

vd 2

VOLUME. 2
FIGURES AND TABLES

The University of Cape Town has been given the right to reproduce this thesis in whole or in part. Copyright is held by the author.

DIGITISED
28 NOV 2016

The copyright of this thesis vests in the author. No quotation from it or information derived from it is to be published without full acknowledgement of the source. The thesis is to be used for private study or non-commercial research purposes only.

Published by the University of Cape Town (UCT) in terms of the non-exclusive license granted to UCT by the author.

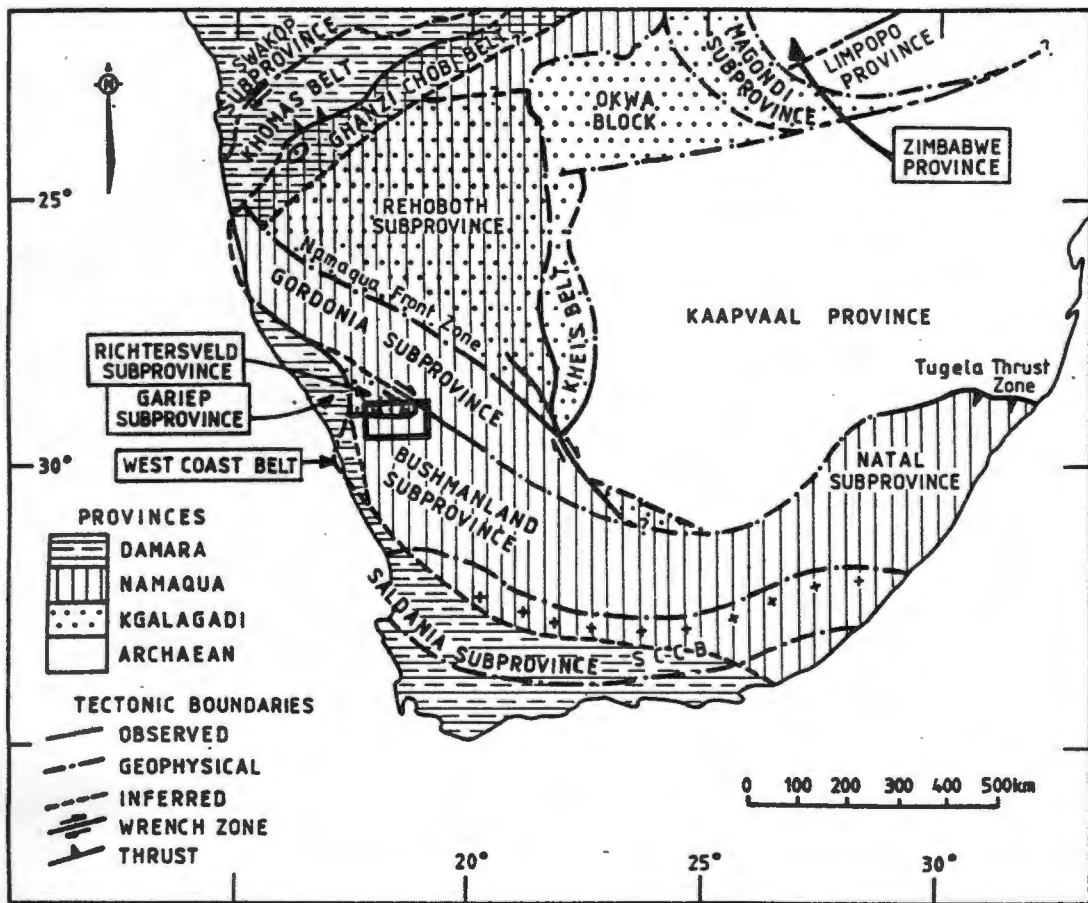


Fig. 1.1 Major Proterozoic tectonic provinces and subprovinces of southern Africa (after Hartnady et al., 1985). Box covers Aggeney's area shown in Fig. 1.4. SCCB = Southern Cape Conductive Belt; + = Beattie magnetic anomaly (after de Beer and Meyer, 1983)



Fig. 1.2 Aerial photograph of Broken Hill mine, looking west. The Black Mountain orebody is seen in the far distance. Photograph courtesy A. Lanham



Fig. 1.3 Panoramic view of Broken Hill looking east. Maanhaarkop is seen in the middle distance and Gamsberg (flat-topped mountain) in the far distance

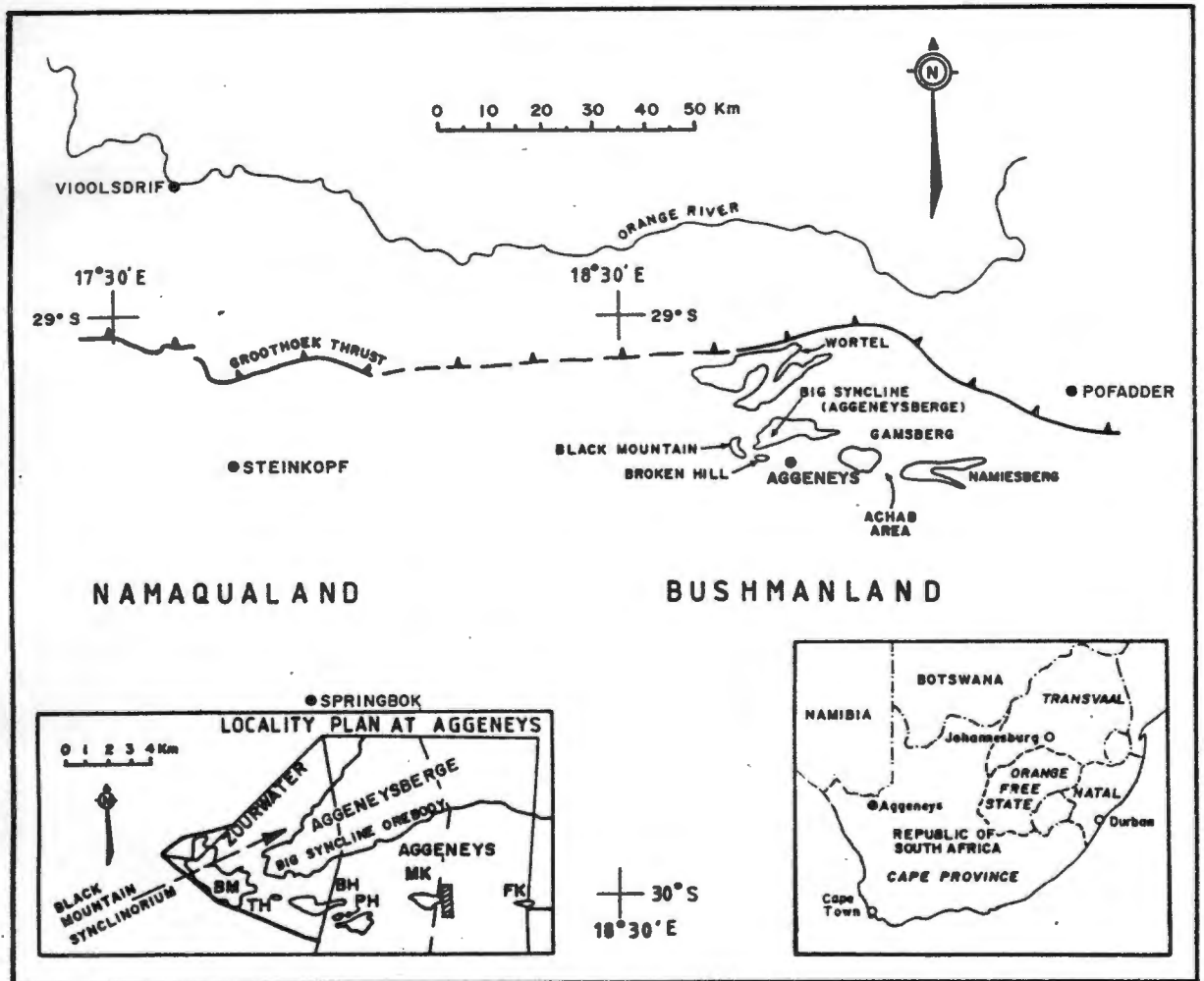


Fig. 1.4 Locality map of southern Africa showing position of inselbergs in the Aggeneys area within the Namaqua Province. Position of Grootthoek Thrust after Blignault et al. (1983, Fig. 14). BH = Broken Hill; MK = Maanhaarkop; FK = Froneman se Kop; BM = Black Mountain; PH = Plant Hill; TH = Tank Hill. Inset shows Aggeneys area relative to political boundaries

Table 1.1 Published ore reserves for the Aggeneys-Gamsberg deposits

Deposit	Reserve type	Million tonnes	Cu%	Pb%	Zn%	Ag ppm
1) Broken Hill	Geological	85	0.34	3.57	1.77	48.1
	Economic	38	0.45	6.35	2.87	82.3
1) Black Mountain	Geological	82	0.75	2.67	0.59	29.8
1) Big Syncline	Geological	101	0.04	1.01	2.45	12.9
2) Gamsberg	Geological	150		0.55	7.1	
Total geological reserves		418	0.23	1.69	3.62	18.7

Published ore reserves for the Aggeneys-Gamsberg deposits

1) From Ryan et.al. (1982)

2) From Rozendaal (1982)

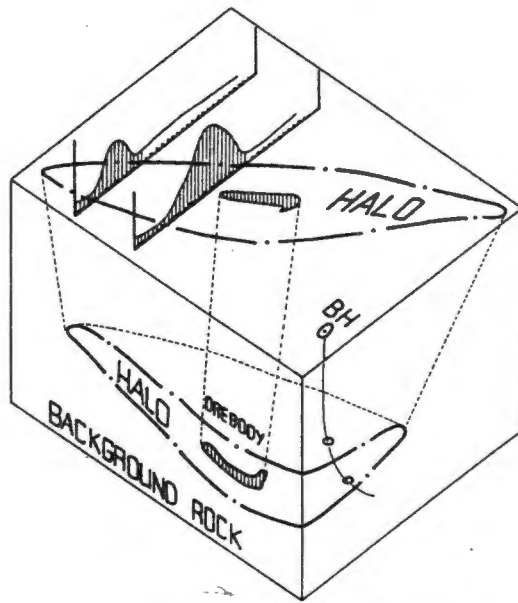


Fig. 2.1 Conceptual representation of an orebody enveloped by its lithogeochemical halo. On the top surface are shown two idealized lithogeochemical sampling profiles for an element of interest with concentration intensity (here shown as positive) increasing both towards the centre of each profile and with proximity to the orebody. Similar profiles could be drawn down the borehole (BH) depicted, with increased geochemical response where the borehole intersects the halo. The Broken Hill orebody only measures 1 000m by 100m in outcrop. Prior knowledge of a halo which envelops Broken Hill-type mineralization would indicate a buried deposit, or alert the explorationist when a borehole had narrowly missed the orebody

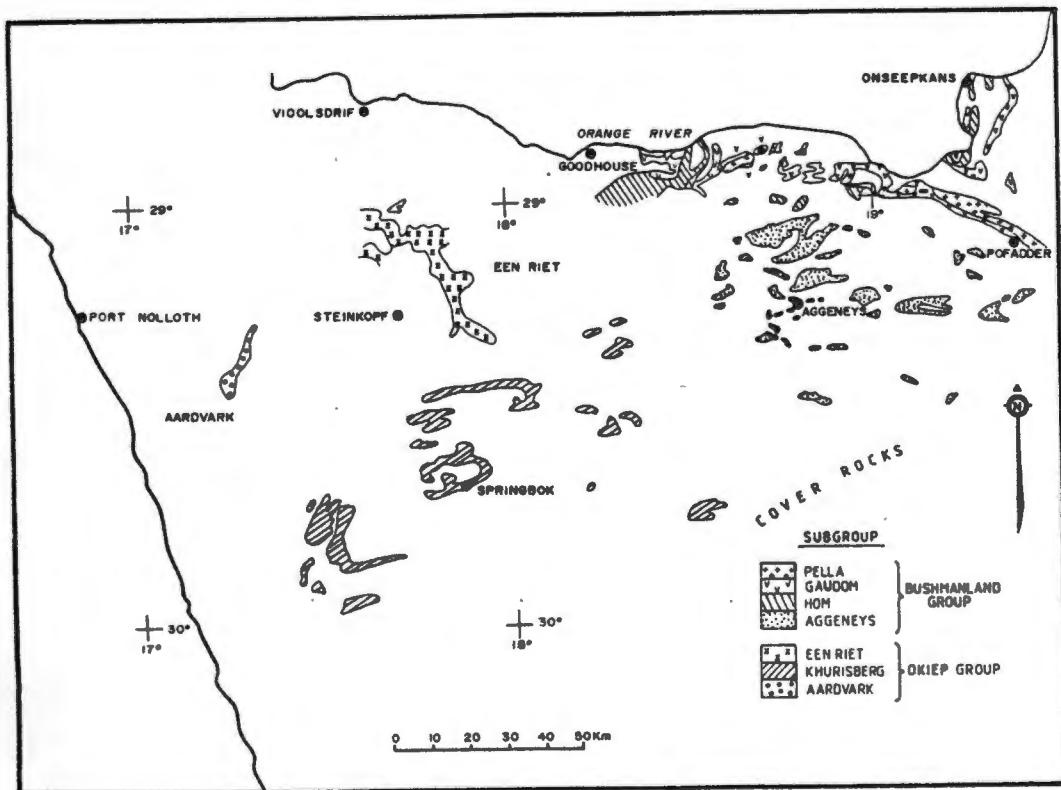


Fig. 3.1 Map showing Subgroups of the Bushmanland Group, and Subgroups of the Okiep Group which are similar to the Aggeneys and Pella Subgroups. Modified after SACS (1980, Figs. 5.1.5 and 5.1.6)

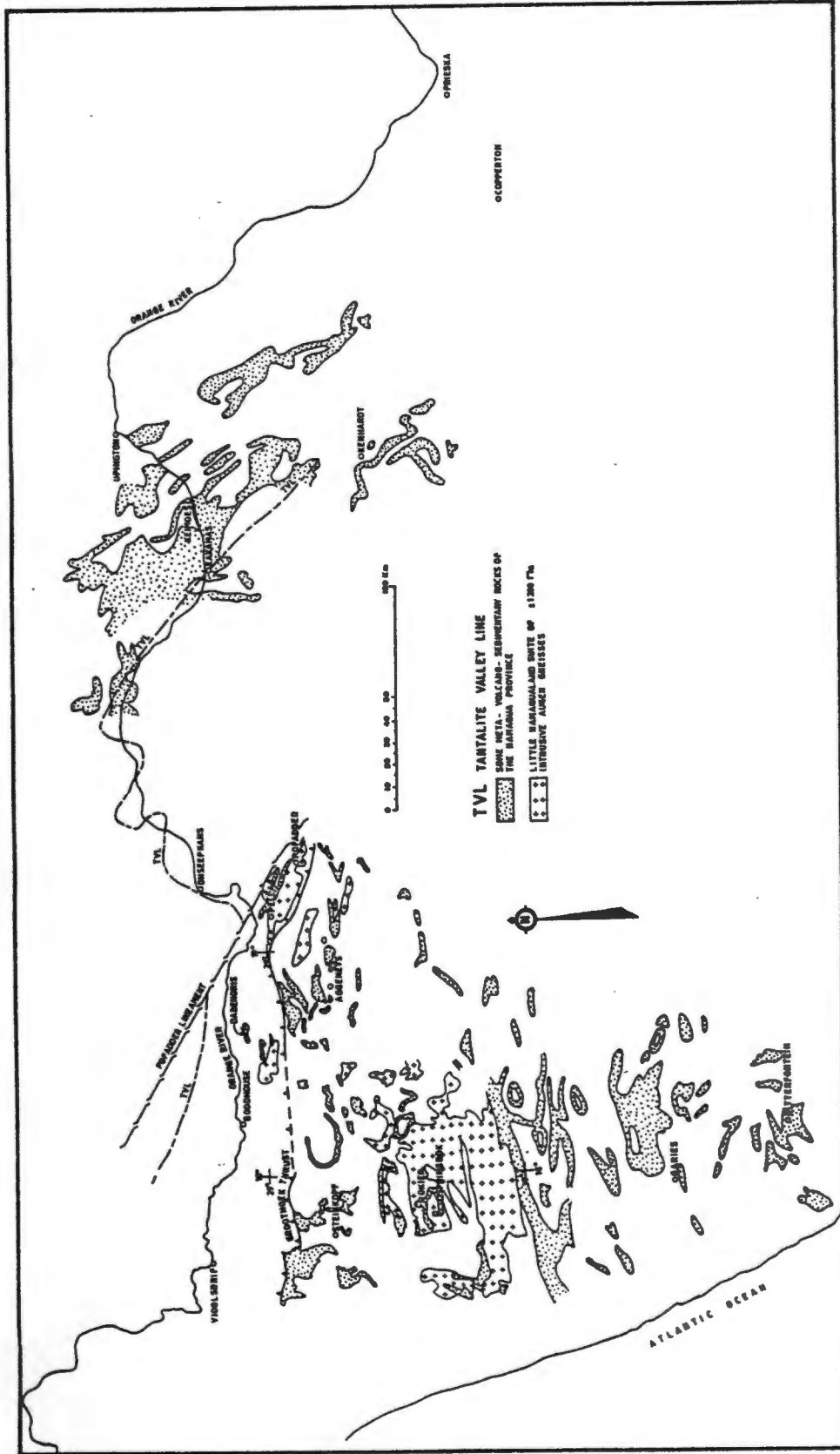


Fig. 3.2 Map showing the Aggeneys Subgroup and all possible correlative supracrustal successions in the Namaqua Province, and the distribution of the Little Namaqualand Suite, from Bitterfontein to Prieska (based on Blignault et al., 1983, Fig. 14; Joubert, 1986; SACS, Fig. 5.1.1 and Moore, 1986, Fig. 1.1)

Table 3.1 SACS (1980) lithostratigraphy of the Bushmanland and Okiep Groups in a generalized structural succession from north (top) to south

BUSHMANLAND GROUP		OKIEP GROUP	
Subgroup	Formation (and lithology)	Subgroup	Lithology
Pella	4. Quartz muscovite schist and conglomerate unit	Een Riet	Metasediments north of Steinkopf
	3. Iron formation unit	Khurisberg	Metaquartzites and schists of the Copper District and environs
	2. Metaquartzite unit		
	1. Schist unit		
Guadom	Mafic gneiss with intercalated metasediments	Aardvark	Metaquartzites and schists on the coastal plain east of Port Nolloth
Hom	Leucoeratic (light grey) gneisses with intercalated metasediments	Garles	All the undifferentiated grey gneisses of Namaqualand
Aggeneys	4. Quartz muscovite schist and conglomerate unit	Bitterfontein	Metaquartzites and schists of southern Namaqualand
	3. Gams Formation (Iron Formation)		
	2. Metaquartzite unit		
	1. Namies Schist Formation		

Table 3.2 Chronology of the major events in the western Namaqua Province

Event	Sedimentary and volcanic	Intrusive	Metamorphic	Tectonic	Reference
Age (Ma)					
600 - 1 000	Gariiep Complex			Subduction ceased along SCCB	De Beer & Meyer (1983)
1 000					
1 000 - 1 200		Little Namaqualand Suite of siliceous augen granite gneiss		Namaqua Orogeny (Kibaran)	Blignault et al. (1983)
1 200			Regional metamorphic peak (high grade in Springbok-Komaggas area)		Clifford et al. (1981)
1 200 - 1 500	Aggeneys-Gamsberg orebody formation				Koepfel (1980)
1 300				Accretion of Namaqualand Metamorphic Complex to Kaapvaal Craton	Joubert (1986)
< 1 500	Jannelsepan Formation mafic metavolcanics				Cornell (1978)
1 600 - 2 020	Bushmanland Group development				Betton (1984); Welke & Smith (1984)
1 730		Vioolsdrif Suite more acid phase. Tantalite Valley line of mafic bodies		Accretion of Richtersveld-Bushmanland microcontinent with Gordonia Subprovince	Reid & Barton (1983) Joubert (1986)
1 900		Vioolsdrif Suite granodiorite and diorite			Reid & Barton (1983)
2 000	Orange River Group, calc-alkaline volcanics (felsic Hom Fm. overlain by basic Gaudom Fm.)			Orange River Orogeny (Eburnian)	Reid & Barton (1983) Blignault et al. (1983)
2 020		Achab Gneiss (Bushmanland basement)			Welke & Smith (1984)

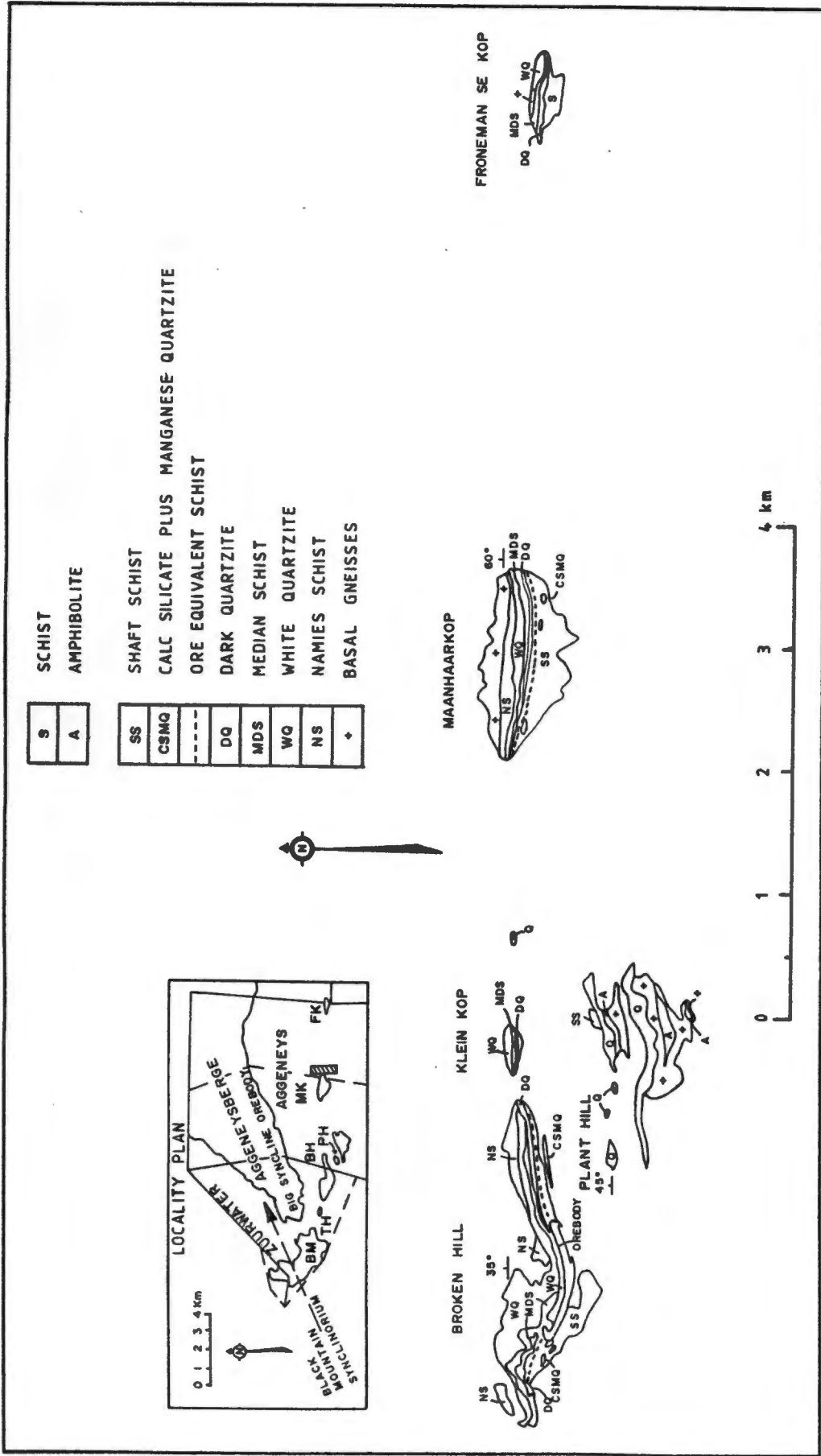


Fig. 4.1 Map of the Aggeneys area showing gross similarity of the geology between Broken Hill, Klein Kop, Maanhaarkop and Froneman se Kop. Locality plan shows relationship of Broken Hill (BH), Maanhaarkop (MK) and Froneman se Kop (FK) forming the southern limb of the Black Mountain (BM) synclinorium. Also indicated are Plant Hill (PH) and Tank Hill (TH).

THICKNESS (m)	CUMULATIVE THICKNESS (m)	PICTURE	LOCAL MINE NAME	SOME PROPOSED FORMAL NAMES
			PINK GNEISS AND AUGEN GNEISS	Basal Gneiss
180	180		SCHIST	Namies Schist
80	260		UPPER QUARTZITE	White Quartzite
50	310		SCHIST	Median Schist
25	335		LOWER QUARTZITE	Dark Quartzite
40	375		HANGINGWALL SCHIST	
40	415		UPPER OREBODY	
15	430		INTERMEDIATE SCHIST	
30	460		LOWER OREBODY	
30	490		UPPER FOOTWALL SCHIST	
10	500		WEAK ZONE	Biotite Graphite Zone
10	510		CALC-SILICATE ROCK AND MANGANESE QUARTZITE	
80	597		LOWER FOOTWALL SCHIST	Upper Shaft Schist
85	682		GREY GNEISS	
90	772		LOWER FOOTWALL SCHIST	Lower Shaft Schist
			SCHIST QUARTZITE	
14	795		AMPHIBOLITE & GREY GNEISS	
			PINK GNEISS	

Fig. 4.2 Structural succession at Broken Hill: the idealized borehole intersection

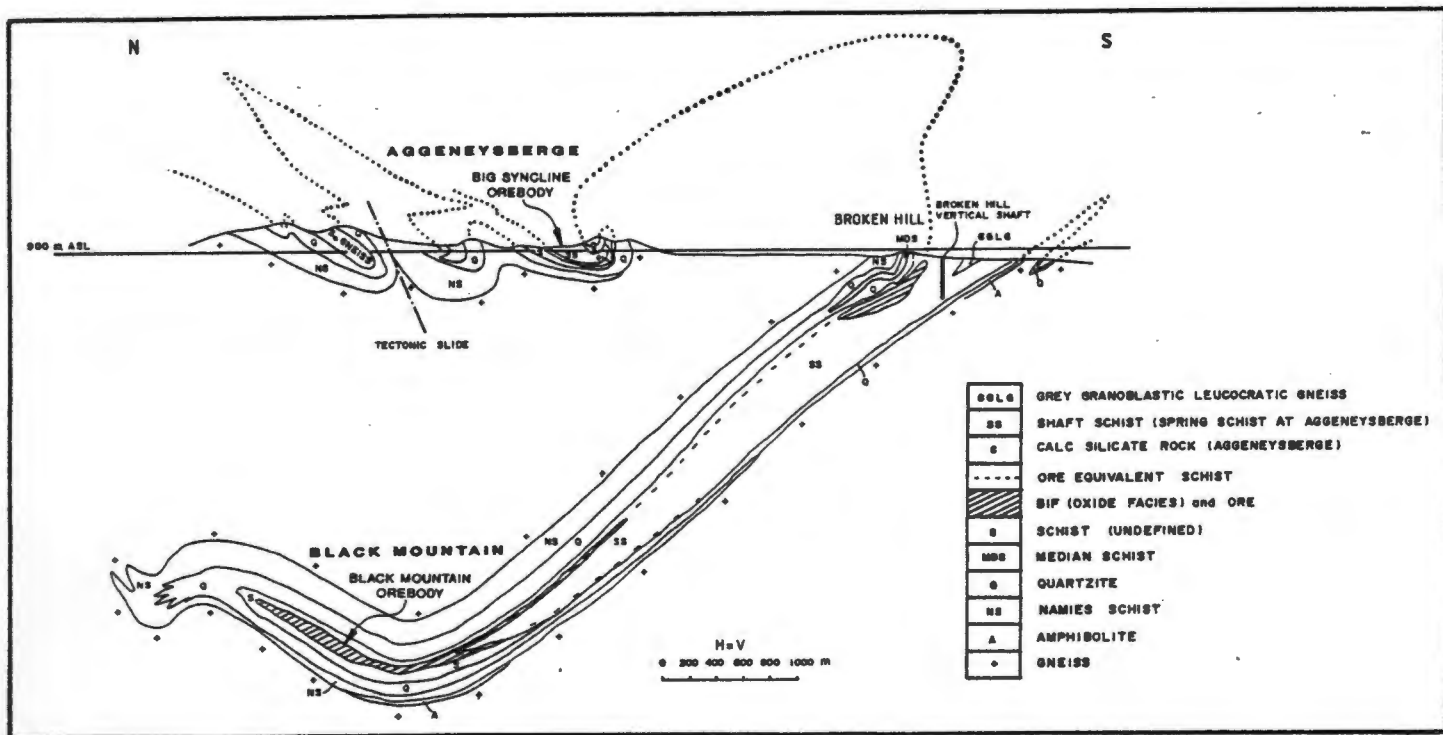


Fig. 4.3 Regional north south section through Broken Hill, Aggeneysberge and Black Mountain showing fold closure positions for Aggeneysberge and Black mountain projected down plunge from surface (after Lipson, 1978, Fig. 87). Location of cross section shown in Fig. 5.3

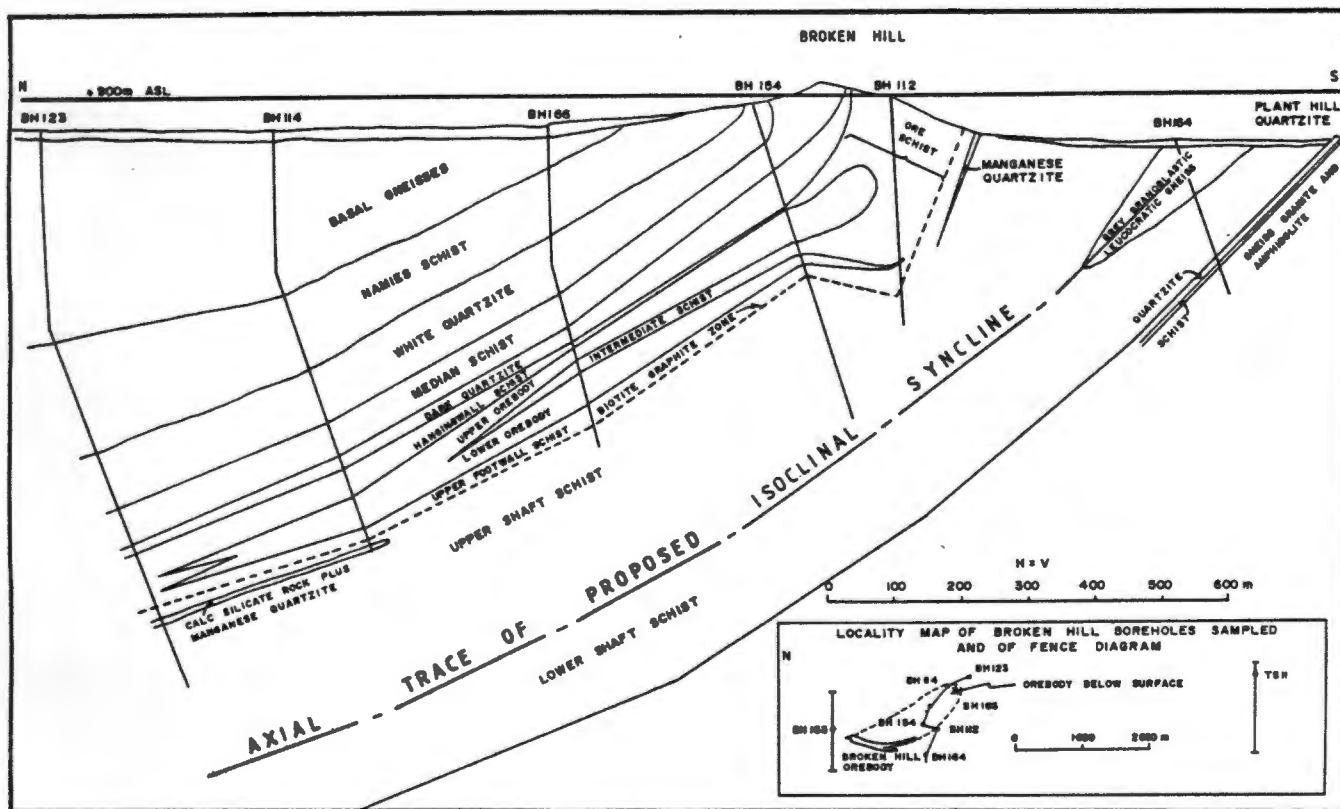


Fig. 4.4 Structural interpretation along a section through Broken Hill and Plant Hill

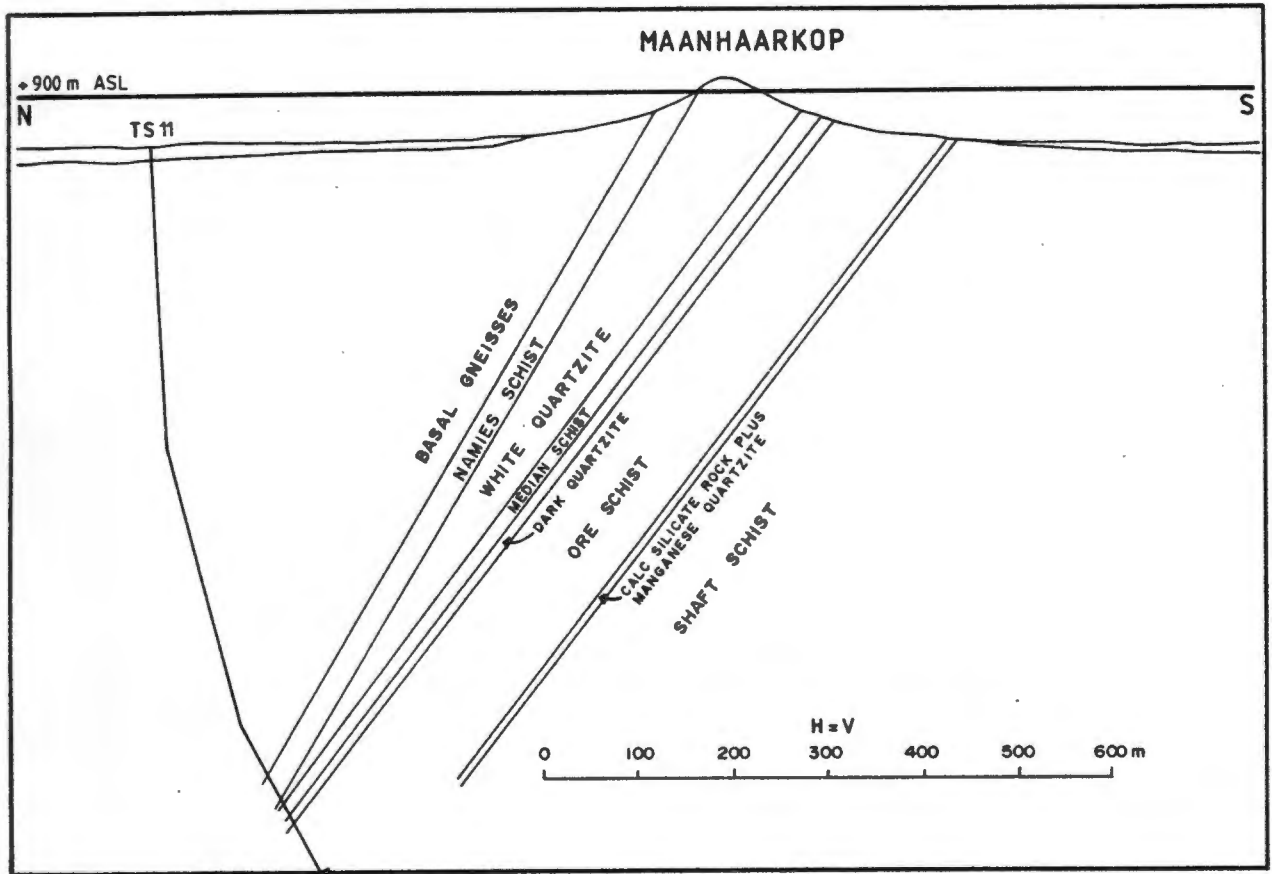


Fig. 4.5 Idealized structural section through Maanhaarkop and borehole TS11

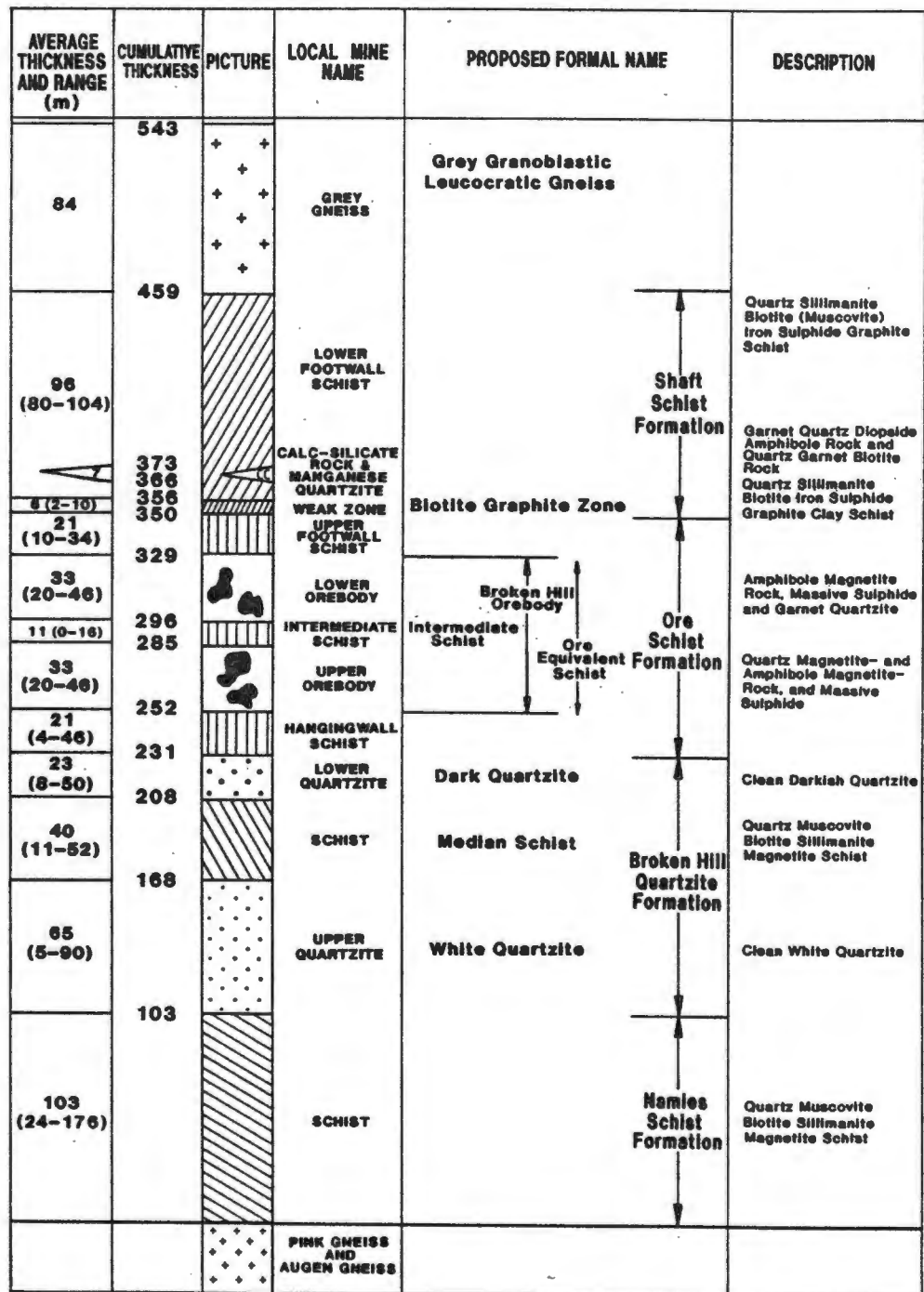


Fig. 4.6 Working stratigraphic column at Broken Hill



Fig. 4.7 Photograph of NS core showing pink hue and common nodular texture

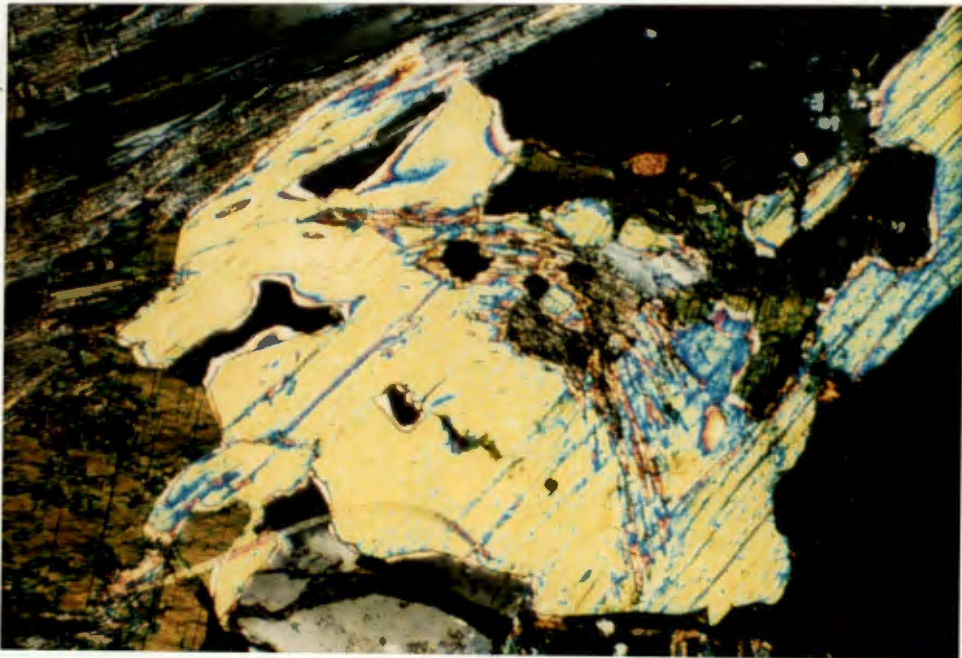


Fig. 4.8 NS (ALP063) showing undeformed muscovite as an alteration product after folded sillimanite. Note also simplectic quartz intergrowths (dark zones in muscovite). Highly birefringent inclusion in quartz is zircon. Crossed nichols. (1cm = 100 micron)



Fig. 4.9 Photograph of SS core showing bottle-green hue and uniformly banded texture. Note green colour of pegmatite at bottom centre



Fig. 4.10 SS (ALP186) showing muscovite as an alteration product after biotite. Plain polarized light. (1cm = 100 micron)



Fig. 4.11 Photograph of conglomerate at Maanhaarkop



Fig. 4.12 Photograph of folded OEGQ layer in OS on west side of Broken Hill orebody. Note pegmatite formed between OEGQ boudins in upper limb of fold



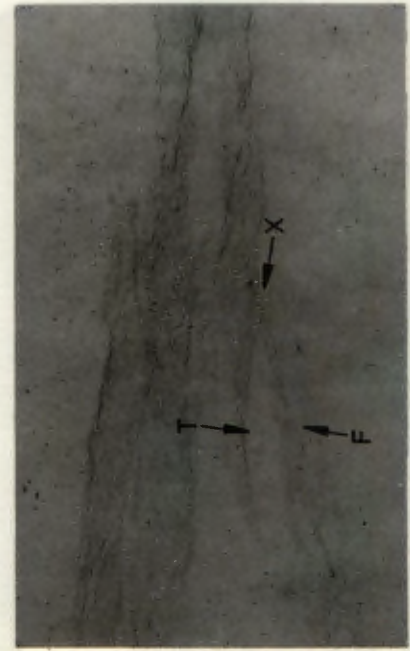
Fig. 4.13 Photograph of IS showing pseudo-pebbles in schist matrix. Note quartzitic band in bottom left, which has started to boudinage



Fig. 4.14 Photograph of OES+GQ core from borehole BH112 beyond the eastern fold closure of the orebody. Note garnet-biotite composition of OES, and the intense refoliation present in the top piece of core

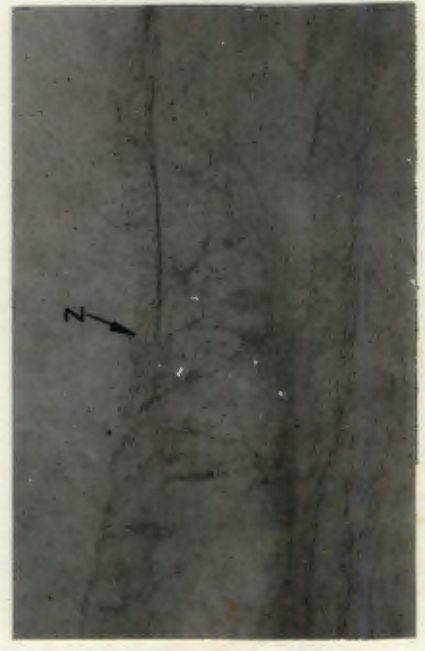


Fig. 4.15 Quartzite with heavy mineral layers showing possible foreset between two subparallel bands



SCALE 1:1

Fig. 4.16 Stereoscopic X-ray radiographs of quartzite. Heavy mineral layers show ripple-like features with cusps pointing southward. Detail also shows apparent foreset "F" being truncated by apparent topset "T" at "X"



SCALE 1:1

Fig. 4.17 Stereoscopic X-ray radiographs of quartzite showing detail of possible raindrop feature located at "Z"



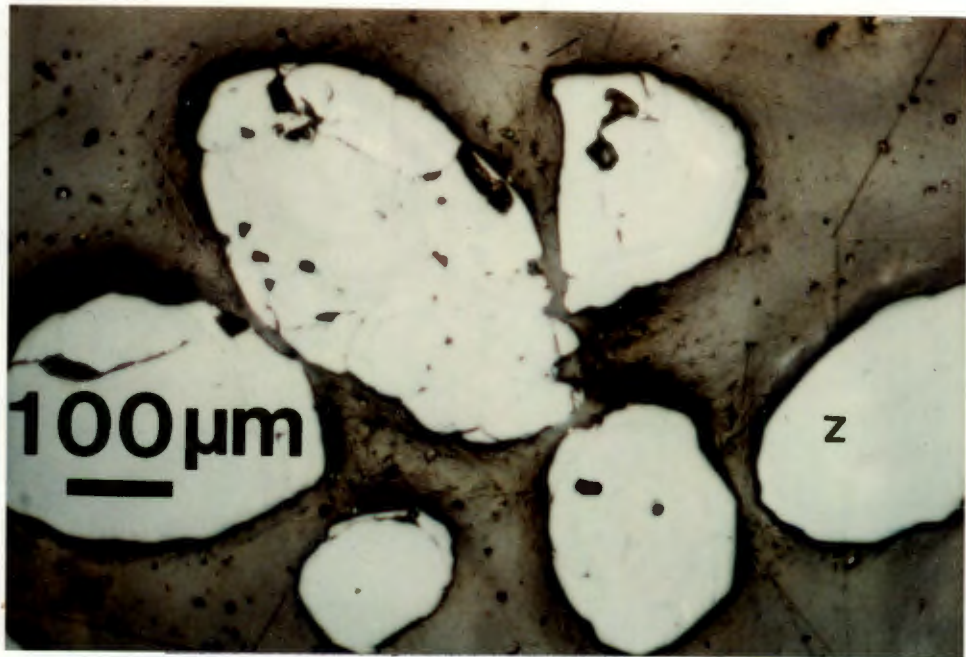


Fig. 4.18 Photomicrograph of well rounded zircon concentrates from BQ (ALP227). Photograph courtesy of G. Martin

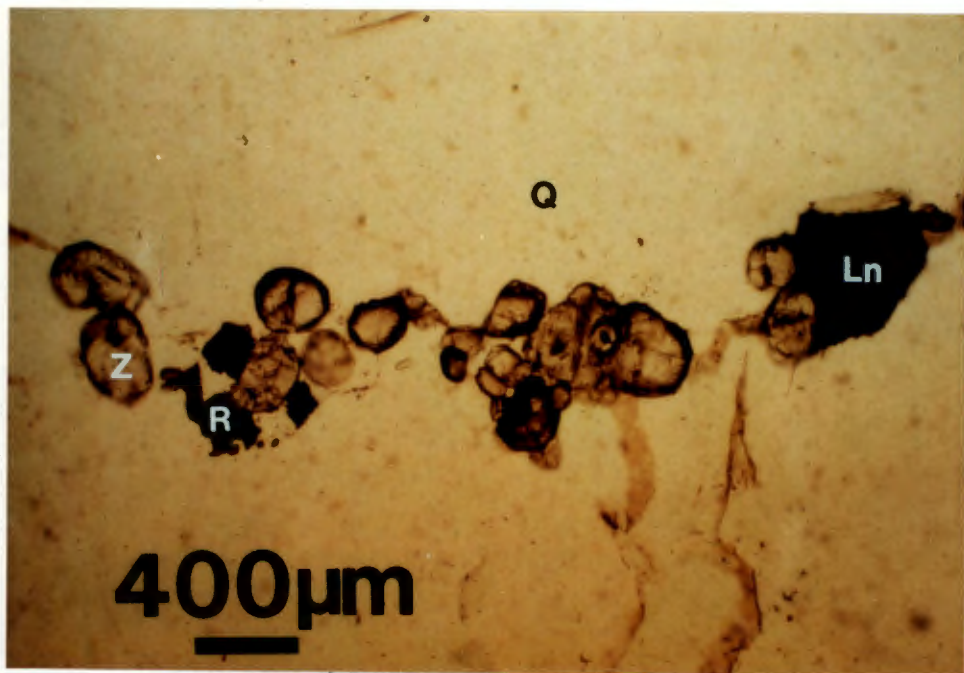


Fig. 4.19 Heavy mineral layer in quartzite with rounded zircon (Z) the dominant mineral. (R = rutile; Ln = limonite). Photograph courtesy of G. Martin

Table 4.1 Zircon grain sizes in Namies Schist and Shaft Schist

ROCK TYPE	SLIDE NO.	NO. OF OBSERVATIONS	MEAN ZIRCON LONG AXES (MICRON)	AV. OF SLIDE MEANS	AV. OF TOTAL MEASUREMENTS
NAMIES SCHIST	ALP 28	8	61		
	ALP 29	5	28		
	ALP 30	8	53		
	ALP 39	14	96		
	ALP 61	3	43	58	70
	ALP 63	6	65		(n = 81)
	ALP 65	15	46		
	ALP 122	12	58		
	ALP 123	10	68		
UPPER SHAFT SCHIST	ALP 56	4	30		
	ALP 57	6	28		
	ALP 58	8	51	39	42
	ALP 59	6	28		(n = 32)
	ALP 154	8	58		
LOWER SHAFT SCHIST	ALP 60	9	37		
	ALP 140	10	39	41	39
	ALP 142	3	50		(n = 34)
	ALP 162	12	38		

Table 4.2 Zircon grain sizes in Broken Hill Quartzites and Median Schist

ROCK TYPE	SLIDE NO.	NO. OF OBSERVATIONS	MEAN ZIRCON LONG AXES (MICRON)	AV. OF SLIDE MEANS	AV. OF TOTAL MEASUREMENTS
White Quartzite	ALP009	6	Mean 80 S.D. 25		77
	ALP124	2	60	79	(S.D. = 27)
	ALP237	3	103		(n = 23)
	ALP232	7	73		
Dark Quartzite	ALP126	1	200		
	ALP011	2	130		77
	ALP233	3	47	95	(S.D. = 48)
	ALP239	3	83		(n = 15)
	ALP240	4	45	5.8	
	ALP238	2	65		
Median Schist	ALP041	5	28	13	58
	ALP125	3	87	15	(S.D. = 33) (n = 8)

* Measurements do not include zircons from heavy mineral layers

Table 4.3 Stratigraphic thicknesses (m) of rock types at Broken Hill

BOREHOLE	NS	UQ	MDS	LQ	HS	UOB	IS	LOB	UFS	BGZ	SS	CSMQ	GGLG	TOTAL
BH123	176	90	50	14	40		14		20	10	80	7		
BH114	118	84	52	20	46		0		21	2		6		
BH166	92	82	48	22	7	20	14	46	34	10	>30			
BH156			40	50	4	46	16	20	10	4	104			
BH112										5			84	
BH164											104			
TS11	24	5	11	8	10									
BH163														
AVERAGE	103	65	40	23	21	33	11	33	21	6	96	7	84	459 (excl. GGLG)
RANGE	24-176	5-90	11-52	8-50	4-46	20-46	0-16	20-46	10-34	2-10	80-104	0-7		

Table 4.4 Physical dimensions of Broken Hill Quartzites

		STRIKE LENGTH	DOWN-DIP EXTENT	THICKNESS
MEASURED	NS	3300	750	103
(m)	SS	3300	750	96
INFERRED	NS	>10	<10	
(km)	SS	>5	>10	

Table 4.5 Physical dimensions of Namies Schist and Shaft Schist

		STRIKE LENGTH	DOWN-DIP EXTENT	THICKNESS
MEASURED	BGZ	3000	750	6
(m)	CSMQ	5 - 400	350 Often Missing	7
INFERRED	BGZ	>5	>1	
(km)	CSMQ	>5	>1	

Table 4.6 Physical dimensions of Biotite Graphite Zone (BGZ) and Calc Silicate Rock plus Manganese Quartzite (CSMQ)

		STRIKE	DOWN-DIP	THICKNESS
		LENGTH	EXTENT	
MEASURED (m)	WQ	3300	750	65
	DQ	900	750	23
INFERRED (km)	WQ	>10	>10?	
	DQ	>10	>10?	

Table 4.7 Physical dimensions of the Broken Hill orebody and Ore Schists

		STRIKE	DOWN-DIP	DOWN-PLUNGE	THICKNESS
		LENGTH	EXTENT	EXTENT	
MEASURED (m)	UOB	600	-	1200	40-60
	LOB	600	-	1200	30-60
	OS	3000	1100	-	110
	HS	3000	1100	-	21
	IS	600	-	1200	11
	UPS	3000	1100	-	21
	OES	3000	1100	-	68
INFERRED (km)	OS	>5	>5		
	HS	>5	-		
	UPS	>5	-		
	OES	>5	-		

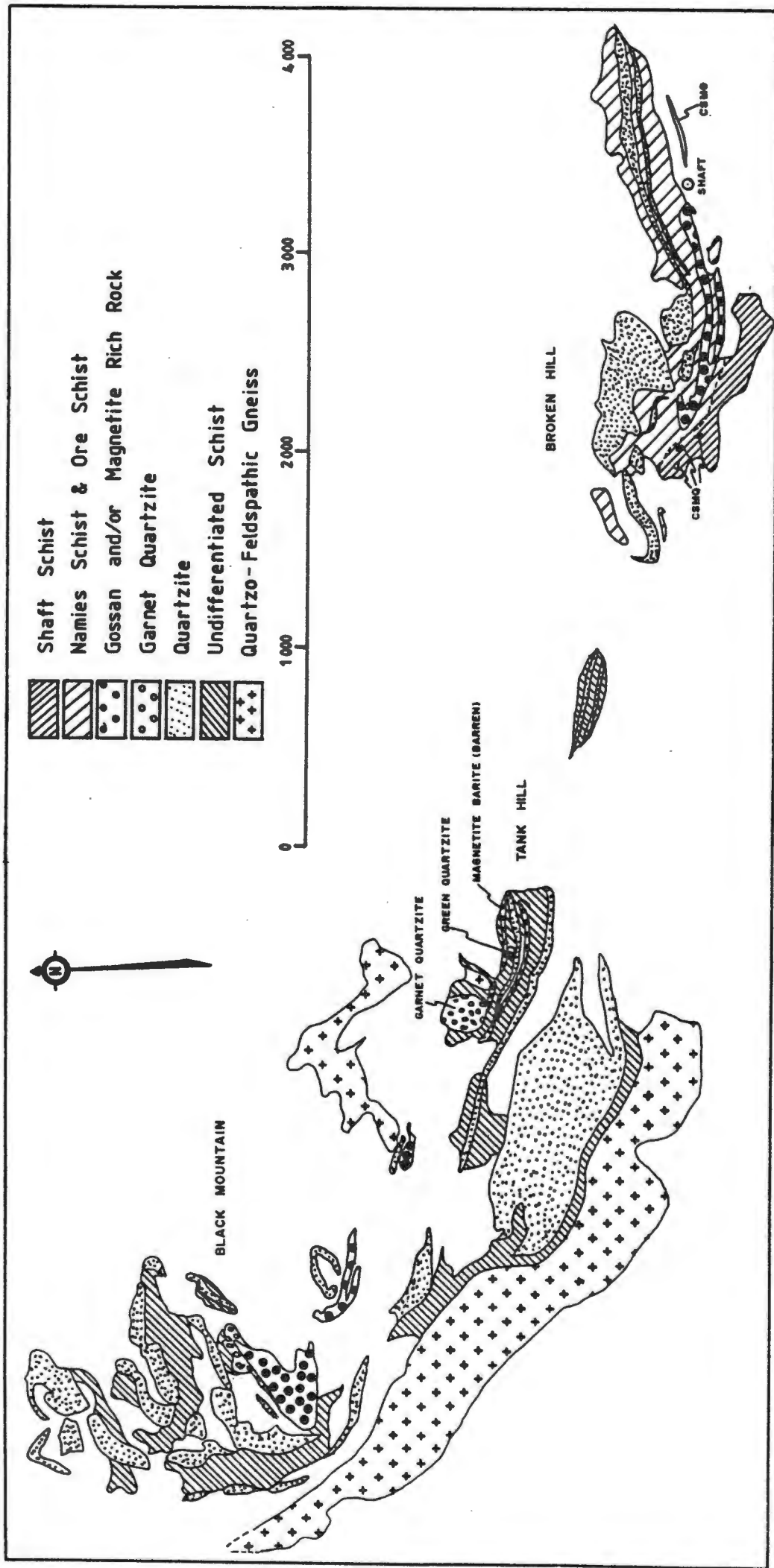


Fig. 5.1 Generalized geological map of Black Mountain, Tank Hill and Broken Hill





Fig. 5.2 Photograph of Tank Hill looking south west. Note the unusual rock-types Garnet Quartzite, Green Quartzite, Massive Magnetite and Barite Magnetite Rock, all lying within the dip slope of a single stratigraphic horizon between the quartzite which forms the ridge of Tank Hill, and gneiss underlying the sand-covered flats. Quartzites in the far distance are separated from Tank Hill by a valley

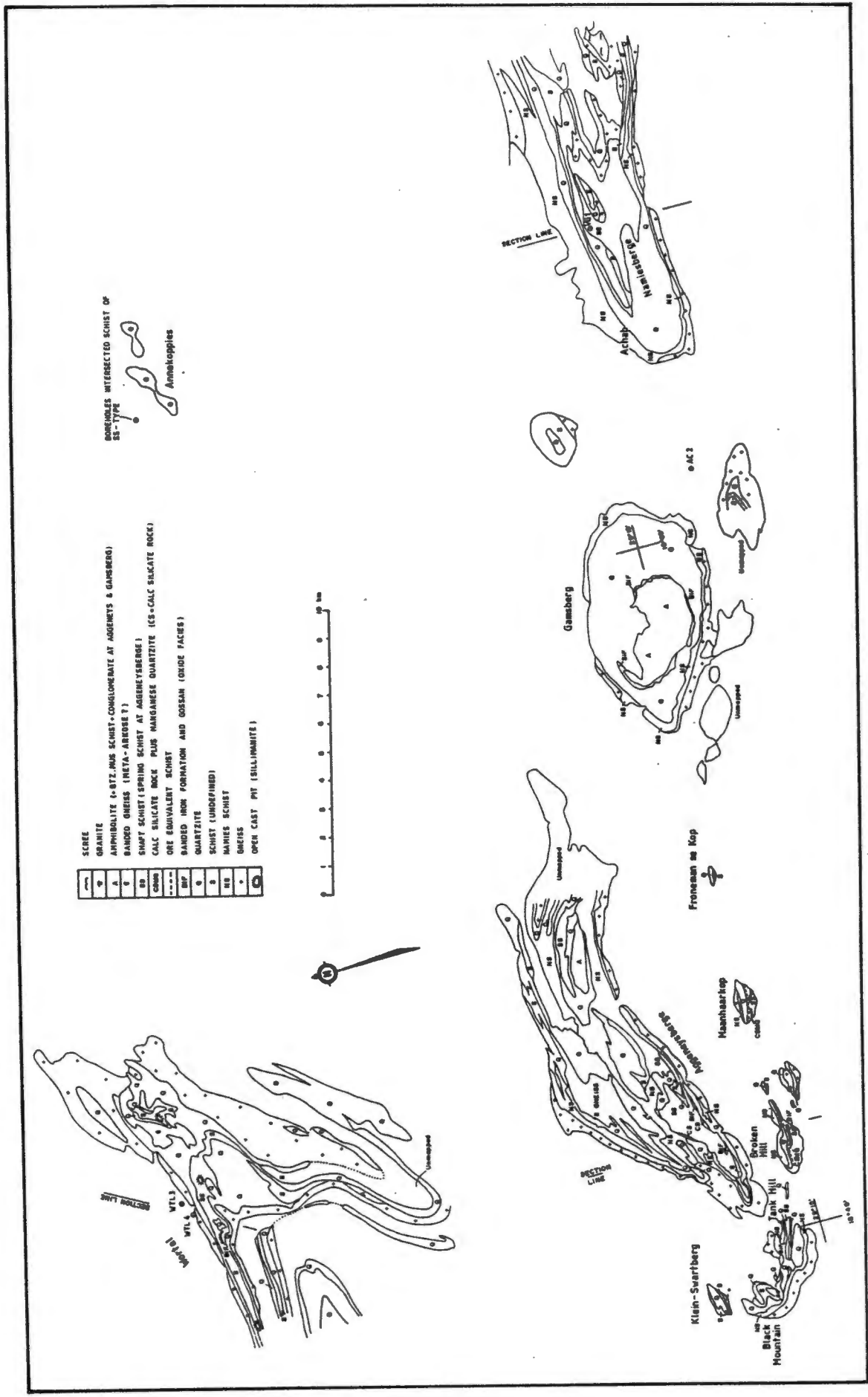


Fig. 5.3 Generalized geological map of the Aggenneys area with some selected inselbergs. Indicated are section lines through Broken Hill-Aggenneysberge (Fig. 4.3), Namiesberg (Fig. 5.4) and Wortel (Fig. 5.6)

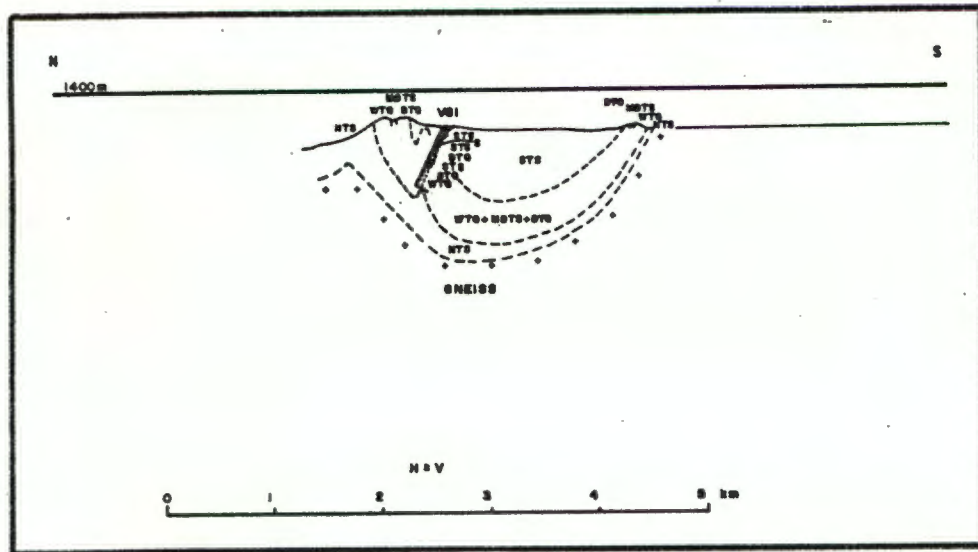


Fig. 5.4 Cross section through Namiesberg and borehole VG1. Abbreviations as in list at start of thesis



Fig. 5.5 Photograph of southern limb of Namiesberg syncline showing Dark-type Quartzite overlying White-type Quartzite

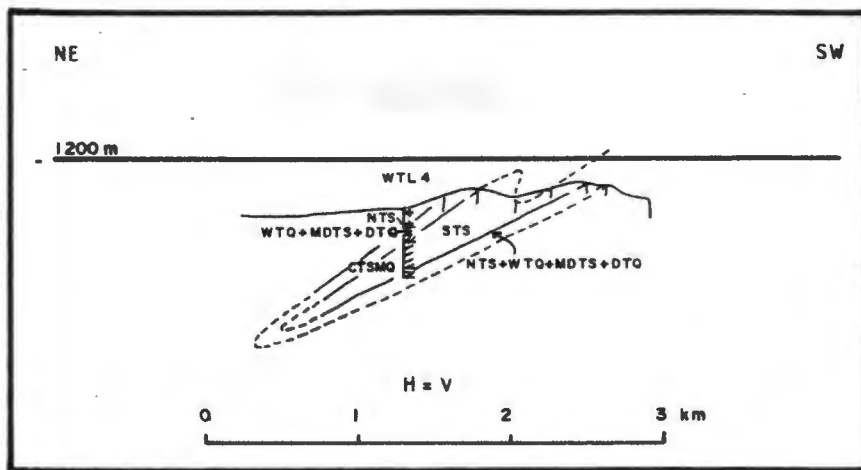


Fig. 5.6 Cross section through Wortel and borehole WTL4. Abbreviations as in list at start of thesis

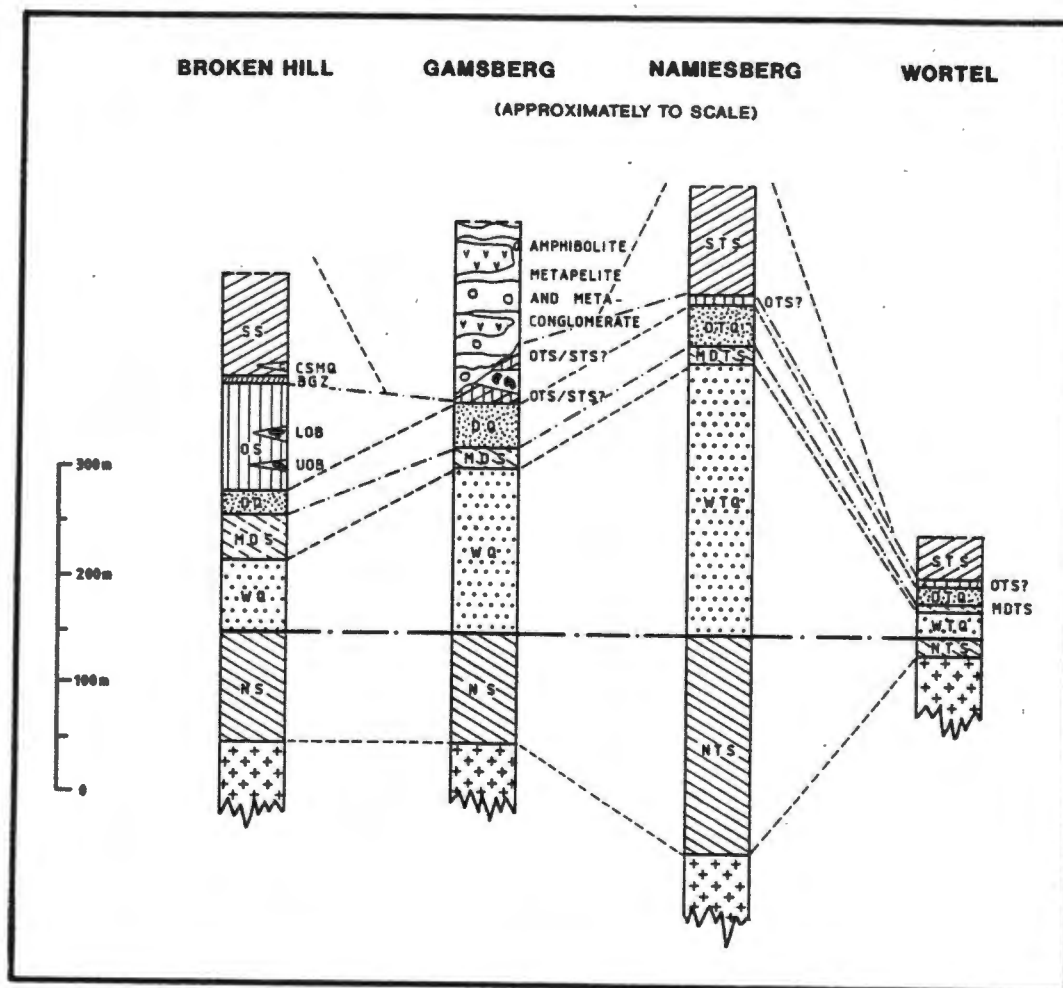
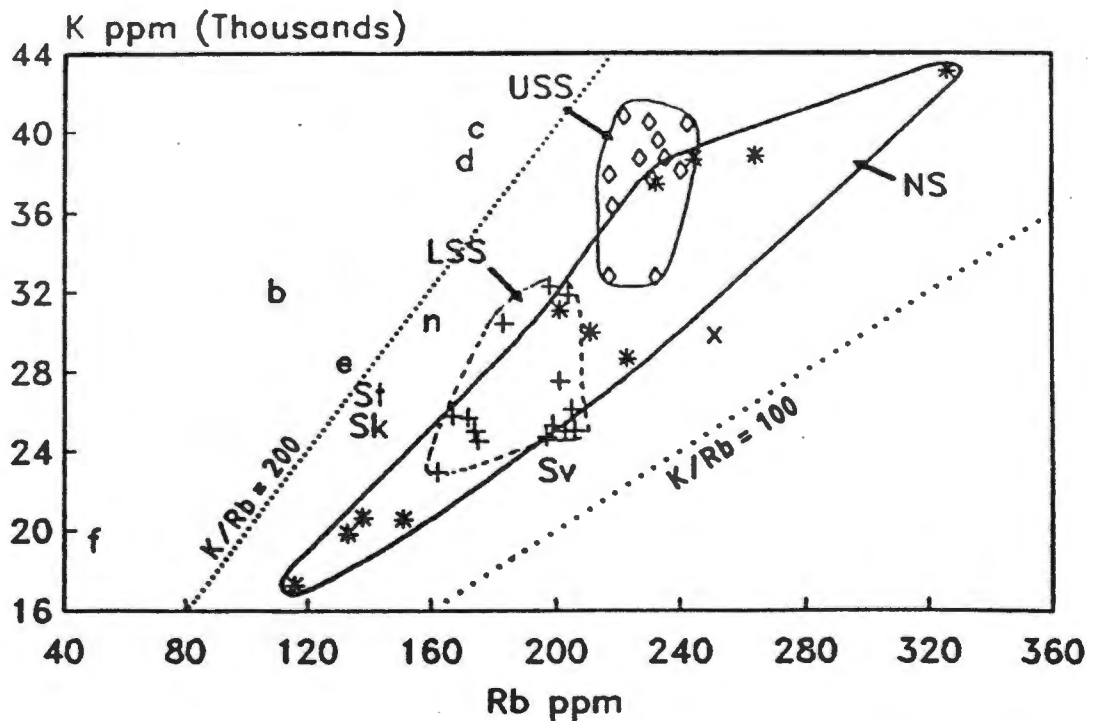


Fig. 5.7 Generalized comparative stratigraphic successions from Broken Hill, Gamsberg, Namiesberg and Wortel. Abbreviations as in list at start of thesis



Legend

Sv Average shale and clay (Vinogradov, 1962, p647)
 Sk Average shale (Krauskopf, 1979, p544)
 St Average shale (Turekian, 1972, p84)

n Average of 54 metapelites; Precambrian; amphibolite facies (Senior & Leake, 1978, p623)
 c Average of 396 shales; Proterozoic; weak metamorphism (Cameron & Garrels, 1980, p190)
 x Average of 13 shales; Phanerozoic; unmetamorphosed (Van de Kamp et al., 1976, p207)
 d Average of 6 metapelites; Phanerozoic; amphibolite facies (Dostal and Capedri, 1978, p411)
 e Av. of 23 metapelites; Phanerozoic; amphibolite facies (Dostal and Capedri, 1978, p411)
 f Average of 24 metapelites; Phanerozoic; granulite facies (Dostal and Capedri, 1978, p411)
 b Average of 27 metapelites; Proterozoic; granulite facies (Barby and Cuney, 1982, p306)

Fig. 6.1 NS and SS K vs Rb concentrations compared with various shales. See legend for shale codes



Fig. 6.2 Photograph of schist from borehole core (touching pencil) and surface outcrop, used to test the chemical effects of surface weathering

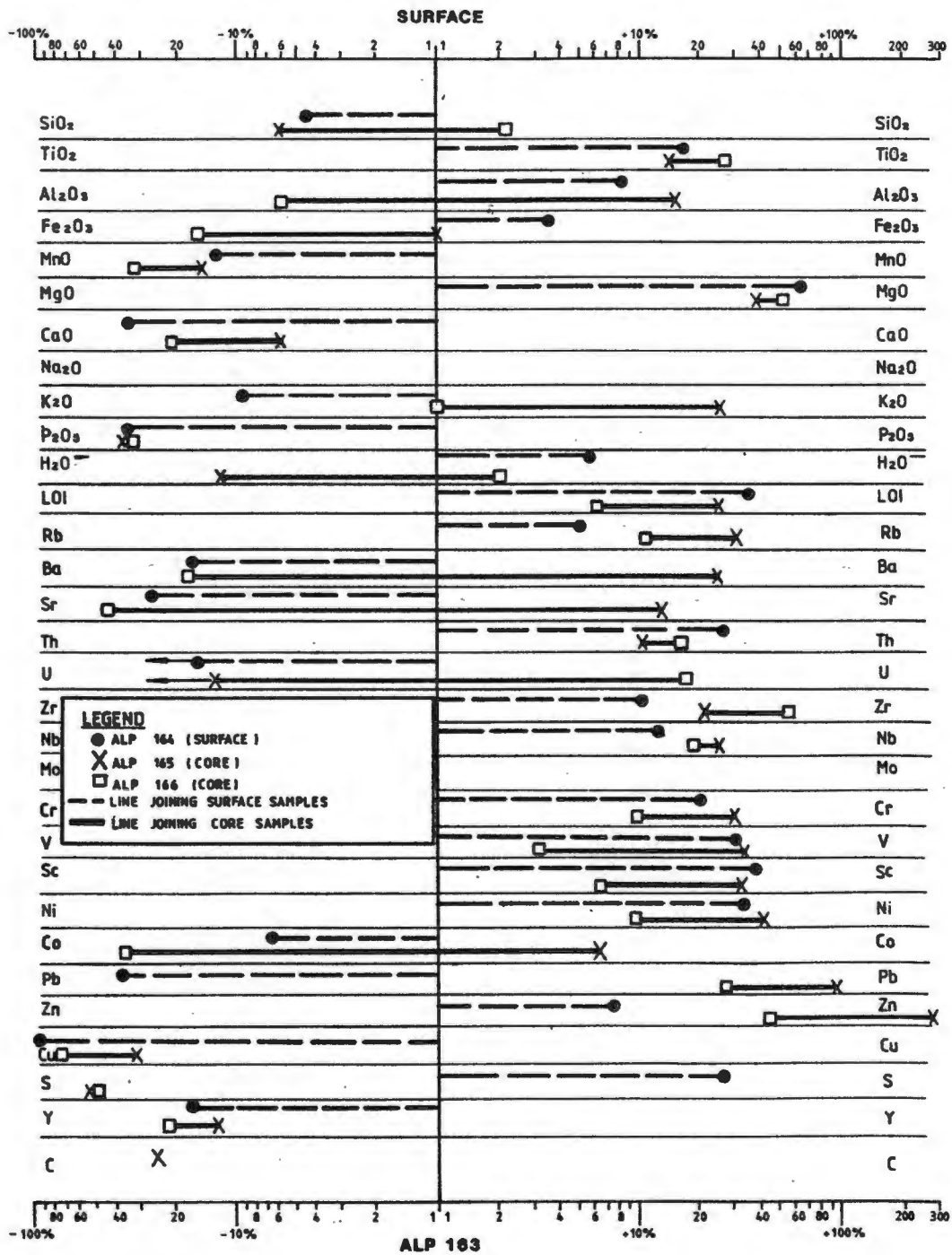


Fig. 6.3 Surface schist weathering orientation study. Percent variation (positive or negative) in element content is with respect to sample ALP163

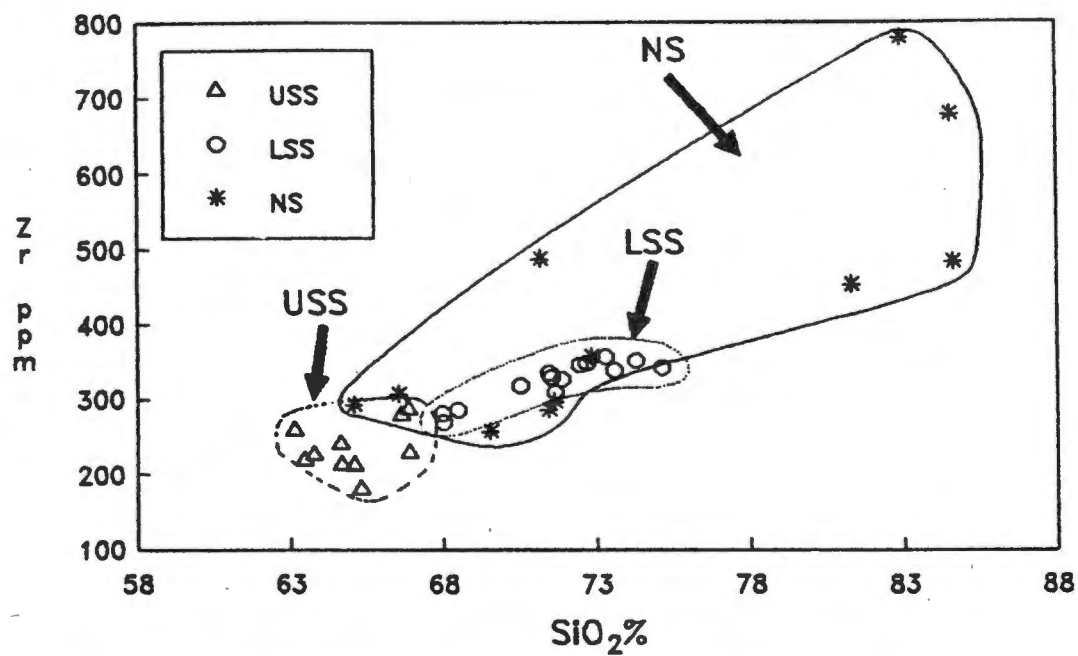


Fig. 6.4 NS and SS Zr vs SiO₂ concentrations

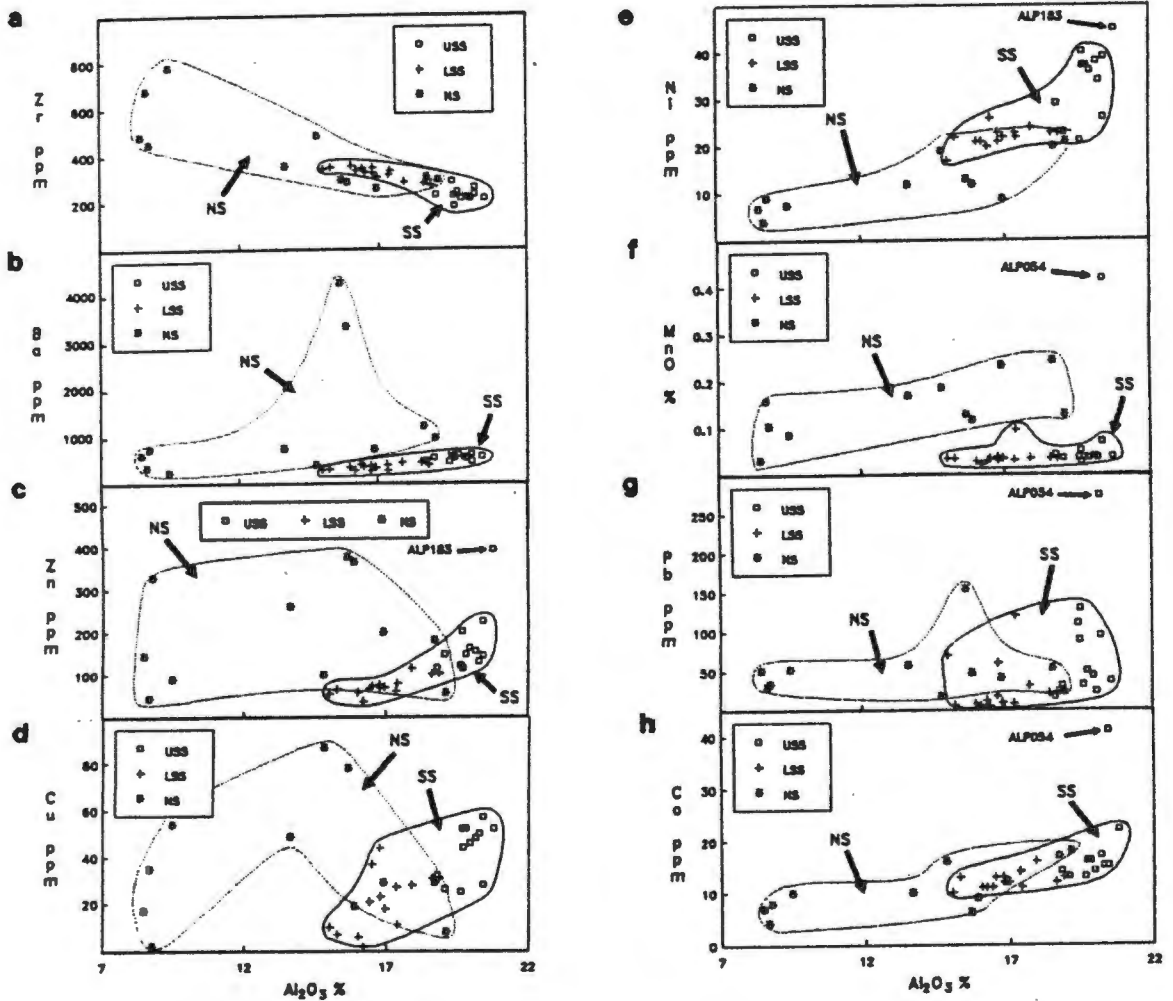


Fig. 6.5 NS and SS element variations vs Al_2O_3 : (a) Zr; (b) Ba; (c) Zn; (d) Cu; (e) Ni; (f) MnO; (g) Pb; (h) Co

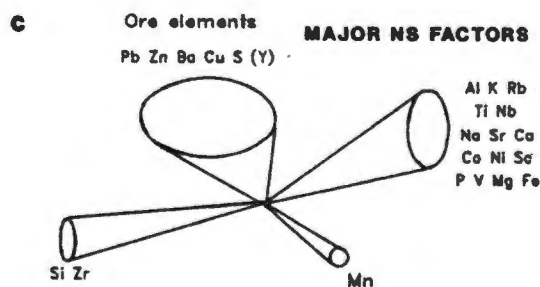
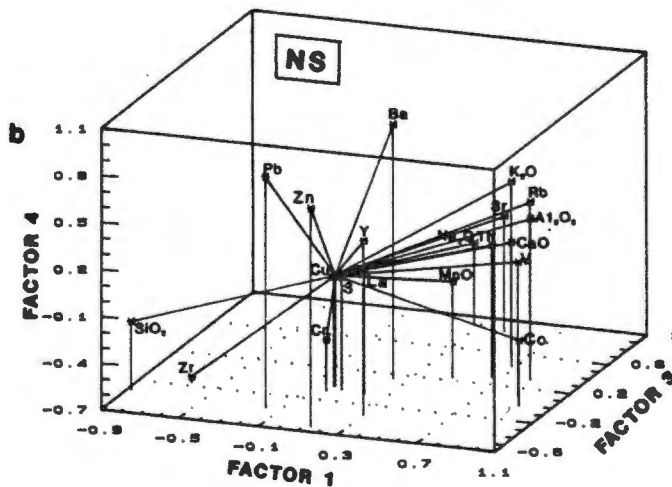
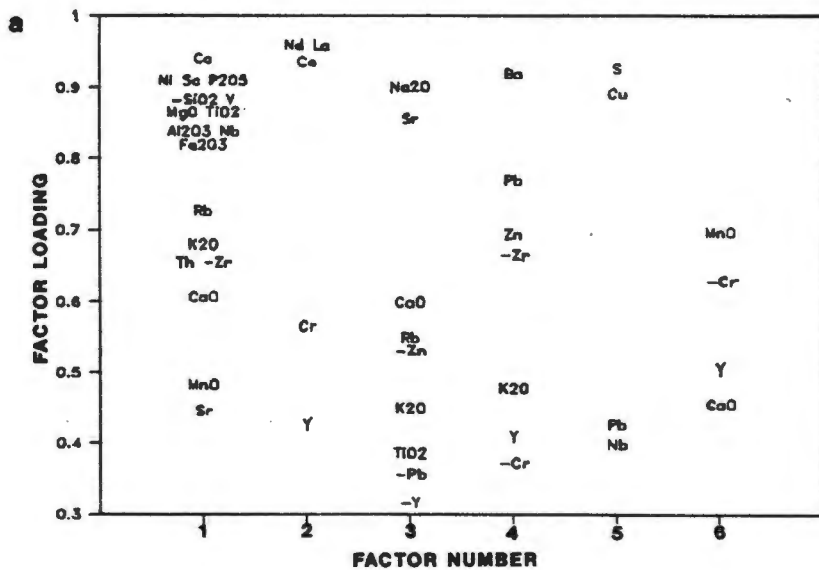


Fig. 6.6 NS factor analysis: (a) loadings on the six factors which cumulatively explain 93.6 % of the variance; (b) geometric representation of Factors 1, 3 and 4 which account for 64.7 % of the total variance. For purposes of clarity the elements Co, Ni, Sc, P₂O₅, V, MgO, TiO₂, Nb and Fe₂O₃ have been omitted as they may be effectively represented by the elements Al₂O₃, K₂O and Rb, as seen in Fig. 6.6 (a) above. The REE's and certain other elements are also omitted in the interests of clarity; (c) 3-D conceptual representation of the major NS factors shown in Fig. 6.6 (b) above.

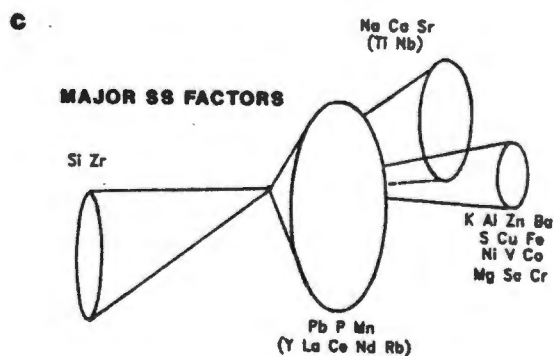
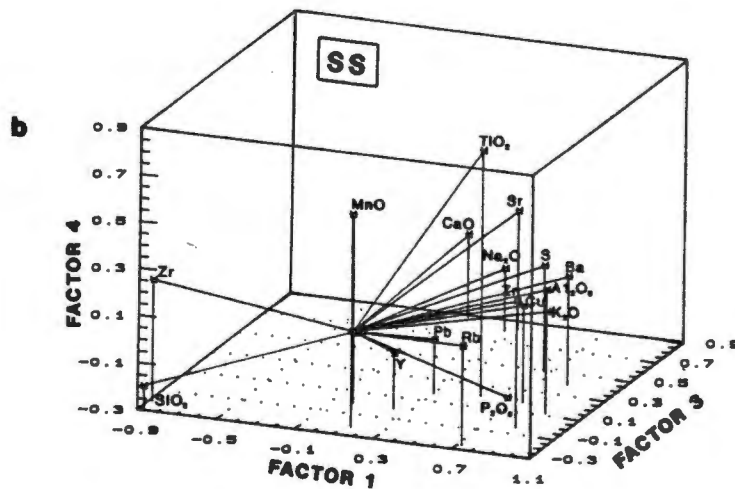
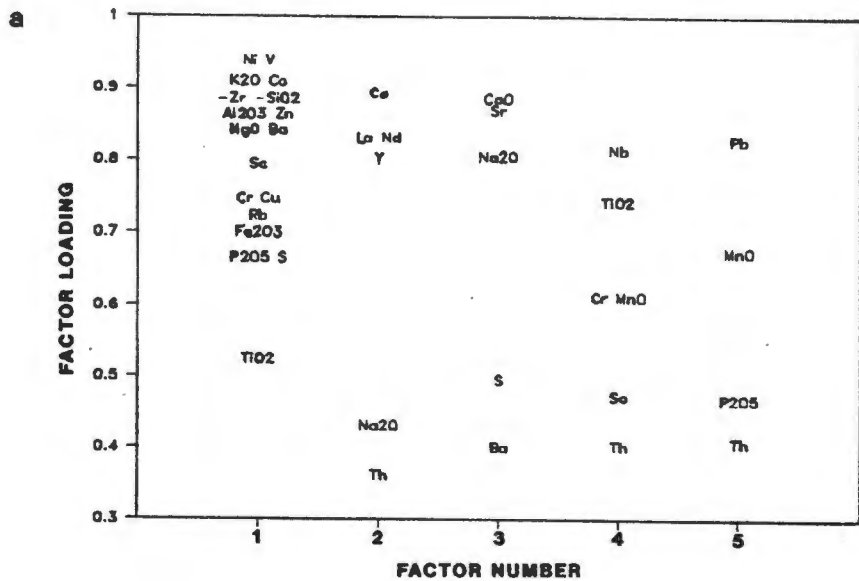


Fig. 6.7 SS factor analysis: (a) loadings on the five factors which cumulatively explain 82.6 % of the variance; (b) geometric representation of Factors 1, 3 and 4 which account for 65.6 % of the total variance. For purposes of clarity the elements Co, Ni, Sc, V, MgO, Cr and Fe₂O₃ have been omitted as they may be effectively represented by the elements Al₂O₃, K₂O and Ba, as seen in Fig. 6.7 (a) above. The REE's and certain other elements are also omitted in the interests of clarity; (c) 3-D conceptual representation of the major NS factors shown in Fig. 6.7 (b) above.

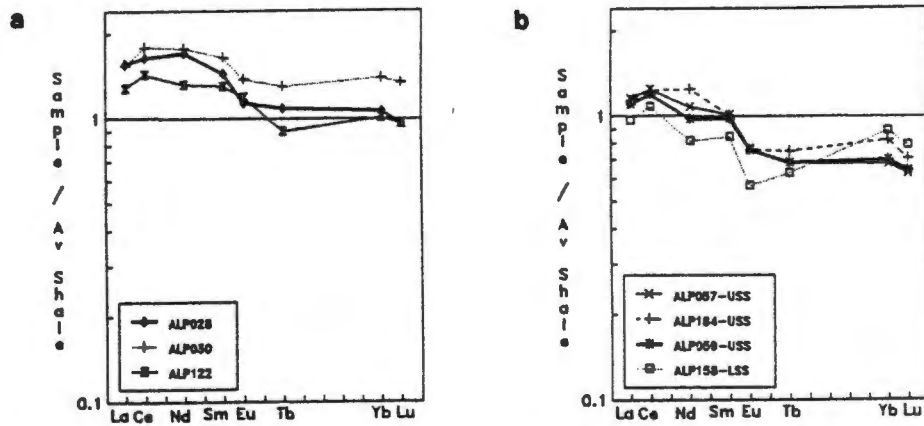


Fig. 6.8 Shale-normalized REE patterns using the INAA analytical method: (a) NS; (b) SS. ALP057, 184 and 059 are USS; ALP158 is LSS. Average shale after Piper (1974)

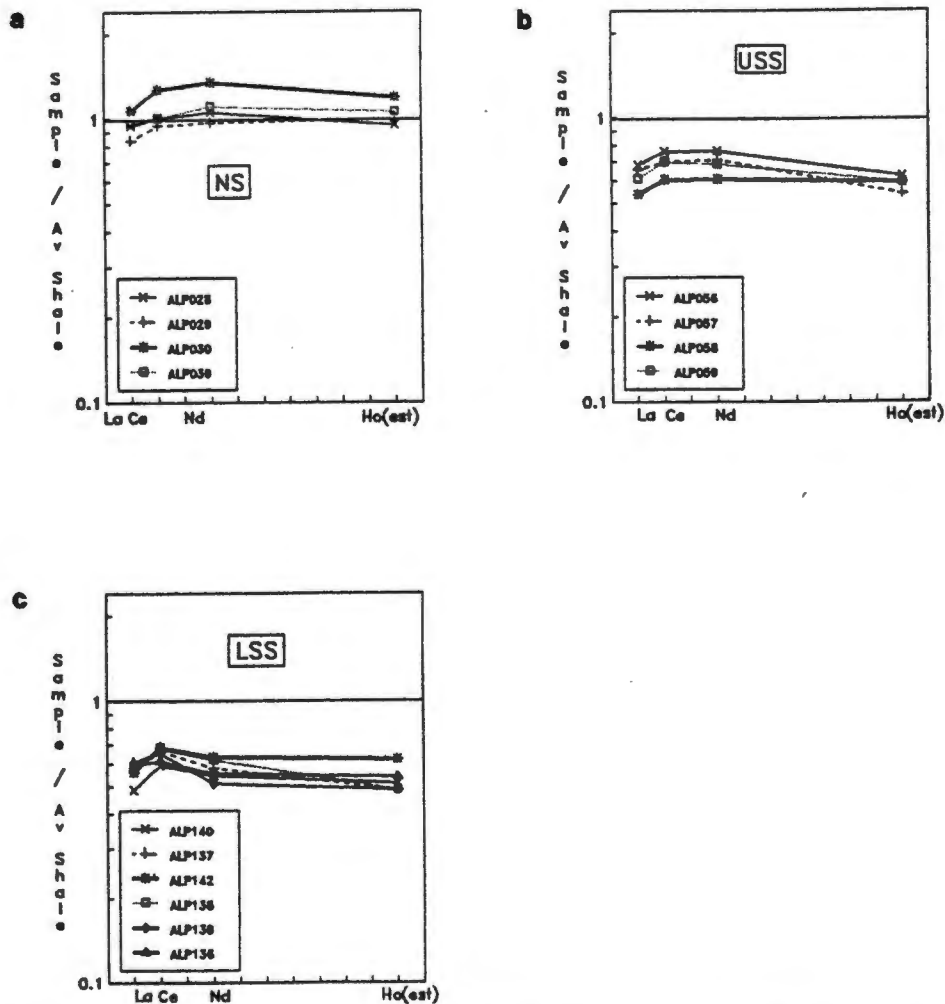


Fig. 6.9 Shale-normalized schist REE patterns, using the XRF analytical method: (a) NS from borehole BH123; (b) USS from borehole BH123; (c) LSS from boreholes BH164 and 156. Estimated Ho (Ho est.) = $Y \cdot 0.0272$ (see Appendix A.2.5).

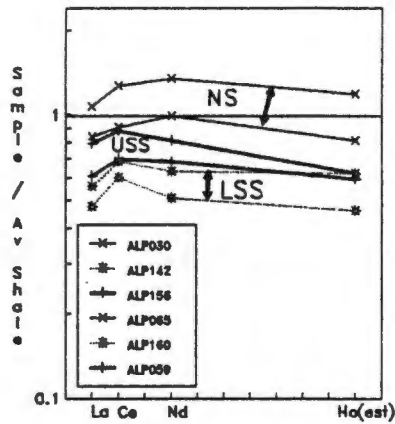


Fig. 6.10 Average shale-normalized REE patterns for the rock-types NS, USS and LSS for XRF-derived data

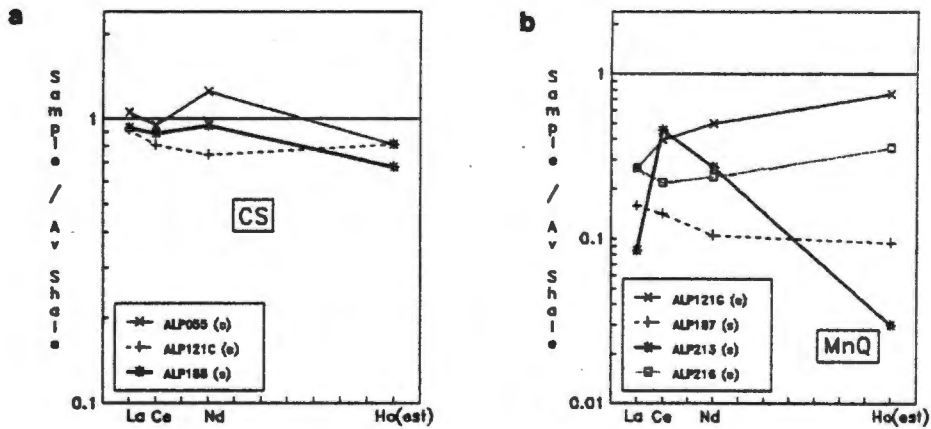


Fig. 6.11 Shale-normalized REE patterns using the XRF analytical method: (a) CS; (b) MnQ (s = surface samples; c = borehole core)

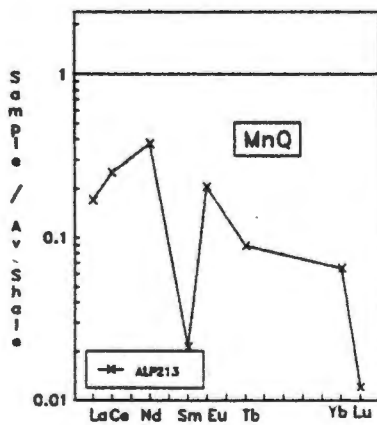


Fig. 6.12 Shale-normalized REE patterns using the INAA method for MnQ sample ALP213

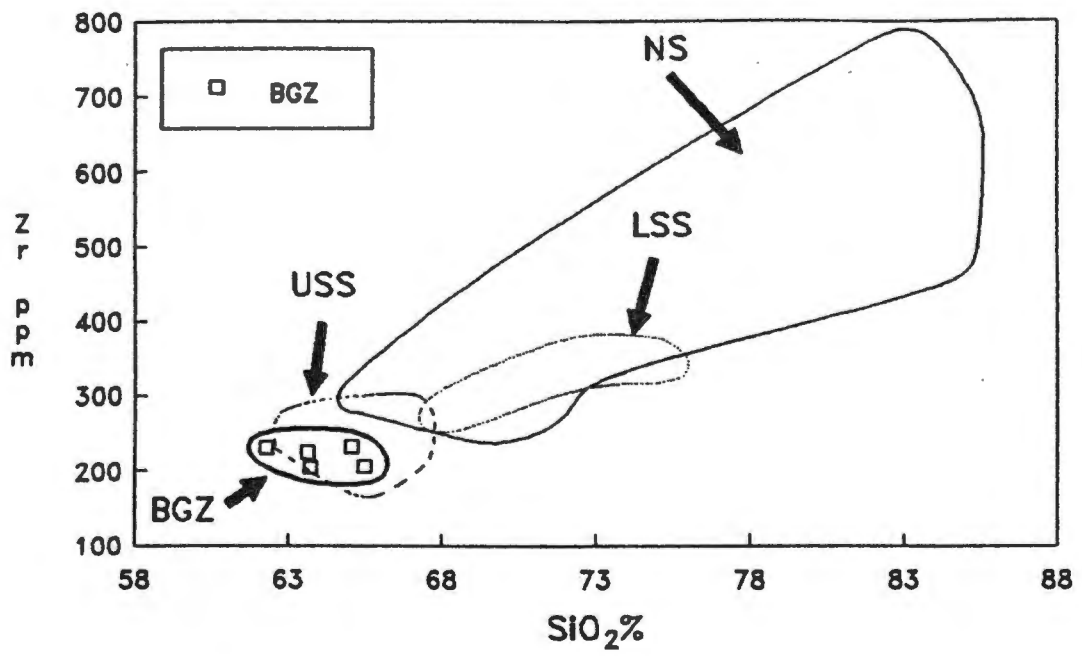


Fig. 6.13 NS, SS and BGZ Zr vs SiO₂ concentrations

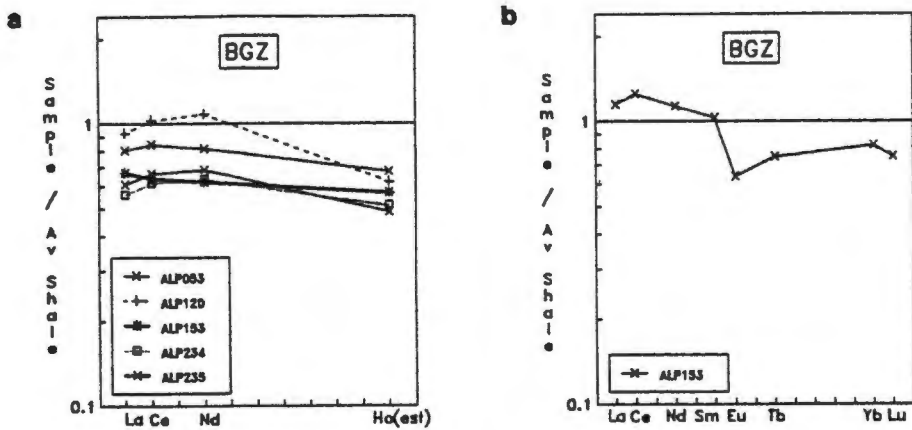


Fig. 6.14 Shale-normalized BGZ REE patterns: (a) XRF data; (b) INAA data

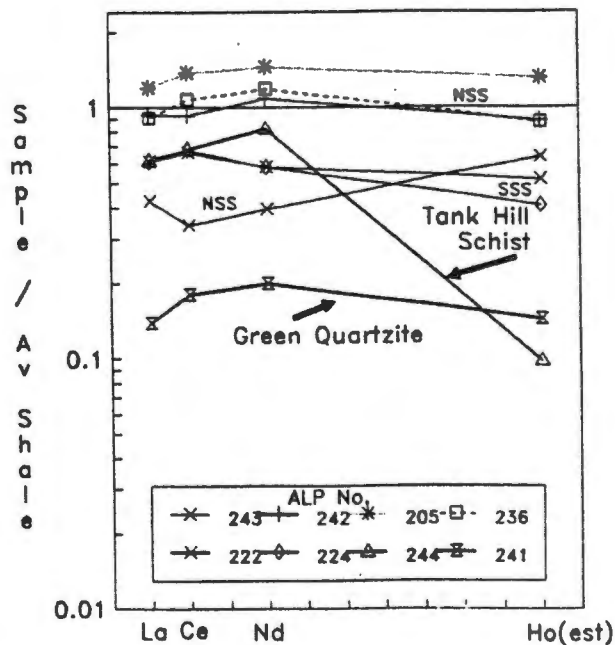


Fig. 6.15 Shale-normalized REE patterns for the Tank Hill rocks using XRF-derived data. Surface NS (NSS) and SS (SSS) are shown for comparison

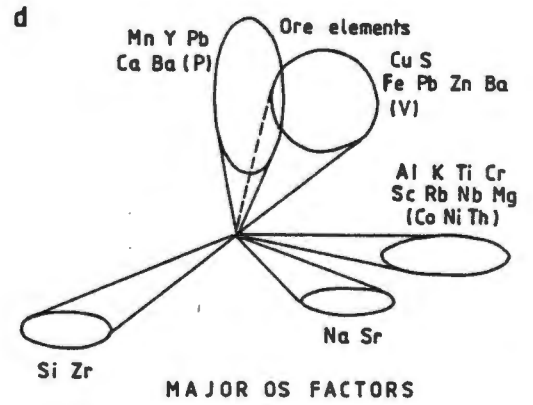
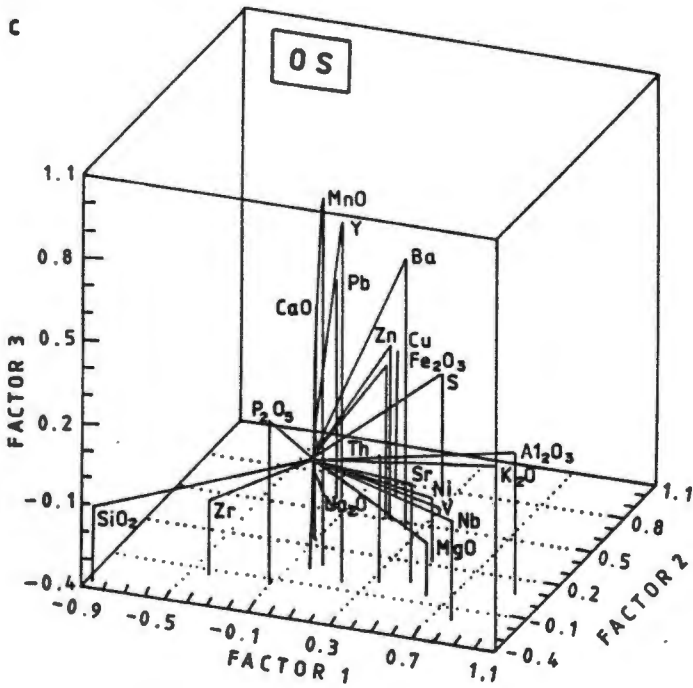
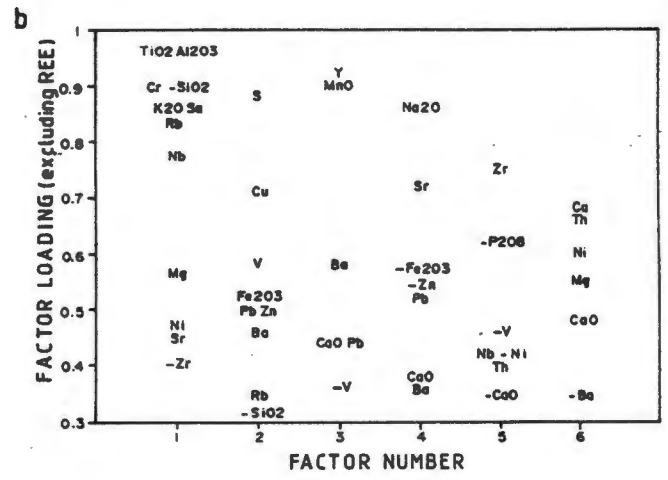
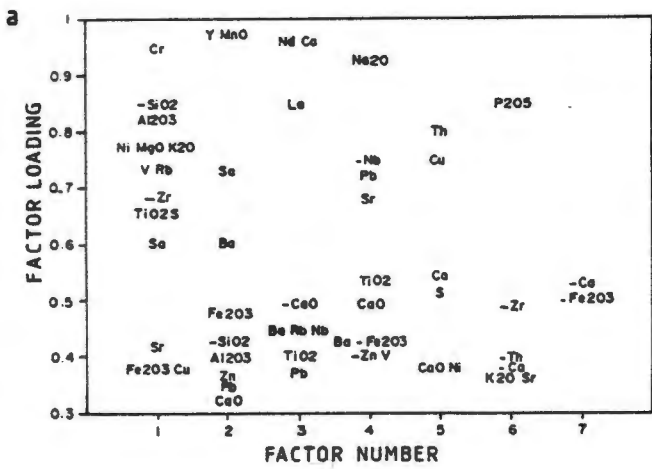


Fig. 6.16 OS factor analysis: (a) including REE, with loadings on the seven factors which cumulatively explain 89.6 % of the variance; (b) excluding REE, with loadings on the 6 factors which cumulatively explain 80.9 % of the variance; (c) geometric representation of Factors 1, 2 and 3 (excluding REE) which account for 52.6 % of the total variance. For purposes of clarity the elements Rb, Cr, Co, Sc and TiO₂ have been omitted as all except Co may be effectively represented by K₂O, as seen in Fig. 6.16 (b) above. Co was omitted because it displays poor correlation with all elements (Table 6.19) and falls in Factor 6 (Fig. 6.16 (b)). The REE's are also omitted in the interests of clarity; (d) 3-D conceptual representation of the major NS factors shown in Fig. 6.16 (c) above

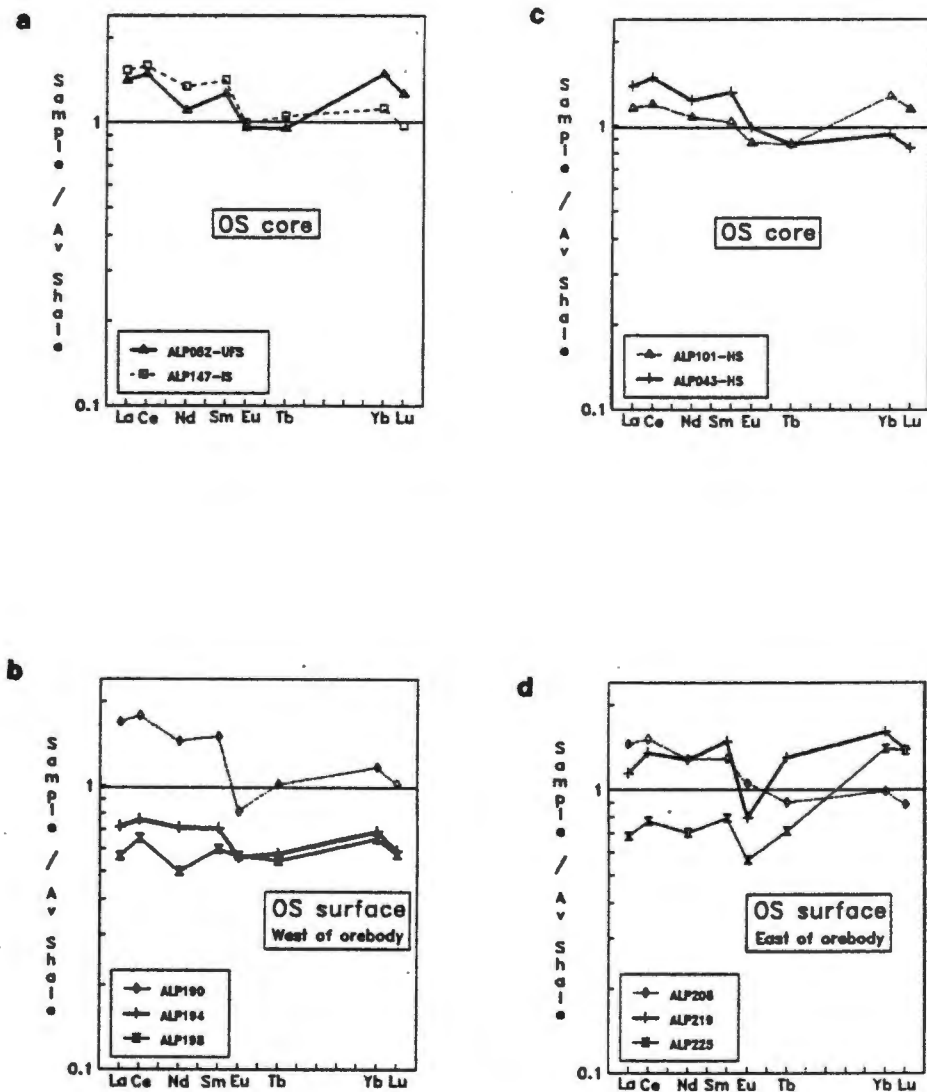


Fig. 6.17 Shale-normalized INAA REE profiles of Ore Schists: (a) UFS (ALP052) and IS (ALP147); (b) HS; (c) OS surface samples west of orebody; (d) OS surface samples east of orebody, with ALP219 and ALP225 from Maanhaarkop

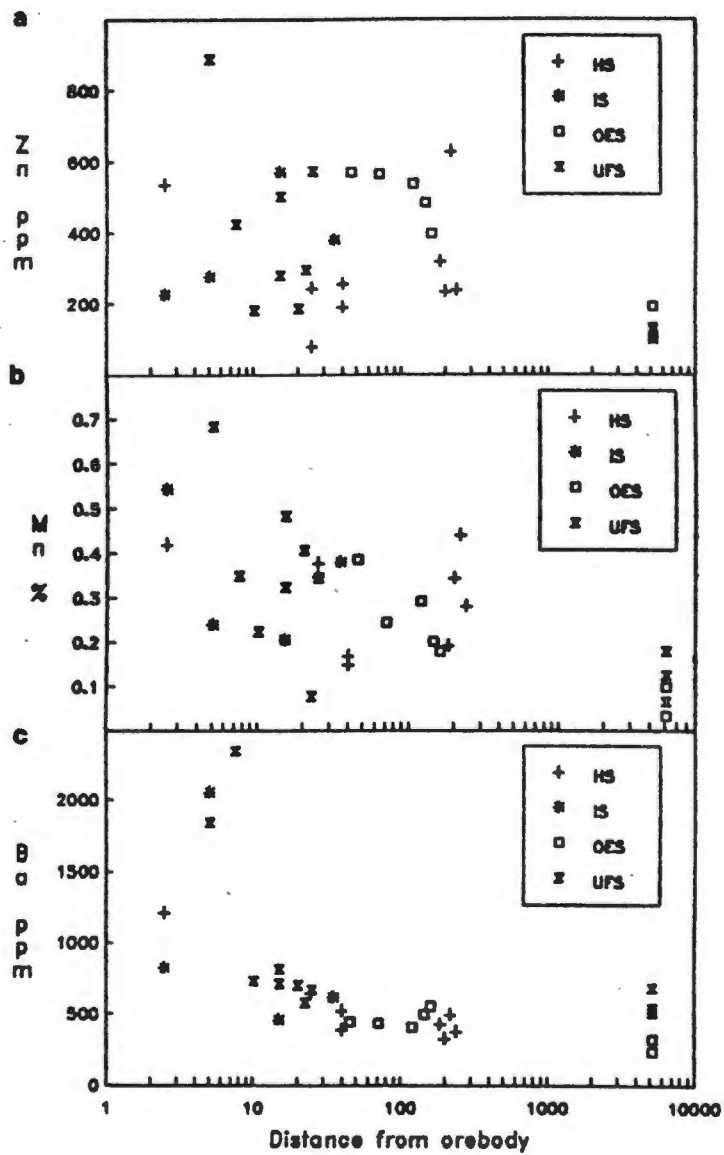


Fig. 6.18 OS borehole core element variations versus distance from the orebody: (a) Zn; (b) Mn; (c) Ba

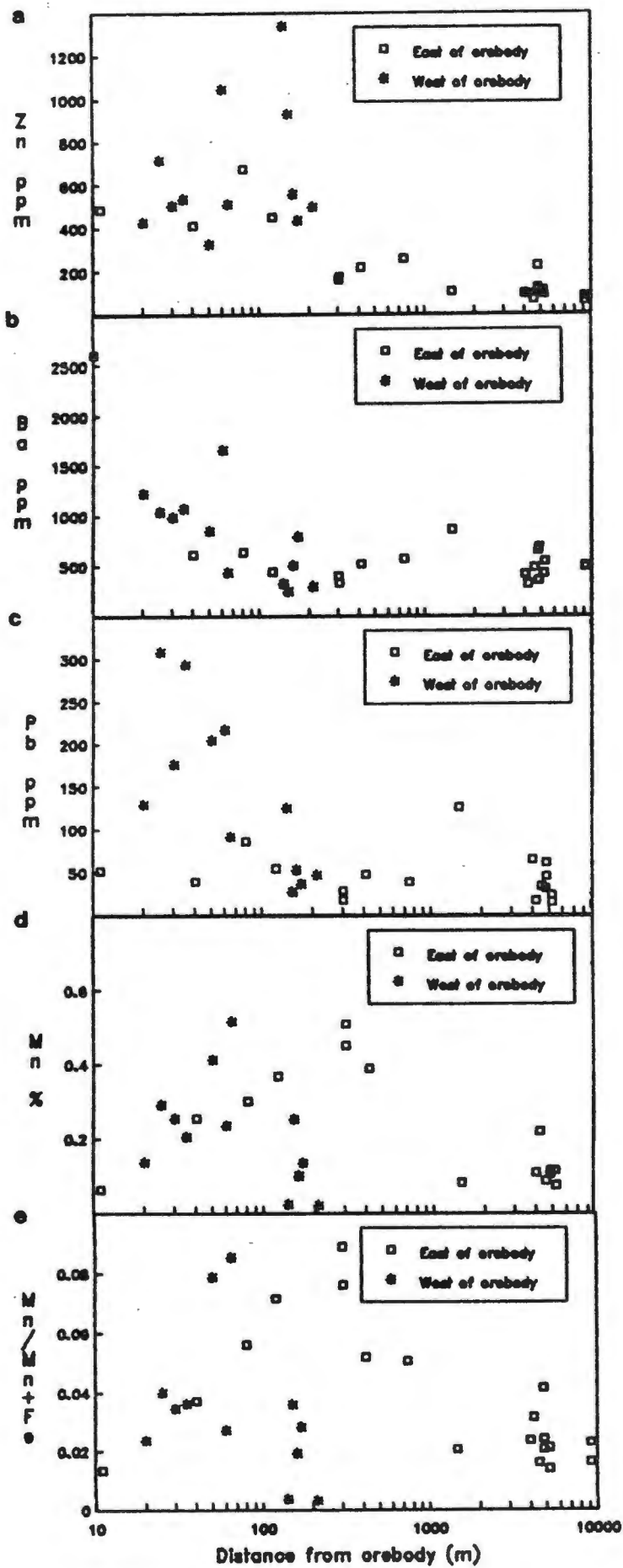


Fig. 6.19 OS surface outcrop element and ratio variations versus distance from the orebody: (a) Zn; (b) Ba; (c) Pb; (d) Mn; (e) Mn/Mn+Fe

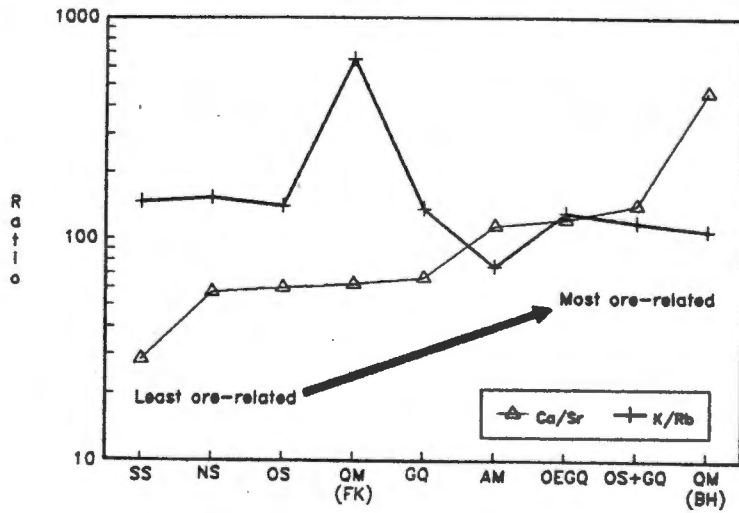


Fig. 6.20 Average K/Rb and Ca/Sr (ppm/ppm) ratios for ore- and non-ore-related rocks

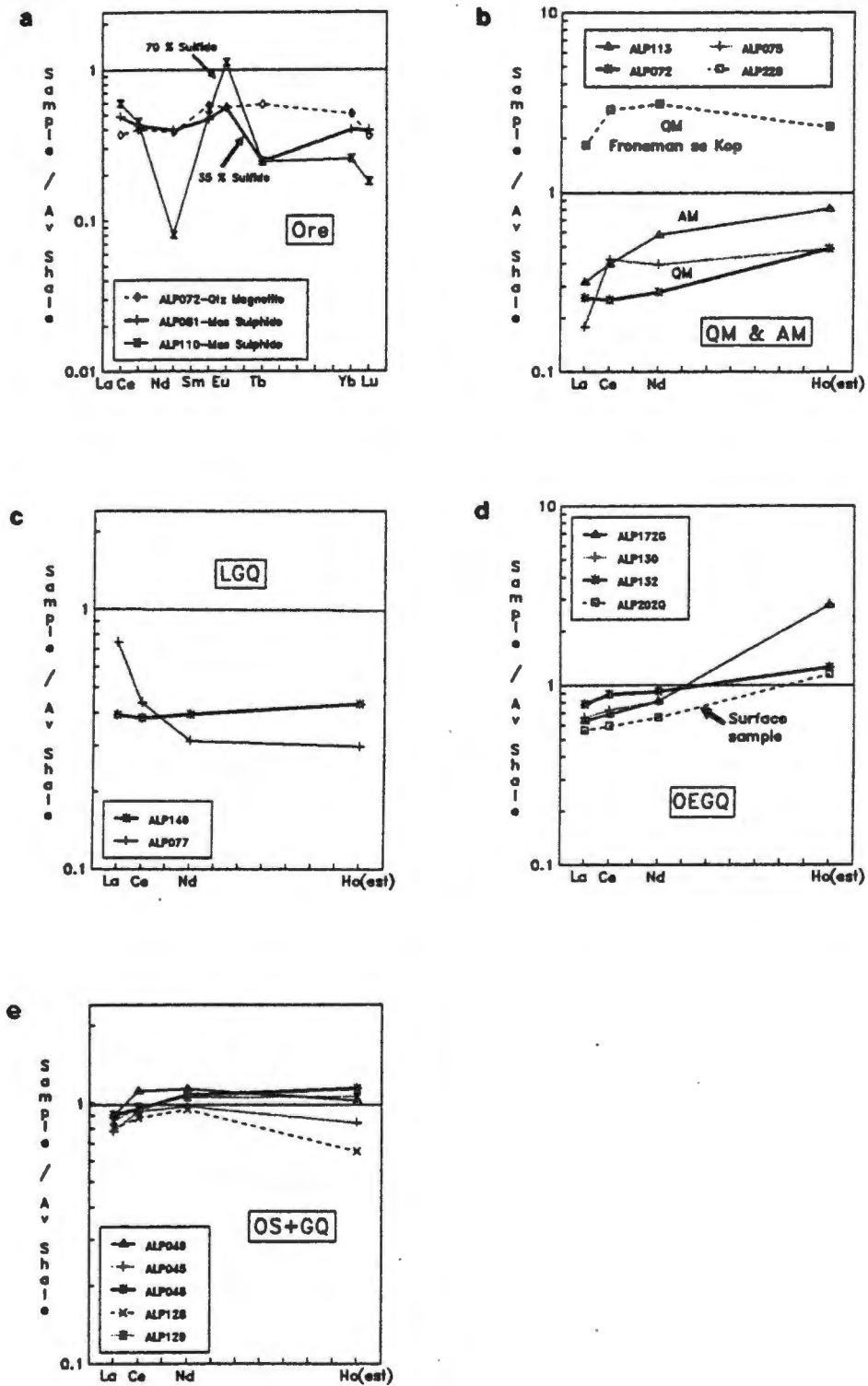


Fig. 6.21 Shale-normalized INAA and XRF REE profiles for various ore-related rocks: (a) Massive Sulphide and Quartz Magnetite Rock from the Broken Hill orebody; (b) Magnetite-rich rocks from the Broken Hill orebody compared with Froneman se Kop Quartz Magnetite Rock; (c) Lower Orebody Garnet Quartzite; (d) Ore Equivalent Garnet Quartzite (ALP130 and ALP132 from Maanhaarkop); (e) Ore Schist plus Garnet Quartzite (ALP128 and ALP129 from Maanhaarkop. INAA data in (a); XRF data in (b) to (e)

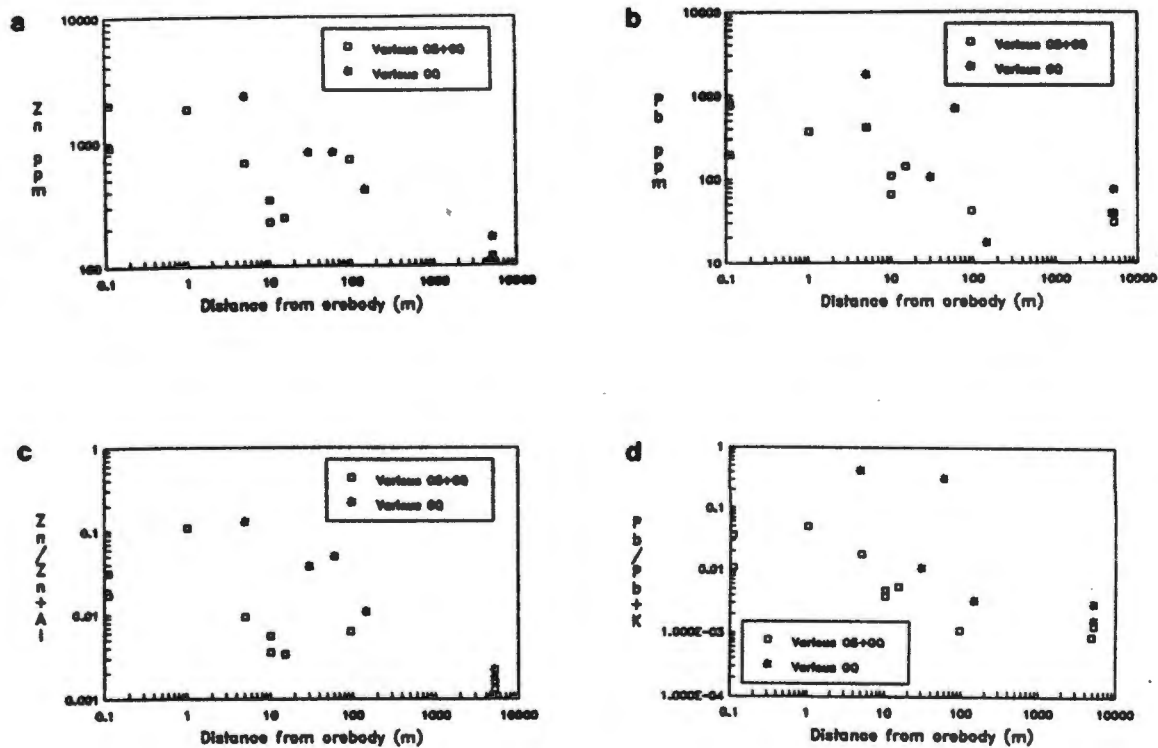


Fig. 6.22 OS+GQ and GQ element and inter-element ratio variations versus distance from the orebody: (a) Zn; (b) Pb; (c) Zn/Zn+Al; (d) Pb/Pb+K

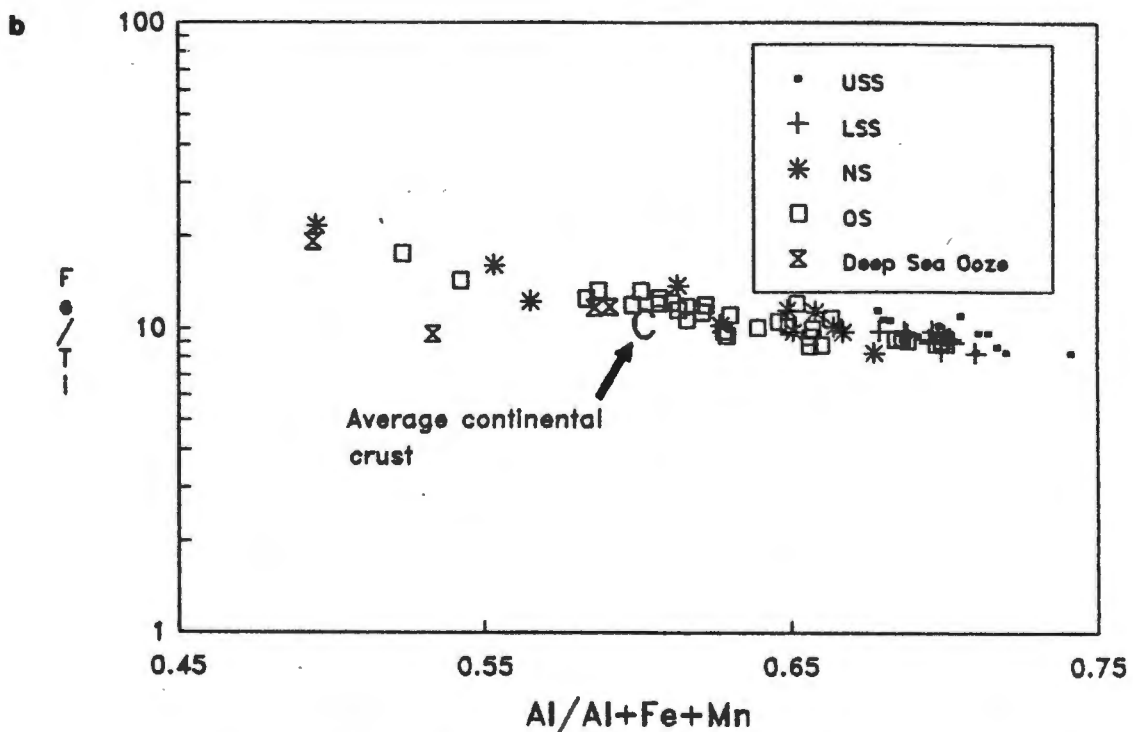
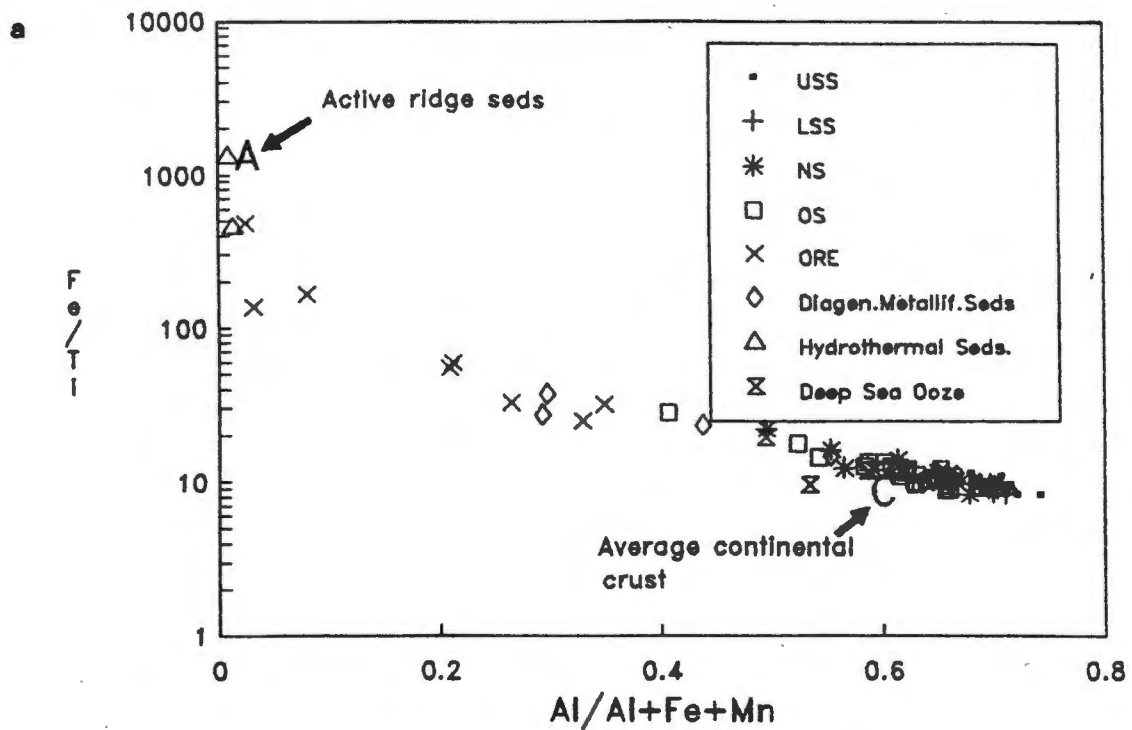


Fig. 6.23 Plot of Fe/Ti vs Al/(Al+Fe+Mn) ratios after Bostrom (1973). All data other than Aggeney's samples from Marchig et al. (1982). (b) is an enlargement of the area in (a) centered on average crust

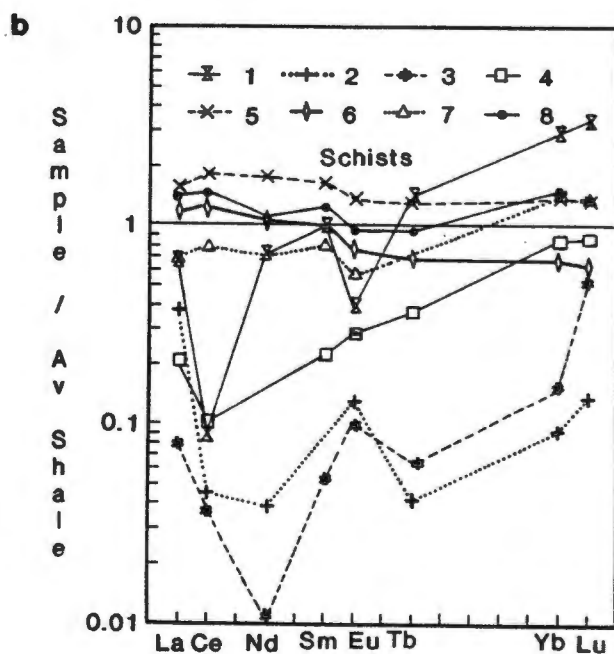
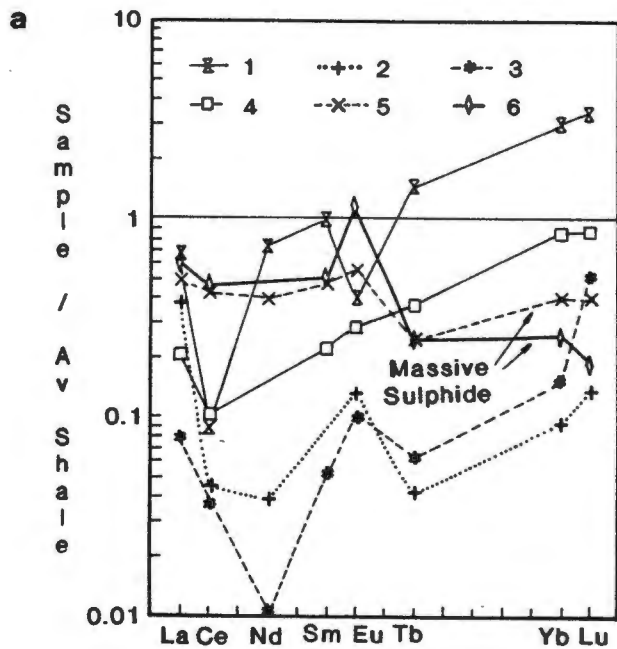


Fig. 6.24 Shale-normalized INAA and XRF REE profiles for various ore-related rocks at Aggeney's compared with metalliferous hydrothermal sediments from the Santorini caldera (1), Atlantis II Deep (2), Galapagos islands (3) and nontronite encrusting basalt on the Juan de Fuca Ridge (4). Comparisons are (a) massive sulphide (5 = ALP081, 6 = ALP110); (b) schists (5 = NS, ALP030; 6 = SS, ALP057; 7 = OS, ALP225; 8 = OS, ALP052). Profiles 1, 2 and 3 from Fleet (1984); profile 4 from Murnane and Clague (1983, sample 11b).

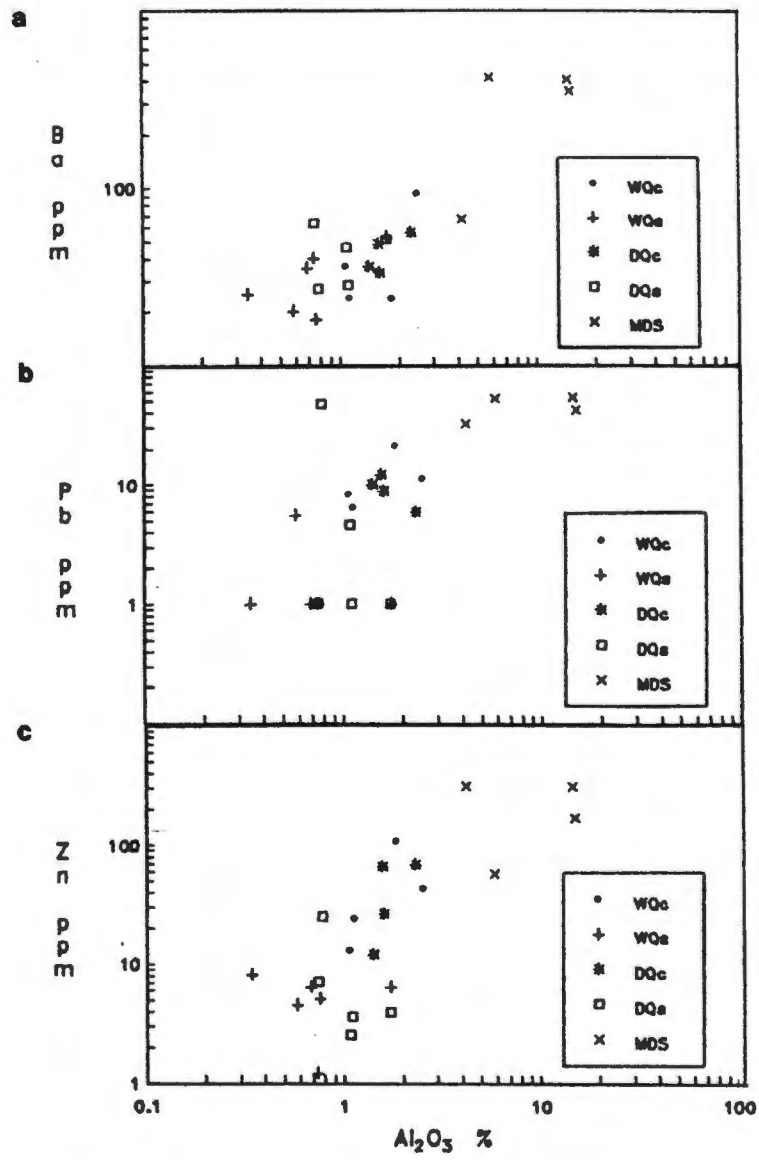


Fig. 6.25 BQ element variations vs Al_2O_3 : (a) Ba; (b) Pb; (c) Zn

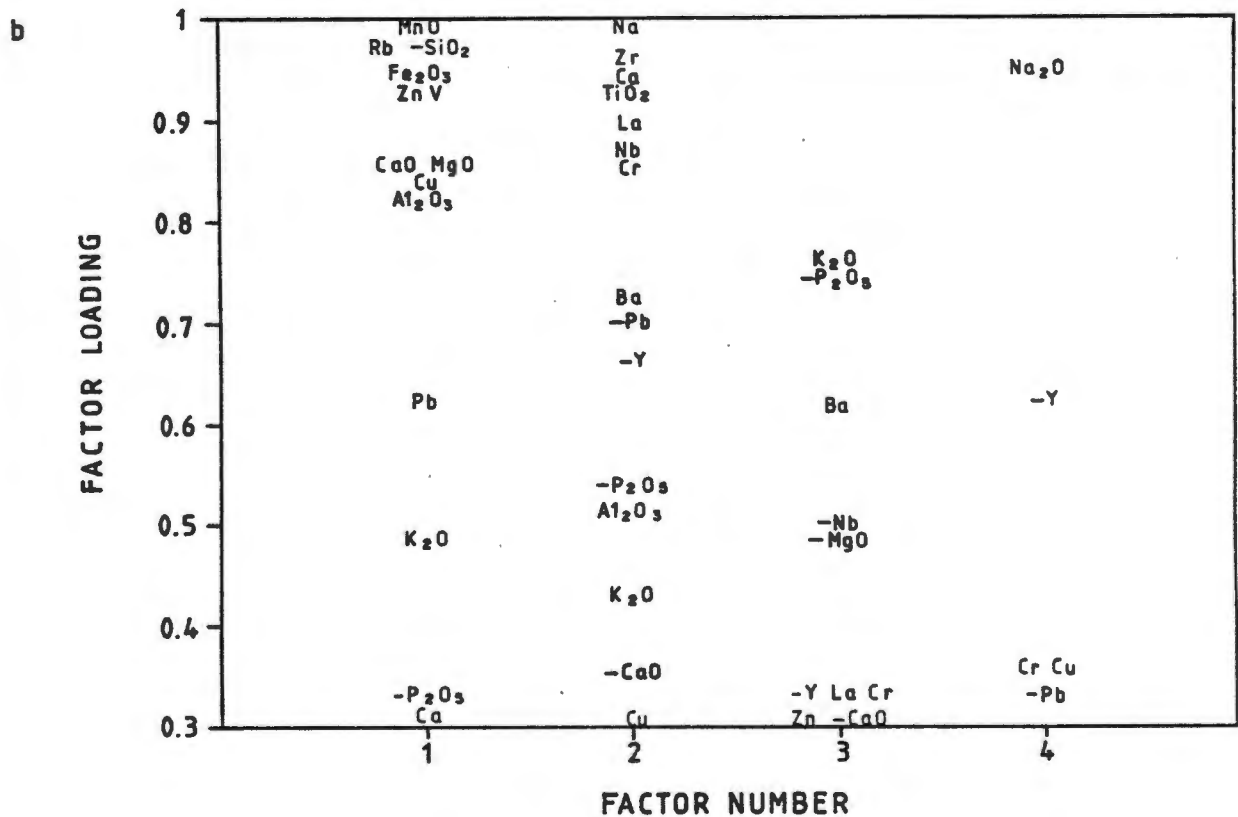
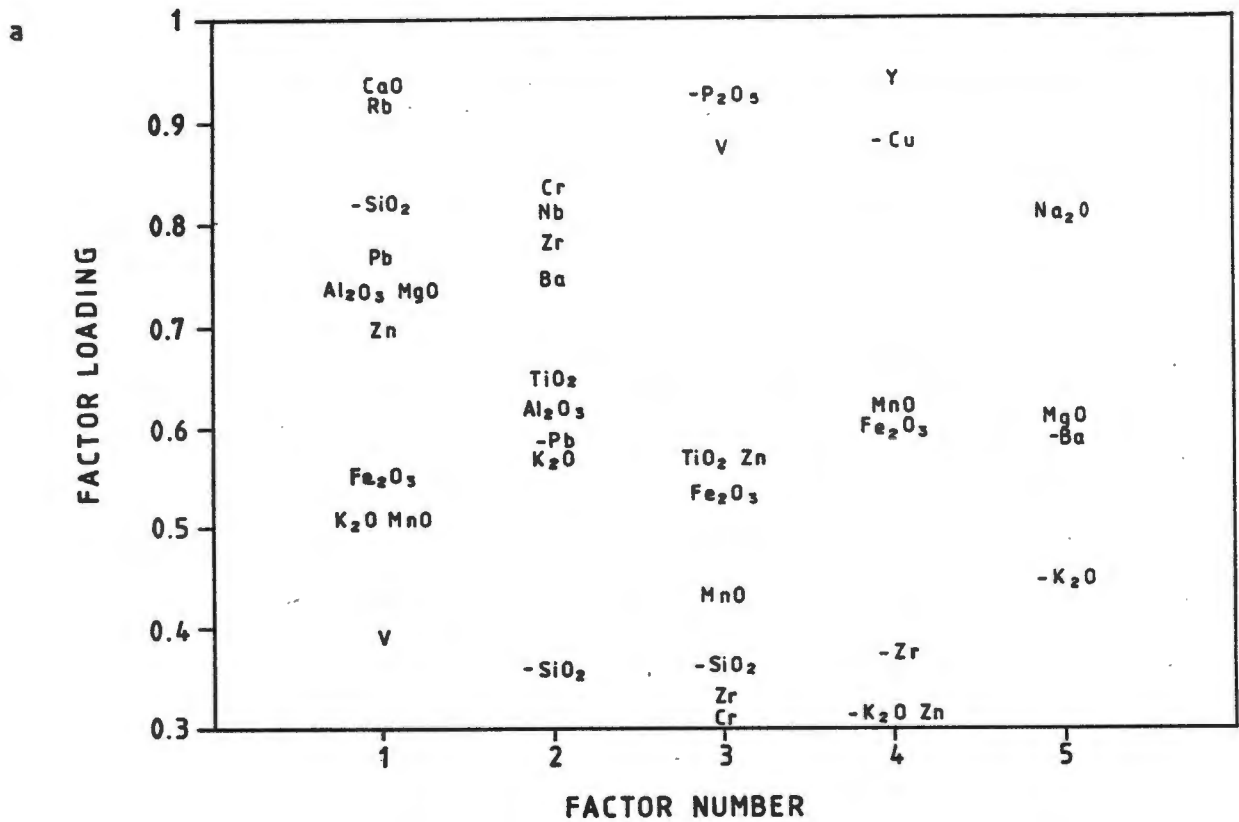


Fig. 6.26 Combined factor analysis for WQ and DQ: (a) excluding REE, with loadings on the five factors which cumulatively explain 92,2 % of the variance; (b) including REE with loadings on the four factors which cumulatively explain 100 % of the variance

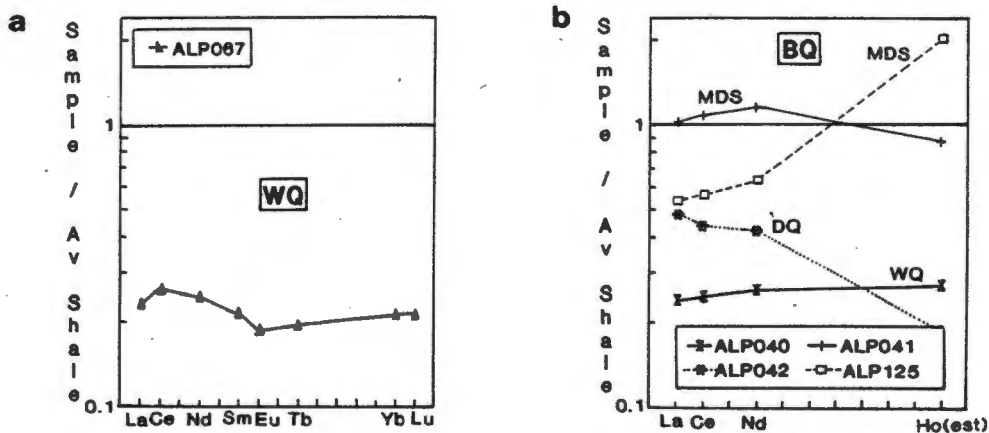


Fig. 6.27 Shale-normalized BQ REE patterns: (a) INAA analysis for a WQ sample; (b) XRF analyses of WQ (ALP040), DQ (ALP042) and MDS (ALP041) from borehole BH123, and MDS from Maanhaarkop (ALP125)

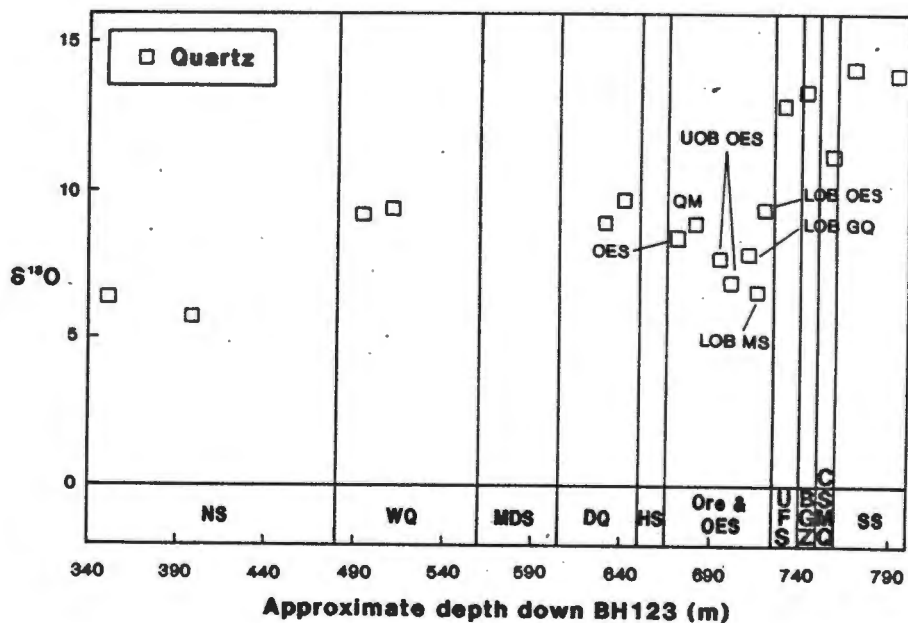


Fig. 6.28 $S^{18}O$ (SMOW) ratios of quartz grains from different parts of the structural succession. Most samples come from borehole BH123 hence all samples have been fitted into their approximate positions within the borehole lithological column. Within the Ore and Equivalent Horizons the following infrequently used abbreviations are: UOB = Upper Orebody; LOB = Lower Orebody; QM = Quartz Magnetite; MS = Massive Sulphide

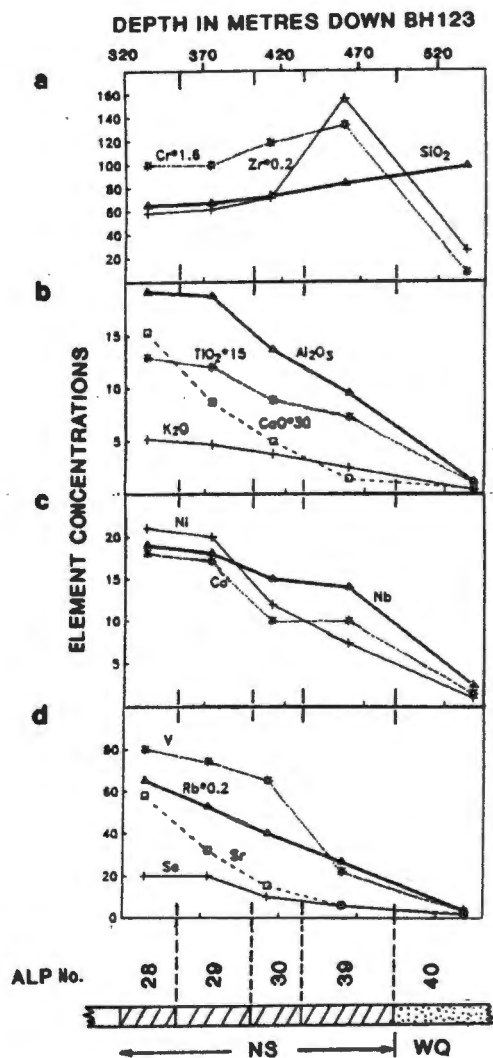


Fig. 6.29 NS element variations down borehole BH123: (a) SiO_2 , Cr and Zr; (b) Al_2O_3 , K_2O , TiO_2 and CaO ; (c) Ni, Nb and Co; (d) V, Rb, Sr and Sc. All elements reported in ppm except SiO_2 , Al_2O_3 , K_2O , TiO_2 and CaO which are in percent. X-axis represents depth in metres down the borehole. Sample numbers and rock types are shown. Zr and Cr are the only elements which do not grade smoothly across the NS-WQ boundary

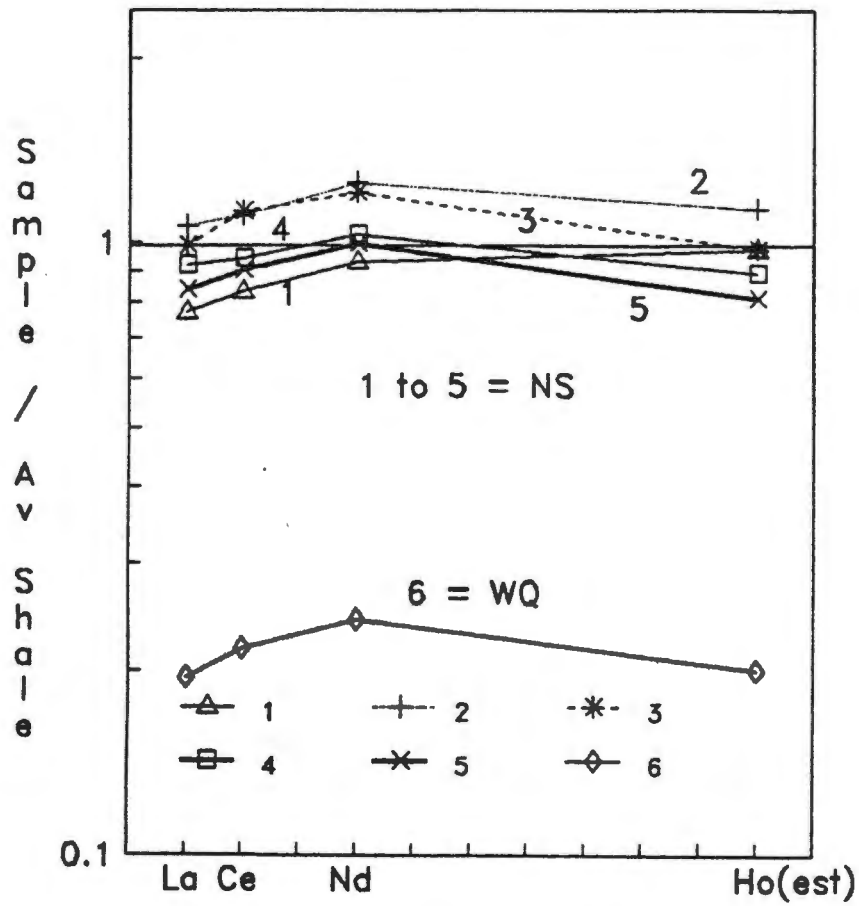


Fig. 6.30 Shale-normalized XRF-derived REE analyses from borehole BH166. Samples 1 to 5 of NS are taken progressively nearer WQ (sample 6).

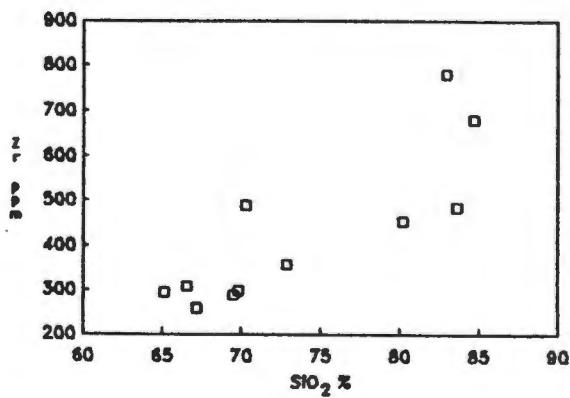


Fig. 6.31 NS Zr vs SiO₂ concentrations

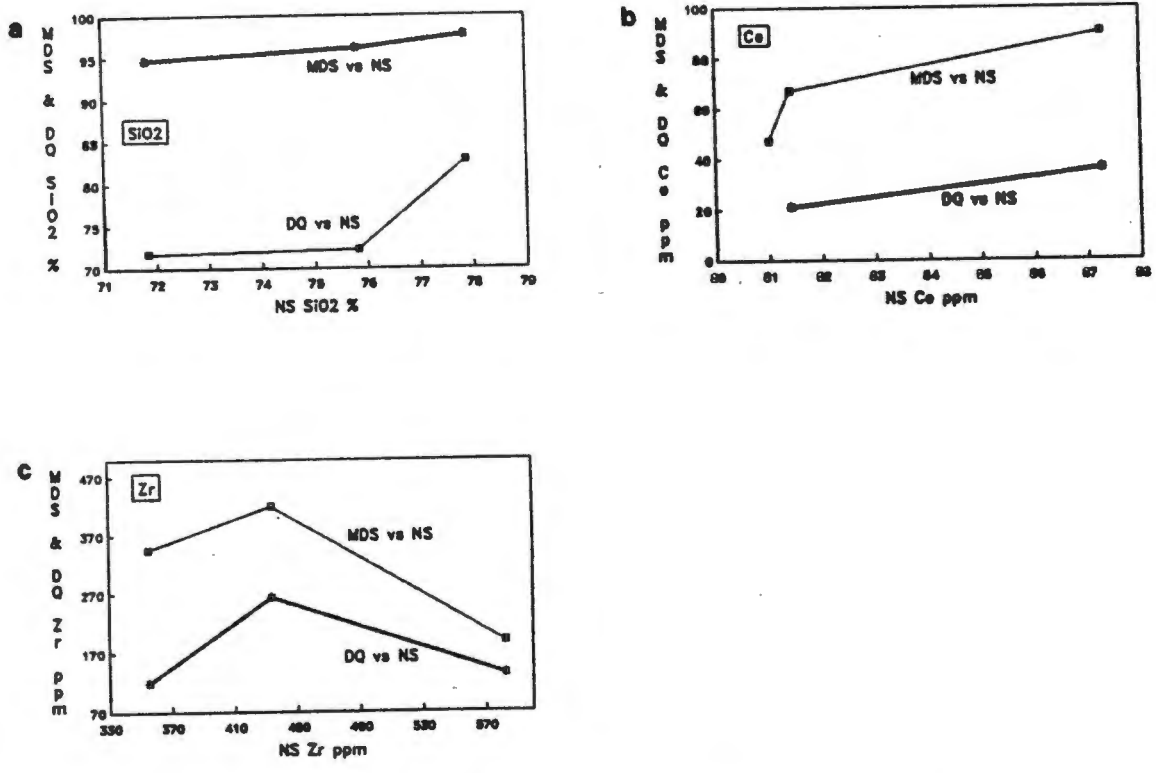


Fig. 6.32 Plots of average element concentrations of NS against MDS and DQ for each of three boreholes: (a) SiO₂; (b) Ce; (c) Zr

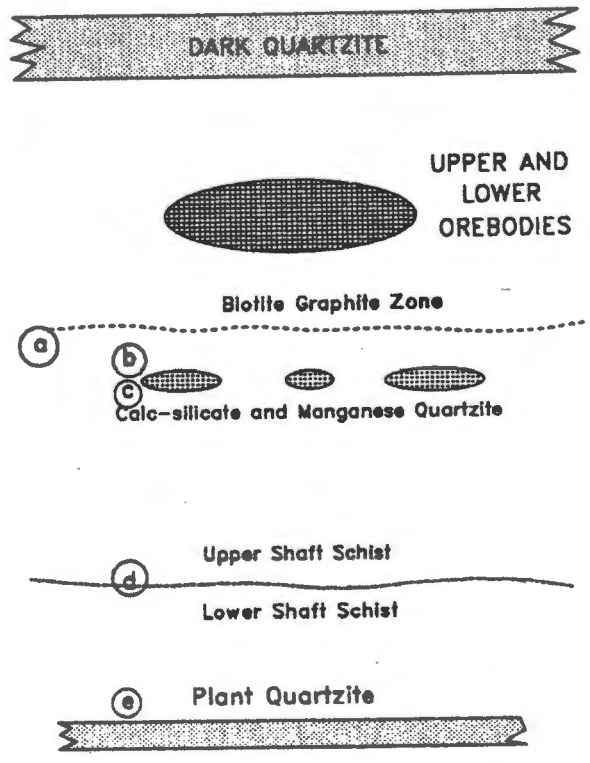


Fig. 6.33 Zones over which geochemical transitions are considered in SS. Zones a. to e. referred to in the text are highlighted.

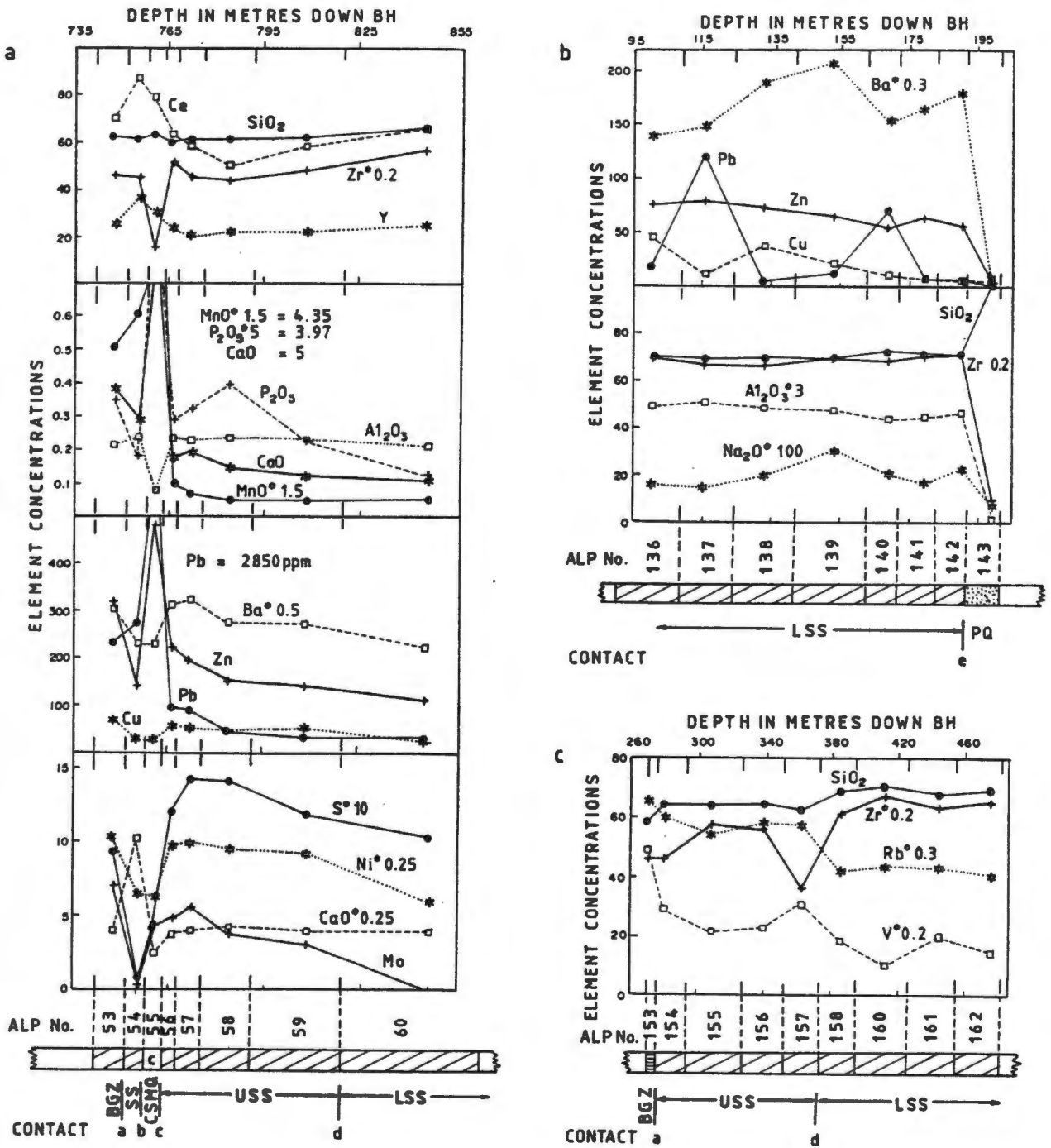


Fig. 6.34 SS element variations down boreholes. Elements in percent are SiO₂, MnO, Na₂O, CaO, Al₂O₃, P₂O₅ and S. All other elements in ppm. X-axis represents depth in metres down the sub-vertical borehole. Sample numbers, rock types and contacts referred to in the text, are shown. Boreholes are (a) BH123; (b) BH156; (c) BH164

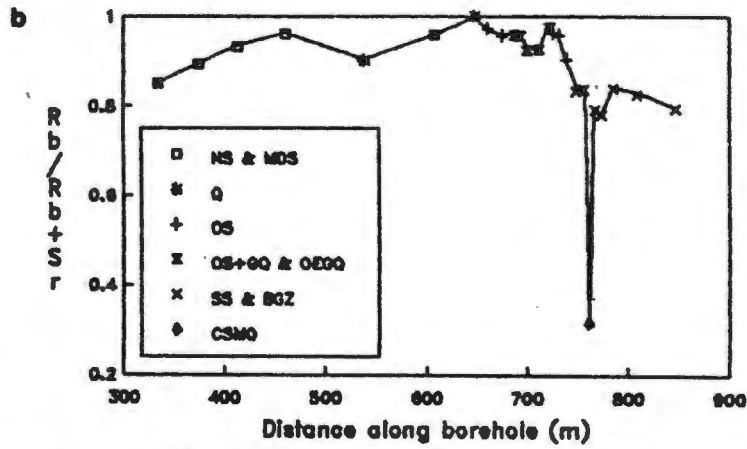
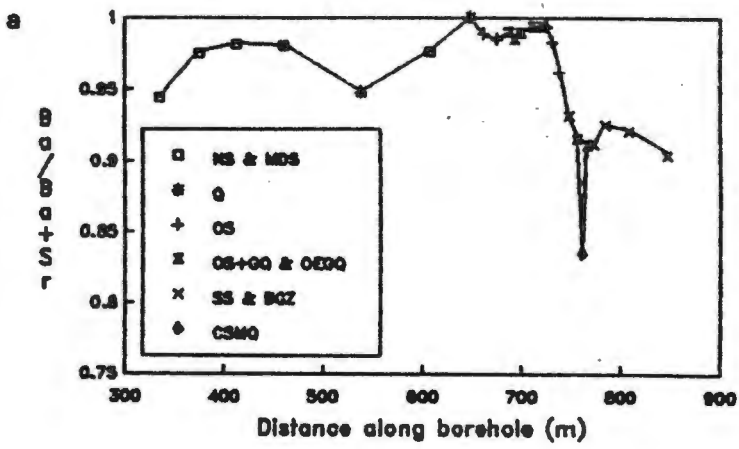


Fig. 6.35 Inter-element ratios versus distance down borehole BH123: (a) Ba/Ba+Sr; (b) Rb/Rb+Sr

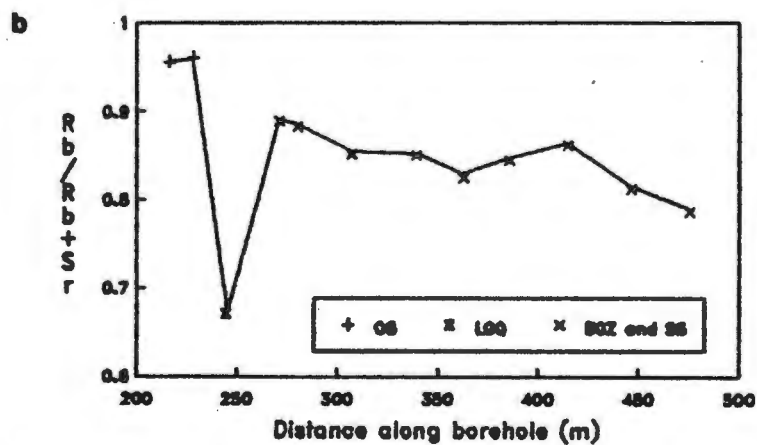
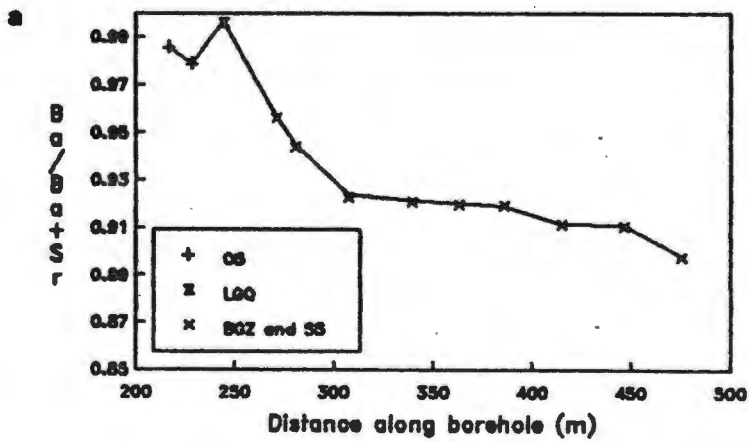


Fig. 6.36 Inter-element ratios versus distance down borehole BH156: (a) Ba/Ba+Sr; (b) Rb/Rb+Sr

Table 6.1 Percentage pegmatite in zones of homogeneous schist

Zone	ALP No.	Rock type	Sample width (m)	LOI %	SiO ₂ %	Pegmatite %
1	51	UFS	7.7	1.8	61	15.3
	52	UFS	7.3	1.8	62	15.1
	54	SS	3.8	2.7	62	15
	56	SS	4.03 12.03	4.8	60	10.4 Wt.ed avg.
	57	SS	8	4.9	61	16.9 = 14.7
	58	SS	16	4.9	61	13.9
	59	SS	32	5.1	62	13.8
2	136	SS	16	3.5	70	13.5
	137	SS	14.8	3.9	69	8.5
	139	SS	20.85	4.1	69	5.9
	140	SS	10.4	3.3	72	13.8
	141	SS	11	3.3	72	12.3
3	154	SS	15.9	4.1	64	7.2
	155	SS	37.7	4.1	64	12.6
	156	SS	21.5	3.7	64	16.1
	157	SS	24.6	3.7	64	13.1
4	158	SS	21.12	3.9	69	10.5
	160	SS	26.85	3.4	71	23.1 or 7.5
	161	SS	27.69	4.1	68	11.2

Table 6.2 Host rock element enrichments and depletions resulting from pegmatites extraction

	Pegmatite has HIGHER, and host rock has LOWER concentrations of the elements shown below			Pegmatite has LOWER, and host rock has HIGHER concentrations of the elements shown below			Pegmatite and host rock have SIMILAR COMPOSITION for elements shown below. Difference between host rock and pegmatite concentrations is:					
	5-10%	10-15%	>15%	-5% to -10%	-10% to -15%	<-15%	<5% and >-5%					
NS av.	Ba Sr Pb		Na	Ti Mg Nb Sc Zn Y	Fe Th Cr Ni Cu	Mn Zr V Co S			Si K Rb	Al P U	Ca LOI	
SS av.	P	Ca	Na Sr U Pb Y	Ti Mg Nb Sc Zn	Fe Zr Cr Ni Cu	Mn LOI V Co S			Si Rb	Al Ba	K Th	
OS av.		K	Ca Na P Ba Sr Pb			Fe Zr Ni	Mg Nb Zn	LOI Se Y	Ti Mn Th Cr V Co	Si U S	Al Cu?	Rb

Table 6.3 Ratios between surface outcrop (s) and borehole core (c) element mean concentrations of NS, USS and OS as an indication of effect of surface weathering on element distribution

	NSs/NSc	USSs/USSc	OSs/OSc
SiO ₂	1.05	1.09	1.02
TiO ₂	0.59	1.00	0.90
Al ₂ O ₃	0.72	0.88	0.92
Fe ₂ O ₃	1.15	0.96	1.10
MnO	0.68	1.23	0.85
MgO	0.34	0.65	0.98
CaO	0.63	0.48	1.23
Na ₂ O	1.31	0.43	1.35
K ₂ O	0.92	0.67	0.88
P ₂ O ₅	1.48	1.50	1.31
Rb	0.96	0.97	0.82
Ba	0.59	0.71	0.95
Sr	1.08	0.38	1.37
Th	0.74	1.58	0.97
Zr	0.64	1.51	0.91
Nb	0.69	1.04	0.83
Cr	1.58	0.91	0.85
V	1.06	0.33	0.81
Sc	0.57	0.90	0.94
Ni	0.93	0.80	0.95
Co	0.54	0.77	0.90
Pb	0.78	0.54	0.62
Zn	0.49	0.46	1.07
Cu	0.15	0.42	1.35
S	0.18	0.01	0.10
Y	0.97	0.73	1.07
La	0.93	0.89	0.85
Ce	0.92	0.92	0.83
Nd	0.93	0.79	0.82

Table 6.4 NS and SS average element concentrations and coefficients of variation (S.D./Mean)

	NS			SS (USS + LSS)			Coefficients of variation		USS n = 11		LSS n = 14	
	Mean	S.D.	n	Mean	S.D.	n	NS	SS	Mean	S.D.	Mean	S.D.
	SiO ₂ %	74.697	7.283	11	68.737	3.803	25	0.10	0.06	65.046	1.253	71.625
TiO ₂ %	0.605	0.174	11	0.73	0.059	25	0.29	0.08	0.762	0.051	0.705	0.051
Al ₂ O ₃ %	13.62	4.116	11	18.161	1.756	25	0.30	0.10	19.827	0.549	16.852	1.077
Fe ₂ O ₃ %	6.164	1.879	11	5.86	0.639	25	0.30	0.11	6.376	0.540	5.455	0.313
MnO %	0.143	0.062	11	0.037	0.015	25	0.43	0.41	0.038	0.011	0.036	0.017
MgO %	0.748	0.45	11	1.484	0.314	25	0.60	0.21	1.782	0.133	1.250	0.173
CaO %	0.167	0.133	11	0.143	0.044	25	0.80	0.31	0.159	0.051	0.130	0.031
Na ₂ O %	0.16	0.113	11	0.275	0.09	25	0.71	0.33	0.300	0.095	0.255	0.077
K ₂ O %	3.565	1.091	11	3.793	0.765	25	0.31	0.20	4.551	0.327	3.197	0.332
P ₂ O ₅ %	0.067	0.031	11	0.045	0.016	25	0.46	0.36	0.057	0.014	0.036	0.009
C %	See Note 1. below			0.28	0.26	14		0.93	0.457	0.229	0.092	0.109
Rb ppm	203	64	11	207	24	25	0.32	0.12	230	7.8	189	15
Ba ppm	1254	1314	11	447	111	25	1.05	0.25	552	55	364	57
Sr ppm	21	15	11	36	13	25	0.71	0.36	41	13	32	11
Th ppm	16	3.1	11	16	2.6	25	0.19	0.16	17	2.5	16	2.3
Zr ppm	425	172	11	283	54	25	0.40	0.19	232	30	323	27
Nb ppm	15	3.1	11	15	1.5	25	0.21	0.10	15	1.8	15	1.2
Cr ppm	72	24	11	102	11	25	0.33	0.11	110	10	95	5.6
V ppm	46	22	11	124	65	25	0.48	0.52	183	48	78	26
Se ppm	11	5.5	11	17	2.0	25	0.50	0.12	19	1.2	16	1.4
Ni ppm	12	5.7	11	27	8.0	25	0.48	0.30	34	7.0	22	2.0
Co ppm	11	4.6	11	14	2.6	25	0.42	0.19	16	2.4	12	1.5
Pb ppm	51	37	11	42	38	25	0.73	0.90	59	37	28	32
Zn ppm	194	122	11	116	74	25	0.63	0.64	171	77	72	20
Cu ppm	37	27	11	31	17	25	0.73	0.55	44	11	21	12
S ppm	294	278	11	7011	4295	25	0.95	0.61	10589	2415	4721	3766
Y ppm	35	5.1	11	21.9	3.3	25	0.15	0.15	23	2.6	21	3.1
La ppm	38	4.4	11	26	4.1	25	0.12	0.16	28	3.9	24	3.1
Ce ppm	84	11	11	58	6.7	25	0.13	0.12	61	6.7	56	5.7
Nd ppm	42	5.5	11	25	3.9	25	0.13	0.16	28	2.9	24	3.6
Note: All major elements are calculated volatile free. The volatile content of the original data, uncorrected for oxidation of iron, is listed below												
H ₂ O %	0.29	0.12	11	0.34	0.18	25	0.41	0.53	0.36	0.12	0.33	0.26
LOI %	1.85	0.68	11	4.06	0.64	25	0.37	0.16	4.60	0.43	3.67	0.40

- Notes: 1. C Of the 5 NS samples analysed for C, 3 are < 0.01 %, and the maximum value is 0.05 %. Only 1 of 14 SS samples analysed has C < 0.01 %.
2. U Only 2 NS samples have U concentrations > LLD, with a maximum of 5.1 ppm. 6 of the SS samples have U concentrations > LLD, with a maximum of 6 ppm.
3. Mo 6 of 7 NS samples analysed for Mo have concentrations < LLD. 15 of the 18 SS samples analysed for Mo are > LLD. The maximum value is 5.6 ppm.

Table 6.5 SS element concentrations relative to NS

SS/NS†			
Element more concentrated in SS		Element less concentrated in SS	
TiO2	= 1.21	SiO2	= 0.92
Al2O3	= 1.33	Fe2O3	= 0.95
MgO	= 1.98	MnO	= 0.26 *
Na2O	= 1.72	CaO	= 0.86
K2O	= 1.06	P2O5	= 0.67
H2O	= 1.17		
LOI	= 2.19 *		
Rb	= 1.02	Ba	= 0.36 *
Sr	= 1.71	Zr	= 0.67
U	=	Nb	= 1
Th	= 1	Pb	= 0.82
Cr	= 1.42	Zn	= 0.6
V	= 2.7 *	Cu	= 0.84
Sc	= 1.55	Y	= 0.63
Ni	= 2.25 *	La	= 0.68
Co	= 1.27	Ce	= 0.69
S	= 23.85 @	Nd	= 0.6
Mo			

Codes: † (Mean SS)/(Mean NS)

* More than 2x concentration (or < 0.5x concentration)

@ More than 5x concentration (or < 0.2x concentration)

Table 6.6 Tests for normality and tests for equality of means for the rock-types NS and SS

	Chi-Squared tests for Normality (on log(10) transformed data)						t-Test for difference between Means (on log(10) transformed data)		
	NS			SS			NS vs SS		
	Chi-Sq statistic	95% C.L.	80% C.L.	Chi-Sq statistic	95% C.L.	80% C.L.	t statistic	95% Confidence levels	99%
SiO2	7.18			8.60		Not	2.58	Different	Same
TiO2	5.73			2.84			-2.44	Different	Same
Al2O3	7.18			8.60		Not	-3.30	Different	Different
Fe2O3	8.64		Not	6.68			0.03	Same	Same
MnO	1.36			29.72	Not	Not	7.17	Different	Different
MgO	4.27			6.04			-4.86	Different	Different
CaO	2.82			9.24		Not	-0.27	Same	Same
Na2O	5.73			4.76			-3.52	Different	Different
K2O	8.64		Not	15.64	Not	Not	-0.84	Same	Same
P2O5	5.73			6.68			1.63	Same	Same
Rb	4.27			11.16	Not	Not	-0.56	Same	Same
Ba	4.27			4.76			2.63	Different	Same
Sr	5.73			6.68			-3.09	Different	Different
Th	11.55	Not	Not	6.68			-0.85	Same	Same
Zr	11.55	Not	Not	9.88		Not	3.00	Different	Different
Nb	10.09		Not	22.04	Not	Not	0.11	Same	Same
Cr	13.00	Not	Not	2.84			-3.97	Different	Different
V	5.73			7.32		Not	-4.97	Different	Different
Se	4.27			18.84	Not	Not	-3.56	Different	Different
Ni	2.82			20.76	Not	Not	-5.42	Different	Different
Co	4.27			7.96		Not	-2.33	Different	Same
Pb	4.27			4.12			1.83	Same	Same
Zn	1.36			5.40			1.76	Same	Same
Cu	2.82			22.68	Not	Not	0.07	Same	Same
S	8.64		Not	34.20	Not	Not	-8.63	Different	Different
Y	1.36			4.76			8.95	Different	Different
La	2.82			4.68			8.42	Different	Different
Ce	5.73			9.74		Not	8.00	Different	Different
Nd	4.27			3.84			9.92	Different	Different

Codes: Same = Same Means

Not = Not Normally distributed

Different = Different Means

Blanks indicate that distribution has passed the test for Normality

Data set sizes:

NS n = 11

SS n = 25

Notes:

1. Chi-Squared statistic calculated as shown by Le Maitre (1982, pp26-28) and tested against values in Le Maitre (1982, Table A5).
2. Both Cu and S in SS are more nearly Normally distributed than Log Normally. For a Normal distribution, Chi-Sq. Cu = 7.32, and S = 11.8, i.e. S is still not acceptably normally distributed.
3. The very high MnO Chi-Squared statistic in SS is caused by a concentration of results in the central cell.
4. t-Statistic (separate) and degrees of freedom are taken from BMDP P3D output.
5. t-Statistic is tested against values in Le Maitre (1982, Table A3).

Table 6.7 NS correlation matrix

	Si	Zr	Y	P	Cu	Pb	Zn	S	Ba	Fe	Mn	K	Rb	Al	Ti	Nb	Sc	Ni	Mg	V	Co	Cr	Th	Ca	Na	Sr	La	Ce	Nd	
Si	1																													
Zr	3	1																												
Y	3	*	1																											
P	-3	-2	*	1																										
Cu				*	1																									
Pb					*	1																								
Zn						*	1																							
S							*	1																						
Ba								*	1																					
Fe									*	1																				
Mn										*	1																			
K											*	1																		
Rb												*	1																	
Al													*	1																
Ti														*	1															
Nb															*	1														
Sc																*	1													
Ni																		*	1											
Mg																			*	1										
V																				*	1									
Co																					*	1								
Cr																						*	1							
Th																							*	1						
Ca																								*	1					
Na																									*	1				
Sr																										*	1			
La																											*	1		
Ce																												*	1	
Nd																													*	1

Pearson product-moment correlation matrix performed on log (10) transformed data
n = 11

Codes:

Si = SiO2
Ti = TiO2
Al = Al2O3
Fe = Fe2O3
Mn = MnO
Mg = MgO
Ca = CaO
Na = Na2O
K = K2O
P = P2O5

Blank = r < 0.521
1 = r > 0.521
2 = r > 0.602
3 = r > 0.735
4 = r > 0.847
- =

Correlation not significant at the 90 % confidence limit
Correlation significant at the 90 % confidence limit
Correlation significant at the 95 % confidence limit
Correlation significant at the 99 % confidence limit
Correlation significant at the 99.8 % confidence limit
Negative correlation

Table 6.8 SS correlation matrix

Si	Zr	Y	P	Cu	Pb	Zn	S	Ba	Fe	Mn	K	Rb	Al	Ti	Nb	Se	Ni	Mg	V	Co	Cr	Th	Ca	Na	Sr	La	Ce	Nd	C
Si	4	-1	-3	-4	-2	-4	-4	-4	-4	-4	-4	-4	-4	-4	-4	-4	-4	-4	-4	-4	-4	-3	-2	-3	-3	-1	-3	-4	Si
Zr	4	*	-1	-4	-4	-4	-4	-4	-4	-4	-4	-4	-4	-4	-1	-4	-4	-4	-4	-4	-4	-3	-2	-2	-3	-3	-3	-3	Zr
Y	-1	-1	*																			2							Y
P	-3	-4		*																									P
Cu	-4	-4		2	*																								Cu
Pb	-4	-4		2	3	*																							Pb
Zn	-4	-4		2	3	4	*																						Zn
S	-4	-4		-1	3	3		*																					S
Ba	-4	-4		1	3	4		2	*																				Ba
Fe	-4	-4		2	3	4		3	4	*																			Fe
Mn	-4	-4		2	3	4		3	4		*																		Mn
K	-4	-4		1	3	4		3	4		2	*																	K
Rb	-4	-4		1	3	4		3	4		4	*																	Rb
Al	-4	-4		1	3	4		3	4		4	4	*																Al
Ti	-4	-4		1	3	4		3	4		4	4	4	*															Ti
Nb	-4	-4		1	3	4		3	4		4	4	4	3	*														Nb
Se	-4	-4		1	3	4		3	4		4	4	4	4	2	*													Se
Ni	-4	-4		1	3	4		3	4		4	4	4	4	4	4	*												Ni
Mg	-4	-4		1	3	4		3	4		4	4	4	4	4	4	4	*											Mg
V	-4	-4		1	3	4		3	4		4	4	4	4	4	4	4	4	*										V
Co	-4	-4		1	3	4		3	4		4	4	4	4	4	4	4	4	4	*									Co
Cr	-4	-4		1	3	4		3	4		4	4	4	4	4	4	4	4	4	4	*								Cr
Th	-4	-4		1	3	4		3	4		4	4	4	4	4	4	4	4	4	4	4	*							Th
Ca	-4	-4		1	3	4		3	4		4	4	4	4	4	4	4	4	4	4	4	4	*						Ca
Na	-4	-4		1	3	4		3	4		4	4	4	4	4	4	4	4	4	4	4	4	4	*					Na
Sr	-4	-4		1	3	4		3	4		4	4	4	4	4	4	4	4	4	4	4	4	4	4	*				Sr
La	-4	-4		1	3	4		3	4		4	4	4	4	4	4	4	4	4	4	4	4	4	4	4	*			La
Ce	-4	-4		1	3	4		3	4		4	4	4	4	4	4	4	4	4	4	4	4	4	4	4	4	*		Ce
Nd	-4	-4		1	3	4		3	4		4	4	4	4	4	4	4	4	4	4	4	4	4	4	4	4	4	4	Nd
C	-4	-4		1	3	4		3	4		4	4	4	4	4	4	4	4	4	4	4	4	4	4	4	4	4	4	C

Pearson product-moment correlation matrix performed on log (10) transformed data
 n = 23 For C, n = 13

Codes:

- Si = SiO2
- Ti = TiO2
- Al = Al2O3
- Fe = Fe2O3
- Mn = MnO
- Mg = MgO
- Ca = CaO
- Na = Na2O
- K = K2O
- P = P2O5

- For n = 23
- Blank = r < 0.352
- 1 = r > 0.352
- 2 = r > 0.413
- 3 = r > 0.526
- 4 = r > 0.640
- =

Correlation not significant at the 90 % confidence limit
 Correlation significant at the 90 % confidence limit
 Correlation significant at the 95 % confidence limit
 Correlation significant at the 99 % confidence limit
 Correlation significant at the 99.8 % confidence limit
 Negative correlation

- For n = 13
- Blank = r < 0.476
- 1 = r > 0.476
- 2 = r > 0.553
- 3 = r > 0.684
- 4 = r > 0.801
- =

Correlation not significant at the 90 % confidence limit
 Correlation significant at the 90 % confidence limit
 Correlation significant at the 95 % confidence limit
 Correlation significant at the 99 % confidence limit
 Correlation significant at the 99.8 % confidence limit
 Negative correlation

Table 6.9 Average coefficients of variation for NS and SS

	USS	LSS	SS total	NS
Major elements (SiO ₂ - P ₂ O ₅)	0.29	0.17	0.33	0.41
Trace elements (Rb - Y)	0.26	0.29	0.35	0.49

Table 6.10 NS and SS factor analysis parameters: (a) variances explained by each factor, and cumulative variances; (b) communalities for each element.

a Variances explained by each factor, and cumulative variances

		Factor 1	Factor 2	Factor 3	Factor 4	Factor 5	Factor 6
NS	% Variance	39.5	13.8	13.1	12.1	9.2	6.1
	Cum. % Va	39.5	53.2	66.3	78.4	87.5	93.6
SS	% Variance	42.6	13.9	12.5	10.5	6.7	
	Cum. % Va	42.6	56.6	69.1	79.5	86.2	

b Communalities for each element

No. of samples included in F.A.	NS 11	SS 23
SiO ₂	1.00	0.98
TiO ₂	0.98	0.91
Al ₂ O ₃	0.98	0.91
Fe ₂ O ₃	0.85	0.73
MnO	0.83	0.88
MgO	0.95	0.95
CaO	0.94	0.84
Na ₂ O	0.94	0.91
K ₂ O	0.99	0.94
P ₂ O ₅	0.99	0.82
Rb	1.00	0.74
Ba	0.96	0.94
Sr	0.98	0.90
Th	0.67	0.63
Zr	0.94	0.95
Nb	0.96	0.68
Cr	0.95	0.96
V	0.97	0.96
Sc	1.00	0.92
Ni	0.97	0.90
Co	0.97	0.85
Pb	0.95	0.90
Zn	0.90	0.92
Cu	0.87	0.65
S	0.87	0.76
Y	0.80	0.71
La	0.97	0.89
Ce	0.99	0.92
Nd	0.98	0.93

The communality for each element represents the sum of the squared factor loadings for each element. If the communality approximates 1, then that element is completely represented by the Factor Analysis.

Table 6.11 CS and MnQ average element concentrations for core and surface samples combined

	CS n = 3 Mean	MnQ n = 4 Mean	USS * n = 11 Mean
SiO2 %	65.099	88.327	65.046
TiO2 %	0.468	0.077	0.762
Al2O3 %	11.165	2.064	19.827
Fe2O3 %	7.099	4.825	6.376
MnO %	1.845	0.705	0.038
MgO %	4.259	0.114	1.782
CaO %	6.859	0.511	0.159
Na2O %	0.471	0.055	0.300
K2O %	1.471	0.142	4.551
P2O5 %	0.306	0.541	0.057
Rb ppm	92	5	230
Ba ppm	1235	63	552
Sr ppm	101	16	41
Th ppm	11	8.7	17
U ppm	6.9	10.5	
Zr ppm	123	23	232
Nb ppm	10.0	3.3	15
Mo ppm	3.4	4.3	
Cr ppm	64	15	110
V ppm	79	33	183
Se ppm	12	1.8	19
Ni ppm	30	10	34
Co ppm	12	13	16
Pb ppm	1987	12087	59
Zn ppm	1611	1079	171
Cu ppm	59	421	44
S ppm	5963	14119	10589
Y ppm	28	11	23
La ppm	40	7.9	28
Ce ppm	73	25	61
Nd ppm	37	11	28

* USS means for comparison

Table 6.12 CS element concentrations relative to USS

CS/USS †			
Element content higher in CS		Element content lower in CS	
SiO ₂ =	1.001	TiO ₂ =	0.614
Fe ₂ O ₃ =	1.113	Al ₂ O ₃ =	0.563
MnO =	48.354 @	K ₂ O =	0.323 *
MgO =	2.390 *		
CaO =	43.221 @		
Na ₂ O =	1.569		
P ₂ O ₅ =	5.383 @		
Ba =	2.239 *	Rb =	0.399 *
Sr =	2.483 *	Th =	0.624
U =		Zr =	0.531
Pb =	33.834 @	Nb =	0.651
Zn =	9.399 @	Cr =	0.582
Cu =	1.341	V =	0.435 *
Y =	1.213	Sc =	0.622
La =	1.413	Ni =	0.871
Ce =	1.207	Co =	0.793
Nd =	1.353	S =	0.563

Codes: † (Mean CS)/(Mean USS)
 * More than 2x concentration (or < 0.5x concentration)
 @ More than 5x concentration (or < 0.2x concentration)

Table 6.13 MnQ element concentrations relative to USS

MnQ/USS †			
Element content higher in MnQ		Element content lower in MnQ	
SiO ₂ =	1.36	TiO ₂ =	0.10 @
MnO =	18.49 @	Al ₂ O ₃ =	0.10 @
CaO =	3.22 †	Fe ₂ O ₃ =	0.76
P ₂ O ₅ =	9.51 @	MgO =	0.06 @
		Na ₂ O =	0.18 @
		K ₂ O =	0.03 @
U		Rb =	0.02 @
Pb =	205.82 @	Ba =	0.11 @
Zn =	6.30 @	Sr =	0.38 †
Cu =	9.57 @	Th =	0.50 †
S =	1.33	Zr =	0.10 @
		Nb =	0.21 †
		Cr =	0.13 @
		V =	0.18 @
		Sc =	0.09 @
		Ni =	0.29 †
		Co =	0.83
		Y =	0.47
		La =	0.28 †
		Ce =	0.41 †
		Nd =	0.38 †

Codes: † (Mean MnQ)/(Mean USS)

* More than 2x concentration (or < 0.5x concentration)

@ More than 5x concentration (or < 0.2x concentration)

Table 6.14 BGZ average element concentrations and standard deviations

		BGZ		USS *	
		n = 5		n = 11	
		Mean	S.D.	Mean	S.D.
SiO ₂	%	64.008	1.139	65.046	1.253
TiO ₂	%	0.796	0.058	0.762	0.051
Al ₂ O ₃	%	20.168	1.445	19.827	0.549
Fe ₂ O ₃	%	7.067	0.596	6.376	0.540
MnO	%	0.186	0.101	0.038	0.011
MgO	%	1.914	0.191	1.782	0.133
CaO	%	0.228	0.093	0.159	0.051
Na ₂ O	%	0.180	0.059	0.300	0.095
K ₂ O	%	4.772	0.257	4.551	0.327
P ₂ O ₅	%	0.080	0.018	0.057	0.014
C	%	0.768	0.357	0.457	0.229
Rb	ppm	251	22	230	7.8
Ba	ppm	649	141	552	55
Sr	ppm	28	13	41	13
Th	ppm	18	3.7	17	2.5
Mo	ppm	5.3	1.2		
Zr	ppm	218	12	232	30
Nb	ppm	16	1.0	15	1.8
Cr	ppm	122	7.7	110	10
V	ppm	239	62	183	48
Se	ppm	19	1.7	19	1.2
Ni	ppm	45	3.8	34	7.0
Co	ppm	19	5.7	16	2.4
Pb	ppm	184	167	59	37
Zn	ppm	636	492	171	77
Cu	ppm	86	50	44	11
S	ppm	6078	3414	10589	2415
Y	ppm	21	2.6	23	2.6
La	ppm	29	5.5	28	3.9
Ce	ppm	63	13	61	6.7
Nd	ppm	29	6.5	28	2.9
Note: All major elements are calculated volatile free. The volatile content of the original data, uncorrected for oxidation of iron, is listed below					
H ₂ O-	%	0.490	0.259	0.359	0.120
LOI	%	4.653	0.458	4.601	0.432

* USS data presented for comparison

- Notes: 1. U Of the five BGZ samples, 3 have detectible U, with a maximum value of 7ppm.
2. Mo All five BGZ samples have detectible Mo, with a maximum value of 7ppm.

Table 6.15 BGZ element concentrations relative to USS: (a) ratios of BGZ/USS on a per element basis; (b) Ca/Sr C/S and K/Na ratios of BGZ and USS

a

BGZ/USS †			
Element content higher in BGZ		Element content lower in BGZ	
TiO ₂ =	1.044	SiO ₂ =	0.984
Al ₂ O ₃ =	1.017	Na ₂ O =	0.600
Fe ₂ O ₃ =	1.108		
MnO =	4.877 *		
MgO =	1.074		
CaO =	1.438		
K ₂ O =	1.049		
P ₂ O ₅ =	1.415		
C =	1.681		
Rb =	1.094	Sr =	0.696
Ba =	1.176	Zr =	0.940
Th =	1.020	Sc =	0.994
U		S =	0.574
Mo		Y =	0.907
Nb =	1.015		
Cr =	1.107		
V =	1.310		
Ni =	1.306		
Co =	1.209		
Pb =	3.127 *		
Zn =	3.713 *		
Cu =	1.959		
La =	1.045		
Ce =	1.036		
Nd =	1.057		

Codes:

† (Mean BGZ)/(Mean USS)

* More than 2x concentration (or < 0.5x concentration)

@ More than 5x concentration (or < 0.2x concentration)

b

ppm/ppm :	BGZ :	USS :
Ca/Sr	58.2	27.7
C/S	1.3	0.4
K/Na	29.7	17.0

Table 6.16 Tank Hill Schist (THS) and Green Quartzite (GrQ) element concentrations

	ALP244 THS	ALP241 GrQ	NSSav n = 4	* SSSav n = 2
SiO ₂ %	72.391	96.649	78.663	71.178
TiO ₂ %	0.687	0.092	0.354	0.761
Al ₂ O ₃ %	13.373	2.185	9.820	17.383
Fe ₂ O ₃ %	6.439	0.189	7.102	6.135
MnO %	0.074	0.007	0.097	0.047
MgO %	0.399	0.066	0.258	1.165
CaO %	0.022	0.032	0.106	0.076
Na ₂ O %	0.190	0.056	0.210	0.128
K ₂ O %	3.742	0.685	3.292	3.041
P ₂ O ₅ %	0.160	0.038	0.099	0.086
Rb ppm	336	35	196	223
Ba ppm	4052	561	746	391
Sr ppm	19	14	23	16
Th ppm	15	<LLD	12	28
U ppm	<LLD			
Zr ppm	219	99	270	350
Nb ppm	16	3.0	10	16
Mo ppm	6.1	1.2		
Cr ppm	67	64	114	101
V ppm	90	12	49	61
Se ppm	14	1.3	6.3	17
Ni ppm	<LLD	<LLD	11	28
Co ppm	<LLD	<LLD	5.9	12
Pb ppm	7109	57	40	32
Zn ppm	7628	10	95	79
Cu ppm	108	<LLD	5.6	18
S ppm	5730		53	149
Y ppm	3.6	5.3	34	17
La ppm	25	5.7	35	25
Ce ppm	57	15	77	56
Nd ppm	31	7.6	39	22

* NSSav = Average of NS surface samples for comparison
 SSSav = Average of SS surface samples for comparison

Table 6.17 Tests for Normality and tests for the equality of means for the rock-types NS, SS and OS

	Chi-Squared tests for Normality (on log(10) transformed data)			t-Test for difference between Means (on log(10) transformed data)					
	OS			NS vs OS			SS vs OS		
	Chi-Sq statis.	95% C.L.	80% C.L.	t statistic	95% Confidence levels	99%	t statistic	95% Confidence levels	99%
SiO2	5.39			3.63	Different	Different	1.62	Different	Same
TiO2	5.39			-3.75	Different	Different	-1.23	Different	Different
Al2O3	5.39			-3.36	Different	Different	-1.87	Same	Same
Fe2O3	4.35			-2.77	Different	Same	-2.52	Different	Different
MnO	4.87			-4.19	Different	Different	0.00	Different	Different
MgO	6.94			-2.82	Different	Same	-1.24	Different	Different
CaO	5.39			0.37	Same	Same	2.14	Same	Same
Na2O	4.35			1.69	Same	Same	4.45	Different	Different
K2O	1.77			-1.37	Same	Same	-0.64	Same	Same
P2O5	5.90			1.24	Same	Same	-1.40	Same	Same
Rb	6.42			-2.09	Same	Same	-0.58	Different	Different
Ba	7.97		Not	1.31	Same	Same	-0.91	Different	Different
Sr	5.90			1.05	Same	Same	2.43	Different	Different
Th	7.45		Not	-3.42	Different	Different	-3.28	Different	Different
Zr	1.26			3.53	Different	Different	-0.46	Same	Same
Nb	7.45		Not	-4.09	Different	Different	-2.81	Different	Different
Cr	13.13	Not	Not	-3.60	Different	Different	2.16	Same	Same
V	16.23	Not	Not	-4.26	Different	Different	0.61	Same	Same
Sc	9.00		Not	-3.48	Different	Different	-0.95	Same	Same
Ni	6.94			-4.76	Different	Different	-1.47	Same	Same
Co	13.65	Not	Not	-3.58	Different	Different	-1.97	Different	Different
Pb	6.94			-1.85	Same	Same	0.24	Different	Different
Zn	6.94			-2.49	Different	Same	-0.19	Different	Different
Cu	41.52	Not	Not	-2.23	Different	Same	-1.13	Different	Different
S	3.84			-0.68	Same	Same	3.37	Different	Different
Y	12.10	Not	Not	1.59	Same	Same	-2.37	Different	Different
La	5.69			0.96	Same	Same	-4.01	Different	Different
Ce	3.23			1.06	Same	Same	-3.37	Different	Different
Nd	11.23	Not	Not	1.27	Same	Same	-3.50	Different	Different

Codes: Same = Same Means
 Not = Not Normally distributed
 Different = Different Means
 Blanks indicate that distribution has passed the test for Normality

Data set sizes:
 NS n = 11
 SS n = 25
 OS n = 31

Notes: 1. Chi-Squared statistic calculated as shown by Le Maitre (1982, pp26-28) and tested against values in Le Maitre (1982, Table A5).
 2. t-Statistic (separate) and degrees of freedom are taken from BMDP P3D output.
 3. t-Statistic is tested against values in Le Maitre (1982, Table A3).

Table 6.18 OEH average element concentrations and coefficients of variation (S.D./Mean)

	OS = HS+IS+UFS+OES n = 31 *			OS+GQ n = 9		OEGQ n = 4 including 1 surface sample		OS SURFACE n = 30	
	Mean	SD	Co-efft of var.	Mean	SD	Mean	SD	Mean	SD
SiO2 %	66.506	4.337	0.07	68.564	5.893	73.129	3.317	67.911	8.618
TiO2 %	0.840	0.124	0.15	0.619	0.128	0.478	0.169	0.754	0.293
Al2O3 %	18.600	2.805	0.15	13.698	3.105	9.024	4.374	17.024	4.880
Fe2O3 %	8.148	1.483	0.18	12.260	6.235	13.497	4.527	8.950	3.596
MnO %	0.364	0.189	0.52	0.560	0.308	0.698	0.475	0.310	0.243
MgO %	1.098	0.352	0.32	0.856	0.195	0.851	0.502	1.072	0.575
CaO %	0.125	0.048	0.39	0.197	0.161	0.308	0.170	0.153	0.132
Na2O %	0.105	0.042	0.40	0.098	0.032	0.082	0.041	0.142	0.084
K2O %	4.083	1.024	0.25	2.904	0.693	1.682	1.292	3.612	1.213
P2O5 %	0.048	0.014	0.28	0.062	0.049	0.097	0.065	0.063	0.028
C %	0.015	0.016	1.06	0.016	0.015			0.040	0.008
Rb ppm	244	42	0.17	204	48	107	81	200	78
Ba ppm	705	488	0.69	813	535	295	131	670	471
Sr ppm	15	8.4	0.55	10	2.4	18	13	21	7.8
Th ppm	19	3.0	0.16	19	3.2	15	1.5	19	12
Zr ppm	267	41	0.15	291	28	355	174	243	45
Nb ppm	20	3.2	0.16	15	3.4	12	6.0	17	4.0
Cr ppm	100	16	0.16	77	13	53	18	85	24
V ppm	93	58	0.62	89	39	79	51	75	22
Se ppm	18	4.0	0.23	13	3.1	19	9.0	17	5.9
Ni ppm	25	7.6	0.30	18	6.0	19	12	24	8.9
Co ppm	19	15	0.76	21	2.4	19	4.8	18	6.6
Pb ppm	122	201	1.65	200	233	203	277	76	68
Zn ppm	345	192	0.56	591	567	375	276	368	309
Cu ppm	55	127	2.33	106	103	121	120	74	117
S ppm	993	2488	2.51	1577	2114	1622	2614	101	66
Y ppm	33	6.9	0.21	35	7.0	73	29	35	17
La ppm	36	5.5	0.15	33	4.3	27	3.1	31	7.5
Ce ppm	79	9.5	0.12	80	15	60	9.0	66	16
Nd ppm	39	4.1	0.10	39	6.3	31	3.5	32	8.4

Note: Mo Adjacent core samples of OS+GQ and OEGQ from borehole TS11 at Maanhaarkop contain 22 and 64 ppm Mo respectively
 Core OS samples ALP119 and ALP135 contain 6.0 and 3.3 ppm Mo from Broken Hill and Maanhaarkop, respectively
 Surface OS samples ALP192, ALP212, ALP164 and ALP219 contain 8, 19, 2.2 and 11 ppm Mo respectively. The first 3 samples come from Broken Hill and the last sample from Maanhaarkop

C 9 OS, 3 OS Surface and 5 OS+GQ samples were analysed for C

* For La, Ce and Nd, n = 19

Table 6.19 OS correlation matrix

	Si	Zr	Y	P	Cu	Pb	Zn	S	Ba	Fe	Mn	K	Rb	Al	Ti	Nb	Sc	Ni	Mg	V	Co	Cr	Th	Ca	Na	Sr	La	Ce	Nd					
Si	*	4	-1																															
Zr	4	*		-1																														
Y	-1	*																																
P	-1		*																															
Cu				*																														
Pb					*																													
Zn						*																												
S							*																											
Ba								*																										
Fe									*																									
Mn										*																								
K											*																							
Rb												*																						
Al													*																					
Ti														*																				
Nb															*																			
Sc																*																		
Ni																	*																	
Mg																		*																
V																			*															
Co																				*														
Cr																					*													
Th																						*												
Ca																							*											
Na																								*										
Sr																									*									
La																										*								
Ce																											*							
Nd																													*					

Pearson product-moment correlation matrix performed on log (10) transformed data
 n = 31 For REE, n = 19

Codes:

Si	=	SiO2	For n = 31
Ti	=	TiO2	Blank = r < 0.
Al	=	Al2O3	1 = r > 0.301
Fe	=	Fe2O3	2 = r > 0.355
Mn	=	MnO	3 = r > 0.456
Mg	=	MgO	4 = r > 0.562
Ca	=	CaO	- =
Na	=	Na2O	
K	=	K2O	For n = 19
P	=	P2O5	Blank = r < 0.389
			1 = r > 0.389
			2 = r > 0.456
			3 = r > 0.575
			4 = r > 0.693
			- =

Correlation not significant at the 90 % confidence limit
 Correlation significant at the 90 % confidence limit
 Correlation significant at the 95 % confidence limit
 Correlation significant at the 99 % confidence limit
 Correlation significant at the 99.8 % confidence limit
 Negative correlation

Correlation not significant at the 90 % confidence limit
 Correlation significant at the 90 % confidence limit
 Correlation significant at the 95 % confidence limit
 Correlation significant at the 99 % confidence limit
 Correlation significant at the 99.8 % confidence limit
 Negative correlation

Table 6.20 OS factor analysis parameters; (a) OS variances explained by each Factor, and cumulative variances; (b) communalities for each element

a		Factor	Factor	Factor	Factor	Factor	Factor	Factor
		1	2	3	4	5	6	7
OS	% Variance	26.0	14.7	14.4	13.6	8.6	7.0	5.3
	Cum. % Var	26.0	40.7	55.1	68.7	77.4	84.3	89.6
OS(-REE)	% Variance	29.2	11.9	11.5	11.3	8.6	8.4	
	Cum. % Var	29.2	41.1	52.6	63.9	72.5	80.9	

b		OS	OS(-REE)
	No. of samples included in P.A.	19	31
	SiO ₂	0.98	0.95
	TiO ₂	0.91	0.96
	Al ₂ O ₃	0.96	0.96
	Fe ₂ O ₃	0.94	0.63
	MnO	0.97	0.90
	MgO	0.77	0.84
	CaO	0.83	0.77
	Na ₂ O	0.97	0.76
	K ₂ O	0.93	0.92
	P ₂ O ₅	0.79	0.56
	Rb	0.95	0.89
	Ba	0.93	0.86
	Sr	0.85	0.83
	Th	0.91	0.71
	Zr	0.86	0.79
	Nb	0.82	0.84
	Cr	0.96	0.91
	V	0.85	0.82
	Se	0.93	0.90
	Ni	0.87	0.85
	Co	0.82	0.64
	Pb	0.90	0.76
	Zn	0.92	0.65
	Cu	0.85	0.59
	S	0.83	0.83
	Y	0.97	0.92
	La	0.85	0.89
	Ce	0.93	0.92
	Nd	0.94	0.93

The communality for each element represents the sum of the squared factor loadings for each element. If the communality approximates 1, then that element is completely represented by the Factor Analysis.

Table 6.21 Some orebody average element concentrations

	Upper Orebody Quartz Magnetite Rock n = 2	Lower Orebody Garnet Quartzite n = 3	Lower Orebody Amphibole Magnetite Rock	Froneman se Kop Quartz Magnetite Rock
	Mean	Mean	ALP113	ALP228
SiO ₂ %	36.603	86.791	39.980	29.103
TiO ₂ %	0.315	0.215	0.279	0.520
Al ₂ O ₃ %	2.183	3.270	5.382	4.623
Fe ₂ O ₃ %	58.289	6.536	38.877	64.142
MnO %	0.151	0.352	7.803	0.188
MgO %	0.320	0.422	1.051	0.001
CaO %	0.387	0.111	0.529	0.225
Na ₂ O %	0.042	0.065	0.049	0.153
K ₂ O %	0.313	0.754	0.090	0.692
P ₂ O ₅ %	0.316	0.036	0.336	0.353
C %		0.020	0.001	
Rb ppm	24	46	10	46
Ba ppm	60	2475	1273	160
Sr ppm	6.0	12	37	266
Th ppm	37	5	18	34
U ppm		<4	<4	12
Zr ppm	127	269	118	627
Nb ppm	2.8	5.5	5.0	5.6
Mo ppm	6.7	3.1	9.0	5.2
Cr ppm	51	52	29	76
V ppm	38	23	37	387
Sc ppm	2.9	2.3	4.3	15
Ni ppm	15	10	43	20
Co ppm	92	19	47	24
Pb ppm	599	746	8000	<4
Zn ppm	2478	1655	10100	143
Cu ppm	2494	288	1390	194
S ppm	6886	11617	40192	254
Y ppm	18	9.3	30	85
La ppm	8.9	16	13	75
Ce ppm	28	25	33	237
Nd ppm	13	10	22	117

Table 6.22 Broken Hill Quartzite (BQ) average element concentrations and standard deviations

n	WQ Core		DQ Core		WQ + DQ Core		WQ Surface		DQ Surface		WQ+DQ Surface		MDS	
	4		4		8		6		5		11		4	
	Mean	S.D.	Mean	S.D.	Mean	S.D.	Mean	S.D.	Mean	S.D.	Mean	S.D.	Mean	S.D.
SiO2 %	96.315	1.351	96.197	1.010	96.256	1.194	98.038	0.547	97.835	0.542	97.945	0.581	78.299	6.201
TiO2 %	0.060	0.006	0.066	0.043	0.063	0.031	0.043	0.008	0.045	0.009	0.044	0.009	0.440	0.255
Al2O %	1.616	0.577	1.706	0.348	1.661	0.479	0.801	0.436	1.073	0.348	0.910	0.439	9.715	4.817
Fe2O %	1.266	0.711	1.386	0.640	1.326	0.679	0.763	0.411	0.602	0.526	0.718	0.487	8.068	1.440
MnO %	0.031	0.032	0.038	0.022	0.035	0.027	0.012	0.003	0.011	0.005	0.012	0.005	0.225	0.085
MgO %	0.162	0.148	0.084	0.033	0.123	0.114	0.026	0.021	0.058	0.026	0.034	0.020	0.725	0.413
CaO %	0.062	0.061	0.022	0.008	0.042	0.048	0.005	0.004	0.004	0.004	0.005	0.004	0.232	0.207
Na2O %	0.064	0.034	0.045	0.004	0.054	0.026	0.043	0.010	0.046	0.017	0.042	0.011	0.092	0.016
K2O %	0.417	0.160	0.446	0.066	0.431	0.123	0.250	0.156	0.308	0.174	0.271	0.175	2.126	1.369
P2O5 %	0.029	0.017	0.009	0.008	0.019	0.017	0.020	0.015	0.017	0.017	0.020	0.016	0.078	0.021
RB ppm	27	10	24	3	26	8	15	11	16	9	16	10	130	76
BA ppm	45	29	43	9	44	22	32	12	43	14	36	15	313	144
SR ppm	3.4	2.9	1.5	0.5	2.5	2.3	2.8	1.2	3.4	1.0	3.1	1.2	19	7.2
ZR ppm	108	26	149	69	129	56	75	12	89	23	81	20	310	84
NB ppm	2.5	0.8	2.6	1.8	2.6	1.4	2.9	2.1	2.6	0.8	2.9	1.6	11	7
CR ppm	5.7	1.4	8.0	3.1	6.9	2.6	5.5	1.0	4.8	0.9	5.2	1.1	49	28
V ppm	3.9	1.7	4.3	1.8	4.1	1.8	2.7	0.5	2.4	0.4	2.5	0.5	47	17
SC ppm	1.3	0.4	1.7	0.7	1.5	0.6	1.7	1.3	1.7	1.4	1.8	1.4	7	4
CO ppm	2.4	2.1	2.6	1.4	2.5	1.8	1.0	0.0	1.9	1.7	1.5	1.3	20	10
PB ppm	12	5.6	9.1	2.2	10	4.5	1.8	1.7	11	18	6.1	13.7	45	9
ZN ppm	47	36	43	24	45	31	5.3	2.2	8.4	8.4	7.1	6.2	209	105
CU ppm	44	22	173	227	108	174	2.4	1.4	15	25	8.3	19	90	101
S ppm	281	129	419	180	350	171	55	43	97	118	80	91	548	358
Y ppm	8.6	2.0	8.2	4.3	8.4	3.4	3.7	1.4	5.3	2.1	4.6	2.0	42	18
LA ppm	8.9	0.7	16	4.0	12	4.2	9.8	1.4	11	2.8	10	2.2	32	7.4
CE ppm	20	1.1	29	7.8	23	6.7	20	5.0	22	5.1	21	5.1	63	17
ND ppm	9.1	0.7	13	3.2	11	2.8	8.9	1.8	10	2.2	10	2.0	32	7.7

Note: All major elements are calculated volatile free. The volatile content of the original data, uncorrected for oxidation of iron, is listed below

H2O- %	0.053	0.045	0.043	0.057		0.002	0.053	0.051	0.011		0.210	0.072
LOI %	0.303	0.052	0.254	0.096		0.204	0.069	0.212	0.053		1.120	0.468

Note 1. Median Schist also has the following elements in excess of lower limit of detection

	Mean	S.D.
Th	14.500	2.693
Ni	13.475	5.884

2. The one median schist analysed for carbon has 0.01% C

3. Both quartzite samples analysed for carbon have values of <0.01% C

Table 6.23 BQ correlation matrix

	Si	Zr	Y	P	Cu	Pb	Zn	Ba	Fe	Mn	K	Rb	Al	Ti	Nb	Mg	V	Cr	Ca	Na	La	Ce	Nd		
Si	*																							Si	
Zr	*	*													2							2	1	3	Zr
Y		*	*							1															Y
P			*	*																					P
Cu					*																				Cu
Pb						*																			Pb
Zn							*																		Zn
Ba								*																	Ba
Fe									*																Fe
Mn										*															Mn
K											*														K
Rb												*													Rb
Al													*												Al
Ti														*											Ti
Nb															*										Nb
Mg																*									Mg
V																	*								V
Cr																		*							Cr
Ca																			*						Ca
Na																				*					Na
La																					*				La
Ce																						*			Ce
Nd																							*		Nd

Pearson product-moment correlation matrix performed on log (10) transformed data
n = 8

Codes:

Si	=	SiO ₂	r < 0.621	Correlation not significant at the 90 % confidence limit
Ti	=	TiO ₂	1 = r > 0.621	Correlation significant at the 90 % confidence limit
Al	=	Al ₂ O ₃	2 = r > 0.707	Correlation significant at the 95 % confidence limit
Fe	=	Fe ₂ O ₃	3 = r > 0.834	Correlation significant at the 99 % confidence limit
Mn	=	MnO	4 = r > 0.925	Correlation significant at the 99.8 % confidence limit
Mg	=	MgO	- =	Negative correlation
Ca	=	CaO		
Na	=	Na ₂ O		
K	=	K ₂ O		
P	=	P ₂ O ₅		

For La, Ce and Nd, n = 5

	r < 0.805	Correlation not significant at the 90 % confidence limit
1 =	r > 0.805	Correlation significant at the 90 % confidence limit
2 =	r > 0.878	Correlation significant at the 95 % confidence limit
3 =	r > 0.959	Correlation significant at the 99 % confidence limit
4 =	r > 0.991	Correlation significant at the 99.8 % confidence limit
- =		Negative correlation

Table 6.24 BQ factor analysis parameters: (a) variances explained by each factor, and cumulative variances; (b) communalities for each element

		Factor 1	Factor 2	Factor 3	Factor 4	Factor 5
BQ(1)	% Variance	48.7	34.1	10.9	6.3	
	Cum. % Variance	48.7	82.7	93.7	100.0	
BQ(2)	% Variance	36.8	22.8	16.1	9.5	7.0
	Cum. % Variance	36.8	59.5	75.7	85.2	92.2

Table ...Communalities for each element

RL Output NO.	90	91
	BQ(1)	BQ(2)
No. of samples included in P.A.	5	8
SiO ₂	1.00	1.00
TiO ₂	1.00	0.81
Al ₂ O ₃	1.00	0.96
Fe ₂ O ₃	1.00	1.00
MnO	1.00	0.87
MgO	1.00	0.96
CaO	1.00	0.96
Na ₂ O	1.00	0.69
K ₂ O	1.00	0.90
P ₂ O ₅	1.00	0.96
Rb	1.00	0.98
Ba	1.00	0.98
Sr		
Th		
Zr	1.00	0.97
Nb	1.00	0.80
Cr	1.00	0.87
V	1.00	0.96
Sc		
Ni		
Co		
Pb	1.00	0.98
Zn	1.00	0.95
Cu	1.00	0.88
S		
Y	1.00	0.97
La	1.00	
Ce	1.00	
Nd	1.00	

BQ(1) Excluding Ni Sc Sr Th Co S

BQ(2) Excluding Ni Sc Sr Th Co S and REE

The communality for each element represents the sum of the squared factor loadings for each element. If the communality approximates 1, then that element is completely represented by the Factor Analysis.

Table 6.25 Relative element abundances and variations in specific zones of SS

Borehole	Below BGZ		SS Above CSMQ Rel. to SS in BH123 ‡		Below CSMQ		Across USS/LSS Boundary		Above Plant Quartzite	
	Increase	Decrease	Higher	Lower	Increase	Decrease	Increase	Decrease	Increase	Decrease
BH123	Ti Al Fe Mn REE Th Pb Nb Co*	Si Mg* Ca* Na P* C* S* LOI Zr Rb Nb V* Sr Cr* Zn* Cu Ba* Mo Ni*	Fe* Mn* Ca* Pb* Co* REE	Mg* Na P* C* S* LOI V* Cr Ba* Zn* Cu Mo Ni*	Si Fe P Co	Ti Mn* Mg* Ca REE Rb Sr Zr REE Se V Sr Zr* Cr* Th* Pb* Zn* Cu Ba Nb Ni	Si Na* Sr Zr REE Th C S LOI Rb V* Zn Cu Ba Nb Mo Ni* Cr	Al Fe Mg Ca K P C S LOI Rb V* Zn Cu Ba Nb Mo Ni* Cr		
BH156	Si Na* S* REE Th Pb	Ti Al Fe Mn* Mg* Ca K P* LOI C Rb Se V* Ni* Cr Zn* Ba* Cu Mo					Si Zr	Al Mg* Fe Ca* K C* S* (Na) (LOI) Rb* Sr V* Se REE Mo (Th) Cr Ba Pb Zn Cu Ni Co		
BH163							Si Ca* Na* Sr* Zr Nb Th	Al Mg K (Fe) P* C* LOI Zn Ba Rb Cu V* Cr Ni* Co		
BH164									Ca Na Ba Sr Nb	Ti Al Mn Mg Zn Cu Ni

‡ = 1 Sample

* = Strong trend

** Note: All variations taken moving down structural succession

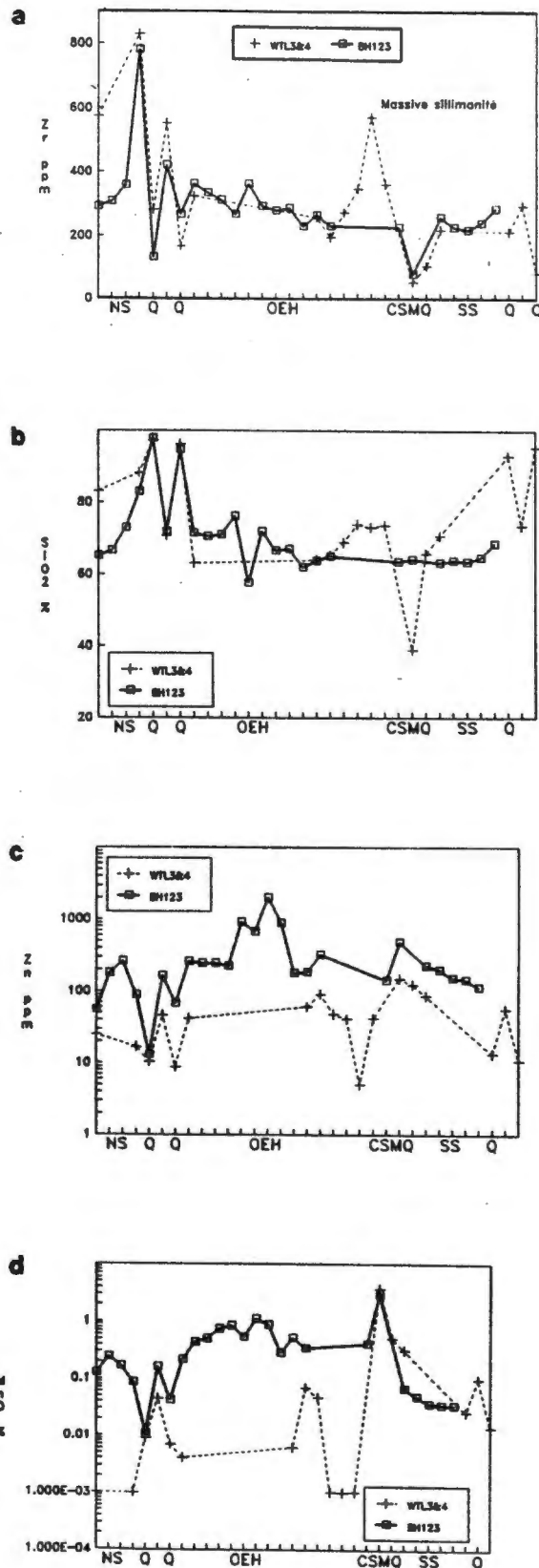


Fig. 7.1 Comparison between element concentrations in Broken Hill borehole BH123 and Wortel holes WTL3 & 4: (a) Zr; (b) SiO₂; (c) Zn; (d) MnO. X-axis represents consecutive rock types down the holes plotted at equally spaced intervals. NS and SS = Broken Hill and Wortel Namies and Shaft Schists; Q = Broken Hill and Wortel quartzites; OEH = Broken Hill OEH and approximate equivalent stratigraphic schist at Wortel; CSMQ = Broken Hill CSMQ and Wortel CTSMQ

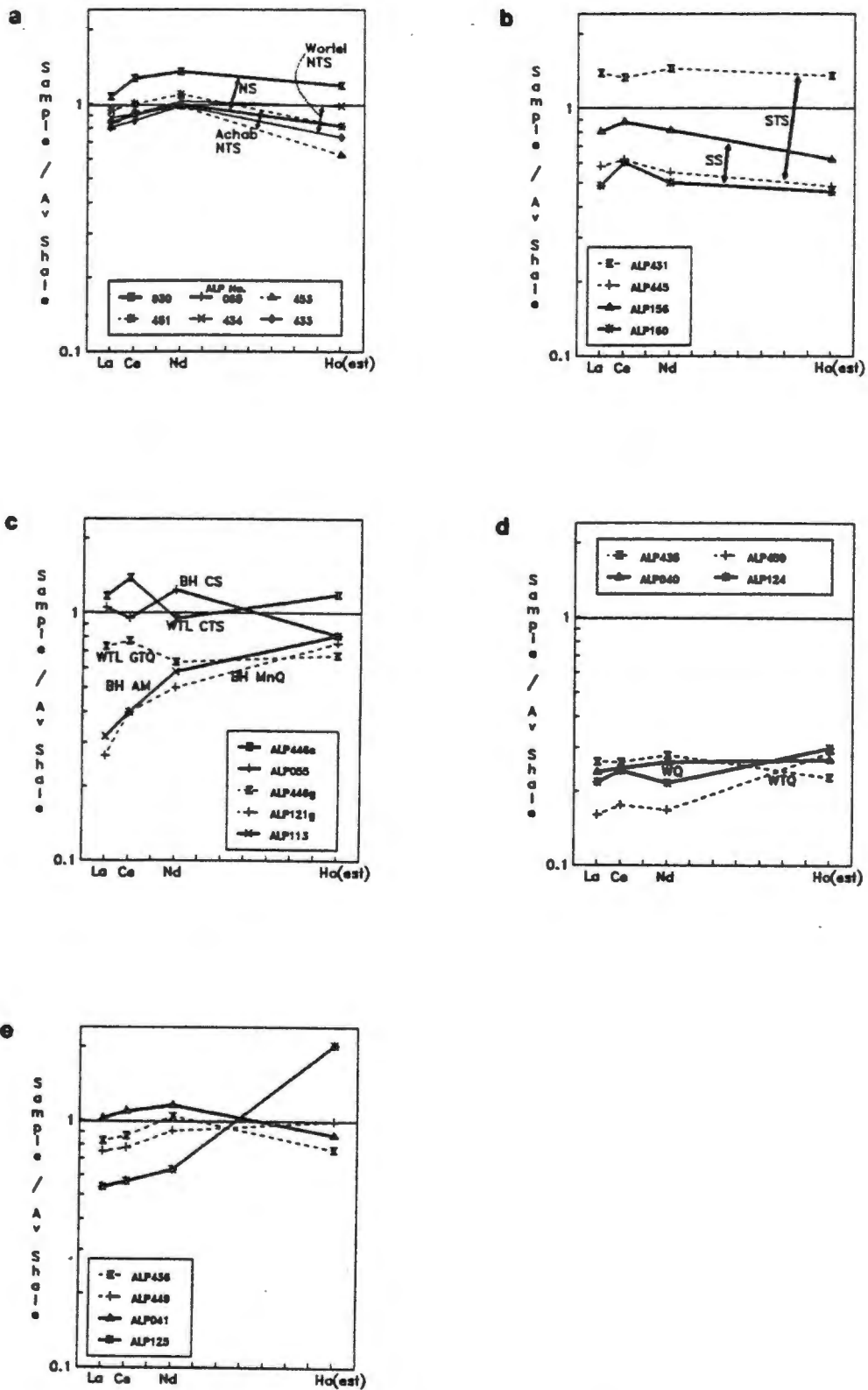


Fig. 7.2 Shale normalized REE patterns for regional rocks compared with Broken Hill analogues, using the XRF analytical method: (a) NS compared with Wortel and Achab NTS; (b) SS compared with Wortel and Namiesberg STS; (c) CSMQ compared with Wortel CTSMQ; (d) WQ compared with Wortel WTQ; (e) MDS compared with Wortel MDTS

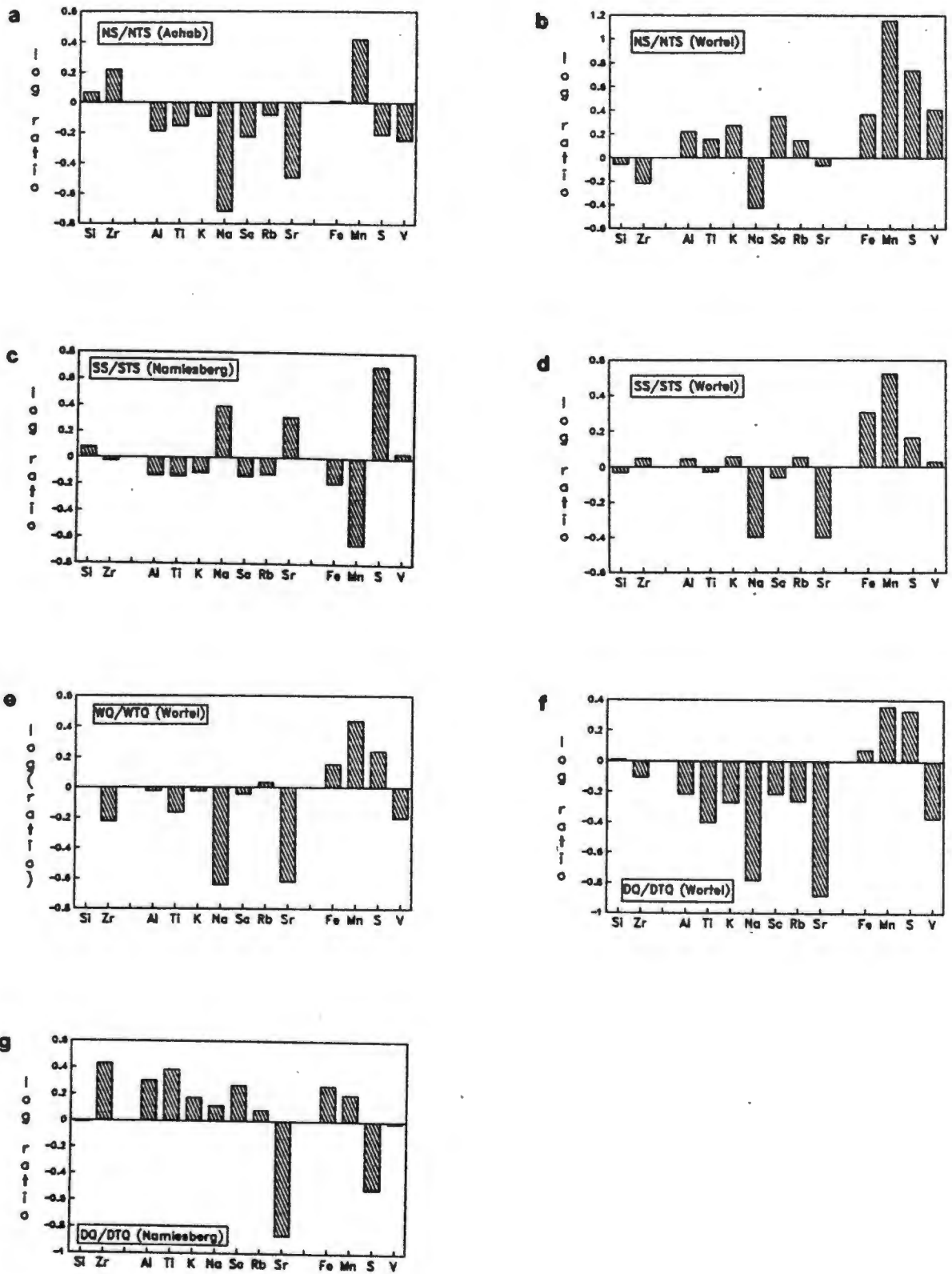


Fig. 7.3 Delta diagrams showing the log ratios of mean element concentration of Broken Hill rock-types to Regional rock-types for borehole core only: (a) NS/NTS (Achab); (b) NS/NTS (Wortel); (c) SS/STS (Namiesberg); (d) SS/STS (Wortel); (e) WQ/WTQ (Wortel); (f) DQ/DTQ (Wortel); (g) DQ/DTQ (Namiesberg). Elements are those less obviously related to the orebody

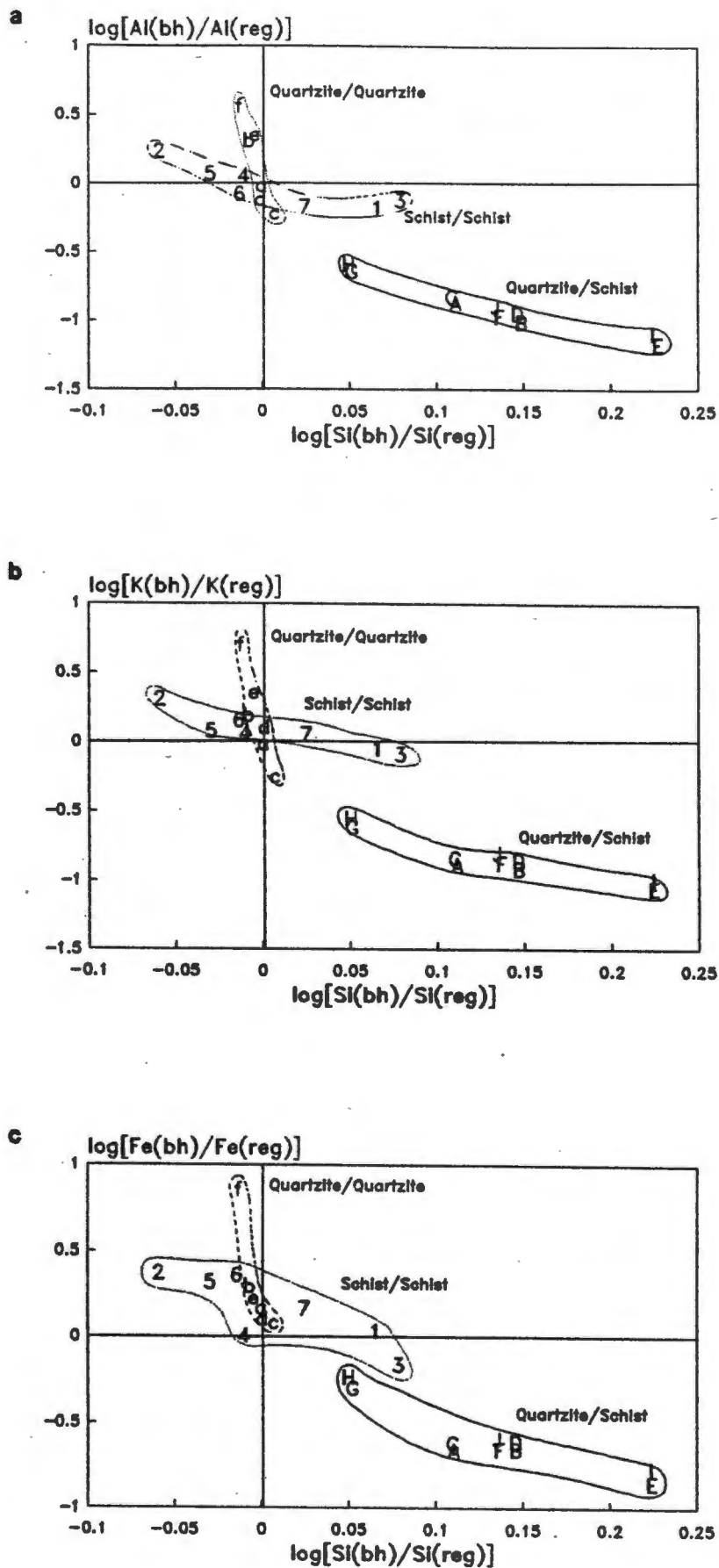


Fig. 7.4 Ratio-ratio diagrams showing the log ratios of the mean concentrations of 3 elements plotted against the log Si ratios for various suites of rocks shown: (a) Al; (b) K; (c) Fe. Legend appears with Fig. 7.5

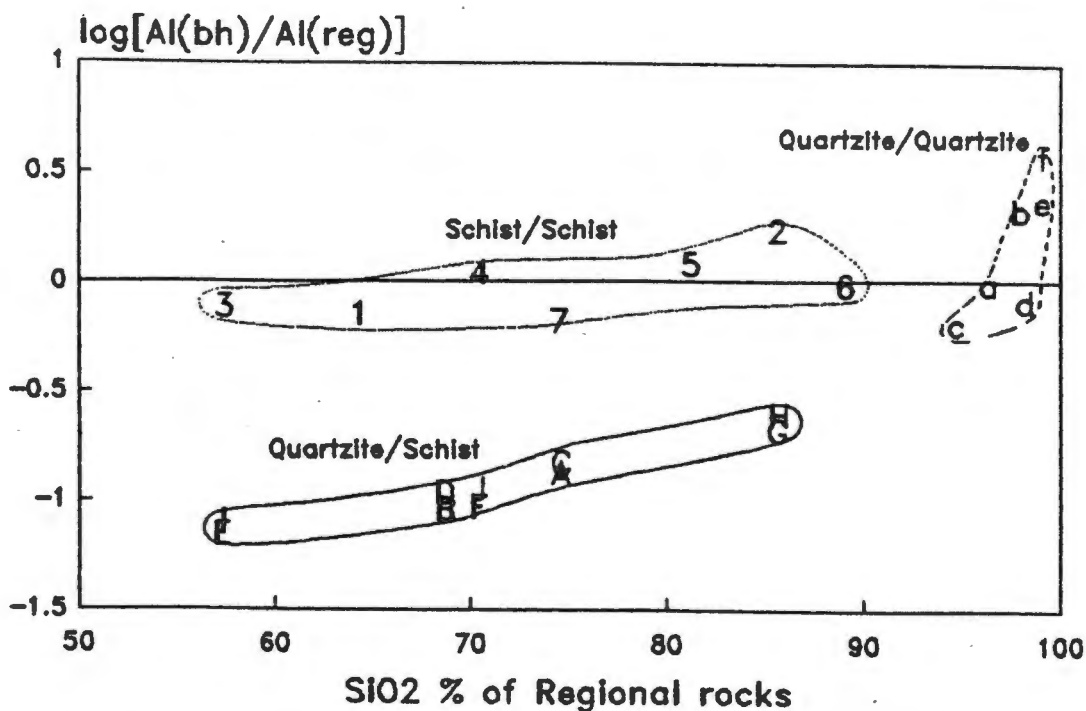


Fig. 7.5 $\log[\text{Al}(\text{bh})/\text{Al}(\text{reg})]$ ratio plotted against the SiO_2 content of the regional rock, for the rock-types shown

Legend to Figs. 7.4 and 7.5

Log Ratios	Code
NS/ACHAB	1
NS/NTSwtl	2
SS/STSnam	3
SS/STSwtl	4
MDSc/MDTSwtl	5
MDSs/MDTSnam	6
NSs/NTSs	7
WQ/WTQwtl	a
DQc/DTQenam	b
DQc/DTQwtl	c
WQs/WTQs	d
DQs/DTQs	e
WQc/WTQenam	f
WQ/NS	A
WQ/SS	B
DQ/NS	C
DQ/SS	D
WQ/STSnam	E
WQ/STSwtl	F
WQ/NTSwtl	G
DQ/NTSwtl	H
DQ/STSnam	I
DQ/STSwtl	J

Where wtl = Wortel
 nam = Namiesberg
 bh = Broken Hill
 reg = Regional (Achab, Namiesberg and Wortel)
 s = surface
 c = core

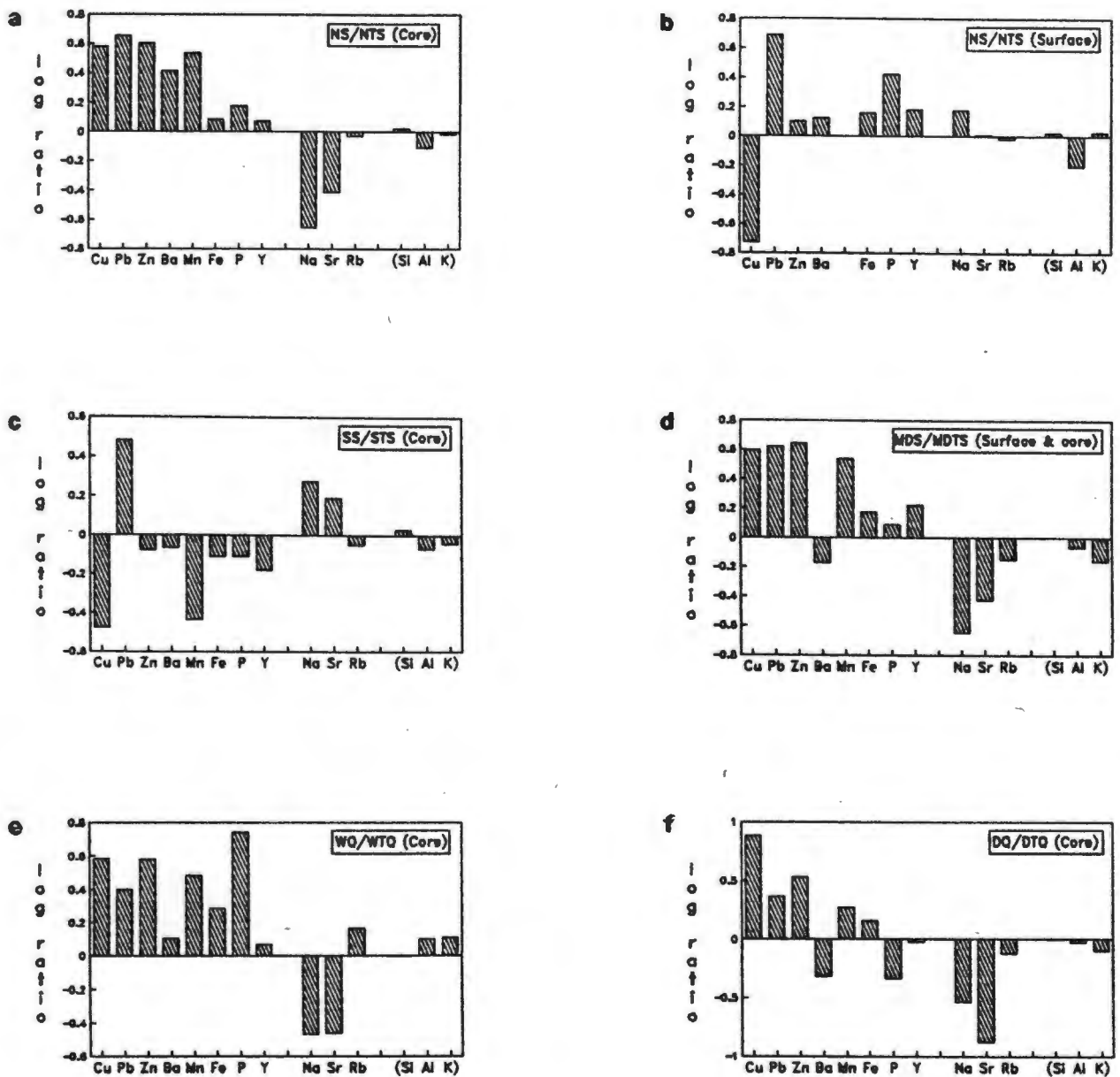


Fig. 7.6 Delta diagrams showing the log ratios of mean ore-related element concentration of Broken Hill rock-types to Regional rock-types for both borehole core and surface samples: (a) NS/NTS (core); (b) NS/NTS (surface); (c) SS/STS (core); (d) MDS/MDTS (surface and core); (e) WQ/WTQ (core); (f) DQ/DTQ (core)

Table 7.1 NTS and STS average element concentrations and coefficients of variation (S.D./Mean)

	NTS		STS		NTS Surface		Coefficients of variation	
	Mean n = 7	S.D.	Mean n = 8	S.D.	Mean n = 9	S.D.	NTS	STS
SiO ₂ %	70.382	9.845	63.915	7.759	74.434	3.890	0.14	0.12
TiO ₂ %	0.741	0.203	0.837	0.197	0.613	0.050	0.27	0.24
Al ₂ O ₃ %	17.368	5.870	21.260	4.336	15.656	2.268	0.34	0.20
Fe ₂ O ₃ %	5.054	1.636	7.509	1.709	4.931	0.539	0.32	0.23
MnO %	0.042	0.021	0.101	0.077	<0.037	0.014	0.51	0.77
MgO %	1.448	0.611	1.799	0.546	1.008	0.273	0.42	0.30
CaO %	0.518	0.255	0.096	0.044	0.097	0.043	0.49	0.46
Na ₂ O %	0.722	0.292	0.145	0.063	0.139	0.097	0.40	0.43
K ₂ O %	3.684	1.214	4.164	1.075	3.078	1.035	0.33	0.26
P ₂ O ₅ %	0.045	0.015	0.058	0.021	0.038	0.008	0.35	0.36
Rb ppm	218	53	230	66	204	56	0.24	0.29
Ba ppm	482	149	521	165	558	263	0.31	0.32
Sr ppm	54	23	23	9.4	22	11	0.43	0.40
Th ppm	16	2.4	23	5.3	17	2.5	0.15	0.23
Zr ppm	385	213	297	65	345	79	0.55	0.22
Nb ppm	20	4.8	22	7.7	15	0.9	0.24	0.35
Cr ppm	99	14	91	12	90	10	0.14	0.13
V ppm	63	29	104	41	69	42	0.46	0.39
Sc ppm	15	6.3	19	4.8	14	1.8	0.43	0.25
Ni ppm	25	9.4	31	6.7	23	6.3	0.37	0.21
Co ppm	11	4.3	18	5.1	9.3	2.5	0.39	0.28
Pb ppm	11	5.1	14	9.4	8.2	6.2	0.45	0.68
Zn ppm	49	24	138	93	75	42	0.50	0.68
Cu ppm	10	14	93	137	31	17	1.45	1.47
S ppm	335	202	1495	1318	133	59	0.61	0.88
Y ppm	29	3.7	33	12	22	4.3	0.13	0.36
La ppm	34	2.8	43	13	27	3.5	0.08	0.31
Ce ppm	75	3.7	86	24	57	7.5	0.05	0.28
Nd ppm	38	2.0	42	14	26	4.2	0.05	0.33
Note: All major elements are calculated volatile free. The volatile content of the original data, uncorrected for oxidation of iron, is listed below.								
H ₂ O-	0.2	0.1	0.4	0.2	0.7	0.2	0.38	0.48
LOI	1.4	0.4	3.9	1.1	5.2	3.0	0.30	0.29

- Notes: 1. C The single NTS core sample analysed for C returned a value of 0.04 %.
Of the 7 STS samples analysed for C, the highest value is 0.06 %.
2. U All NTS samples have U concentrations of <3.3 ppm.
2 of the 8 STS samples have detectible U, with concentrations of 5 ppm.
3. Mo All NTS samples have Mo concentrations of <2 ppm.
STS samples average 3.3 ppm Mo with a maximum of 6.8 ppm.

Table 7.3 STS correlation matrix

Si	Zr	Y	P	Cu	Pb	Zn	S	Ba	Fe	Mn	K	Rb	Al	Ti	Nb	Sc	Ni	Mg	V	Co	Cr	Th	Ca	Na	Sr	La	Ce	Nd	
Si	*	-2	-3	-3	-4	-4	-2	-4	-3	-3	-3	-3	-4	-4	-4	-4	-3	-1	-3	-3	-3	-3	-1	-1	1	-3	-3	-3	Si
Zr	*																												Zr
Y	-2	*																											Y
P	-3	-2	*																										P
Cu	-3	-3	3	*																									Cu
Pb	-3	-3	2	2	*																								Pb
Zn	-4	-3	2	2	2	*																							Zn
S	-4	-4	3	4	2	2	*																						S
Ba	-2	-2	1	1	1	1	1	*																					Ba
Fe	-4	-2	3	3	3	3	3	3	*																				Fe
Mn	-3	-4	3	3	2	2	2	2	3	*																			Mn
K	-3	-3	4	4	2	1	4	4	4	4	*																		K
Rb	-3	-3	2	4	2	1	3	3	4	3	3	*																	Rb
Al	-4	-3	2	4	3	1	3	3	3	3	4	3	*																Al
Ti	-4	-4	2	3	3	4	4	2	4	4	3	3	3	*															Ti
Nb	-4	-4	3	3	2	4	4	2	4	4	4	4	4	4	*														Nb
Sc	-4	-4	2	2	2	3	3	1	3	3	2	3	3	3	3	*													Sc
Ni	-3	-4	3	3	2	4	4	3	4	3	3	4	4	4	3	3	*												Ni
Mg	-3	-3	1	1	1	1	1	1	1	1	1	1	1	1	1	1	1	*											Mg
V	-1	-3	2	2	2	2	3	3	3	3	4	4	3	4	3	3	3	3	*										V
Co	-3	-1	2	2	2	2	2	1	1	1	1	2	3	1	1	1	1	3	2	*									Co
Cr	-3	-3	3	4	2	1	3	4	3	3	3	4	3	3	2	3	2	3	3	3	*								Cr
Th	-3	-3	1	1	1	1	2	2	2	2	2	3	3	3	2	2	2	2	2	2	2	*							Th
Ca	-1	-3	2	2	2	2	2	2	1	3	2	2	3	3	2	2	2	2	2	2	2	2	*						Ca
Na	-1	-3	2	2	2	2	2	2	3	2	2	4	3	1	2	2	3	3	4	4	4	4	2	*					Na
Sr	1	-2	2	3	2	2	2	2	3	2	2	4	3	1	2	2	3	3	4	4	4	4	2	2	*				Sr
La	-3	1	-1	2	2	2	2	2	2	2	2	2	2	2	2	2	2	2	2	2	2	2	2	2	2	*			La
Ce	-3	-3	2	2	3	2	3	1	3	3	2	2	2	3	3	3	2	2	2	2	2	2	4	1	2	*			Ce
Nd	-3	-3	2	2	2	1	3	1	3	3	1	2	2	3	3	2	2	2	2	2	2	2	3	3	1	4	*		Nd

Pearson product-moment correlation matrix performed on log (10) transformed data
n = 8

Codes:

Si = SiO2
Ti = TiO2
Al = Al2O3
Fe = Fe2O3
Mn = MnO
Mg = MgO
Ca = CaO
Na = Na2O
K = K2O
P = P2O5

Blank = r < 0.621
1 = r > 0.621
2 = r > 0.707
3 = r > 0.834
4 = r > 0.925
- =

Correlation not significant at the 90 % confidence limit
Correlation significant at the 90 % confidence limit
Correlation significant at the 95 % confidence limit
Correlation significant at the 99 % confidence limit
Correlation significant at the 99.8 % confidence limit
Negative correlation

Table 7.4 Wortel CTSMQ element concentrations and comparative rock-types from Broken Hill

		CTS n = 1	LAM n = 1	CS n = 3 Mean	GTQ n = 1	LGQ n = 3 Mean	MNQ n = 4 Mean
SiO ₂	%	38.891	39.980	65.099	65.669	86.791	88.327
TiO ₂	%	0.211	0.279	0.468	0.439	0.215	0.077
Al ₂ O ₃	%	5.246	5.382	11.165	9.513	3.270	2.064
Fe ₂ O ₃	%	45.498	38.877	7.099	19.587	6.536	4.825
MnO	%	3.734	7.803	1.845	0.518	0.352	0.705
MgO	%	3.262	1.051	4.259	2.967	0.422	0.114
CaO	%	1.519	0.529	6.859	0.522	0.111	0.511
Na ₂ O	%	0.010	0.049	0.471	0.039	0.065	0.055
K ₂ O	%	0.398	0.090	1.471	0.593	0.754	0.142
P ₂ O ₅	%	0.828	0.336	0.306	0.153	0.036	0.541
Rb	ppm	39	10	92	35	46	4.6
Ba	ppm	122	1273	1235	145	2475	63
Sr	ppm	59	37	101	20	12	16
Th	ppm	<9.4	18	11	<6.4	5.2	8.7
U	ppm	<7.2	<7.2	7	<4.9	<4	11
Zr	ppm	55	118	123	104	269	23
Nb	ppm	<2.9	5.0	10	5.9	5.5	3.3
Mo	ppm	12	9.0	3.4	4.2	3.1	4.3
Cr	ppm	35	29	64	63	52	15
V	ppm	95	37	79	100	23	33
Se	ppm	6.6	4.3	12	12	2.3	1.8
Ni	ppm	14	43	30	38	10	10
Co	ppm	124	47	12	42	19	13
Pb	ppm	<10	8000	1987	19	746	12087
Zn	ppm	150	10100	1611	124	1655	1079
Cu	ppm	53	1390	59	6.3	288	421
S	ppm	4020	38780	5963	830	11617	14119
Y	ppm	44	30	28	25	9.3	11
La	ppm	48	13	40	30	16	7.9
Ce	ppm	115	33	73	64	25	25
Nd	ppm	36	22	37	24	10	11

CTSMQ = Calc Silicate-type Rock and Manganese-type Quartzite

CTS = Calc Silicate-type Rock

LAM = Lower Orebody Amphibole Magnetite

CS = Calc Silicate Rock

GTQ = Garnet-type Quartzite

LGQ = Lower Orebody Garnet Quartzite

MNQ = Manganese Quartzite

Table 7.5 Regional Quartzite element concentrations

	WTQ n = 3		MDTS n = 3		DTQ n = 4	
	Mean	SD	Mean	SD	Mean	SD
SiO ₂ %	97.321	1.546	77.682	8.026	96.305	2.017
TiO ₂ %	0.066	0.034	0.597	0.270	0.097	0.095
Al ₂ O ₃ %	1.291	0.768	11.215	3.348	1.817	1.139
Fe ₂ O ₃ %	0.652	0.374	5.412	2.052	0.958	0.362
MnO %	0.010	0.003	0.065	0.025	0.020	0.008
MgO %	0.013	0.017	1.077	0.423	0.007	0.010
CaO %	0.129	0.168	0.397	0.304	0.055	0.040
Na ₂ O %	0.188	0.231	0.407	0.286	0.155	0.128
K ₂ O %	0.325	0.173	3.085	1.664	0.567	0.344
P ₂ O ₅ %	0.005	0.006	0.063	0.034	0.019	0.012
Rb ppm	19	10	183	90	31	15
Ba ppm	35	22	464	276	89	85
Sr ppm	10	11	52	35	11	7.4
Th ppm	<4.1		13	3.8	4.5	3.7
U ppm	<3.2		1.2	1.7	<3.2	
Zr ppm	138	102	373	126	122	69
Nb ppm	2.8	1.3	14	4.6	4.0	1.8
Mo ppm	<1.2		2.2	0.4	0.7	1.2
Cr ppm	9.1	1.3	68	8.6	7.3	4.5
V ppm	5.5	2.2	53	32	7.3	5.1
Sc ppm	1.3	0.2	10	5.7	1.8	1.4
Ni ppm	2.3	1.8	17	9.1	2.7	2.6
Co ppm	1.6	0.5	16	2.6	2.7	1.3
Pb ppm	4.7	2.6	11	8.8	3.9	3.0
Zn ppm	12	2.3	48	6.3	12	3.0
Cu ppm	11	7.8	23	17	23	28
S ppm	206	146	323	395	783	868
Y ppm	7.3	3.2	25	10	8.6	2.9
La ppm	7.4	2.4	32	1.4	12	3.2
Ce ppm	15	5.3	66	4.0	23	8.0
Nd ppm	6.7	3.0	35	3.1	11	3.8

Table 7.6 Regional Quartzite correlation matrix

	Si	Zr	Y	P	Cu	Pb	Zn	Ba	Fe	K	Rb	Al	Ti	Nb	V	Cr	Ca	Na	La	Ce	Nd		
Si	*																					Si	
Zr		*																					Zr
Y			*																				Y
P				*																			P
Cu					*																		Cu
Pb						*																	Pb
Zn							*																Zn
Ba								*															Ba
Fe									*														Fe
K										*													K
Rb											*												Rb
Al												*											Al
Ti													*										Ti
Nb														*									Nb
V															*								V
Cr																*							Cr
Ca																	*						Ca
Na																		*					Na
La																			*				La
Ce																				*			Ce
Nd																					*		Nd

Pearson product-moment correlation matrix performed on log (10) transformed data
n = 7

Codes:

Si = SiO2
Ti = TiO2
Al = Al2O3
Fe = Fe2O3
Mn = MnO
Mg = MgO
Ca = CaO
Na = Na2O
K = K2O
P = P2O5

1 =
2 =
3 =
4 =
- =

Correlation not significant at the 90 % confidence limit
Correlation significant at the 90 % confidence limit
Correlation significant at the 95 % confidence limit
Correlation significant at the 99 % confidence limit
Correlation significant at the 99.8 % confidence limit
Negative correlation

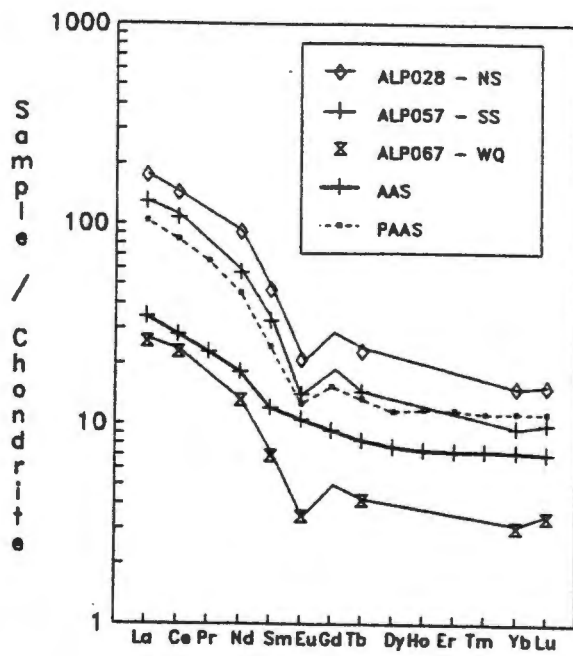


Fig. 8.1 (a) Chondrite normalised NS (ALP028), SS (ALP057), and WQ (ALP067) INAA REE patterns compared with those of Australian Archaean shales (AAS) and post-Archaean Australian shales (PAAS). Chondrite values used for normalization are from Taylor and Gorton (1977). AAS analysis is from Taylor and McLennan (1981), while PAAS values come from Nance and Taylor (1976)

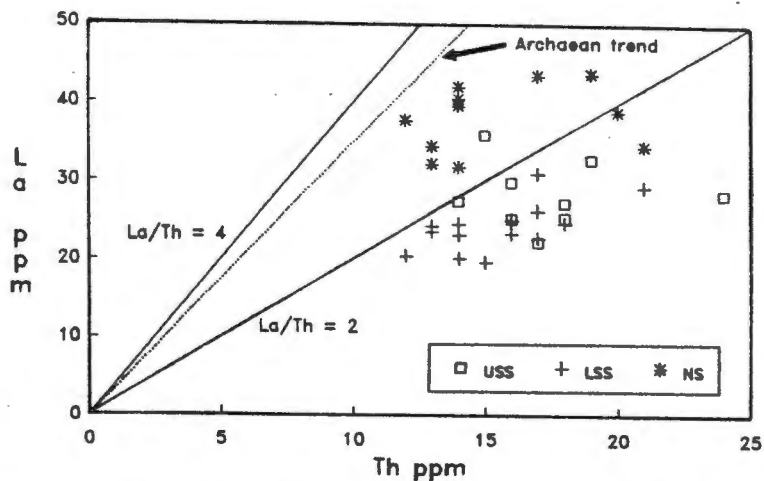


Fig. 8.2 NS and SS La vs Th concentrations on plots after McLennan et al. (1983)

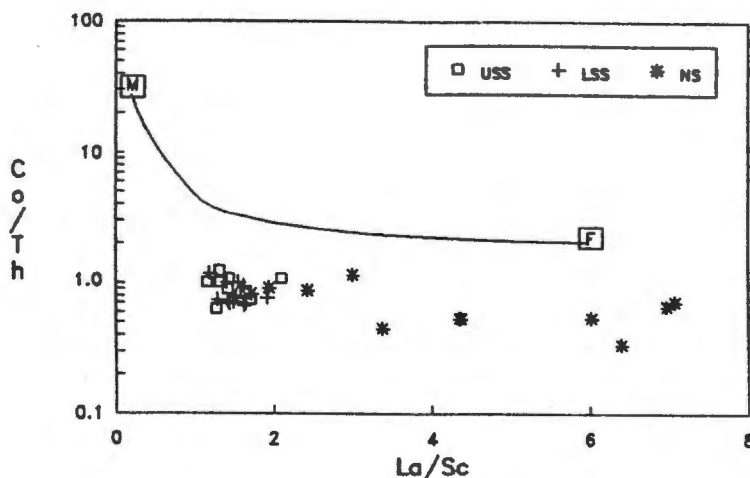


Fig. 8.3 NS and SS Co/Th vs La/Sc concentrations on plots after McLennan et al. (1983). M = average Archaean mafic volcanic rocks; F = average Archaean felsic volcanic rocks

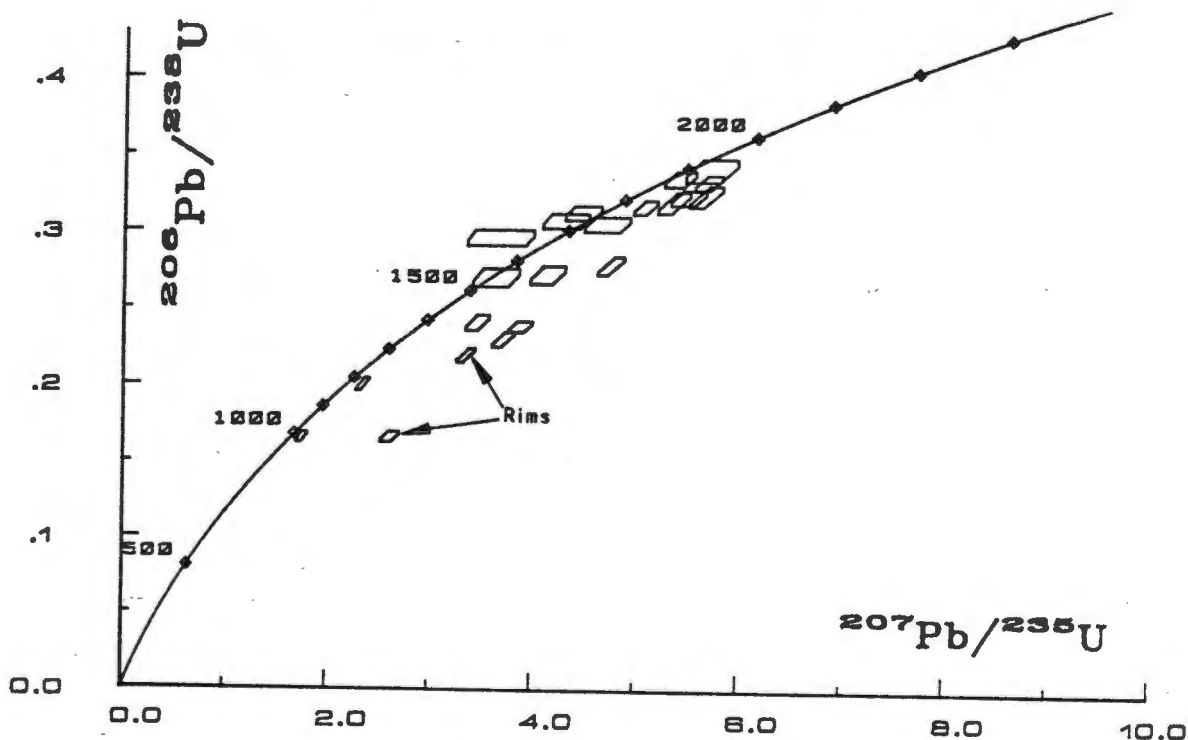


Fig. 8.4 Concordia diagram of ion microprobe results from single zircons from WQ (after Armstrong et al., 1988)

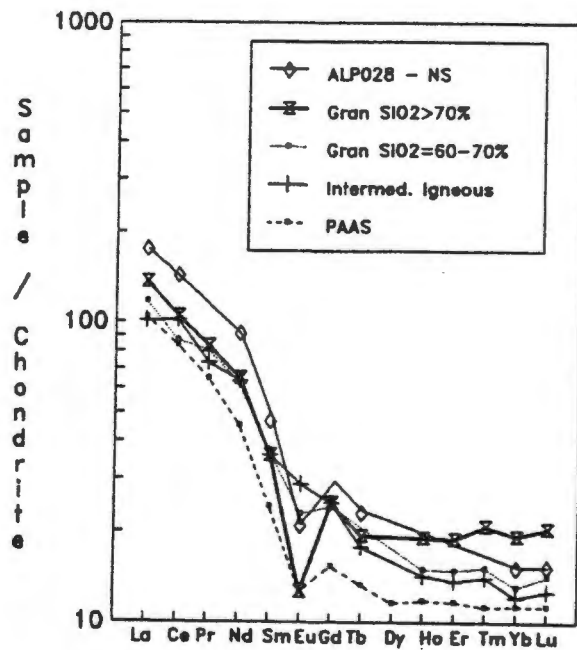


Fig. 8.5 Chondrite normalised BS (ALP028) REE patterns compared with those of siliceous to intermediate rocks and to PAAS. Chondrite values used for normalization are from Taylor and Gorton (1977). Granite and intermediate rock REE values are taken from Haskin et al. (1968), while PAAS values come from Nance and Taylor (1976)

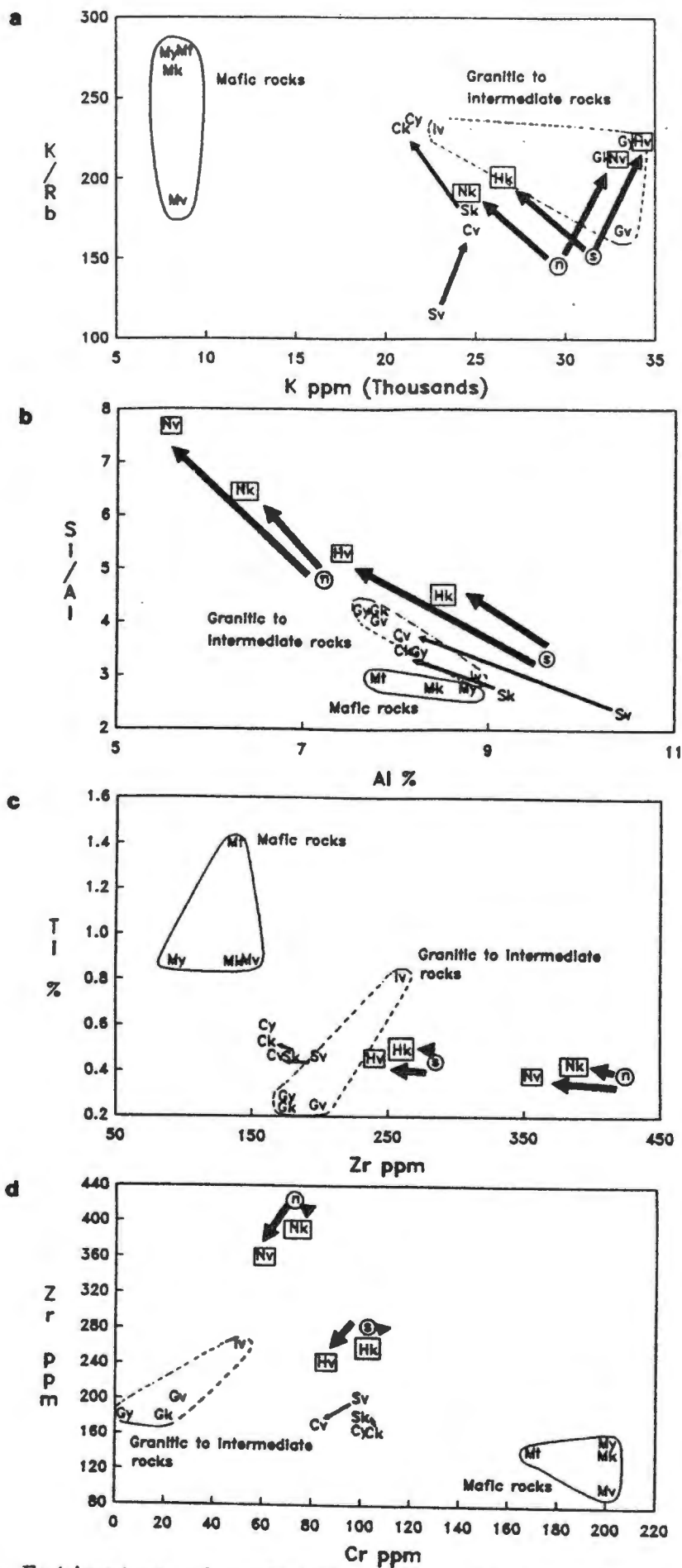


Fig. 8.6 Estimates of average crust which produced BS, using plots of: (a) K/Rb vs K ; (b) Si/Al vs Al ; (c) Ti vs Zr ; (d) Zr vs Cr . Average rock-types annotated thus: n = NS; s = SS; N and H = calculated crust which produced NS and SS, respectively; v = data from Vinogradov (1962); k = data from Krauskopf (1979); t = data from Turekian (1972); y = data from Taylor (1964); s = shale average; c = crustal average; M = mafic rocks; I = intermediate rocks ($SiO_2 < 60\%$); G = granite ($SiO_2 > 60\%$)

Table 8.1 BS CIA values relative to various rock-types and clays

	Granitic rocks	Muscovite	Montmor.-illite	Kaolinite-chlorite	Average shale	NS	SS
CIA	45 - 55	75	75 - 85	100	70 - 75	75.5	79.1

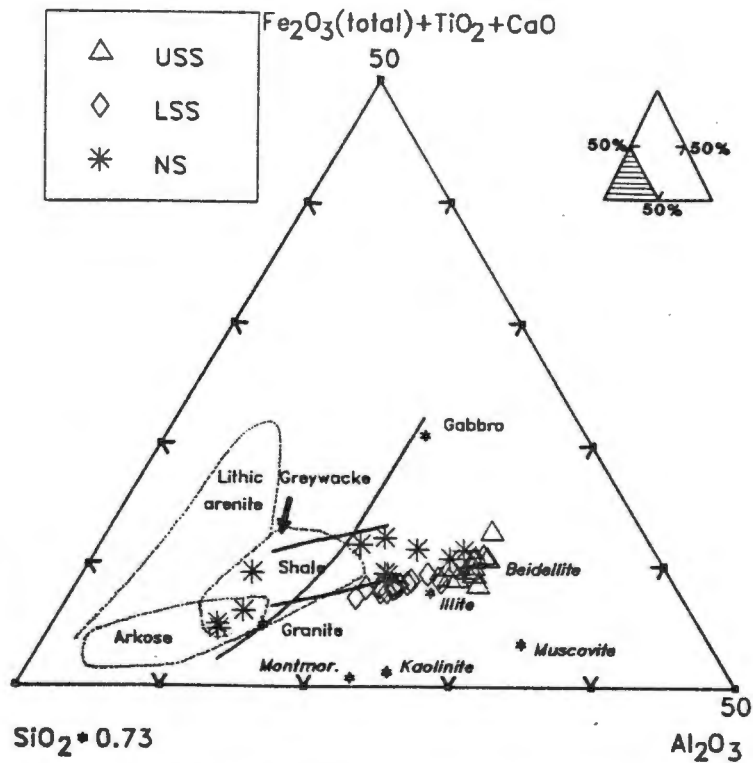


Fig. 9.1 Fields of NS and SS relative to sedimentary and igneous fields defined by de la Roche (1966) in the ternary diagram $\text{Fe}_2\text{O}_3(\text{total})+\text{TiO}_2+\text{CaO} - \text{SiO}_2 \cdot 0.73 - \text{Al}_2\text{O}_3$. Solid line passing through gabbro and granite defines the igneous trend. Ternary diagram represents the subset shown in the locality figure

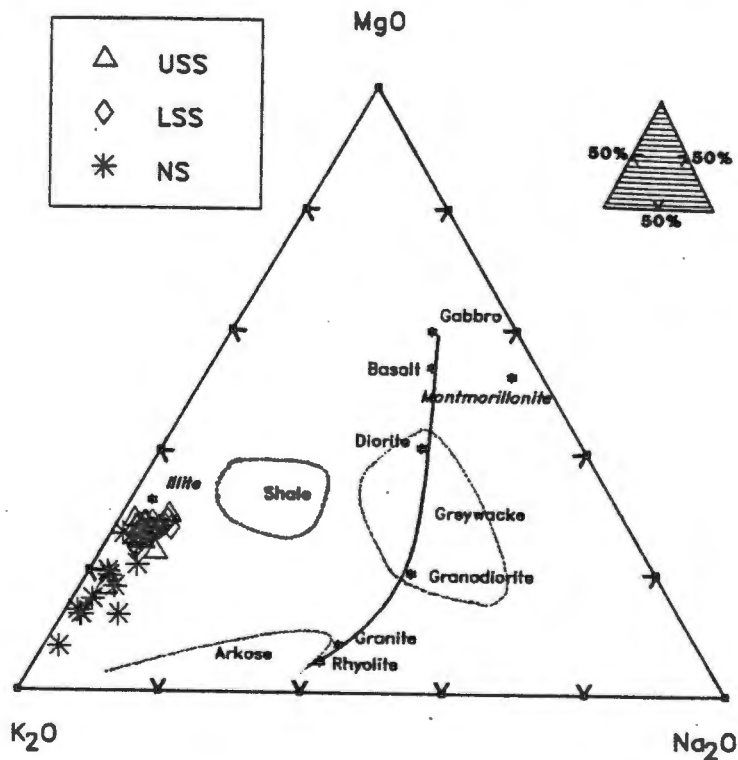


Fig. 9.2 Fields of NS and SS relative to sedimentary and igneous fields defined by de la Roche (1966) in the ternary diagram $\text{MgO} - \text{K}_2\text{O} - \text{Na}_2\text{O}$. Solid line passing through gabbro and granite defines the igneous trend. Ternary diagram represents the full field shown in the locality figure

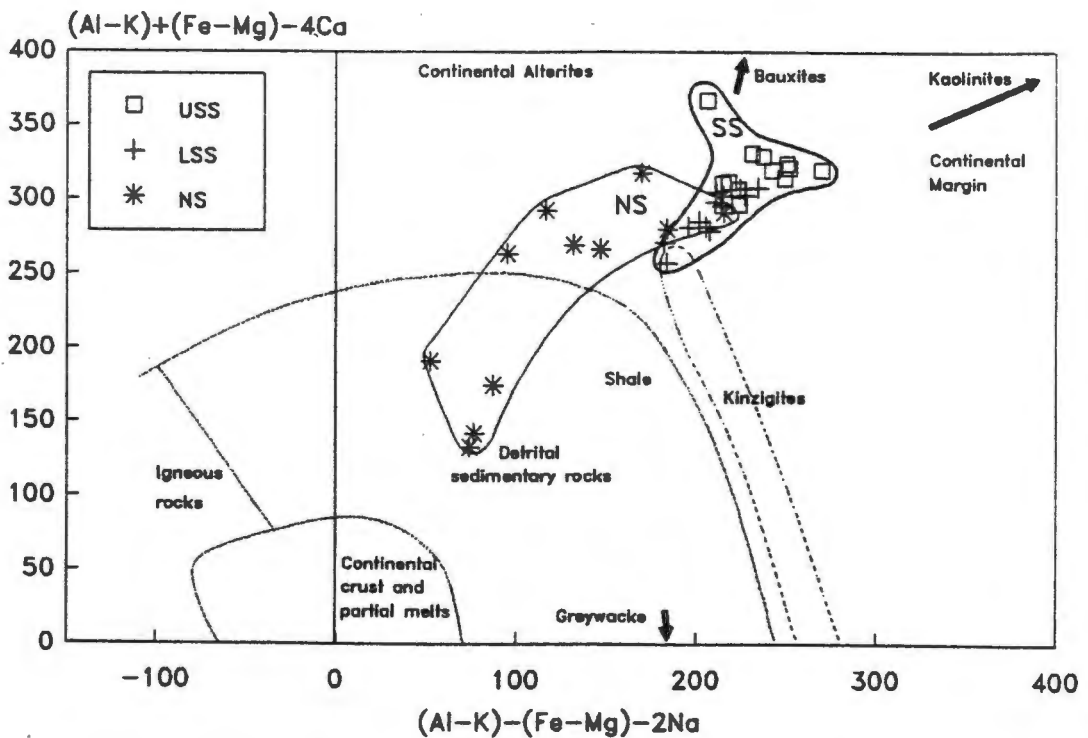


Fig. 9.3 Fields of NS and SS in the binary diagram $(Al-K)+(Fe-Mg)-4Ca$ vs $(Al-K)-(Fe-Mg)-2Na$ of de la Roche (1978) which shows progressive chemical changes that accompany the transformation of igneous rocks to various types of highly mature sediment

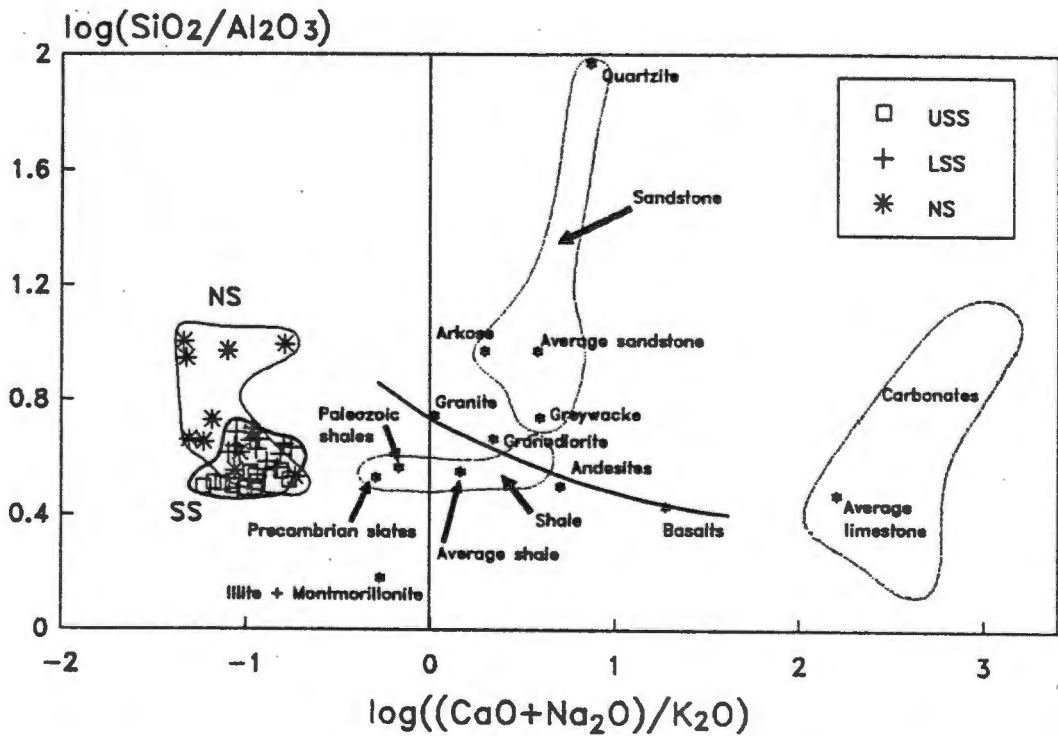


Fig. 9.4 Fields of NS and SS relative to sedimentary and igneous fields defined by Garrels and MacKenzie (1971) in the binary diagram $\log(SiO_2/Al_2O_3)$ vs $\log((CaO+Na_2O)/K_2O)$

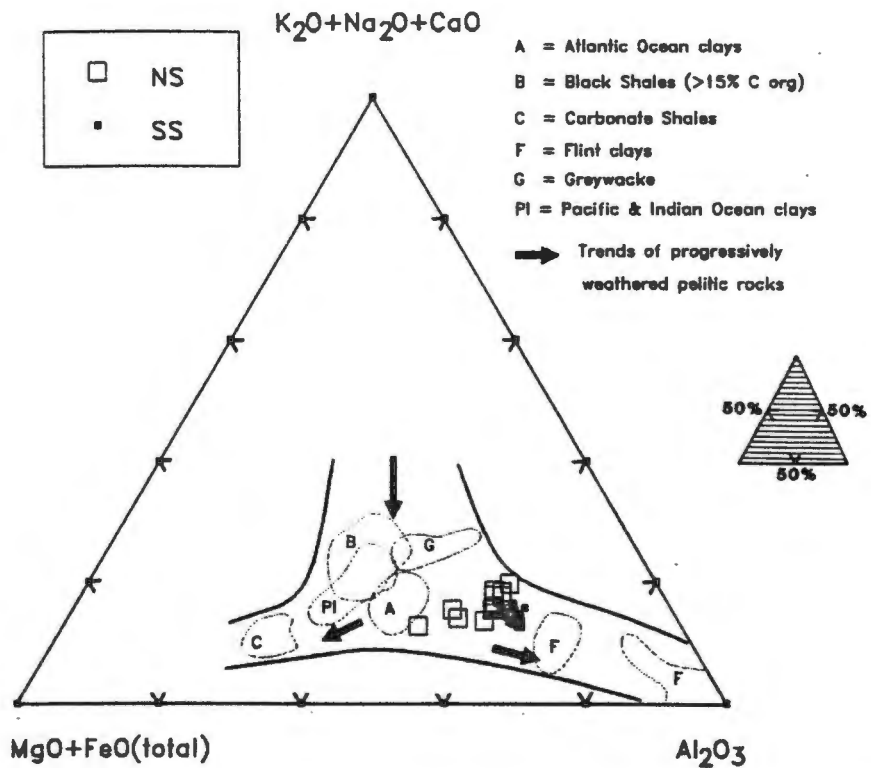


Fig. 9.5 Fields of NS and SS relative to progressively more mature pelitic rocks in the ternary diagram $K_2O+Na_2O+CaO - MgO+FeO(total) - Al_2O_3$, from Englund and Jorgensen (1973). Ternary diagram represents the full field shown in the locality figure

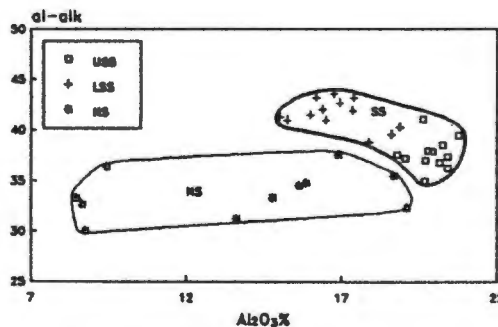


Fig. 9.6 Fields of NS and SS in binary diagram of Niggli al-alk vs Al_2O_3

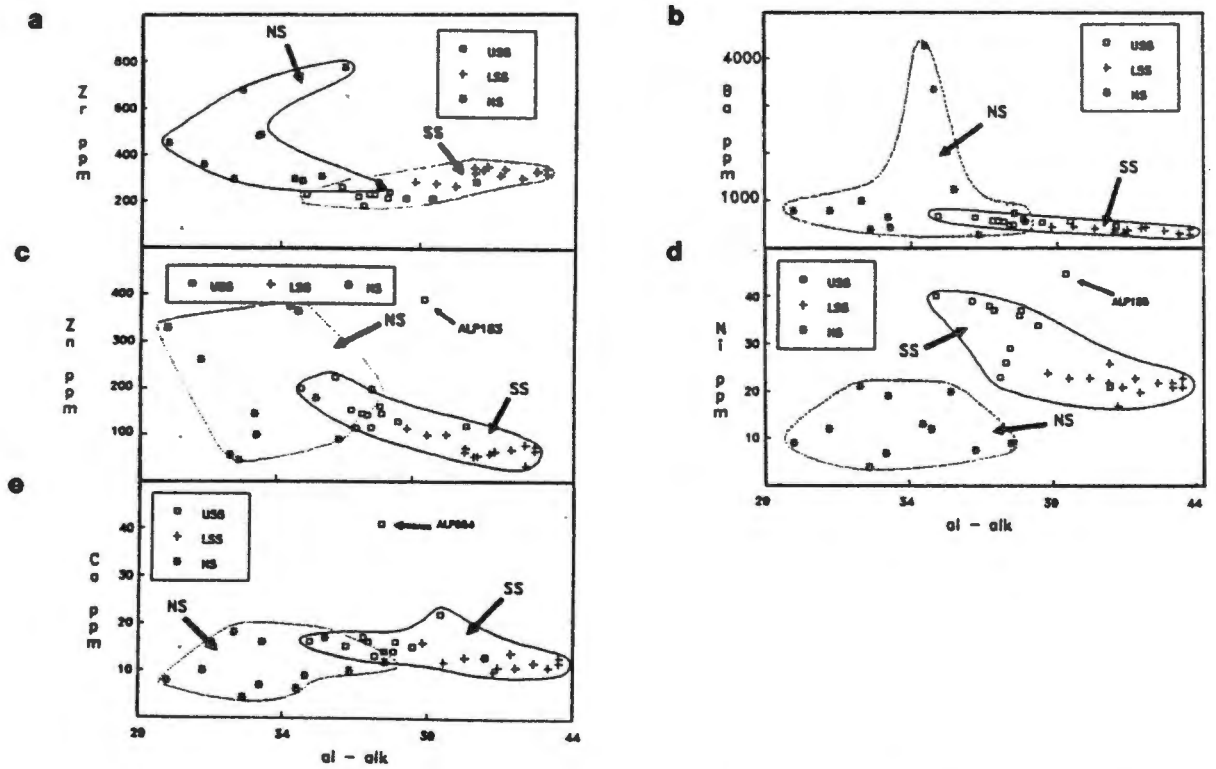


Fig. 9.7 Fields of NS and SS in binary diagrams of trace elements vs Niggli al-alk: (a) Zr; (b) Ba; (c) Zn; (d) Ni; (e) Co

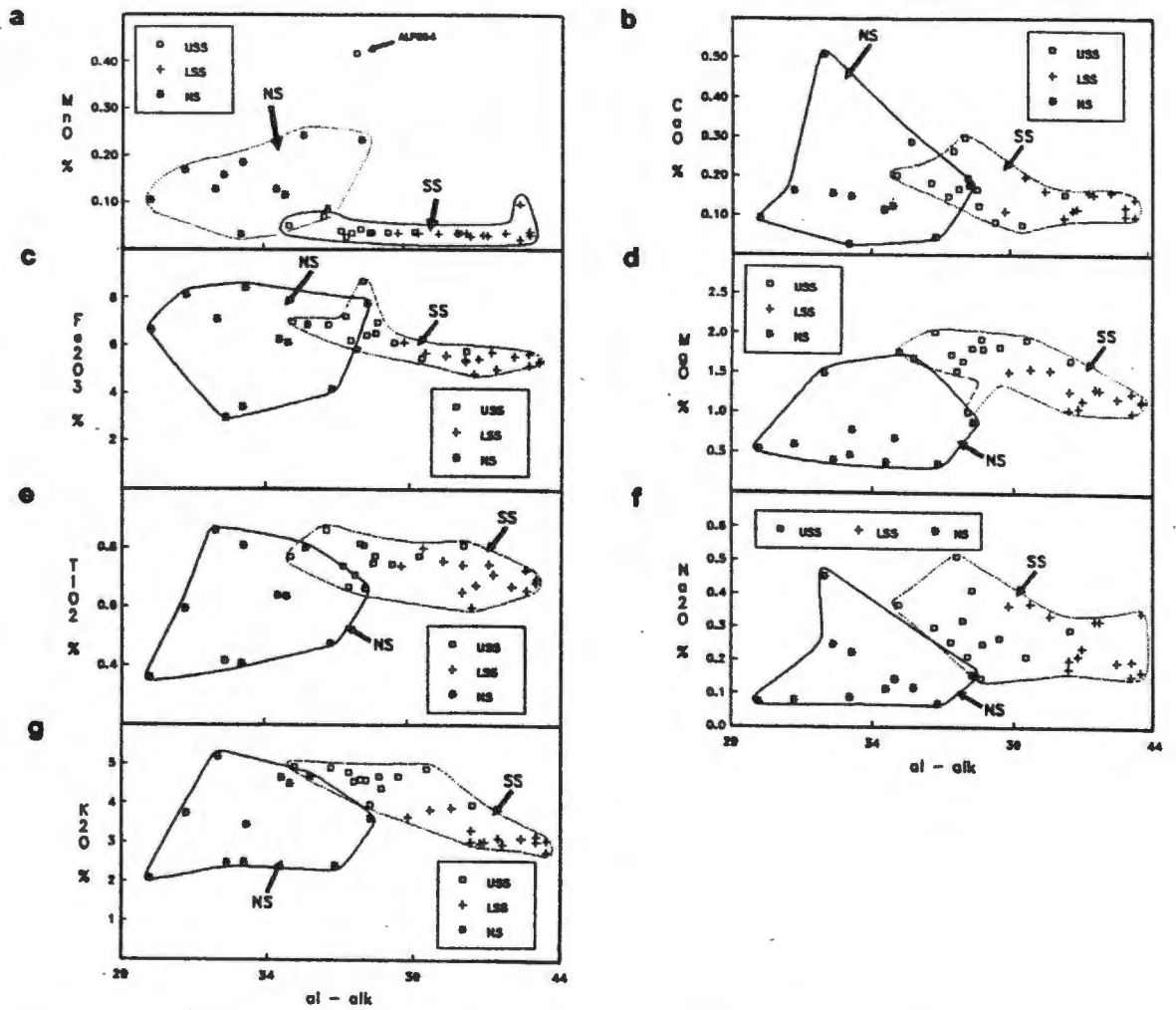


Fig. 9.8 Fields of NS and SS in binary diagrams of major elements vs Niggli al-alk: (a) MnO; (b) CaO; (c) Fe₂O₃; (d) MgO; (e) TiO₂; (f) Na₂O; (g) K₂O

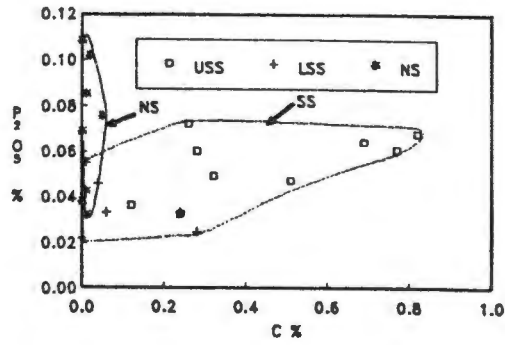


Fig. 9.9 Fields of NS and SS in binary diagram of P_2O_5 vs C

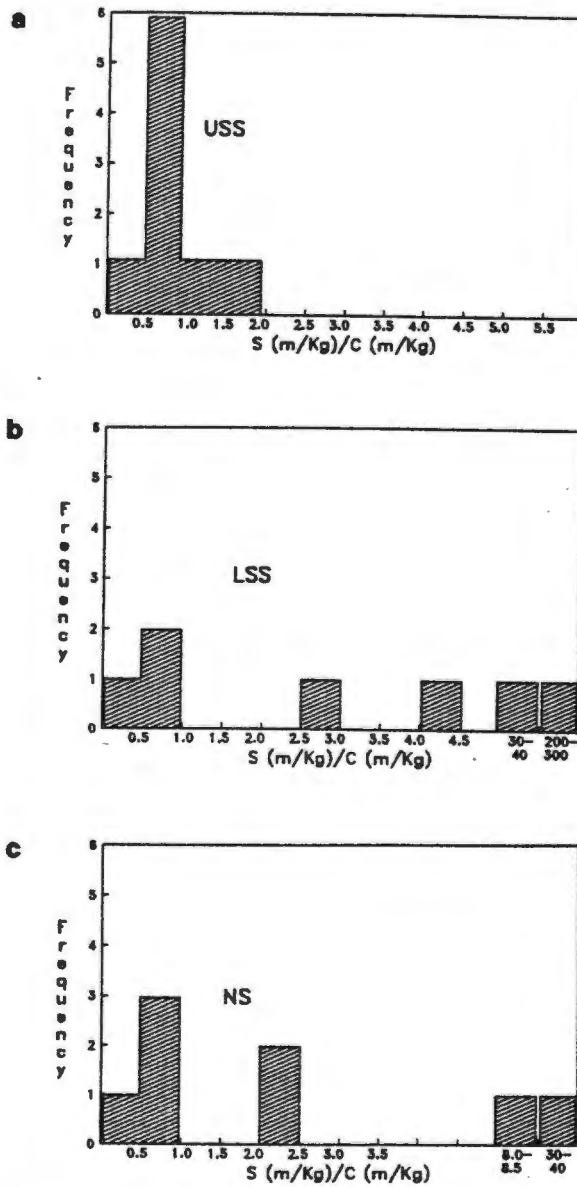


Fig. 9.10 Histograms of S/C ratios: (a) USS; (b) LSS; (c) NS

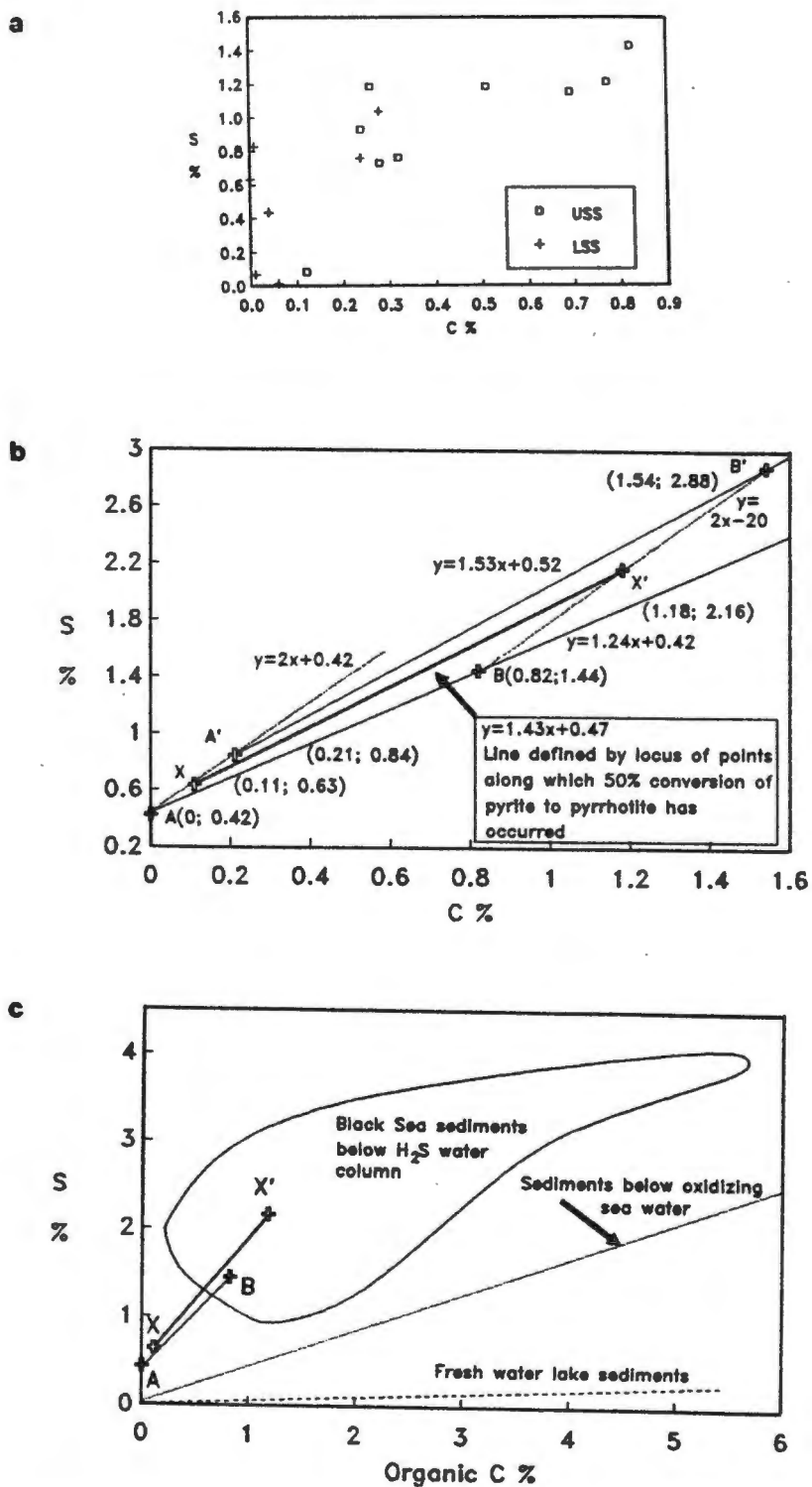


Fig. 9.11 S vs C plots relating to SS: (a) SS S vs C raw data; (b) Graphic representation of the conditions bounding the pre-metamorphic S and C concentrations in SS (see Appendix H for details); (c) SS S vs C curves relative to sediments deposited below various water types. Black Sea sediments from Levinthal (1983); sediments from below normal oxidizing sea water taken from Levinthal (1983) and Berner (1984); modern fresh water lake sediments from Berner (1984)

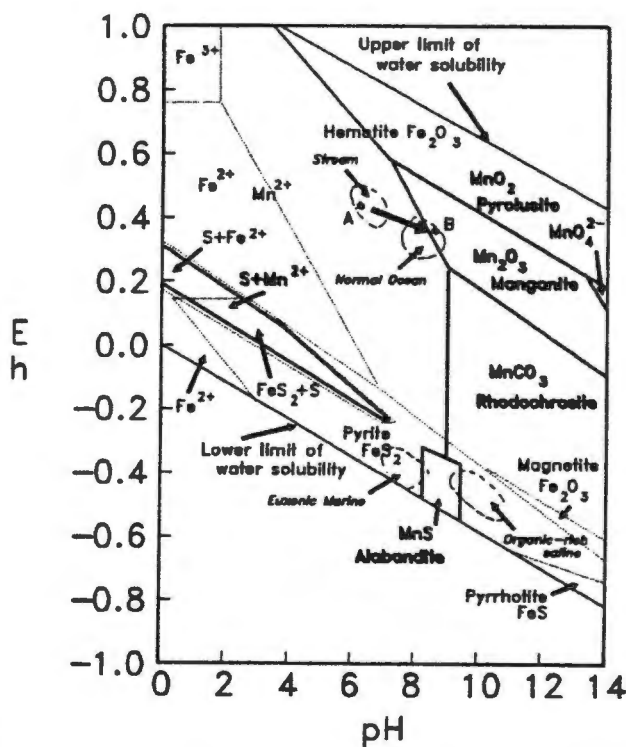


Fig. 9.12 Stability relations in Eh-pH space between some Fe and Mn compounds in water at 25°C and 1 atmosphere total pressure. Dark and light lines mark the Mn and Fe fields, respectively. The Fe^{3+} , Fe^{2+} and Mn^{2+} fields are aqueous, of which the Mn^{2+} field is by far the largest. Activity of total dissolved S = $10^{-1}m$. At lower S concentrations the fields of sulphides shrink markedly. Activity for total dissolved CO_2 = $10^{-4}m$ for Mn, and 0 for Fe. The field of siderite virtually disappears for total dissolved CO_2 < $10^{-3}m$. Modified after Garrels and Christ (1965, pp221, 243 and 381). Also plotted are fields of various naturally occurring waters taken from Baas Becking et al. (1960). The arrow from A to B marks the change in conditions when fresh water mixes with sea water

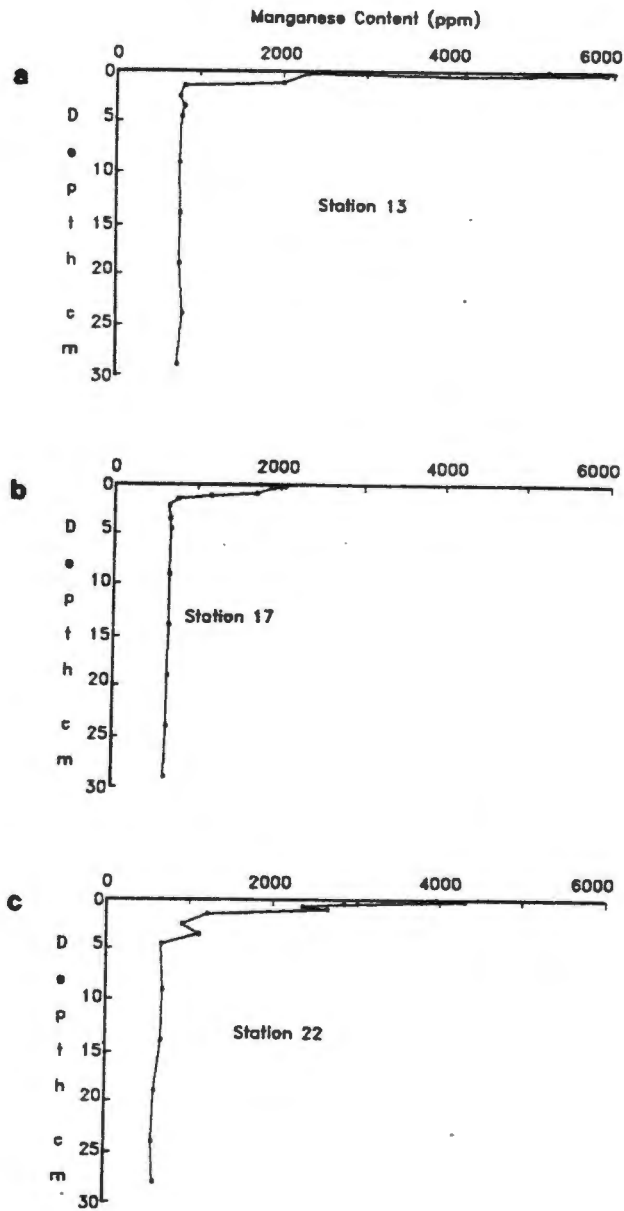


Fig. 9.13 Profiles of total Mn in Laurentian Trough sediments (from Sundby et al., 1981)

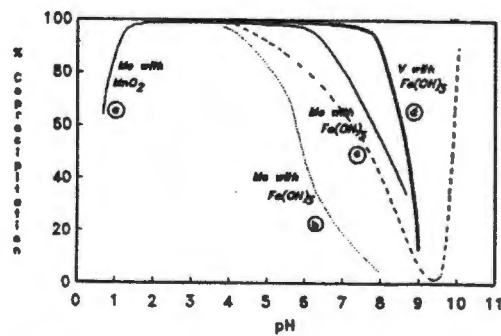


Fig. 9.14 Co-precipitation of Mo by Mn and Fe oxides under varying pH conditions, after Evans et al. (1974-1978). Curves as follows: a. from Chan and Riley (1966); b. and d. Ishibashi et al. (1962); c. Kim and Zeitlin (1968)

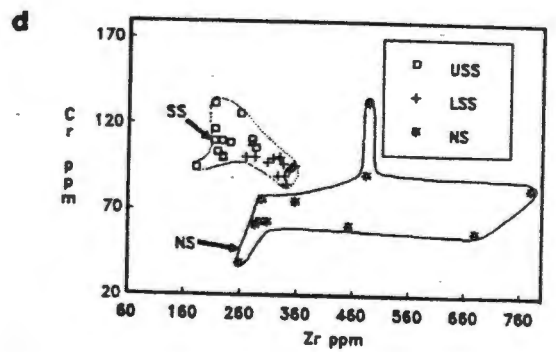
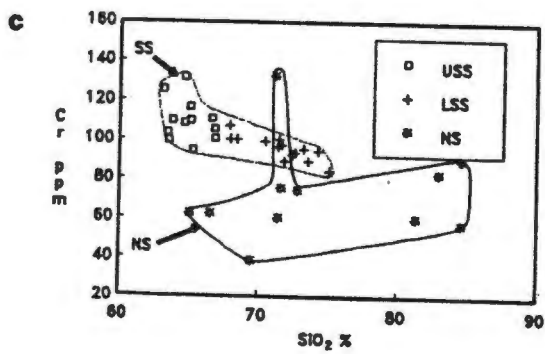
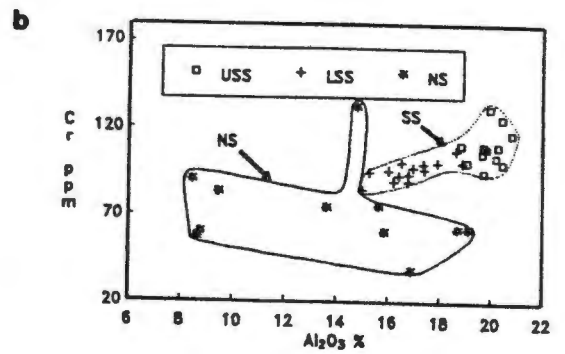
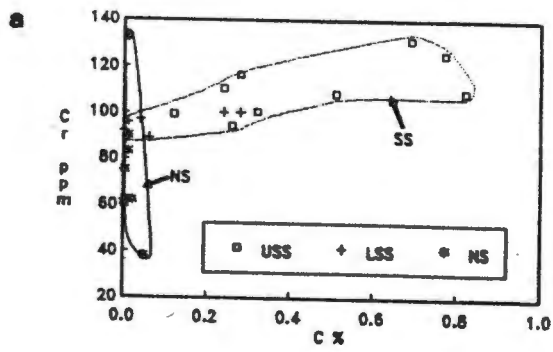


Fig. 9.15 Fields of NS and SS in binary diagram of Cr versus various elements: (a) Cr vs C; (b) Cr vs Al_2O_3 ; (c) Cr vs SiO_2 ; (d) Cr vs Zr

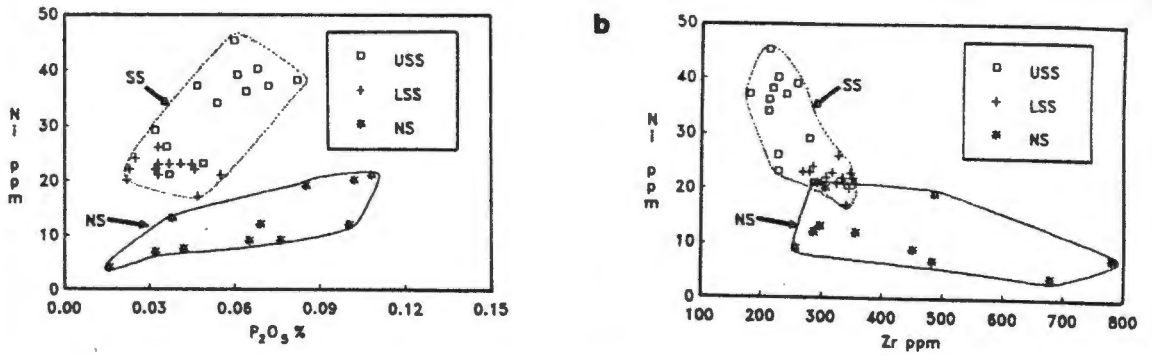


Fig. 9.16 Fields of NS and SS in binary diagram of Ni versus various elements: (a) Ni vs P_2O_5 ; (b) Ni vs Zr

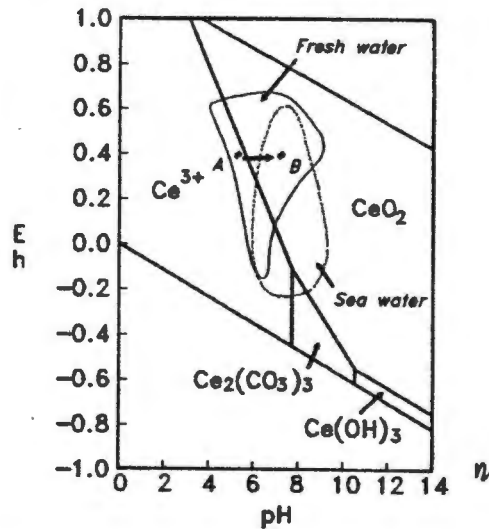


Fig. 9.17 Stability relations for Ce in Eh-pH space, at 25°C and 1 bar pressure. Activities of ions are M^{3+} , M^{2+} and $M^{4+} = 10^{-6}$; total $CO_2 = 10^{-3}$ (after Brookins, 1983). Water fields after Baas Becking et al. (1960). The line joining A to B represents the approximate redox change encountered when particles pass from river water into the sea.

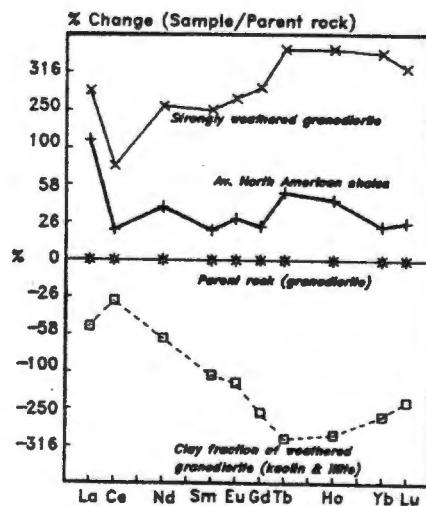


Fig. 9.18 Variations in rare earth concentrations during weathering of granodiorite (after Nesbitt, 1979).

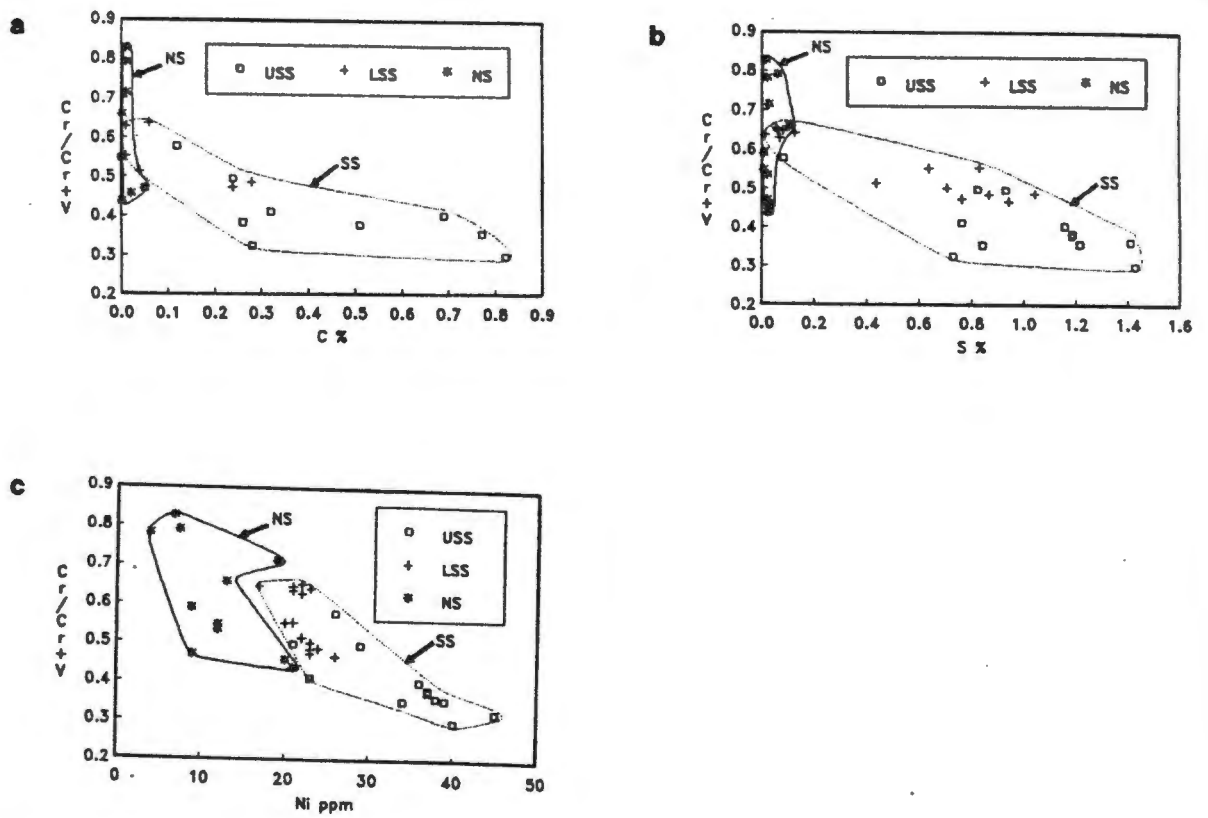


Fig. 9.19 Fields of NS and SS in binary diagram of $Cr/(Cr+V)$ versus various elements: (a) C; (b) S; (c) Ni

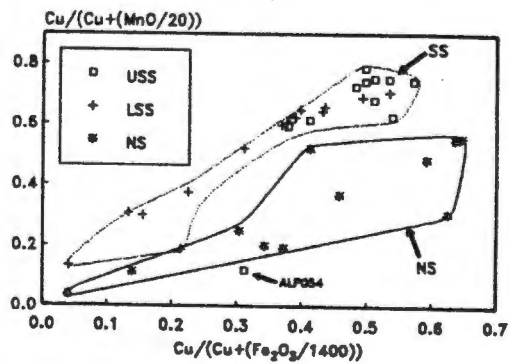


Fig. 9.20 Fields of NS and SS in binary diagram of $Cu/(Cu+(MnO/20))$ versus $Cu/(Cu+(Fe_2O_3/1400))$

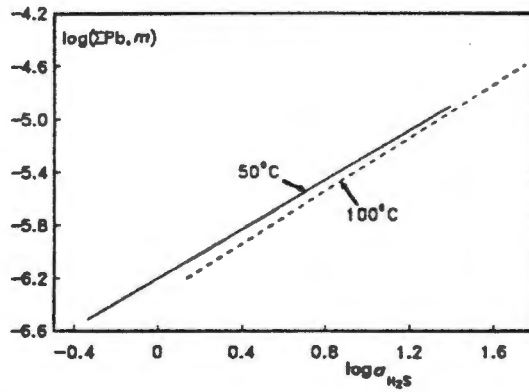


Fig. 9.21 The dependence of Pb concentrations on a_{H_2S} for galena saturated solutions at 50°C and 100°C (after Giordano and Barnes, 1979)

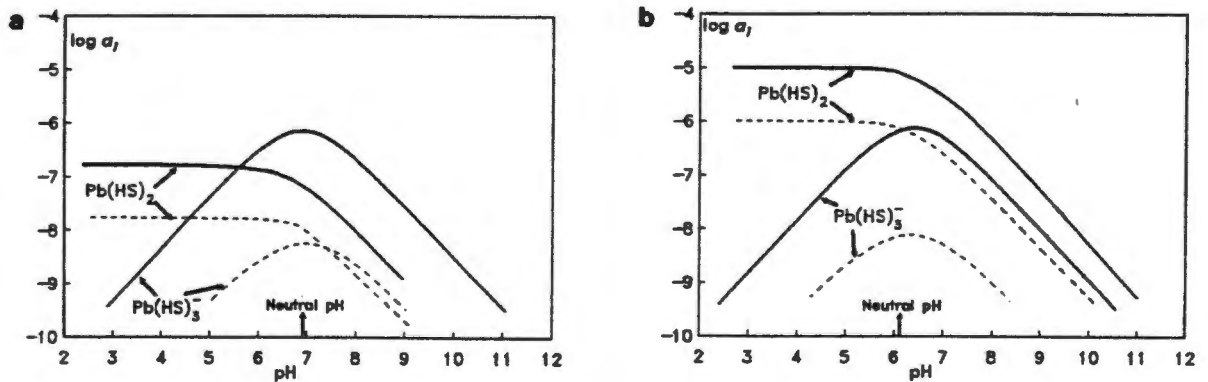


Fig. 9.22 Activities of the complexes $Pb(HS)_2$ and $Pb(HS)_3^-$: (a) 30°C; (b) 100°C. Total S activity = 1 for heavy line and 0.1 for light line. After Giordano and Barnes (1979)

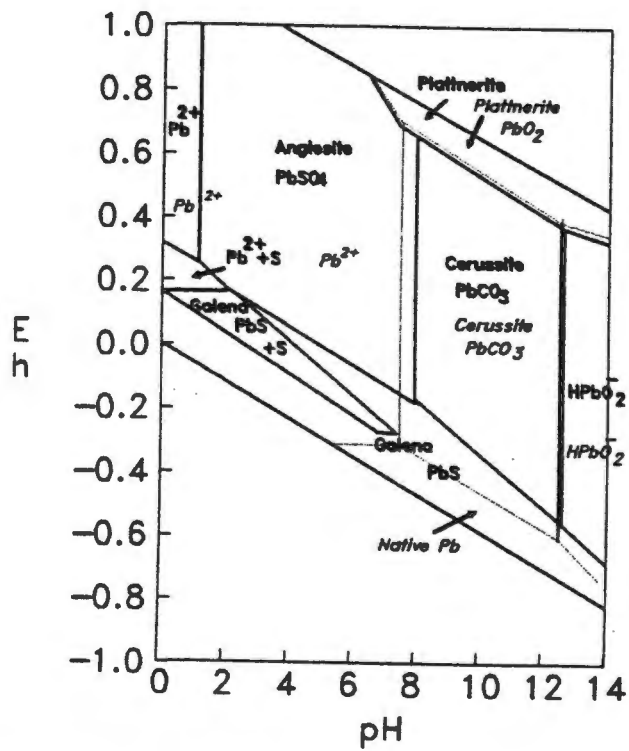


Fig. 9.23 Stability relations in Eh-pH space between various Pb compounds in water at 25°C and 1 atmosphere total pressure. Aqueous Pb covers a wide field in the absence of dissolved S, and this field shrinks to be restricted to the strongly acid range with increase in S content to 10^{-1} m . Dark lines represent fields for conditions of $P_{\text{CO}_2} = 10^{-4} \text{ m}$ and $P_{\text{S}} = 10^{-1} \text{ m}$; light lines for $P_{\text{CO}_2} = 10^{-4} \text{ m}$ and $P_{\text{S}} = 0 \text{ m}$. After Garrels and Christ (1965, pp234 and 237)

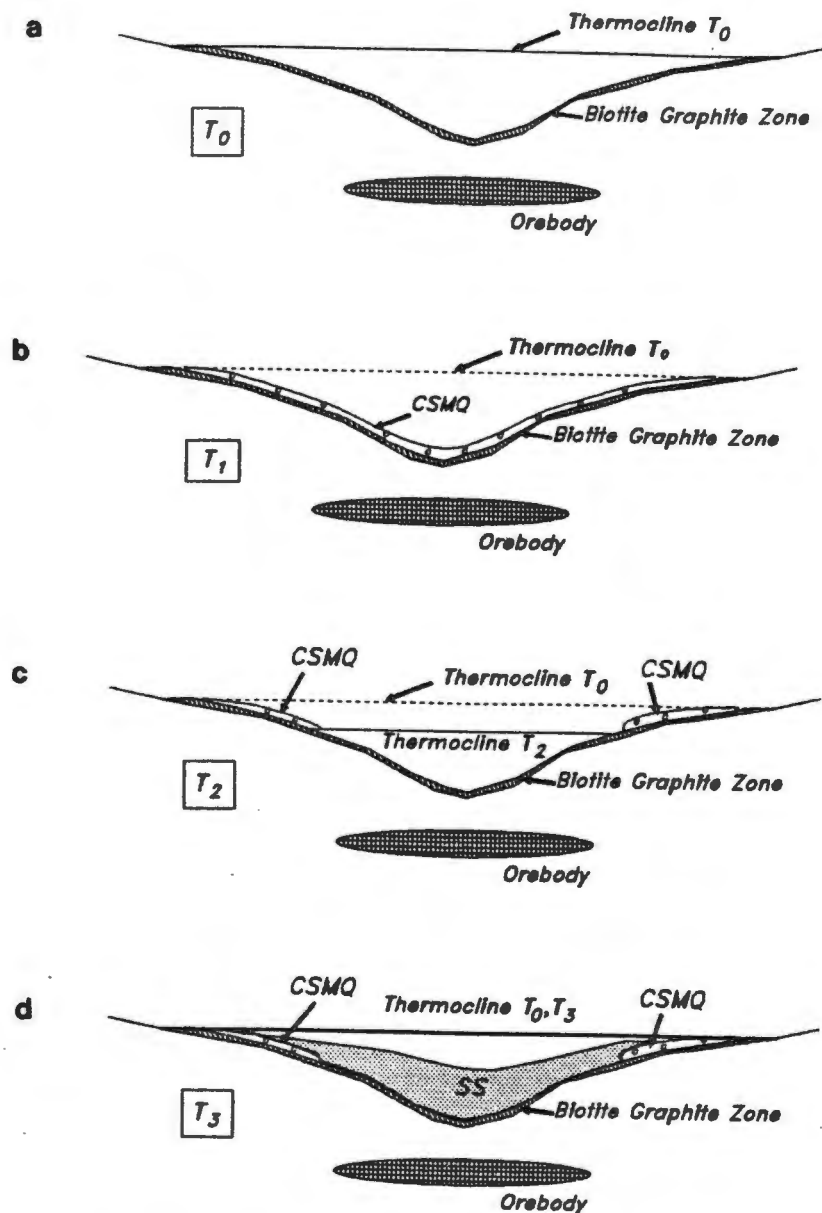


Fig. 9.24 Schematic model of basin geometry control on distribution of CSMQ lenses: (a) BGZ forms above Broken Hill orebody and beneath stable thermocline at time T_0 ; (b) after disruption of the thermocline, CSMQ precipitates (time T_1); (c) below the newly established thermocline (T_2) in the deepest part of the basin, CSMQ goes back into solution, leaving lenses of CSMQ on the flanks of the basin above the T_2 line; (d) the thermocline at time T_3 is re-established at the approximate position of the T_0 thermocline level, with deposition of SS preserving the CSMQ lenses

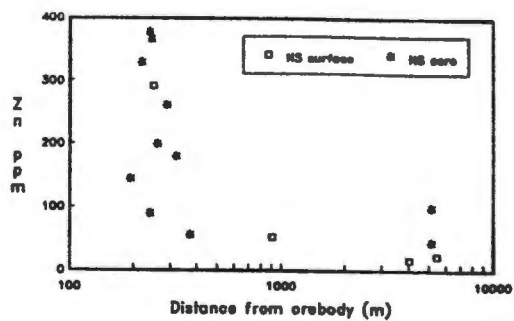


Fig. 9.25 NS Zn variations for surface outcrop and borehole core samples versus distance from the Broken Hill orebody

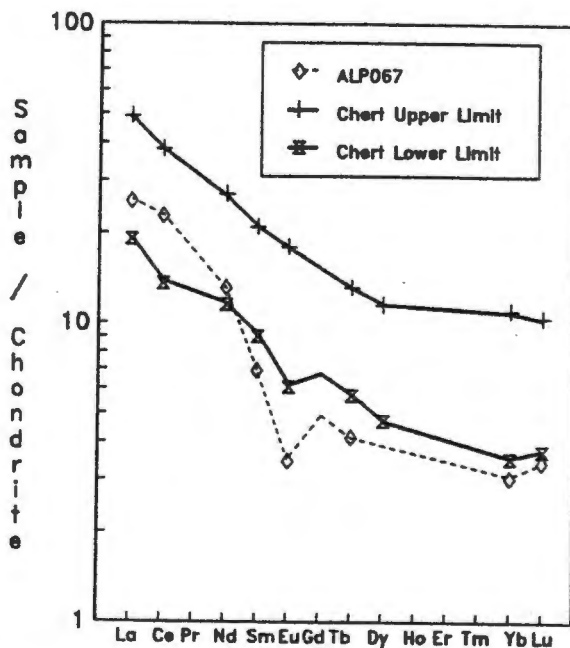


Fig. 9.26 Chondrite normalized WQ REE pattern (ALP067) compared with those from basalt associated deep ocean chert of Crerar et al. (1982)

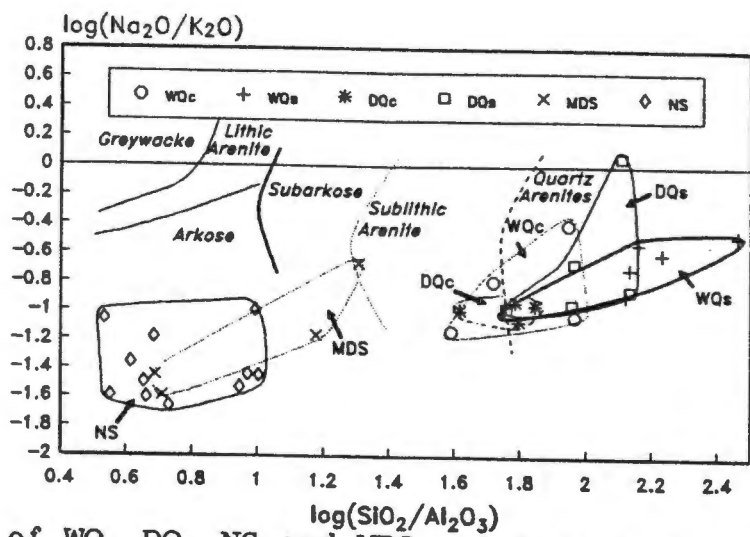


Fig. 9.27 Fields of WQ, DQ, NS and MDS relative to the sandstone fields of Pettijohn et al. (1972, p62) in the binary diagram $\log(\text{Na}_2\text{O}/\text{K}_2\text{O})$ versus $\log(\text{SiO}_2/\text{Al}_2\text{O}_3)$. c = core; s = surface

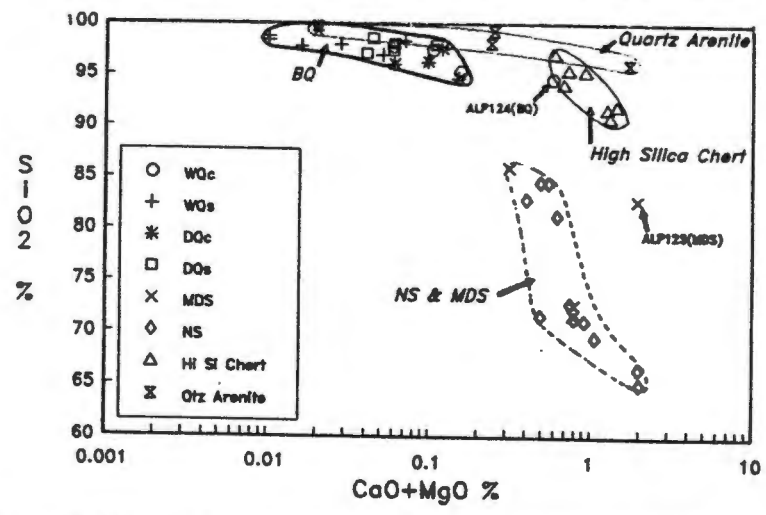


Fig. 9.28 Fields of WQ, DQ, NS and MDS relative to fields of quartz arenite and high silica chert in the binary diagram SiO_2 versus $\text{CaO}+\text{MgO}$.

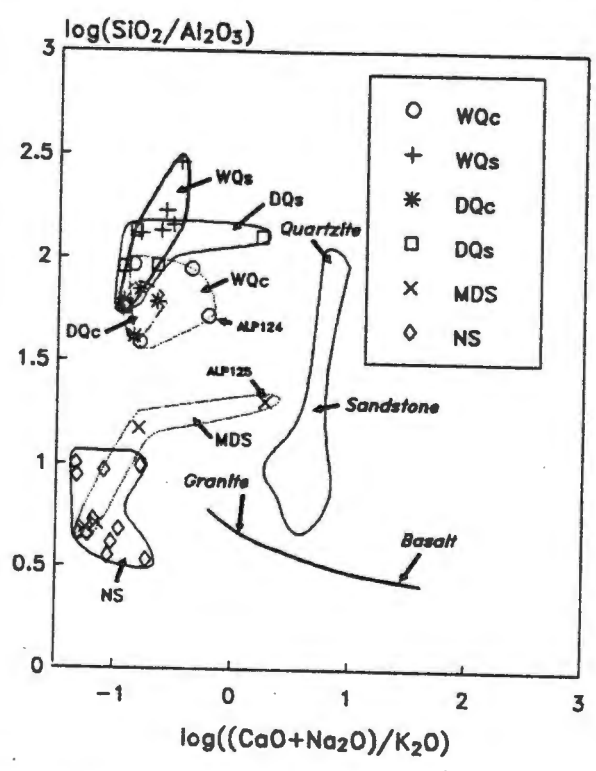


Fig. 9.29 Fields of WQ, DQ, NS and MDS relative to the sandstone-quartzite field of Garrels and MacKenzie (1971) in the binary diagram of $\log(\text{SiO}_2/\text{Al}_2\text{O}_3)$ versus $\log((\text{CaO}+\text{Na}_2\text{O})/\text{K}_2\text{O})$. Heavy line from granite to basalt defines the igneous trend

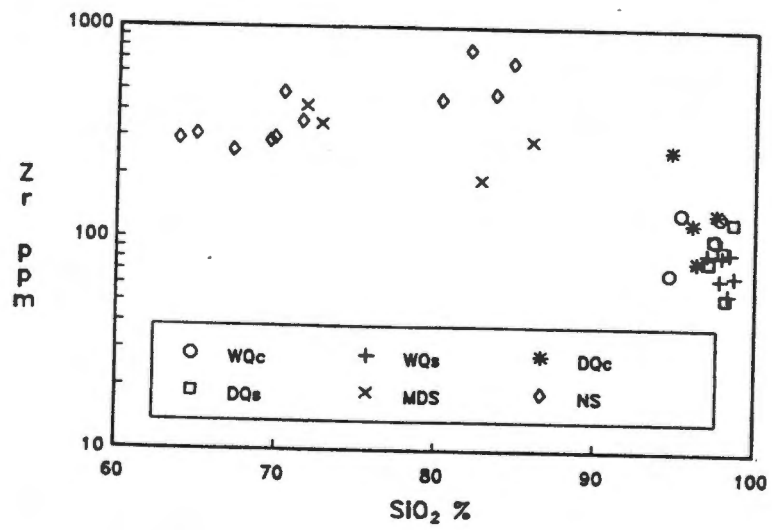


Fig. 9.30 Scatter plot of WQ, DQ, MDS and NS in binary diagram of Zr versus SiO₂

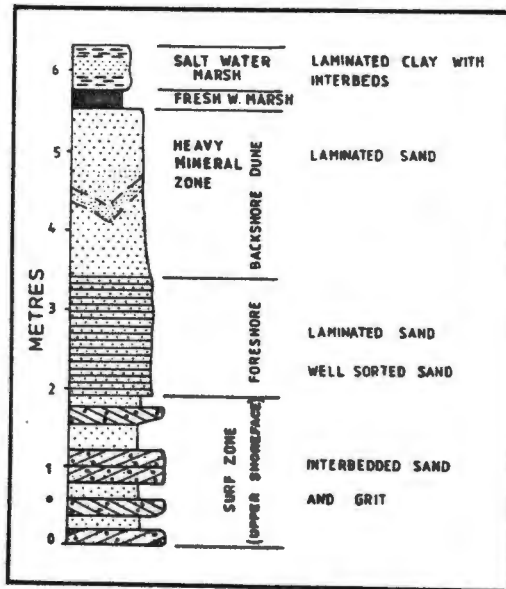


Fig. 9.31 Profile of a prograding beach barrier from Reinson (1979)

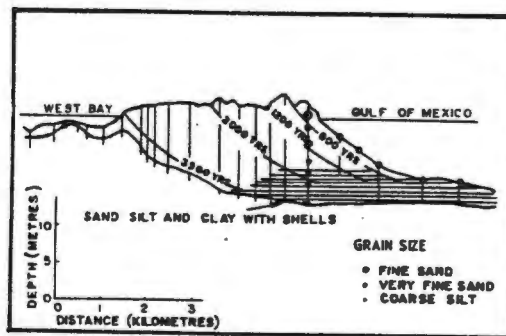


Fig. 9.32 Diachronous rock types in the prograding Galveston beach barrier island (after Bernard et al., 1962)

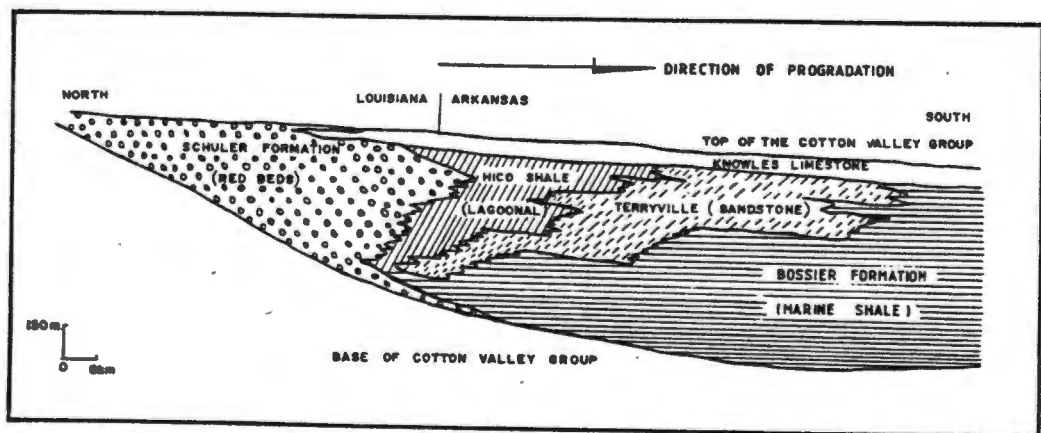


Fig. 9.33 Lithofacies of the Cotton Valley Group (after Thomas and Mann, 1966)

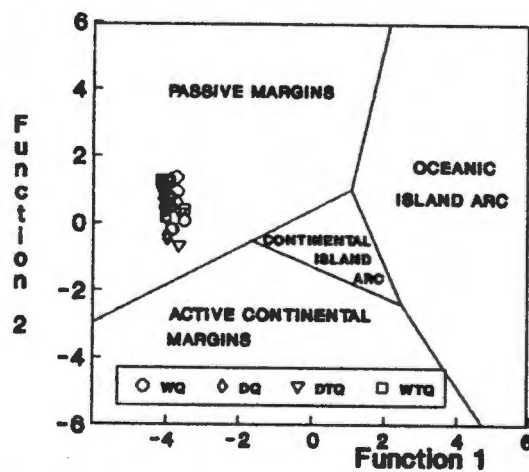


Fig. 9.34 Plot of discriminant scores of surface outcrop and borehole core samples from Broken Hill and Regional Quartzites in Function 1 and Function 2 space (after Bhatia, 1983). WQ = White Quartzite; DQ = Dark Quartzite; T = -type

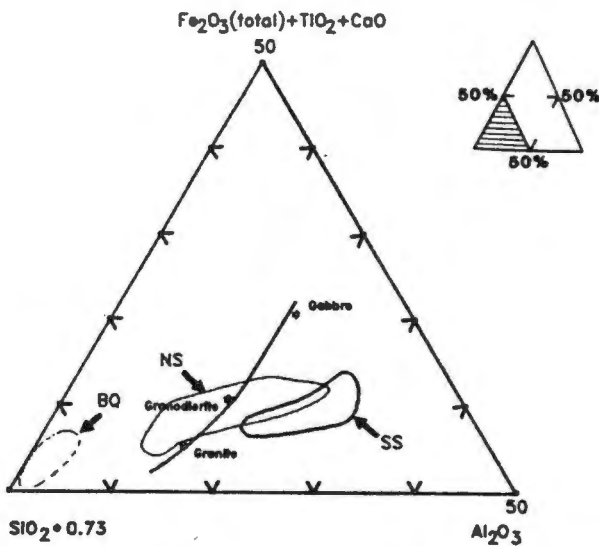


Fig. 9.35 Ternary diagram with apices of Fe_2O_3 (total) + TiO_2 + CaO , $\text{SiO}_2 \cdot 0.73$, and Al_2O_3 , showing initial residual alumina enrichment away from a granodioritic igneous composition, followed by progressively increasing SiO_2 content of NS and then BQ

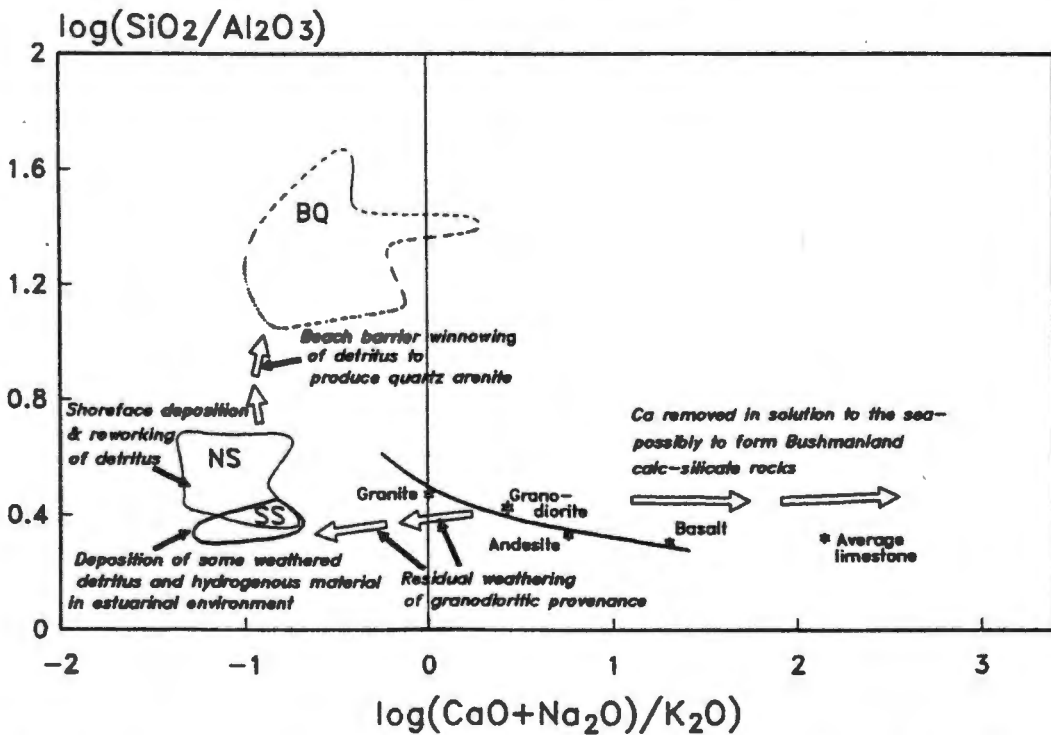


Fig. 9.36 Plot of $\log (\text{SiO}_2/\text{Al}_2\text{O}_3)$ vs $\log ((\text{CaO}+\text{Na}_2\text{O})/\text{K}_2\text{O})$ after Garrels and McKenzie (1971), showing the proposed geochemical model for the conversion of a granodioritic provenance via pelites of SS and NS composition, to quartz arenites having the composition of BQ

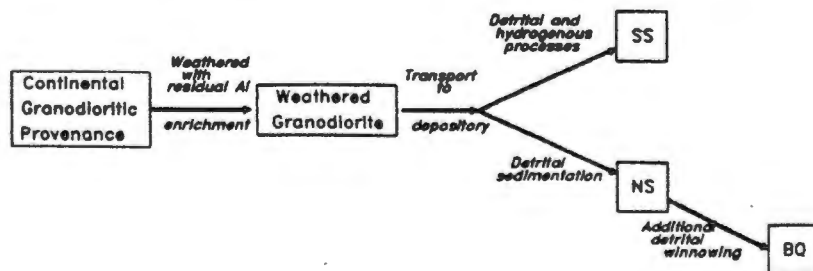


Fig. 9.37 Model flow diagram for genesis of SS, NS and BQ from an initial granodioritic provenance

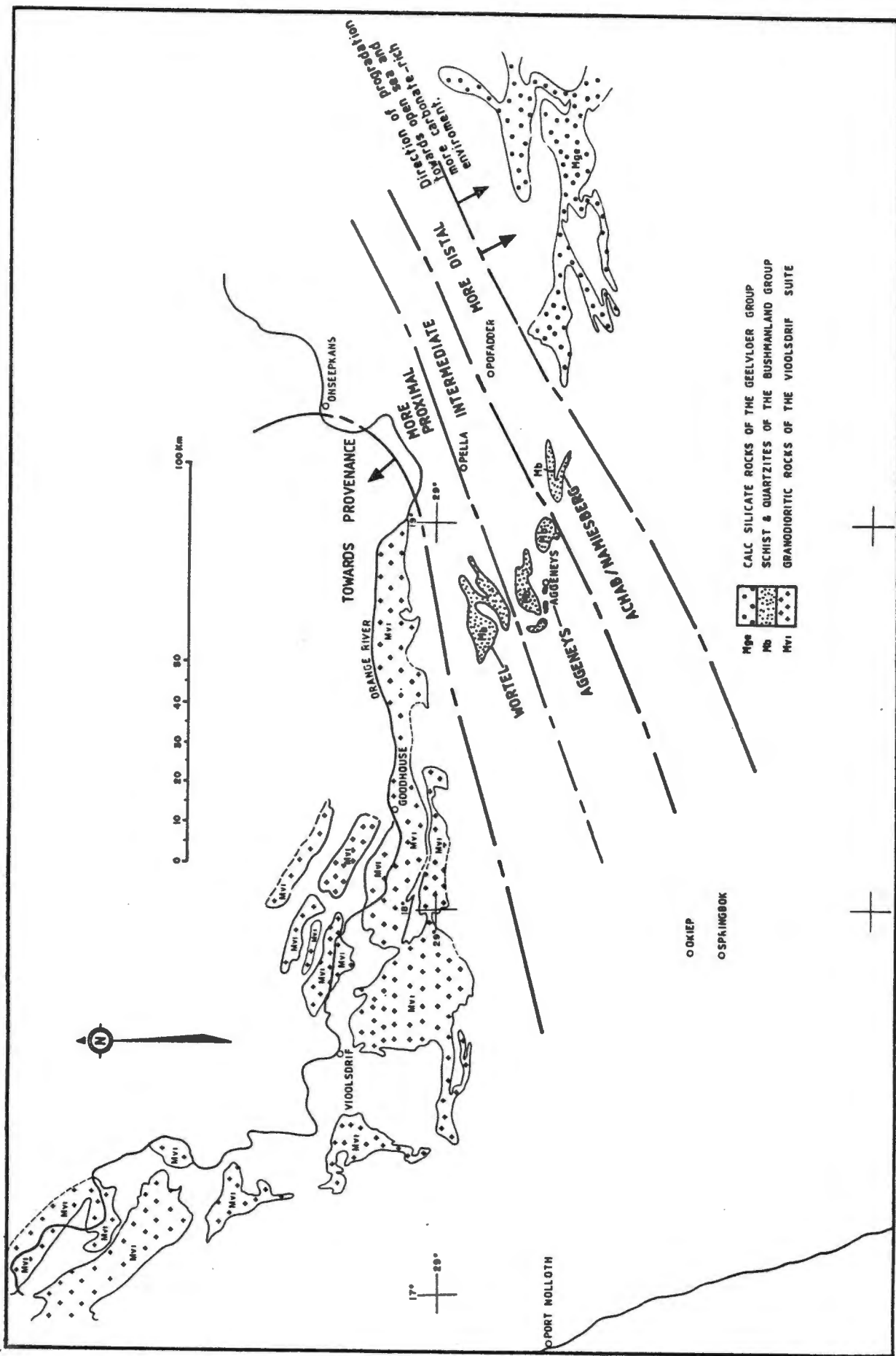


Fig. 9.38 Model showing paleo-geographical relationships between provenance, proximal and distal environments during sedimentation of the Aggeneys Subgroup

Table 9.1 Average Shale composition and comparison with average NS and SS: (a) Average Shale, average NS and SS; (b) Ratio between average element concentration of NS and average shale; (c) Ratio between average element concentrations of SS and average shale

	(a)			(b)		(c)	
	Average NS Shale †		SS	NS/Av. Shale		SS/Av. Shale	
	Mean	Mean	Mean	Element more concentrated in NS	Element less concentrated in NS	Element more concentrated in SS	Element less concentrated in SS
SiO ₂ %	53.407	74.697	68.737	SiO ₂ = 1.40	TiO ₂ = 0.80	SiO ₂ = 1.29	TiO ₂ = 0.96
TiO ₂ %	0.757	0.605	0.73	Fe ₂ O ₃ = 1.01	Al ₂ O ₃ = 0.78	Al ₂ O ₃ = 1.04	Fe ₂ O ₃ = 0.96
Al ₂ O ₃ %	17.417	13.62	18.161	MnO = 1.40	MgO = 0.32 *	K ₂ O = 1.27	MnO = 0.36 *
Fe ₂ O ₃ %	6.077	6.164	5.86	K ₂ O = 1.19	CaO = 0.05 @		MgO = 0.63
MnO %	0.102	0.143	0.037		Na ₂ O = 0.14 @		CaO = 0.04 @
MgO %	2.343	0.748	1.484		P ₂ O ₅ = 0.40 *		Na ₂ O = 0.24 *
CaO %	3.377	0.167	0.143				P ₂ O ₅ = 0.27 *
Na ₂ O %	1.130	0.16	0.275				
K ₂ O %	2.987	3.565	3.793	Rb = 1.27	Sr = 0.05 @		
P ₂ O ₅ %	0.169	0.067	0.045	Ba = 1.90	Nb = 0.98	Rb = 1.29	Ba = 0.68
Rb ppm	160	203	207	Th = 1.37	Cr = 0.74	Th = 1.37	Sr = 0.09 @
Ba ppm	660	1254	447	Zr = 2.36 *	V = 0.35 *	Zr = 1.57	Nb = 0.98
Sr ppm	383	21	36	Pb = 2.55 *	Se = 0.87	Cr = 1.06	V = 0.95
Th ppm	12	16	16	Zn = 2.20 *	Ni = 0.15 @	Se = 1.34	Ni = 0.33 *
Zr ppm	180	425	283	Y = 1.05	Co = 0.56	Pb = 2.10 *	Co = 0.71
Nb ppm	15	15	15	Ce = 1.29	Cu = 0.73	Zn = 1.31	Cu = 0.61
Cr ppm	97	72	102	Nd = 1.40	S = 0.11 @	S = 2.60 *	Y = 0.66
V ppm	130	46	124		La = 0.96		La = 0.66
Se ppm	13	11	17				Ce = 0.89
Ni ppm	81	12	27				Nd = 0.83
Co ppm	20	11	14				
Pb ppm	20	51	42				
Zn ppm	88	194	116				
Cu ppm	51	37	31				
S ppm	2633	294	7011				
Y ppm	33	35	22				
La ppm	40	38	26				
Ce ppm	65	84	58				
Nd ppm	30	42	25				

Codes: * More than 2x concentration (or < 0.5x concentration)
 @ More than 5x concentration (or < 0.2x concentration)

† Average of shales given by Vinogradov (1962), Krauskopf (1979) and Turekian (1972)

Table 9.2 Analyses of NS and SS and various shales for comparison

	Av. NS	Breisanden:ALP028 Mem. AlO3 muscovite sandstone (2)	ALP028 NS	Muddy silt BV592 (1)	Blue mud 525 (1)	ALP030 NS	S152 (1)	SS av.	Kull- grofta Mem. A72 (2)	Av. Black Sea Shale seds. 379A (3)	Black Sea seds. (4)	Av. Argill. pelagic. seds. (5)	Av. Silice pelagic. seds. (5)
SiO2 %	74.70	77.40	65.08	69.06	66.34	72.83	80.14	68.74	67.05	N.G.	57.20	60.38	70.55
TiO2 %	0.61	0.73	0.86	0.97	0.89	0.59	0.46	0.73	1.33	0.33	0.71	0.92	0.72
Al2O3 %	13.62	11.68	19.09	17.17	17.12	13.61	8.67	18.16	21.13	13.23	17.49	19.07	14.68
Fe2O3 %	6.16	4.00	7.09	6.70	7.72	8.13	4.27	5.86	4.98	2.86	7.90	8.98	7.09
MnO %	0.14	0.01	0.13	0.06	0.11	0.17	0.06	0.04	0.03	0.02	0.06	0.52	0.55
MgO %	0.75	0.42	1.49	1.27	2.27	0.59	1.22	1.48	1.14	1.16	3.55	3.73	2.15
CaO %	0.17	0.95	0.51	0.79	0.95	0.16	1.69	0.14	0.13	2.10	2.15	1.01	0.83
Na2O %	0.16	0.61	0.45	1.63	1.97	0.08	1.82	0.28	0.30	0.94	N.G.	1.67	1.04
K2O %	3.57	3.79	5.19	2.20	2.50	3.73	1.60	3.79	3.81	2.41	2.70	3.56	2.10
P2O5 %	0.07	0.41	0.11	0.16	0.13	0.10	0.07	0.05	0.09	N.G.	0.18	0.15	0.30
C %		0.41						0.28	0.82	3.50	0.82	0.24	0.22
Rb ppm	203	140	326	146	138	201	70	207	163		107		
Ba ppm	1254	525	971	515	297	769	266	447	656	300	564	2000	1050
Sr ppm	21	29	58	116	103	15	146	36	30	200	148	450	230
Th ppm	16	6	20			19		16	10			19	
Zr ppm	425	255	292	350	212	356	240	283	280	70	130	126	170
Nb ppm	15		19			15		15					
Mo ppm			6			<		3		10	9	17	38
Cr ppm	72	179	62	75	76	74	40	102	182	100		55	97
V ppm	46	119	80	86	117	65	109	124	214	150		390	460
Se ppm	11	8	20			10		17	16	10	50		
Ni ppm	12	58	21	31	29	12	20	27	56	50		300	330
Co ppm	11	8	18	10	12	10	8	14	17	10		100	200
Pb ppm	51		24	17	17	58	14	42		20	23	175	180
Zn ppm	194	158	55			260		116	240	<300	106		
Cu ppm	37		8	23	19	49	6	31		70	50	400	370
S ppm	300	11500	218			203		7011	12800		1300		
Y ppm	35		35			44		22		30	29		
La ppm	38		39			44		26		30		90	80
Ce ppm	84		83			105		58				130	
Nd ppm	42		40			51		25					

Note: All recalculations volatile free and major element conversions to oxides, by the author

- (1) Recent sediments from Gulf of Paria (Hirst, 1962a, b)
- (2) Jurassic sediments from Norway (Dypvik, 1979)
- (3) Average black shale (USA) (Vine and Tourtelot, 1970, p.261)
- (4) Recent Black Sea sediments (corrected for sea salt contamination) (Calvert and Batchelor, 1978)
- (5) Average pelagic sediments from Atlantic, Pacific and Indian Oceans and Mediterranean Sea (El Wakeel and Riley, 1961)

< <LLD
N.G. Not given

Table 9.3 Ratios of BGZ to various black shales

BGZ/A72 (2)		BGZ/Av.Bl.Shale (3)		BGZ/Bl. Sea seds. (4)	
Element more concentrated in BG	Element less concentrated in BG	Element more concentrated in BG	Element less concentrated in BG	Element more concentrated in BG	Element less concentrated in BG
Fe2O3 = 1.42	SiO2 = 0.95	TiO2 = 2.41 *	CaO = 0.11 @	SiO2 = 1.12	Fe2O3 = 0.89
MnO = 5.72 @	TiO2 = 0.60	Al2O3 = 1.52	Na2O = 0.19 @	TiO2 = 1.12	MgO = 0.11 @
MgO = 1.68	Al2O3 = 0.95	Fe2O3 = 2.47 *	C = 0.22 *	Al2O3 = 1.15	CaO = 0.19 @
CaO = 1.76	Na2O = 0.58	MnO = 9.30 @		MnO = 3.10 *	P2O5 = 0.22 *
K2O = 1.25	P2O5 = 0.93	MgO = 1.65		K2O = 1.77	C = 0.94
	C = 0.94	K2O = 1.98			
Rb = 1.54	Ba = 0.99	Ba = 2.16 *	Sr = 0.14 @	Rb = 2.35 *	Sr = 0.19 @
Th = 1.78	Sr = 0.95	Zr = 3.11 @	Mo = 0.53	Ba = 1.15	Mo = 0.59
V = 1.12	Zr = 0.78	Cr = 1.22	Ni = 0.90	Zr = 1.68	Sc = 0.38 *
Se = 1.18	Cr = 0.67	V = 1.59	Y = 0.71	Pb = 7.98 @	Y = 0.73
Co = 1.11	Ni = 0.80	Se = 1.88	La = 0.98	Zn = 6.00 @	
Zn = 2.65 *	S = 0.47 *	Co = 1.88		Cu = 1.72	
		Pb = 9.18 @		S = 4.68 @	
		Cu = 1.23			

Codes: * More than 2x concentration (or < 0.5x concentration)

@ More than 5x concentration (or < 0.2x concentration)

(2) Kullgrofta Member, Jurassic sediments from Norway (Dypvik, 1979)

(3) Average Black Shale (USA) (Vine and Tourtelot, 1970, p261)

(4) Recent Black Sea sediments (corrected for sea salt contamination) (Calvert and Batchelor, 1978)

Table 9.4 Estimated SS original clay composition compared with illite and montmorillonite

%	Illite	Montmorillonite	SS clay estimate
SiO ₂	62.8	66.6	63 - 64
TiO ₂	0.9		0.75 - 0.90
Al ₂ O ₃	20.4	25.9	19 - 20
Fe ₂ O ₃ (total)	5.8	1.0	7 - 8
MgO	2.3	4.2	1.6 - 2.2
CaO	1.8	2.1	0.2 - 0.3
Na ₂ O	0.4	0.1	0.38 - 0.50
K ₂ O	5.6	0.1	5.0 - 5.5

- Note 1. Illite and montmorillonite compositions are from Deer et al. (1971; pp251-252). Recalculated volatile free by the present author.
2. SS clay element concentration estimates are read off at the lowest al-alk end of the SS spectrum in Figs. 9.8b-g
3. SS clay value of SiO₂ is an approximation calculated by difference

Table 9.5 MnO/(MnO+Fe₂O₃) ratios for NS and SS compared with various shales

Description	USS *	LSS	SS(USS+LSS) *	Av. Bl. Shale (1)	Bijaigarh Bl.Sh. (2)	Kullgrofta Bl.Sh. (3)	Bonteigen Bl.Sh. (4)
SHAFT n	11	14	25			1	3
SCHIST							
MnO/(MnO+Fe ₂ O ₃) Mean	0.006	0.007	0.006	0.007	0.002	0.006	0.005
S.D.	0.001	0.003	0.002				0.001

Description	NS	Average Shale (5)	Average Shale (6)	Skjermyrbekken: Red Silt.St.(7)
NAMIES n	11			
SCHIST				
MnO/(MnO+Fe ₂ O ₃) Mean	0.023	0.016	0.123	0.021
S.D.	0.011			

* Excludes ALP054 with MnO/(MnO+Fe₂O₃) = 0.042

1. Vine and Tourtelot (1970, p. 261)

2. Singh (1980, p. 96)

3. Dypvik (1979) Kullgrofta Member, Ramsa Formation (sample A-72)

4. Dypvik (1979) Bonteigen Member, Ramsa Formation (samples A-85; C-8; C-20)

5. Turekian and Wedepohl, quoted in Vine and Tourtelot (1970)

6. Green, quoted in Vine and Tourtelot (1970)

7. Dypvik (1979) Skjermyrbekken Member, Nybrua Formation (sample F-18)(SiO₂ = 52%).

Dalland (1975) refers to both these Members as having formed under lagoonal conditions. Individual plots of organic C vs S for both Members give positive S intercepts, suggesting reducing overlying waters. Only samples with ignition loss of <10% are used.

Dalland (1975) refers to this as a red/brown siltstone formed under near-shore oxidizing conditions exposed to the open sea. Only the sample with ignition loss <10% is used

Table 9.6 CS average composition, comparative rocks and ratios

	CS n = 3 Mean	Leira Fm. (1)	BH Calc sil. (2)	BH Calc sil. (3)	BH Calc sil. (4)	CS av./ Leira Fm.	CS av./ BH CS(2)	CS av./ BH CS(3)	CS av./ BH CS(4)
SiO2 %	65.10	63.19	56.01	60.78	48.75	1.03	1.16	1.07	1.34
TiO2 %	0.47	0.86	0.38	0.32	0.63	0.55	1.23	1.47	0.75
Al2O3 %	11.17	17.52	9.51	11.07	25.16	0.64	1.17	1.01	0.44 *
Fe2O3 %	7.10	5.57	5.19	4.87	3.60	1.28	1.37	1.46	1.97
MnO %	1.84	0.11	0.49	0.27	0.07	16.96 @	3.76 *	6.72 @	25.60 @
MgO %	4.26	1.39	7.02	8.88	0.76	3.06 *	0.61	0.48 *	5.59 @
CaO %	6.86	5.36	19.86	12.04	12.88	1.28	0.35 *	0.57	0.53
Na2O %	0.47	1.92	0.95	0.84	0.92	0.25 *	0.50 *	0.56	0.51
K2O %	1.47	3.82	0.51	0.85	0.36	0.39 *	2.89 *	1.73	4.07 *
P2O5 %	0.31	0.27	0.08	0.07	0.15	1.13	4.03 *	4.28 *	2.04 *
Rb ppm	92	145				0.63			
Ba ppm	1235	789			67300	1.57			0.02 @
Sr ppm	101	198				0.51			
Th ppm	11	10				1.09			
U ppm	6.9								
Zr ppm	123	215				0.57			
Nb ppm	10.0								
Mo ppm	3.4								
Cr ppm	64	71				0.90			
V ppm	79	132				0.60			
Se ppm	12	16				0.74			
Ni ppm	30	41				0.73			
Co ppm	12	7.6				1.62			
Pb ppm	1987								
Zn ppm	1611	68				23.69 @			
Cu ppm	59								
S ppm	5963	11900				0.50 *			
Y ppm	28								
La ppm	40								
Ce ppm	73								
Nd ppm	37								

Codes: * More than 2x enrichment or depletion

@ More than 5x enrichment or depletion

- (1) Marine calcareous sandstone with intercalations of siltstone (average of samples E-13, F-1 and F-3) from Andoya area, Northern Norway (Lower Cretaceous) (Dypvik, 1979).
- (2) Layered calc silicate rocks of the Ettlewood type from the Broken Hill region, Australia (average of 11 analyses; Stroud et al., 1983, p.261)
- (3) Layered calc silicate rocks of the King Gunnia type from the Broken Hill region, Australia (average of 6 analyses; Stroud et al., 1983, p.261).
- (4) Leucocratic poorly to non-layered calc silicate rocks from the Broken Hill region, Australia (average of 5 analyses; Stroud et al., 1983, p.268)

Note: All averages and recalculations volatile free by the author

Table 9.7 MnQ average composition, comparative cherts and ratios

	MnQ n = 4 Mean	Massive Chert (1)	Conception Gp. Chert (2)	Japanese Chert (3)	MnQ av./ Massive Chert (1)	MnQ av./ Conception Chert (2)	MnQ av./ Japanese Chert (3)
%							
SiO ₂ %	88.33	96.97	81.10	96.22	0.91	1.09	0.92
TiO ₂ %	0.08	Tr	0.31	0.08		0.25 *	0.96
Al ₂ O ₃ %	2.06	0.40	10.14	1.74	5.16 @	0.20 @	1.19
Fe ₂ O ₃ %	4.82	0.54	0.73	0.77	8.93 @	6.61 @	6.27 @
MnO %	0.71	0.30	0.03	0.02	2.35 *	23.51 @	35.27 @
MgO %	0.11	0.49	0.26	0.44	0.23	0.44 *	0.26 *
CaO %	0.51	0.11	0.57	0.35	4.65 *	0.90	1.46
Na ₂ O %	0.05	0.06	3.66	0.08	0.91	0.01 @	0.68
K ₂ O %	0.14	0.06	2.76	0.40	2.37 *	0.05 @	0.36 *
P ₂ O ₅ %	0.54	<0.01	Tr	0.04			13.53 @
Rb ppm:	5						
Ba ppm:	63						
Sr ppm:	16						
Th ppm:	8.7						
U ppm:	10.5						
Zr ppm:	23			23			1.01
Nb ppm:	3.3						
Mo ppm:	4.3						
Cr ppm:	15						
V ppm:	33						
Se ppm:	1.8						
Ni ppm:	10			14			0.72
Co ppm:	13			3.3			3.91 *
Pb ppm:	12087			8.2			1474.02 @
Zn ppm:	1079						
Cu ppm:	421			60			7.02 @
S ppm:	14119						
Y ppm:	11						
La ppm:	7.9						
Ce ppm:	25						
Nd ppm:	11						

Note: Volatile free corrections for average LOI in samples (1) and (2) (0.89 and 0.50, respectively) were not made as their influence on the derived ratios is insignificant

Codes: * More than 2x concentration (or < 0.5x concentration)
@ More than 5x concentration (or < 0.2x concentration)

- (1) Massive chert 0.1 metres above volcanogenic manganese ore, Noda-Tamagawa mine, Japan (Watanabe et al., 1970). Note that these cherts are frequently enriched in U (up to ore grade), Ni, Co, V, Mo, As and Sb.
- (2) Bedded and banded chert derived from acid, vitric, subareal volcanic sources which accumulated in sea water. Selected sample is the most SiO₂ rich of seven analyses from Hughes (1976).
- (3) Bedded and banded chert from Central Japan which are derived from remains of radiolaria and sponge spicules. Average of 69 samples all calculated on a water and carbonate free basis (Sugisaki et al., 1982).

Table 9.8 Average analyses of WQ and DQ borehole core, and selected sandstone and chert analyses for comparison

Code	Broken Hill Quartzites		Quartz arenites					High silica cherts							Bas. Chert	
	WQ	DQ	1	2	3	4	5	6	7	8	9	10	11	12	13	14
n	4	4										17	20	83	1	2
SiO ₂ %	96.32	96.20	96.03	98.11	99.21	99.28	99.68	91.62	95.69	95.45	91.92	94.08	90.86	95.30	96.97	82.29
TiO ₂ %	0.06	0.07	0.20		0.05	0.03	0.02			0.15	0.17	0.05	0.15	0.10	tr.	0.03
Al ₂ O ₃ %	1.62	1.71	1.11	0.31	0.62	0.35	0.20	1.95	2.55	2.14	3.19	0.52	2.38	1.99	0.40	0.26
Fe ₂ O ₃ %	1.27	1.39	0.64	1.21	0.09	0.09	0.01	1.50		0.96	2.76	2.53	3.24	0.98	0.54	5.97
MnO %	0.03	0.04								0.21	0.09	0.43	0.48	0.04	0.30	0.11
MgO %	0.16	0.08	0.10	0.10	0.02	0.06	0.01	1.20		0.57	1.08	0.33	0.91	0.54	0.49	0.19
CaO %	0.06	0.02	1.61	0.14		0.19	<0.01	0.05	1.76	0.16	0.36	0.35	0.39	0.38	0.11	0.81
Na ₂ O %	0.06	0.05	0.10	0.10	0.01		0.08	0.56		0.09	0.05	0.51	0.60	0.12	0.06	0.48
K ₂ O %	0.42	0.45	0.20	0.03	0.02			2.89		0.33	0.49	0.28	0.74	0.51	0.06	0.14
P ₂ O ₅ %	0.03	0.01						0.23				0.15	0.20	0.06	0.00	0.10
Rb ppm	27	24										9.7	31	29		7.5
Ba ppm	45	43										450	1600	140		225
Sr ppm	3.4	1.5										35	74	37		83
Th ppm	<	4.1										4.1	8.0	3.1		
Zr ppm	108	149										14	42	25		
Nb ppm	2.5	2.6										2.5	5.3	2.7		1.0
Mo ppm	<	<										15	13	8.5		17
Cr ppm	5.7	8.0										22	12	38		35
V ppm	3.9	4.3														
Sc ppm	1.3	1.7														
Ni ppm	<	<										26	45	14		27
Co ppm	2.4	2.6										6.6	10	3.5		13
Pb ppm	12	9.1										12	14	8.0		6.0
Zn ppm	47	43										35	77	29		50
Cu ppm	44	173										130	320	59		47
S ppm	281	419														
Y ppm	8.6	8.2										13	30	6.6		2.5
La ppm	8.9	16														
Ce ppm	20	29														
Nd ppm	9.1	13														

All blanks indicate that the element in question has not been analysed for

All values calculated volatile free by the author

< = Below lower limit of detection

1. Quartz arenites (Pettijohn et al., 1972, p.60)
2. Sioux quartzite (Precambrian). (Pettijohn et al., 1972, p. 215, analysis No.C)
3. St. Peter sandstone (Ordovician). (Pettijohn et al., 1972, p. 215, analysis No.E)
4. Tuscarara quartzite (Silurian). (Pettijohn et al., 1972, p.215, analysis No.G)
5. Oriskany sandstone (Devonian). (Pettijohn et al., 1972, p. 215, analysis No.H)
6. Monterey Formation cherty shale, California (Bramlette, 1946, p. 13, analysis No.4)
7. Monterey Formation opaque flint, California (Bramlette, 1946, p. 13, analysis No.11)
8. Palest chert associated with pillow lavas and serpentinite, N. W. Italy (Thurston, 1972, p.332)
9. Green chert (Thurston, 1972, p.332, analysis No.6)
10. Hydrothermal cherts from DSDP Leg 32, sites 303 and 304 (Adachi et al., 1986, p.136)
11. Porcellanites from DSDP Leg 32, sites 303 and 304 (Adachi et al., 1986, p.136)
12. Kamiasso cherts of Central Japan (Sugisaki et al., 1982)
13. Volcanically derived massive chert from hanging wall of Noda-Tamagawa Mn orebody (Watanabe, 1970)
14. Basal chert directly above basalt (Adachi et al., 1986, p.134; average of analyses 55 and 56 by present author)

Table 9.9 Relative silica and aluminium relationships between Broken Hill and Regional rock-types

Rock-type	Compared areas	Si	Al
WQ	BH vs Nam	BH < Nam	BH >> Nam
	BH vs Wtl	BH = Wtl	BH = Wtl
	Nam vs Wtl	Nam > Wtl	Nam < Wtl
DQ	BH vs Nam	BH < Nam	BH > Nam
	BH vs Wtl	BH > Wtl	BH < Wtl
	Nam vs Wtl	Nam >> Wtl	Nam << Wtl
SS	BH vs Nam	BH >> Nam	BH < Nam
	BH vs Wtl	BH < Wtl	BH > Wtl
	Nam vs Wtl	Nam << Wtl	Nam >> Wtl
NS	BH vs Ach	BH > Ach	BH < Ach
	BH vs Wtl	BH < Wtl	BH > Wtl
	Ach vs Wtl	Ach << Wtl	Ach >> Wtl

Codes used: BH = Broken Hill
 Nam = Namiesberg
 Wtl = Wortel
 Ach = Achab

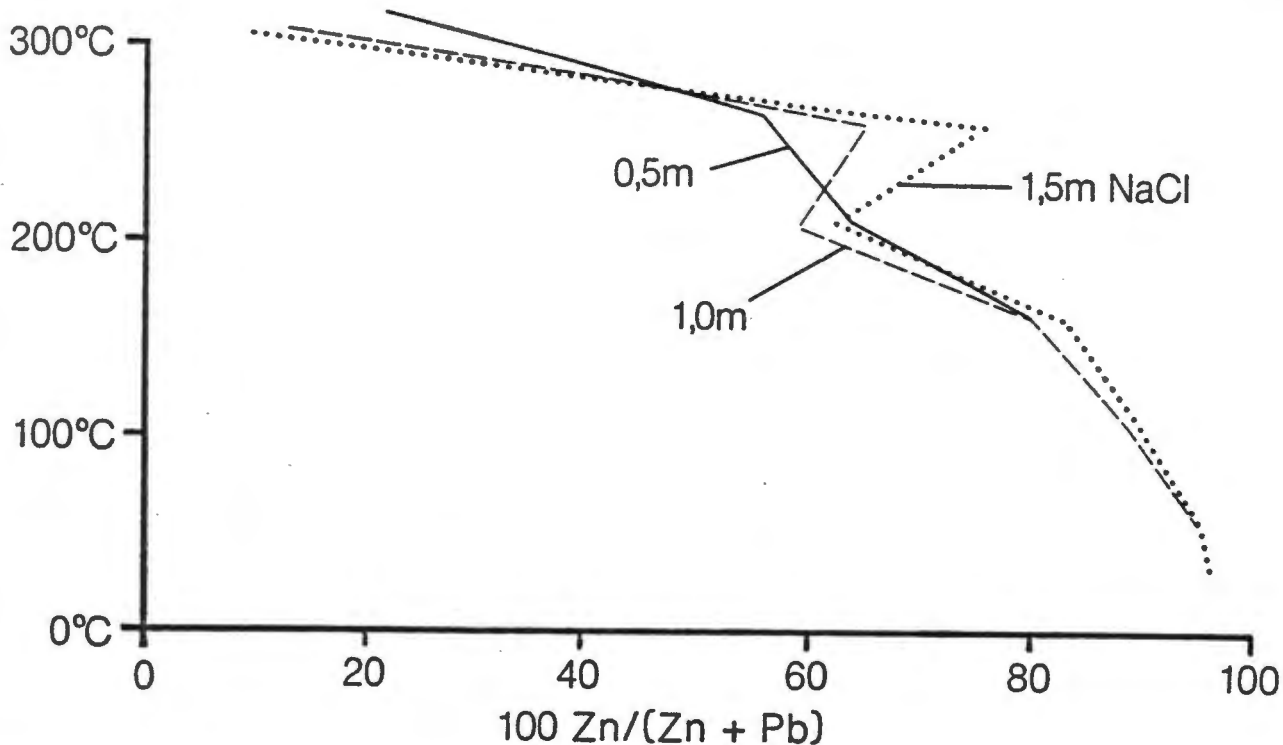


Fig. 10.1 Effects of temperature on the $100 \cdot \text{Zn}/(\text{Zn} + \text{Pb})$ ratio for salinities of 0.5, 1.0 and 1.5m NaCl (after Huston and Large, 1987)

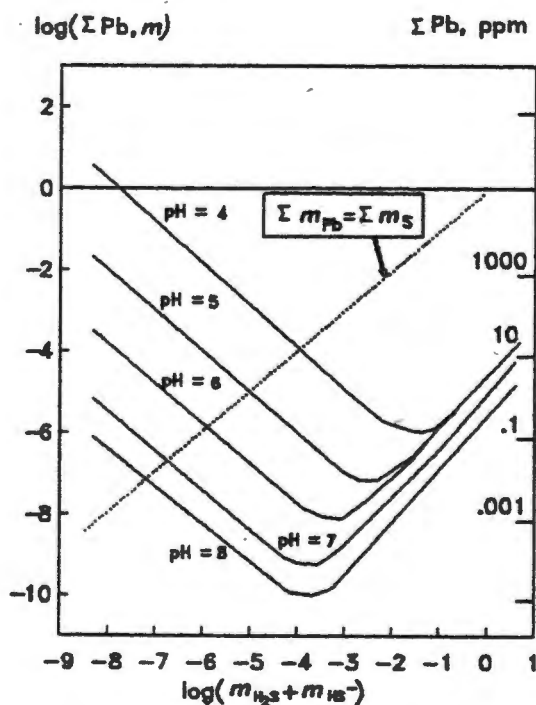


Fig. 10.2 PbS solubility at 150°C in 3m NaCl solutions. Lines with negative slopes on the left side of the diagram are dominated by chloride complexes, and those with positive slopes by sulphide complexes (after Giordano and Barnes, 1979)

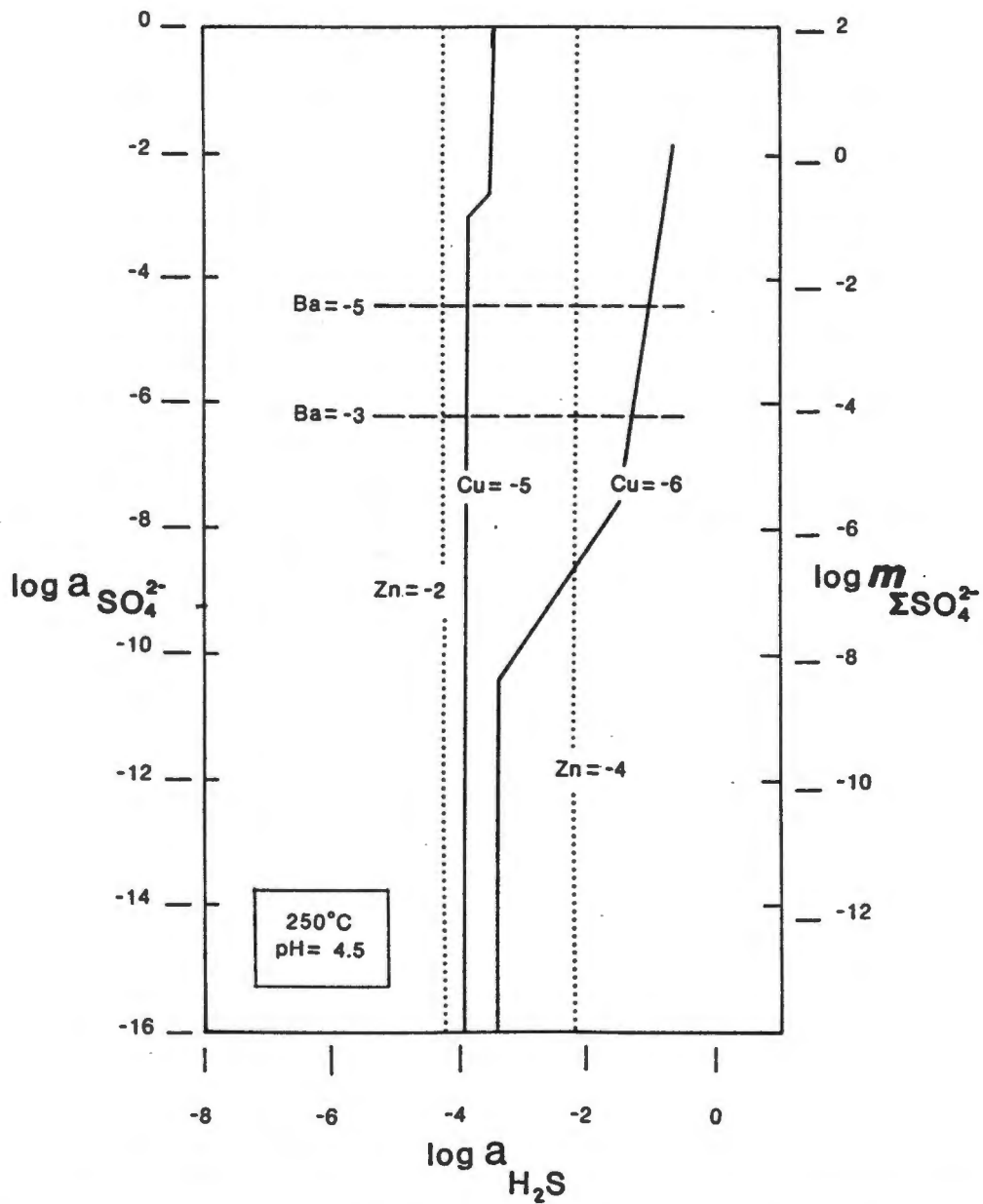


Fig. 10.3 Concentration of metals in solution in equilibrium with various minerals: Ba with barite; Cu with chalcopyrite or bornite; Zn with sphalerite (after Ohmoto et al., 1983)

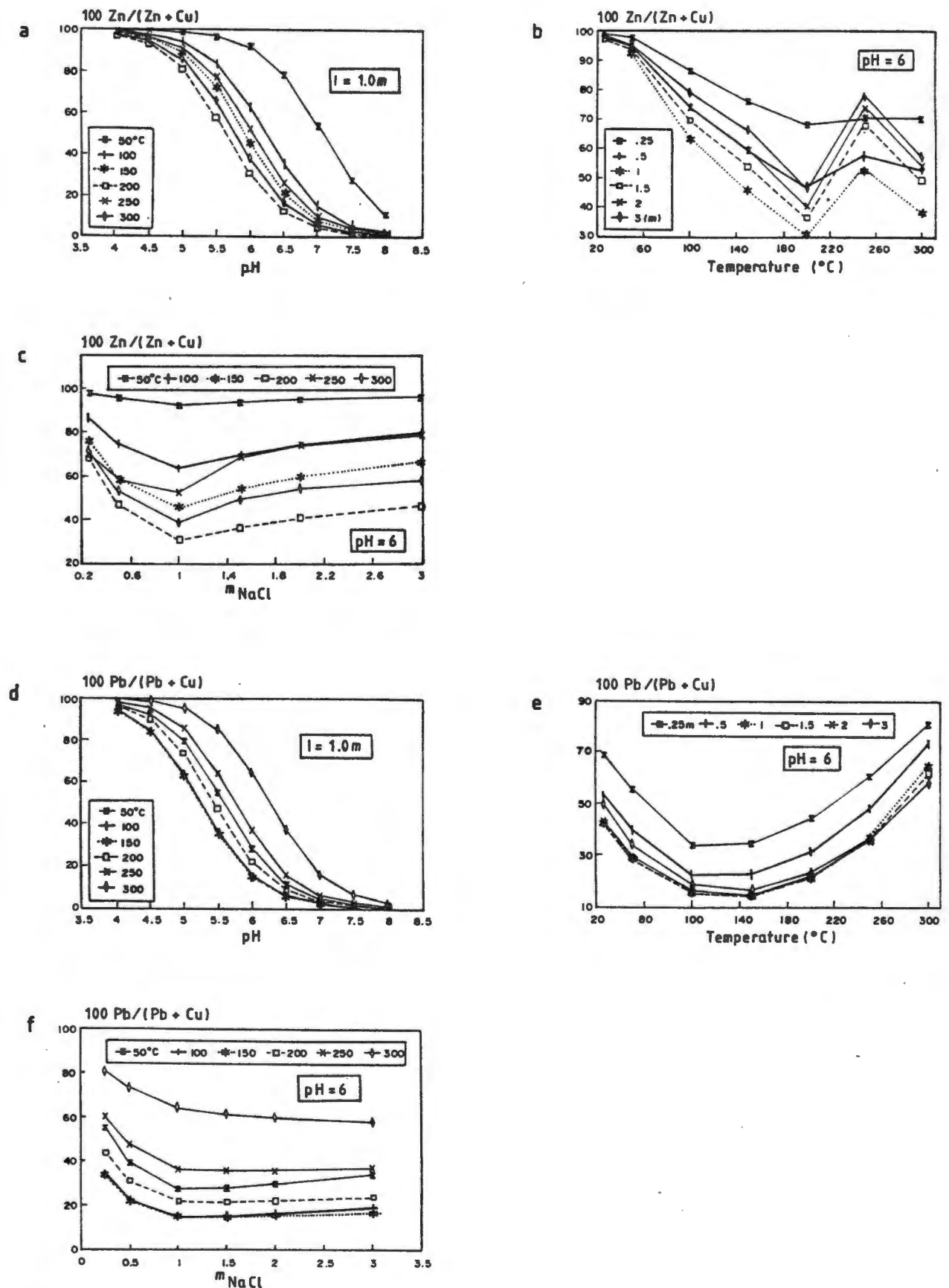


Fig. 10.4 Effect of pH, temperature and salinity on the Zn/Cu and Pb/Cu ratios: (a) effect of pH on the $100 \cdot \text{Zn}/(\text{Zn} + \text{Cu})$ ratio at $I = 1.0m$; (b) effect of temperature on the $100 \cdot \text{Zn}/(\text{Zn} + \text{Cu})$ ratio at $\text{pH} = 6$; (c) effect of salinity on the $100 \cdot \text{Zn}/(\text{Zn} + \text{Cu})$ ratio at $\text{pH} = 6$; (d) effect of pH on the $100 \cdot \text{Pb}/(\text{Pb} + \text{Cu})$ ratio at $I = 1.0m$; (e) effect of temperature on the $100 \cdot \text{Pb}/(\text{Pb} + \text{Cu})$ ratio at $\text{pH} = 6$; (f) effect of salinity on the $100 \cdot \text{Pb}/(\text{Pb} + \text{Cu})$ ratio at $\text{pH} = 6$

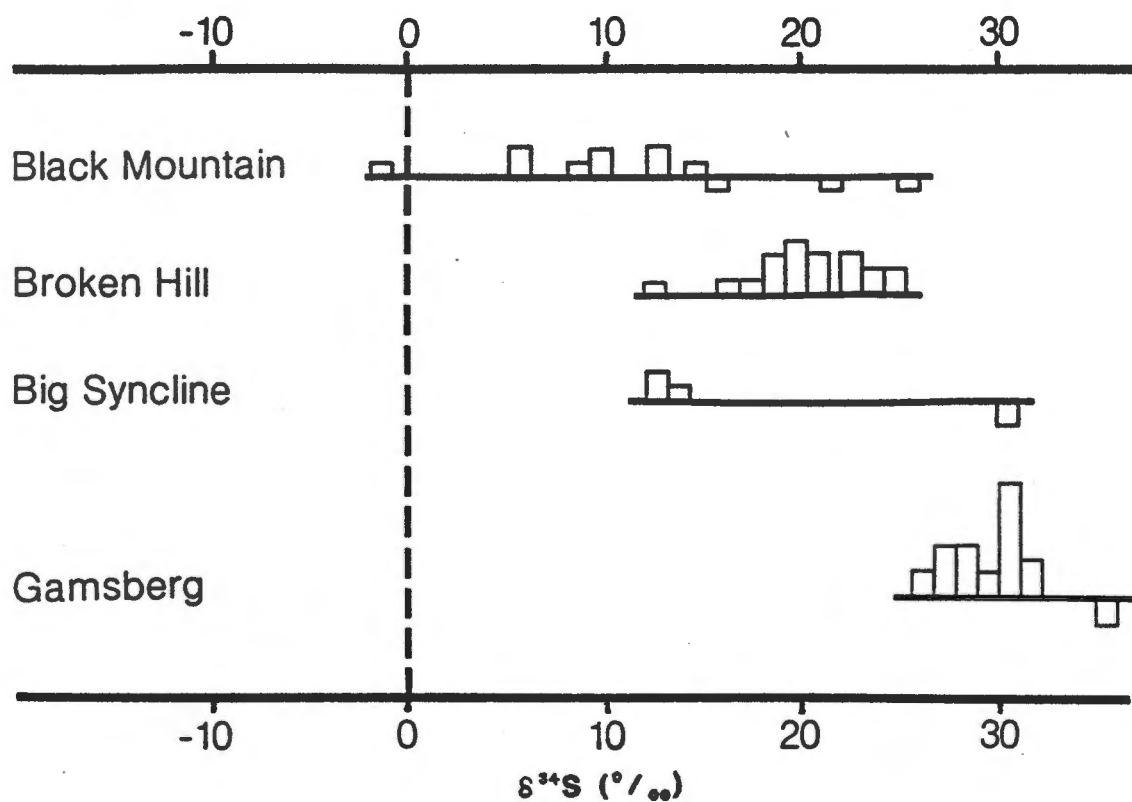


Fig. 10.5 $\delta^{34}\text{S}$ values for Aggeneys-Gamsberg ore deposits. Values are for sulphides above and barite below the line (after von Gehlen et al. (1983))

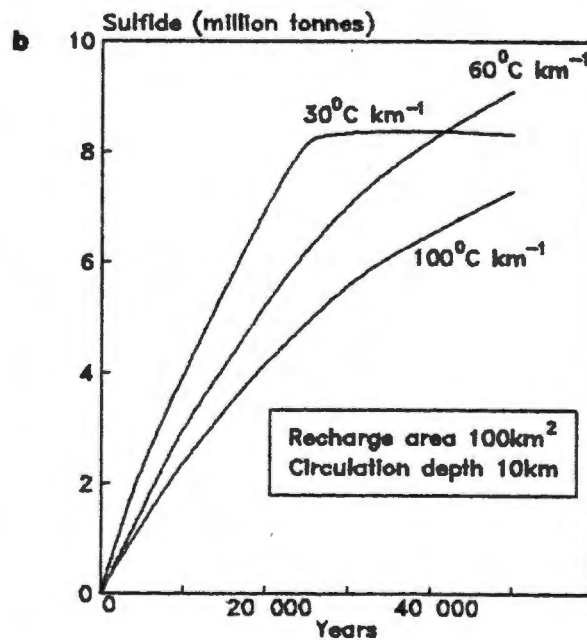
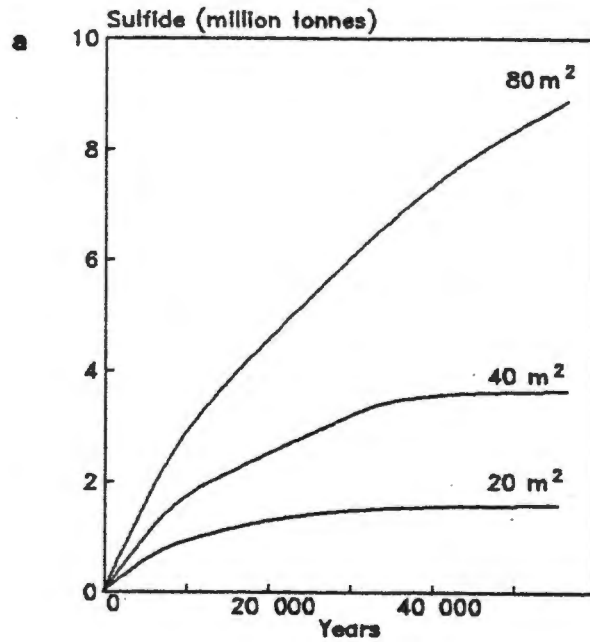


Fig. 10.6 Relationship between potential sulphide mass producible (including Fe sulphide) and time for (a) various cross sectional areas of downflow, and (b) various geothermal gradients (after Strens et al., 1987)

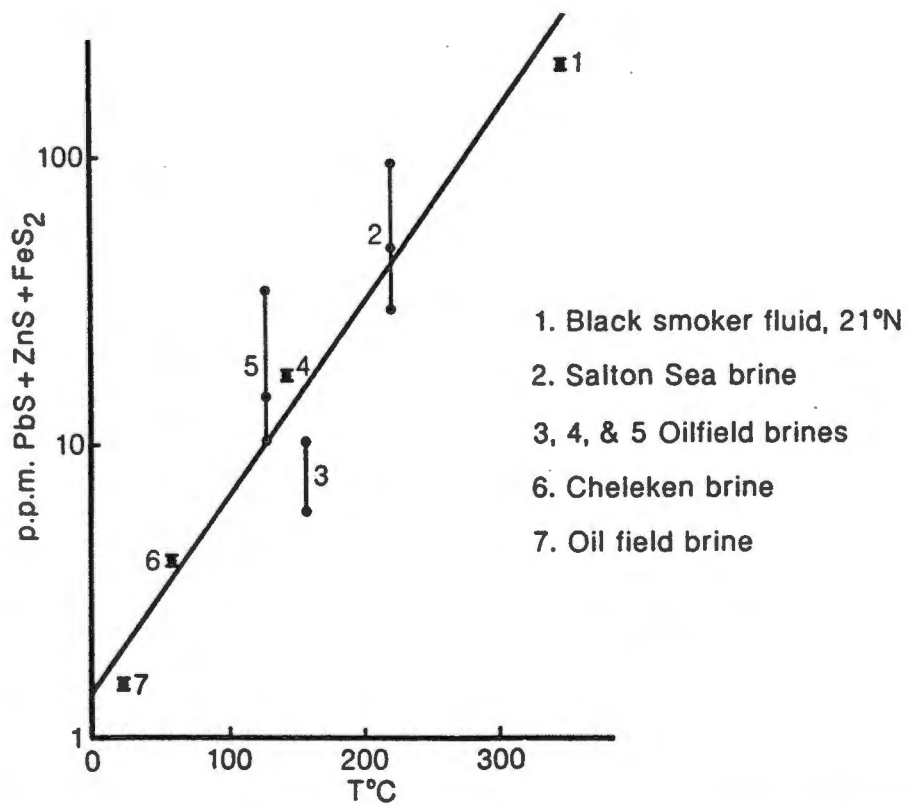


Fig. 10.7 Temperature-concentration relationships for total sulphide mass producible in hydrothermal brine (after Strens et al., 1987)

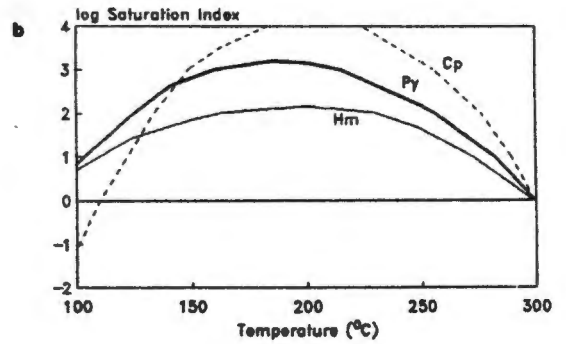
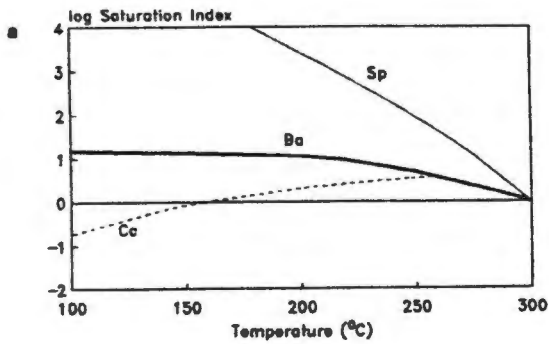


Fig. 10.8 Changes in the saturation indices of minerals during cooling from a 300°C Kuroko fluid on mixing with sea water. Sp = sphalerite; Ba = barite; Cp = chalcopyrite; Py = pyrite; Hm = hematite. The saturation indices of minerals are dependent on fluid redox conditions in (b) but not in (a) (after Ohmoto et al., 1983)

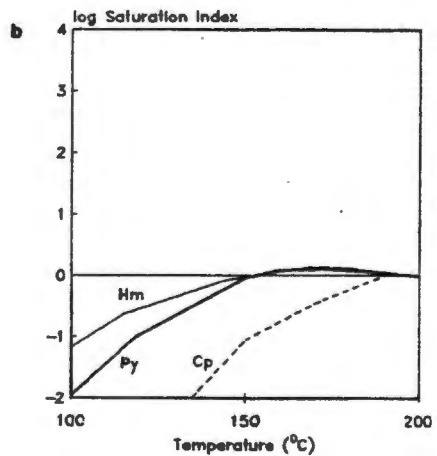
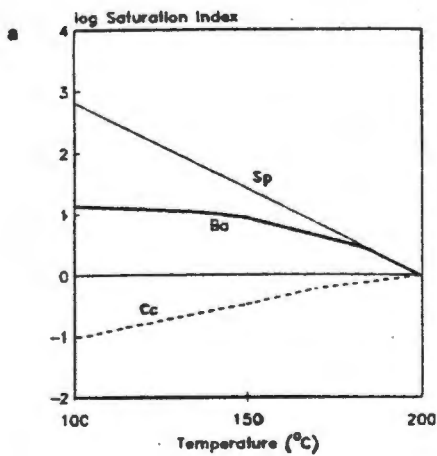


Fig. 10.9 Changes in the saturation indices of minerals during cooling from a 200°C Kuroko fluid. Abbreviations as for Fig. 10.8 (after Ohmoto et al., 1983)

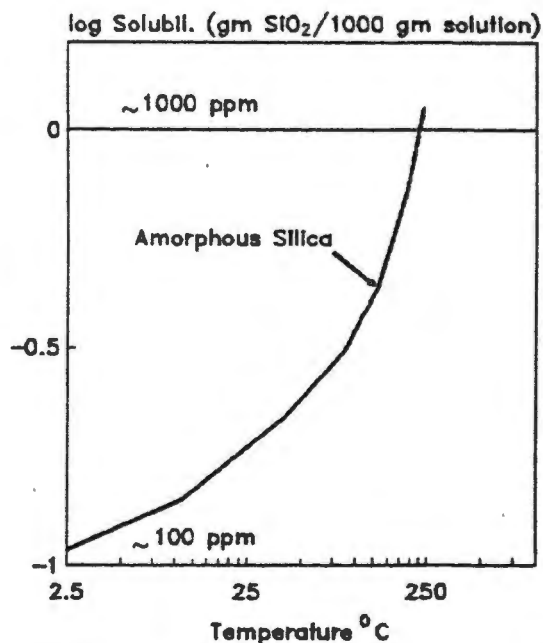


Fig. 10.10 Solubility of amorphous silica in water between 25 and 250°C (after Holland and Mallinin, 1979)

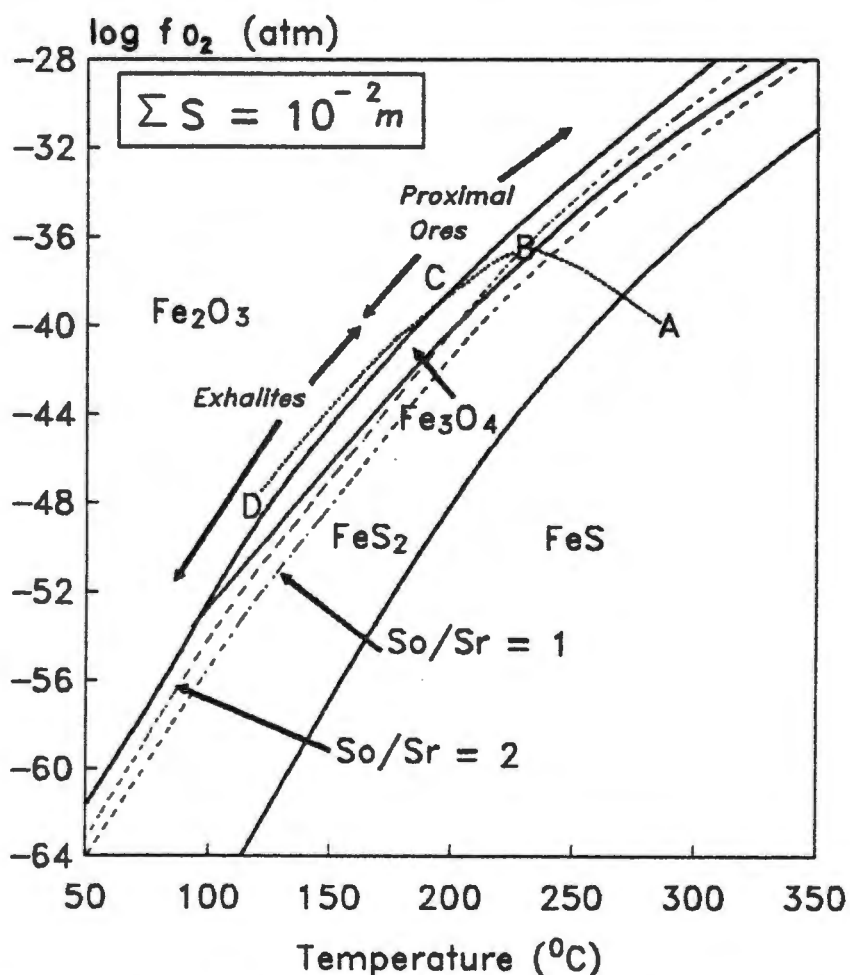


Fig. 10.11 Relationship between proximal ores and exhalites shown in f_{O_2} - temperature space for pH between 5 at 350°C and 7 at 50°C with total S = $10^{-2}m$ and 1m NaCl. Modified after R. R. Large (1977)

Table 10.1 Average base metal contents of some common crustal rocks

	Ultramafic	Basaltic	High Ca Granite	Low Ca Granite	Shales
Cu	10	87	30	10	45
Pb	1	6	15	19	20
Zn	50	105	60	39	95
Ba	0.4	330	420	840	58

Data from Turekian (1972)

Table 10.2 Equilibrium constants used in the Cu-Pb-Zn ratio calculations

Reaction	log K						
	25°C	50°C	100°C	150°C	200°C	250°C	300°C
(1) $2\text{CuCl}_2 + \text{H}_2\text{S} = \text{Cu}_2\text{S} + 4\text{Cl}^- + 2\text{H}^+$	23.04	20.51	16.20	12.66	9.51	6.49	3.44
(2) $2\text{CuCl}_2 + \text{H}_2\text{S} = \text{Cu}_2\text{S} + 6\text{Cl}^- + 2\text{H}^+$	22.84	20.27	15.87	12.24	8.91	5.79	2.54
(3) $2\text{CuCl} + \text{H}_2\text{S} + \text{H}_2 = \text{Cu}_2\text{S} + 2\text{Cl}^- + 4\text{H}^+$	77.57	72.87	64.72	58.59	53.26	49.15	45.45
(4) $2\text{CuCl}_2 + \text{H}_2\text{S} + \text{H}_2 = \text{Cu}_2\text{S} + 4\text{Cl}^- + 4\text{H}^+$	78.27	73.46	65.11	58.80	53.26	49.05	44.95
(5) $2\text{CuCl}_2 + \text{H}_2\text{S} + \text{H}_2 = \text{Cu}_2\text{S} + 6\text{Cl}^- + 4\text{H}^+$	35.61	32.49	27.15	22.66	18.62	15.15	11.46
(6) $2\text{CuCl}_2 + \text{H}_2\text{S} + \text{H}_2 = \text{Cu}_2\text{S} + 8\text{Cl}^- + 4\text{H}^+$	37.91	34.55	28.74	24.00	19.72	15.85	11.86
(7) $\text{ZnCl}_2 + \text{H}_2\text{S} = \text{ZnS} + 2\text{Cl}^- + 2\text{H}^+$	3.95	3.28	1.93	0.44	-1.00	-2.47	-3.93
(8) $\text{ZnCl}_2 + \text{H}_2\text{S} = \text{ZnS} + 2\text{Cl}^- + 2\text{H}^+$	3.75	3.12	1.81	0.37	-0.99	-2.96	-4.90
(9) $\text{ZnCl}_2 + \text{H}_2\text{S} = \text{ZnS} + 3\text{Cl}^- + 2\text{H}^+$	4.03	3.54	2.37	1.31	-0.01	-0.08	-2.23
(10) $\text{ZnCl}_2 + \text{H}_2\text{S} = \text{ZnS} + 4\text{Cl}^- + 2\text{H}^+$	4.18	3.13	1.69	0.12	-1.24	-3.51	-4.85
(11) $\text{PbCl}_2 + \text{H}_2\text{S} = \text{PbS} + 2\text{Cl}^- + 2\text{H}^+$	6.44	5.46	3.78	2.04	0.47	-1.10	-2.60
(12) $\text{PbCl}_2 + \text{H}_2\text{S} = \text{PbS} + 2\text{Cl}^- + 2\text{H}^+$	5.88	4.76	2.83	0.95	-0.98	-2.90	-4.97
(13) $\text{PbCl}_2 + \text{H}_2\text{S} = \text{PbS} + 3\text{Cl}^- + 2\text{H}^+$	6.19	5.23	3.24	1.29	-0.79	-2.95	-5.47
(14) $\text{PbCl}_2 + \text{H}_2\text{S} = \text{PbS} + 4\text{Cl}^- + 2\text{H}^+$	6.39	5.37	3.52	1.77	-0.11	-1.95	-3.79
(15) $\text{Na}^+ + \text{Cl}^- = \text{NaCl}$	-0.90	-1.00	-0.95	-0.75	-0.35	0.05	0.65

Equilibrium constants for equations 1 to 6 were calculated from Helgeson (1969) and for equations 7 to 15 were taken from Huston and Large (1987)

Table 10.3 Zinc/copper and lead/copper ratios of saturated solutions at varying temperatures, salinities and pH's as calculated from thermochemical data

$$\begin{aligned} \text{Pb/Cu ratio} &= 100\text{Pb}/(\text{Pb} + \text{Cu}) \\ &= 100/(1 + (\text{Cu}/\text{Pb}) \cdot (64/207)) \end{aligned}$$

Temp	pH = 4						pH = 5					
	I=.25m	I=.5m	I=1.0m	I=1.5m	I=2m	I=3.0m	I=0.25m	I=0.5m	I=1.0m	I=1.5m	I=2m	I=3.0m
25	100	99	99	99	99	99	96	92	88	88	88	91
50	99	98	97	98	98	98	93	87	80	80	81	83
100	98	97	95	95	95	96	84	74	64	64	66	69
150	98	97	95	94	95	95	84	74	63	63	64	66
200	99	98	97	96	97	97	89	82	74	73	74	75
250	99	99	98	98	98	98	94	90	85	85	85	85
300	100	100	99	99	99	99	98	97	95	94	94	93

Temp	pH = 6						pH = 7					
	I=.25m	I=.5m	I=1.0m	I=1.5m	I=2m	I=3.0m	I=0.25m	I=0.5m	I=1.0m	I=1.5m	I=2m	I=3.0m
25	69	54	42	41	43	49	18	10	7	7	7	9
50	55	40	28	28	30	34	11	6	4	4	4	5
100	34	22	15	15	16	18	5	3	2	2	2	2
150	35	22	15	14	15	16	5	3	2	2	2	2
200	44	31	22	22	22	23	7	4	3	3	3	3
250	61	48	37	36	36	36	13	8	5	5	5	5
300	81	73	65	62	60	57	30	22	15	14	13	12

$$\begin{aligned} \text{Zn/Cu ratio} &= 100\text{Zn}/(\text{Zn} + \text{Cu}) \\ &= 100/(1 + (\text{Cu}/\text{Zn}) \cdot (64/65)) \end{aligned}$$

Temp	pH = 4						pH = 5					
	I=.25m	I=.5m	I=1.0m	I=1.5m	I=2m	I=3.0m	I=0.25m	I=0.5m	I=1.0m	I=1.5m	I=2m	I=3.0m
25	100	100	100	100	100	100	100	100	100	100	100	100
50	100	100	100	100	100	100	100	100	99	99	99	100
100	100	100	99	100	100	100	98	97	94	96	97	97
150	100	99	99	99	99	99	97	93	89	92	94	95
200	100	99	98	98	99	99	96	90	81	85	87	89
250	100	99	99	100	100	100	96	93	92	96	97	97
300	100	99	98	99	99	99	96	92	86	91	92	93

Temp	pH = 6						pH = 7					
	I=.25m	I=.5m	I=1.0m	I=1.5m	I=2m	I=3.0m	I=0.25m	I=0.5m	I=1.0m	I=1.5m	I=2m	I=3.0m
25	99	99	98	97	98	98	95	89	81	79	80	83
50	98	95	92	93	95	96	81	67	54	59	63	70
100	86	74	63	69	74	79	39	22	15	18	22	27
150	76	59	45	54	59	66	24	12	8	10	13	16
200	68	47	30	36	40	46	18	8	4	5	6	8
250	70	58	52	68	74	78	19	12	10	18	22	26
300	70	53	38	49	54	57	19	10	6	9	10	12

Table 10.4 Zinc/lead, zinc/copper and lead/copper ratios of the Aggeneys-Gamsberg orebodies

	Gamsberg	Big Syncline	Broken Hill	Black Mountain
Zn/Pb	93	71	33	18
Zn/Cu	99.8	98	84	44
Pb/Cu	97	96	91	78

Table 10.5 $\delta^{34}\text{S}$ values for sulphide and sulphate (barite) from the Aggeneys-Gamsberg area

	Sulphide $\delta^{34}\text{S}$ permil	Sulphate $\delta^{34}\text{S}$ permil
Black Mountain	+ 8.9 +- 3.7	+20.6 +- 4.3
Broken Hill	+19.8 +- 3.1	
Big Syncline	+12.8 +- 0.7	+30.2 +- 0.1
Gamsberg	+29.2 +- 1.8	+35.4 +- 0.2

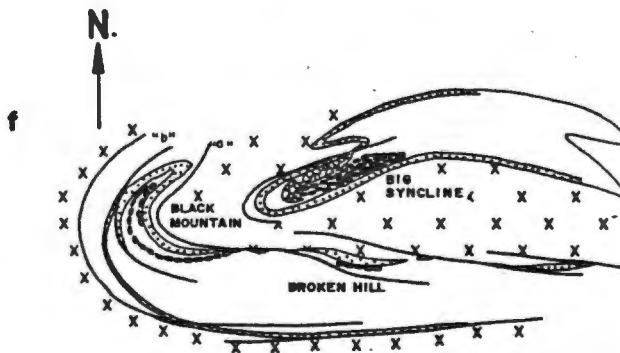
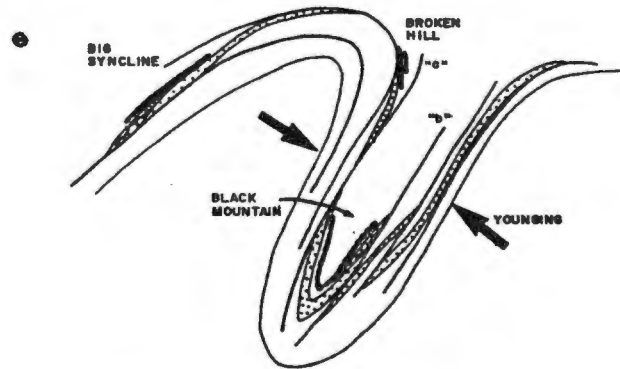
Data from von Gehlen et al. (1983)

Table 10.6 Summary of conditions which obtained to produce the Aggeneys-Gamsberg orebodies

Parameter	Black Mountain	Broken Hill	Big Syncline	Gamsberg
Major metals	Cu, Pb	Pb, Zn, Cu	Zn, Pb	Zn
Accessory deposit	Barite			Barite
Basement	Silicic-potassic granite gneiss throughout; becoming more mafic at depth?			
Amphibolite below	Yes	No	No	No
Amphibolite above	No	No	Yes?	Yes
S ^{**} S Sulphide	8.9	19.8	12.8	29.2
S ^{**} S Sulphate	20.6		30.2	35.4
Basin redox conditions	Oxidizing	Fairly oxidizing	Slightly reducing	Reducing
Fluid Sr/So	<1?	>1	>1	>>1
Fluid Salinity (m)	0.8 - 2.0	0.4 - 1.2	0.3 - 1.5	0.25 - 0.4
Fluid Temperature (deg C)	300	280	180 - 260	100 - 150
Fluid pH	5.6 - 6.2	4.7 - 5.4	4.1 - 4.6	4.0 - 4.5

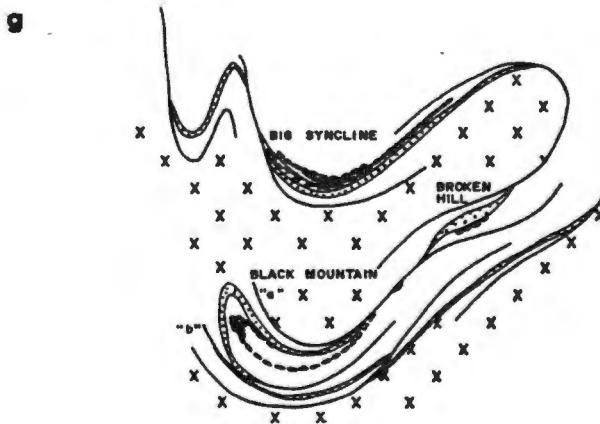
N

S






N

S



N**S****a** 2.0 - 1.7 Ga**LEGEND**

- NF NAMAQUA FRONT ZONE
- PM PASSIVE MARGIN
- VA VOLCANIC ARC (INFERRED)
- MB MARGINAL BASIN
- SCCB SOUTHERN CAPE CONDUCTIVITY BELT
- RSP RICHTERSVELD SUBPROVINCE
- BSP BUSHMANLAND SUBPROVINCE
-  CONTINENTAL CRUST
-  MATURE SEDIMENTS
-  IMMATURE SEDIMENTS
-  OCEANIC CRUST (INFERRED)

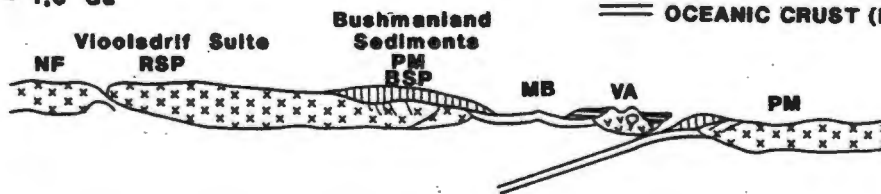
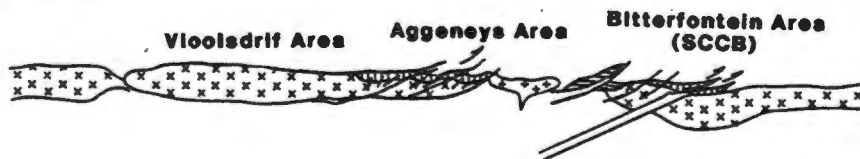
b 1.7 - 1.6 Ga**c** 1.2 - 1.0 Ga

Fig. 11.2 Schematic representation of geotectonic model for development of the Namaqualand Metamorphic Complex as it affects the Bushmanland Group: (a) Generation of Violsdrif Suite and basement to the Bushmanland Group, resulting from south-directed subduction; (b) Sedimentation of Bushmanland Group above rifted passive margin against marginal basin. Simultaneous north-directed, shallow dipping subduction along SCCB, with generation of volcanic arc, and sedimentation of both mature passive margin and immature volcanic arc detritus; (c) Collision of continents causing south vergence and reactivation of normal faults in the Aggeneys area

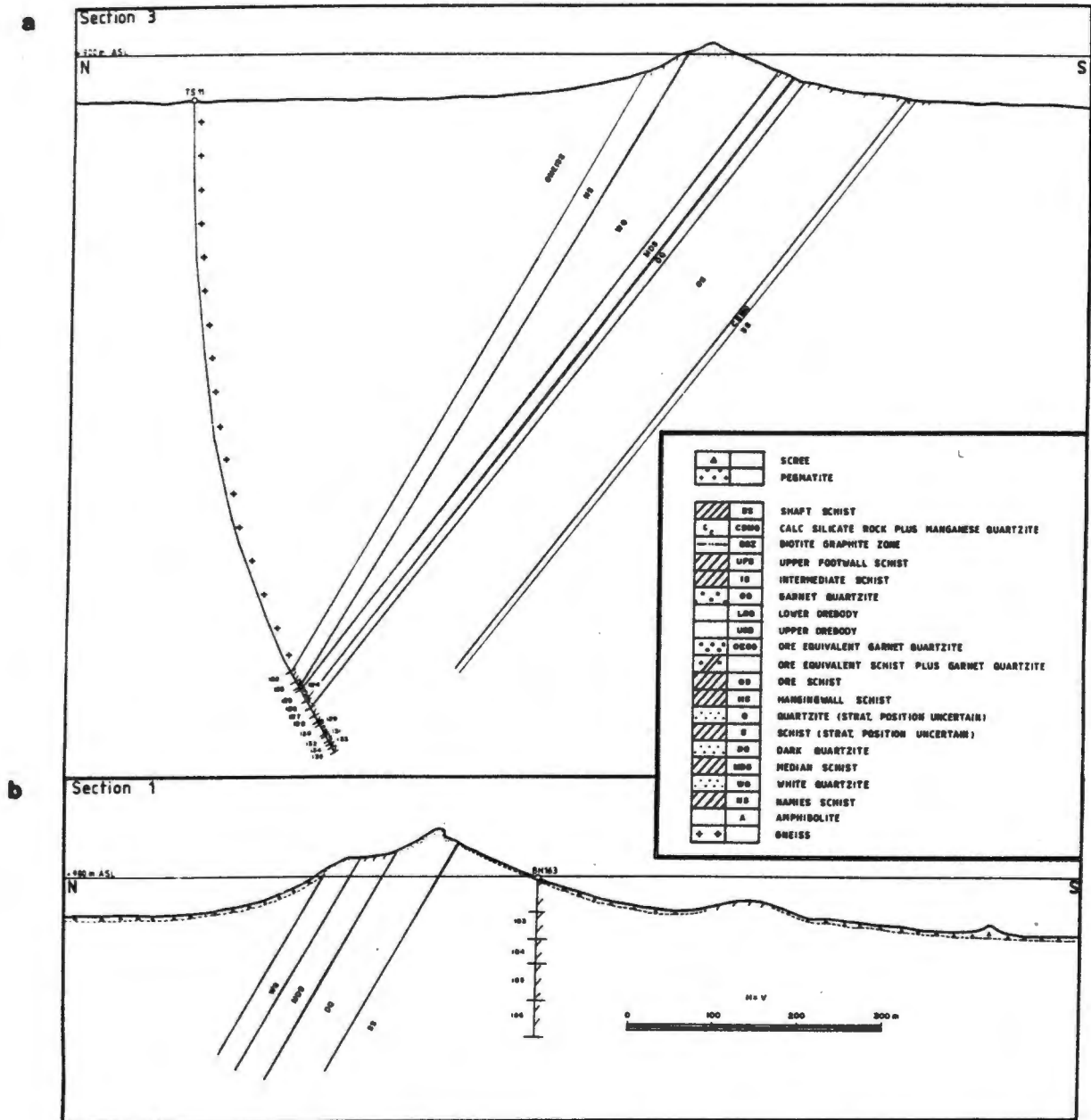
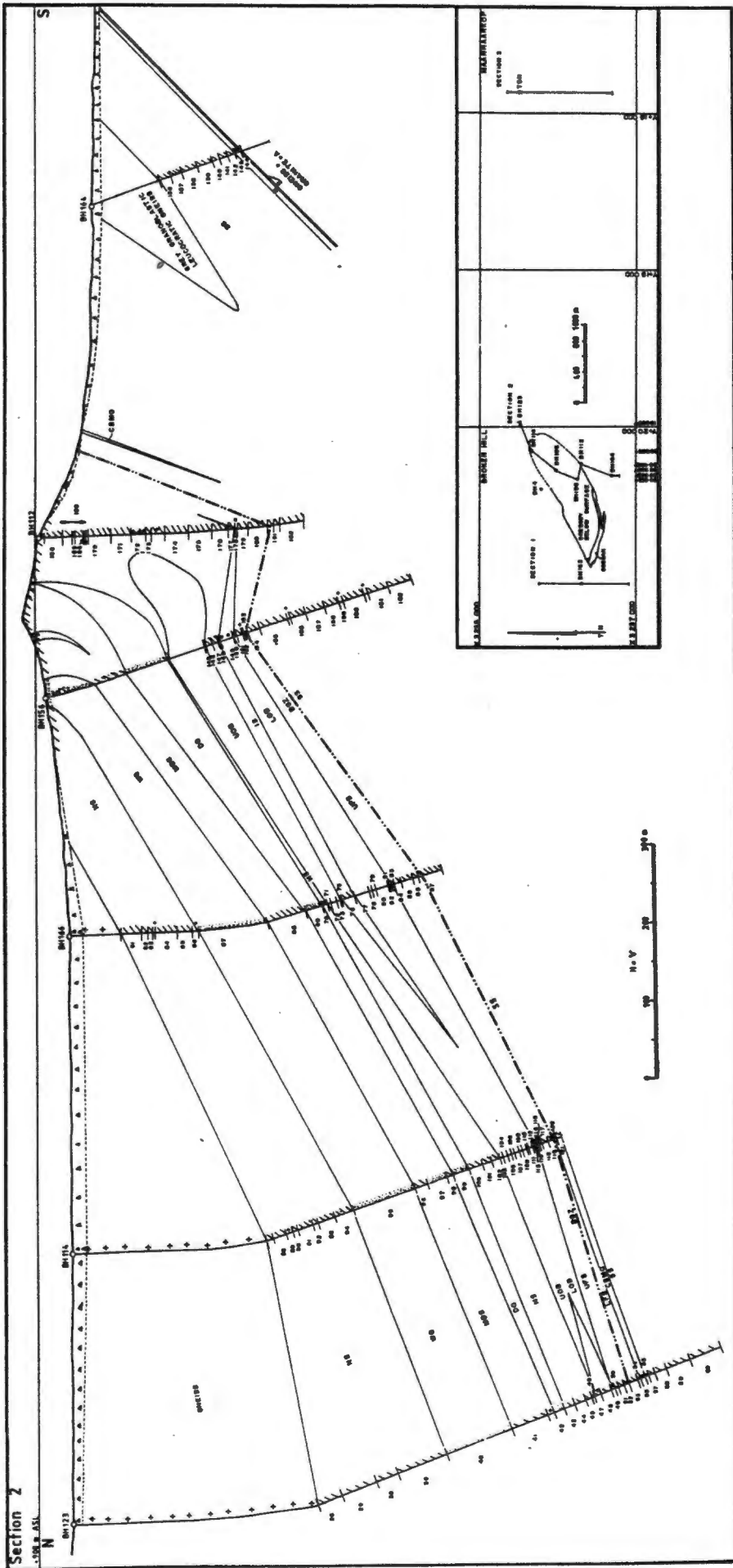
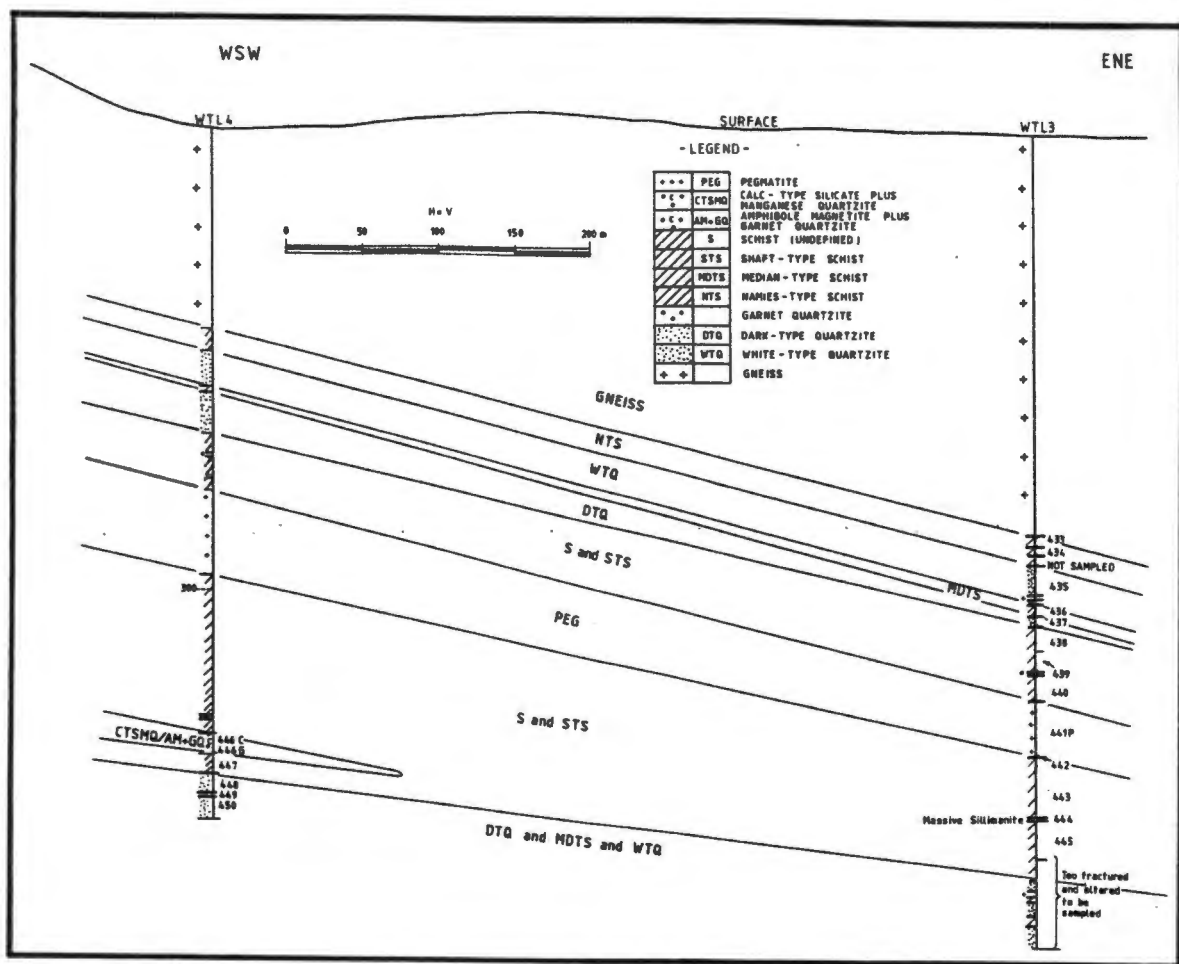


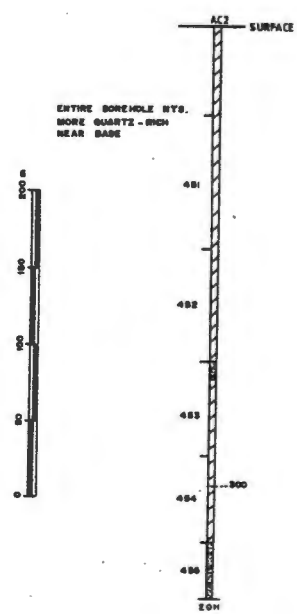
Fig. A.1 Cross section through sampled boreholes showing sample numbers and lithologies: (a) Section through TS11 at Maanhaarkop; (b) Section through BH163 at Broken Hill; (c) Fence diagram through BH123 to BH164 at Broken Hill; (d) Section through WTL3 and 4 at Wortel; (e) Section through AC2 at Achab; (f) Section through VG1 at Namiesberg. Locations of Broken Hill and Maanhaarkop boreholes are shown in the locality plan with Fig. A.1c. while locations of the Achab and Namiesberg boreholes appear in Fig. A.2c. The locations of the Wortel boreholes appear in Fig. 5.3



d



e



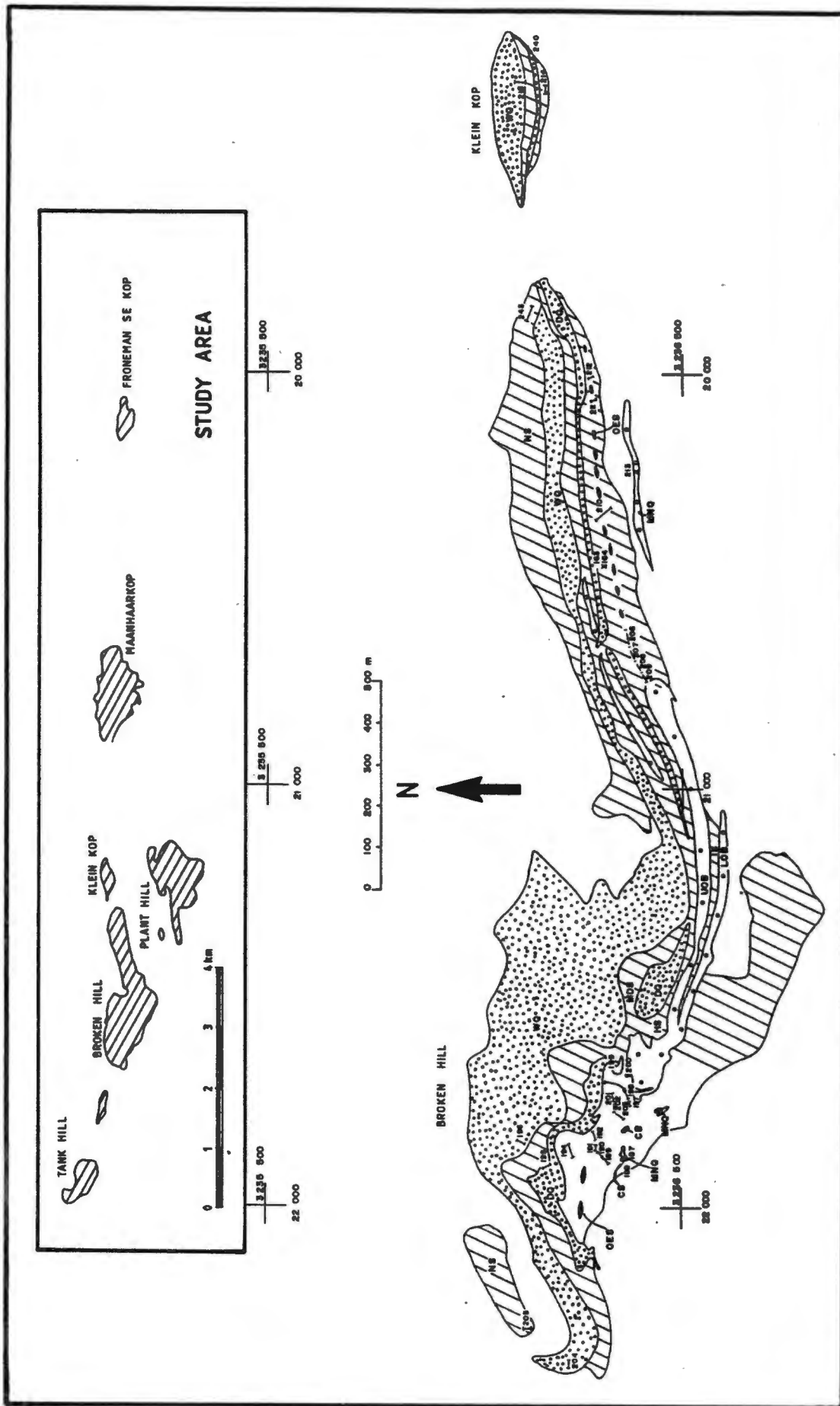
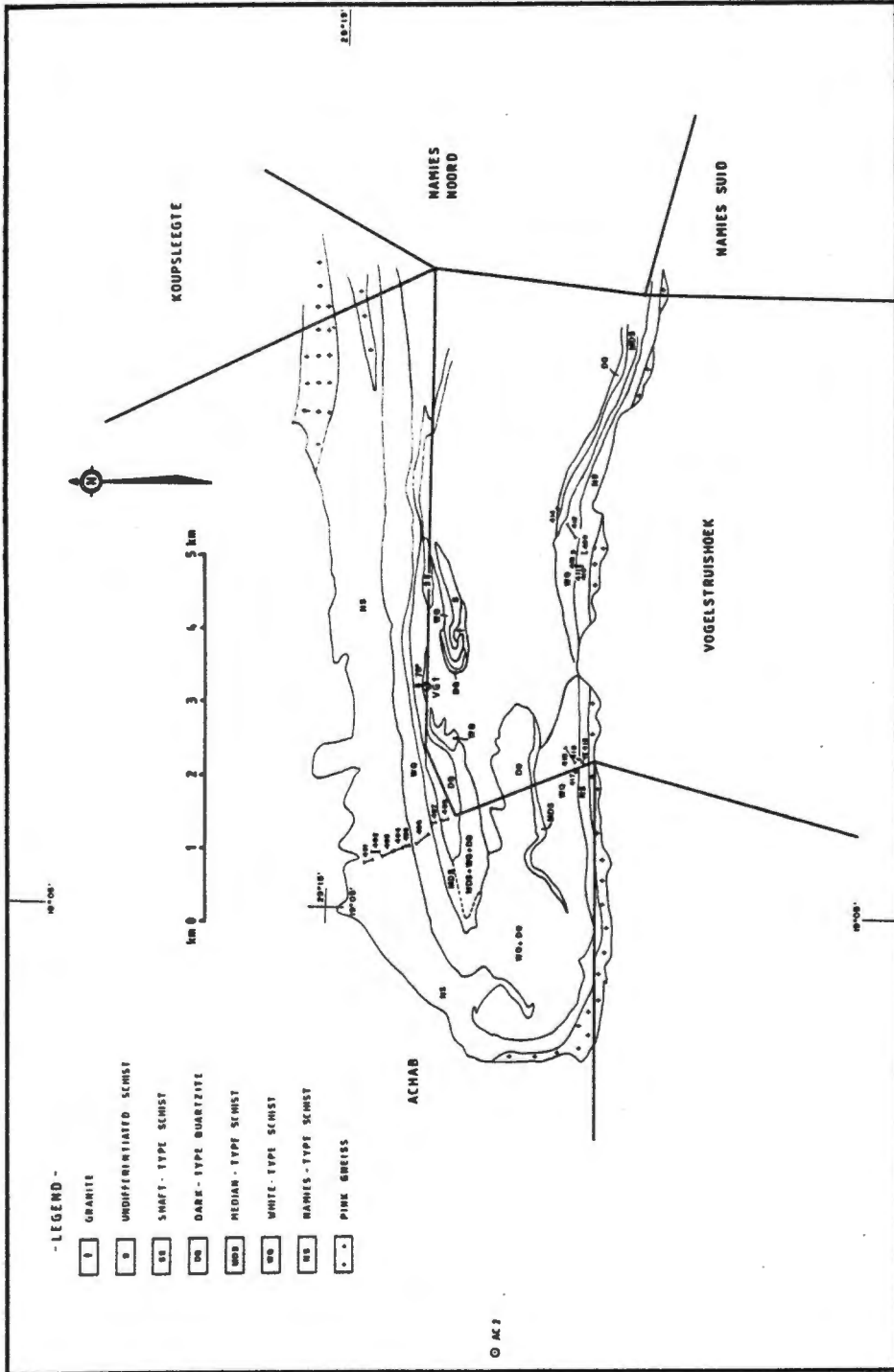


Fig. A.2 Geological maps showing locations of surface samples: (a) Broken Hill - Klein Kop; (b) Tank Hill, Maanhaarkop, Froneman se Kop; (c) Namiesberg



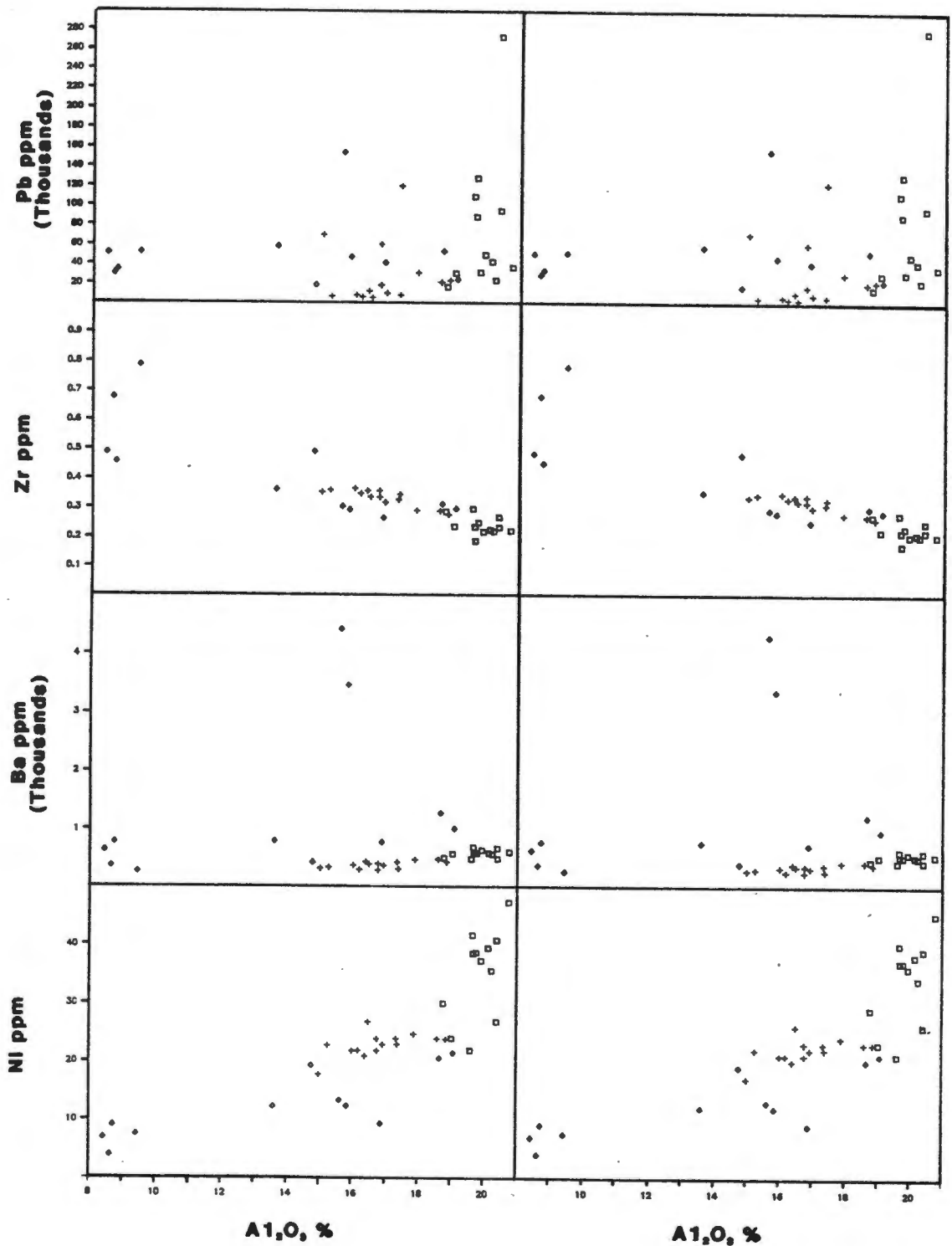


Fig. A.3 Comparison between volatile-included and volatile-free trace element data (left hand side and right hand sides, respectively), when plotted against volatile-free Al₂O₃. Differences between the two pairs of diagrams are negligible except where high Al₂O₃ concentrations coincide with elevated trace element values. Diamond = NS; Plus = LSS; Box = USS

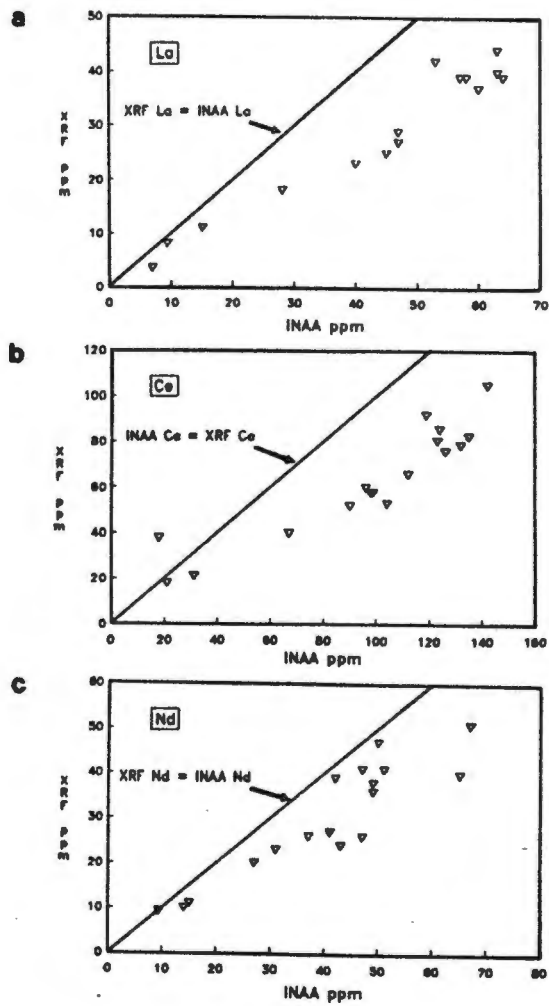


Fig. A.4 Comparison between XRF-derived rare earth element analyses and INAA data for the same samples: (a) La; (b) Ce; (c) Nd

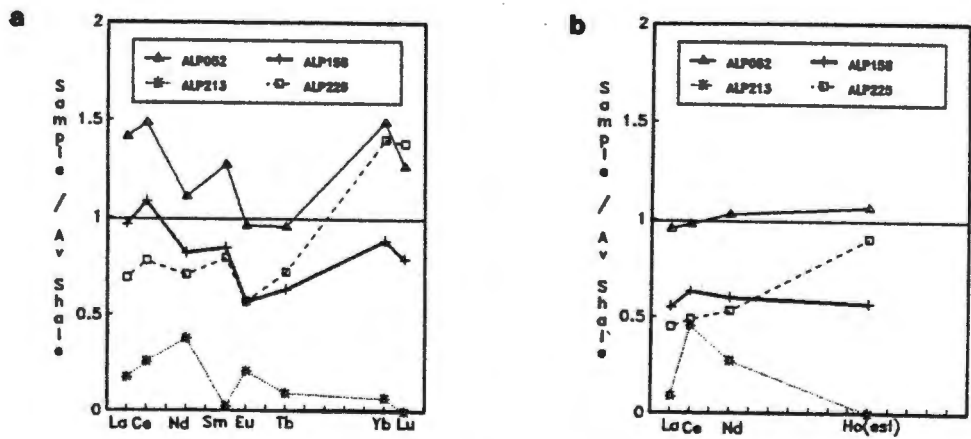


Fig. A.5 REE analyses of four samples by (a) INAA and (b) XRF analytical techniques, illustrating the applicability of the XRF-derived Ho estimate as an indication of relative HREE concentration



Fig. C.1 Photomicrograph of BGZ (ALP235) showing extensive brecciation and rounding of quartz grains in a clay and sericite matrix. Crossed nicols. (1cm = 400 micron)

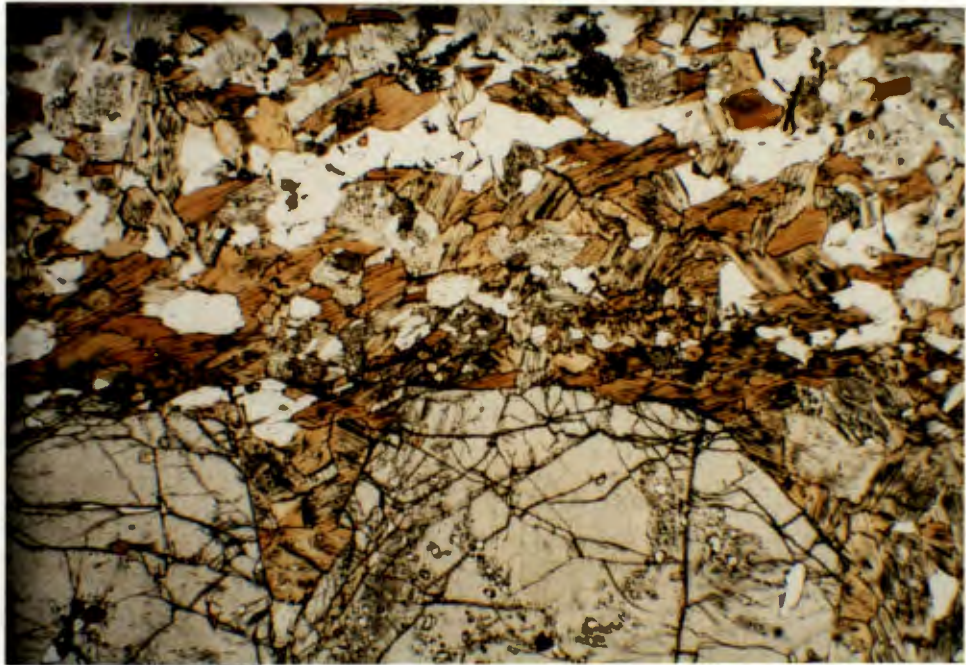


Fig. C.2 Photomicrograph of CS (ALP188) showing mineral banded nature, with garnet-dominated band below, followed by a biotite-rich band and then a quartz-rich band above. Plain polarized light. (1cm = 400 micron)

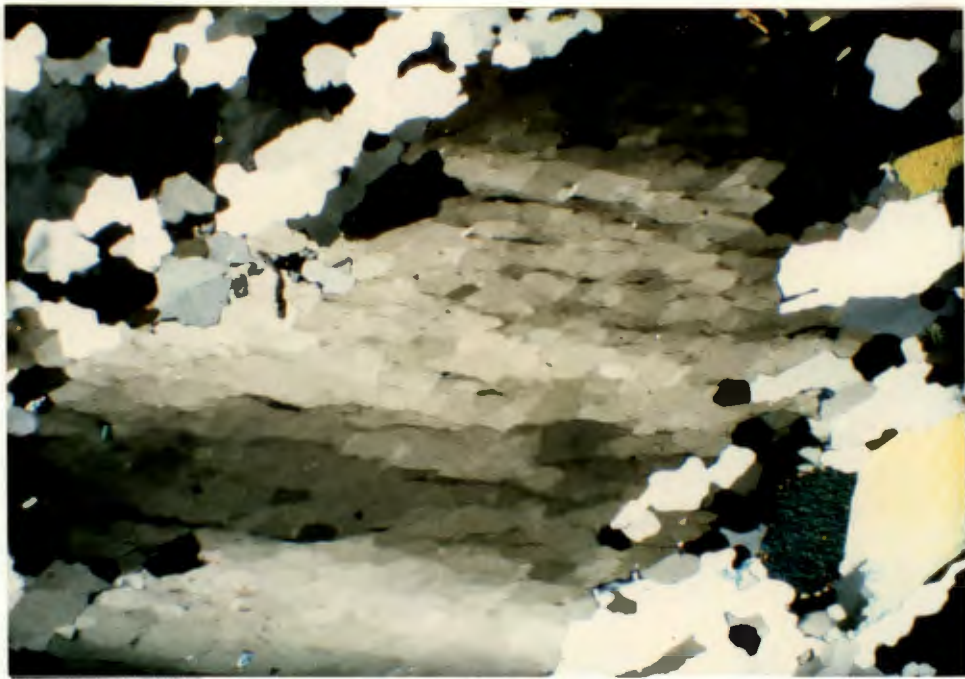


Fig. C.3 Photomicrograph of DQ (ALP239) showing severely strained quartz grain surrounded by a mortar texture of polygonized quartz grains. Muscovite appears near the top right-hand corner. Crossed nicols. (1cm = 400 micron)

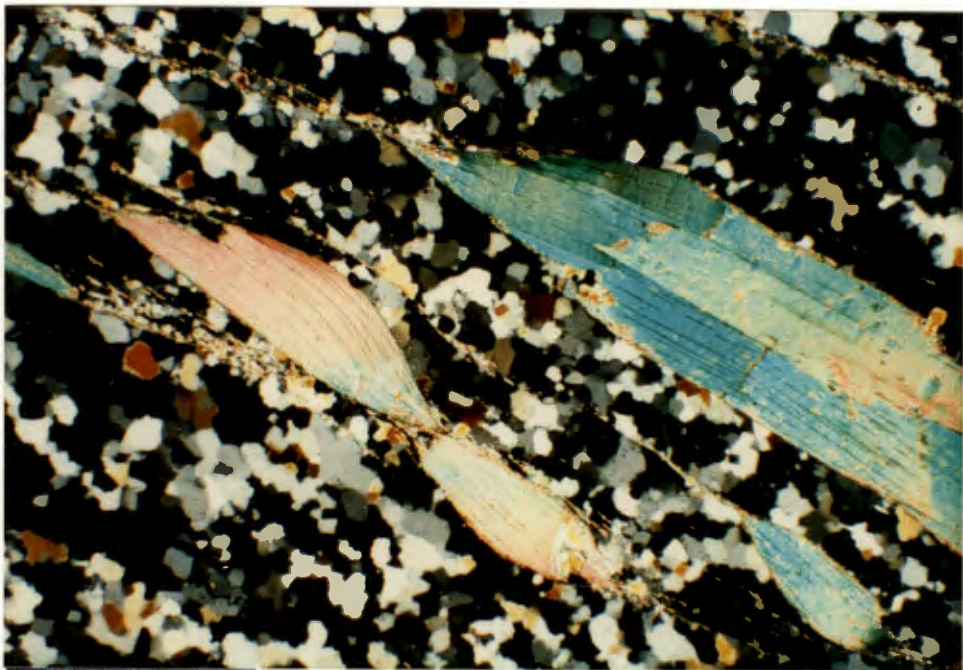


Fig. C.4 Photomicrograph of DQ (ALP126) showing sheared, wispy muscovite in a matrix of recrystallized quartz grains. Crossed nicols. (1cm = 400 micron)



Fig. E.1 Photograph of amphibolite xenoliths intruded by augen gneiss in quarry south of Broken Hill. Main xenolith is approximately 10cm wide

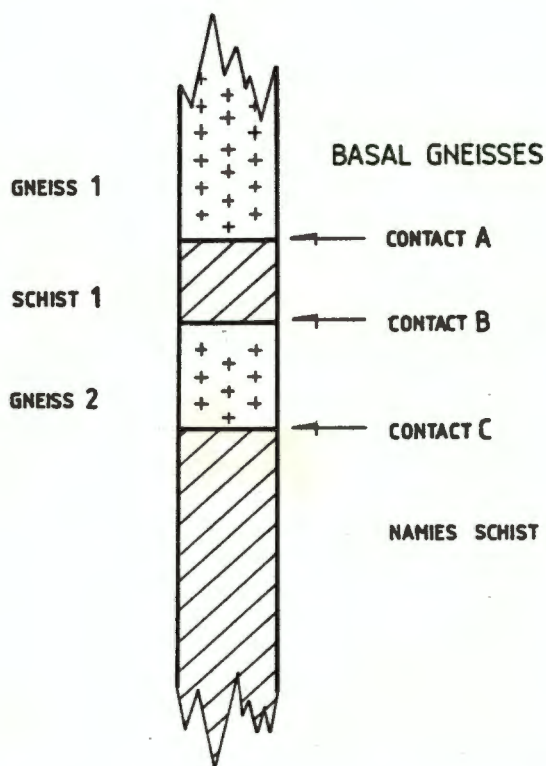


Fig. E.2 Schematic structural borehole intersection through the contact zone between Basal Gneiss and Namies Schist

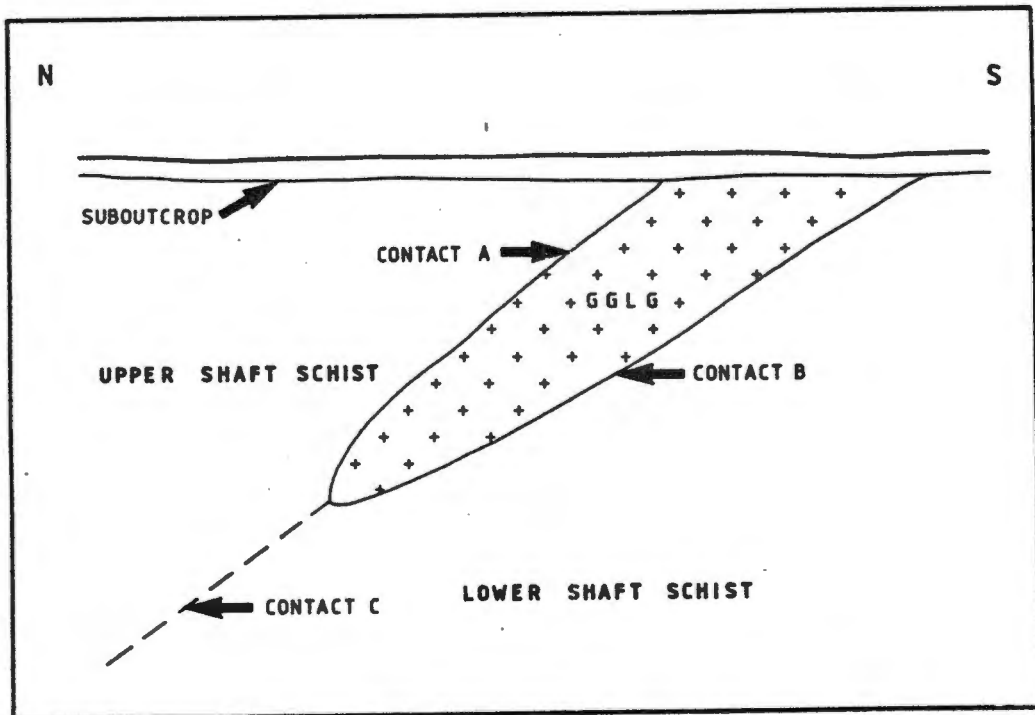


Fig. E.3 Schematic cross section through Shaft Schist showing position of Grey Granoblastic Leucocratic Gneiss (GGLG) as well as the contact between USS and LSS

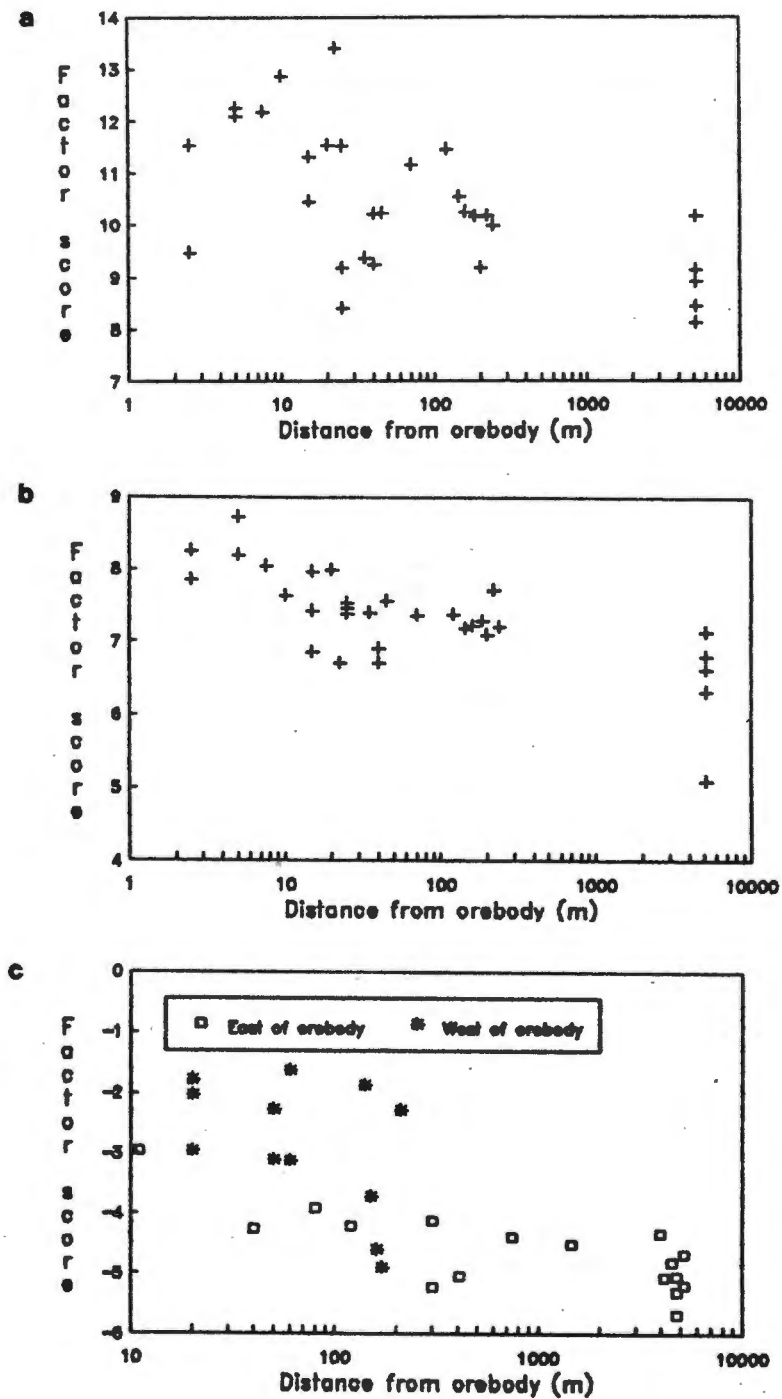


Fig. F.1 OS "ore factor" score variations with distance from the orebody: (a) OS borehole core Factor 2; (b) OS borehole core Factor 3; (c) OS surface outcrop Factor 3

Lithogeochemical Exploration Strategy for deposits of the Aggeney-type in the
North West Cape: Regional scale

Treat core and surface samples separately

Stratigraphy not known from
geology and petrography

Stratigraphy known from
geology and petrography

Establish stratigraphy using:
1. Means
2. Element variability
3. Correlation matrices
4. Factor analysis
5. Discriminant function anal.
6. REE

Stratigraphy still not known

Stratigraphy now known

1 Delta diagrams:
Use the elements Cu Pb Zn Ba Mn Fe P
[Na Sr decrease] while monitoring
Si Al K behaviour to compare schist
alternatively with NTS and STS, and
quartzite alternatively with WTQ
and DTQ

Process data using techniques which
distinguish between fertile and barren
terrane

1 Delta diagrams. Compare:
SS with STS (*) using Pb
NS with NTS using Pb Zn Ba Mn Fe
P Y (Cu) (**) [Na and Sr decrease]
MDS with MDTs using Cu Pb Zn Mn Fe
P Y [Na and Sr decrease]
WQ with WTQ using Mn Fe P Y
(Cu Pb Zn Ba)
DQ with DTQ using Cu Pb Zn Fe
Mn Fe [Sr decrease].

2 Correlation matrices:
For NTS, poor correlation between the
ore-related elements Zn S Ba and
elements such as Al K Ti Se Ni,
suggest the possible presence of a
nearby orebody

3 In NTS and OTS samples, REE patterns
showing positive slopes towards the
HREE's, may indicate the presence of a
nearby orebody

Use individual rock suites from
defined areas

1 Factor analysis: The presence of a
separate ore factor represents a
positive indication of
mineralization
In addition to schist and quartzite,
these techniques may work for
other rock-types such as gneiss

Detailed sampling of prospective
area using local scale
lithogeochemical exploration strategy;
shown in Fig. G.2

(*) The T in NTS and STS etc. refers to rock-types collected from the Achab, Namiesberg and Wortel areas
(**) Elements in parentheses only display the given trends in limited cases

Fig. G.1 Flow chart displaying the regional scale lithogeochemical exploration strategy for locating ore deposits of the Broken Hill-type in the north west Cape

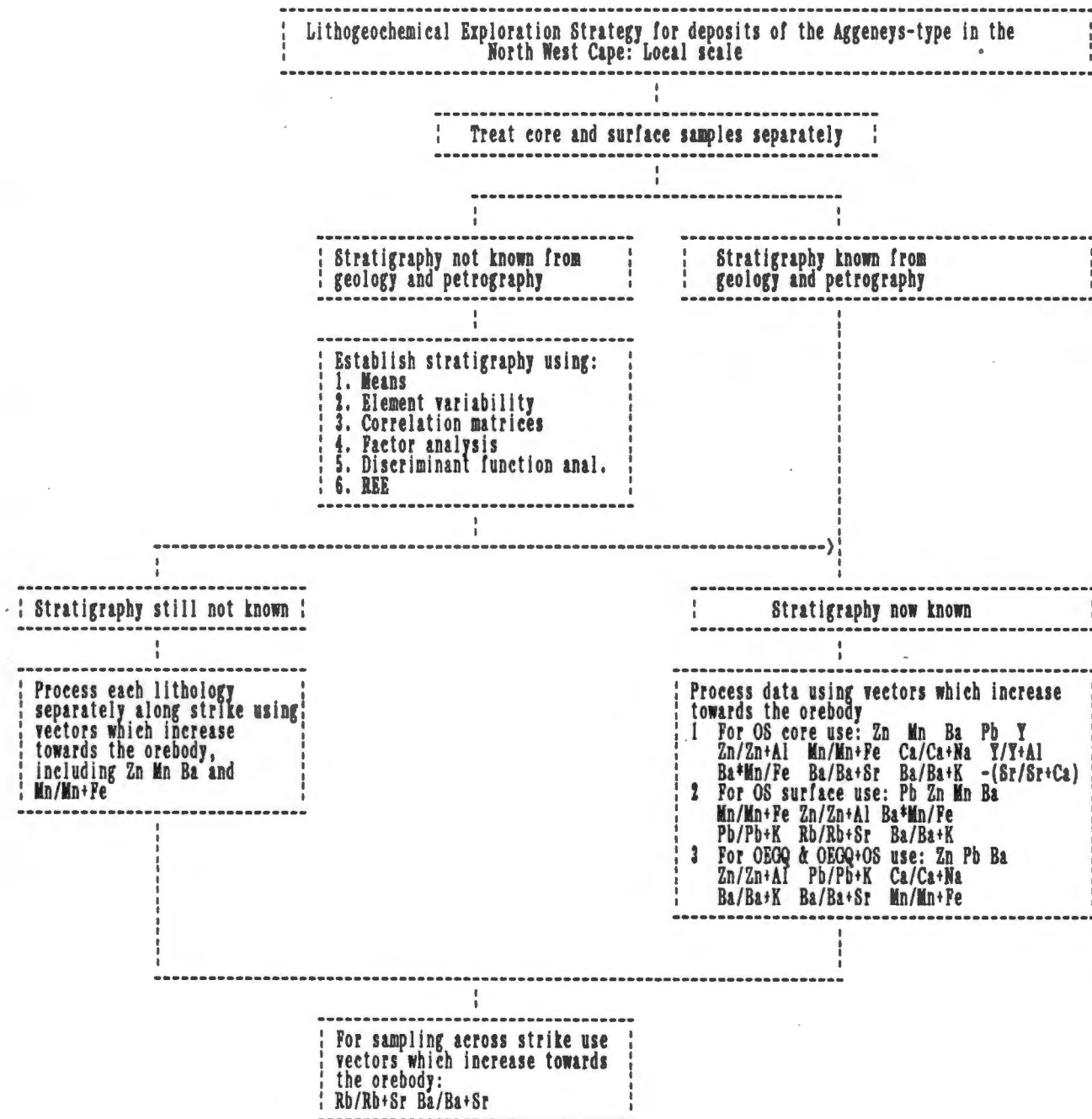


Fig. G.2 Flow chart displaying the local scale lithogeochemical exploration strategy for locating ore deposits of the Broken Hill-type in the north west Cape

Table A.1 Instrumental conditions adopted for major and trace element analyses using XRF spectrometers in the laboratories of the University of Cape Town Geochemistry Department

Element	Spectro- meter	Line	Tube	KV	MA	Crystal	Collimator	Detector	Time		Sample type
									Pk	Bg	
Mu	PW1220	Mo KaC	Mo	70	28	LiF(220)	F	S			B
Si	SRS-1	Ka	Cr	60	45	PET	C	F V	100		F
Ti	SRS-1	Ka	Cr	60	45	LiF(200)	F	F V	40		F
Al	SRS-1	Ka	Cr	60	45	PET	C	F V	100		F
Fe	SRS-1	Ka	Cr	60	45	LiF(220)	F	F V	100		F
Mn	SRS-1	Ka	Cr	60	45	LiF(220)	F	F V	100		F
Mg	SRS-1	Ka	Cr	60	45	TLAP	F	F V	200		F
Ca	SRS-1	Ka	Cr	60	45	LiF(200)	F	F V	40		F
Na	SRS-1	Ka	Cr	60	45	TLAP	C	F V	200	100	B
K	SRS-1	Ka	Cr	60	45	LiF(200)	C	F V	40		F
P	SRS-1	Ka	Cr	60	45	Ge	C	F V	100		F
S	PW1400	Ka	Cr	50	55	Ge	C	F V	80	40	B
Ba	SRS-1	La	Cr	60	45	LiF(200)	F	F V	100	40	B
Se	SRS-1	Ka	Cr	60	45	LiF(200)	F	F V	100	40	B
Rb	SRS-1	Ka	W	60	50	LiF(220)	F	S	100	40	B
Sr	SRS-1	Ka	W	60	50	LiF(220)	F	S	100	40	B
Y	SRS-1	Ka	W	60	50	LiF(220)	F	S	100	40	B
Zr	SRS-1	Ka	W	60	50	LiF(220)	F	S	100	40	B
Nb	SRS-1	Ka	W	60	50	LiF(220)	F	S	100	40	B
Mo	SRS-1	Ka	W	60	50	LiF(220)	F	S	100	40	B
U	SRS-1	La	W	60	50	LiF(220)	F	FS	100	40	B
Th	SRS-1	La	W	60	50	LiF(220)	F	FS	100	40	B
Pb	SRS-1	Lb	W	60	50	LiF(220)	F	FS	100	40	B
Zn	PW1400	Ka	Au	50	55	LiF(220)	F	FS V	80	40	B
Cu	PW1400	Ka	Au	50	55	LiF(220)	F	FS V	80	40	B
Ni	PW1400	Ka	Au	50	55	LiF(220)	F	FS V	80	40	B
Co	PW1400	Ka	W	50	55	LiF(220)	F	S V	80	40	B
Cr	PW1400	Ka	W	50	55	LiF(220)	F	S V	80	40	B
V	PW1400	Ka	W	50	55	LiF(220)	F	S V	80	40	B
La	PW1400	La	W	50	55	LiF(220)	F	FS V	160	80	B
Ce	PW1400	Lb	W	50	55	LiF(220)	F	FS V	160	80	B
Nd	PW1400	La	W	50	55	LiF(220)	F	FS V	160	80	B

Collimator: F = Fine, C = Coarse; Detector: F = Flow, S = Scintillation;

V = Run under vacuum; Sample Type: F = Fusion Disk, B = Briquette

Mu = mass absorption coefficient for Mo Ka Compton for 400000 counts (fixed count method)

Table A.2 Typical lower limits of detection (LLD) and absolute errors (1 standard deviation) for Bushmanland schists from this study analysed by the XRF technique. Since quartzite samples have lower mass absorption coefficients, their LLD and error values are approximately 1/3 lower than for schist

	LLD	Absolute error (1 std. dev.)
Oxide %		
SiO ₂	0.03	0.022
TiO ₂	0.006	0.01
Al ₂ O ₃	0.02	0.08
Fe ₂ O ₃	0.02	0.12
MnO	0.03	0.01
MgO	0.08	0.08
CaO	0.01	0.04
Na ₂ O	0.08	0.09
K ₂ O	0.004	0.03
P ₂ O ₅	0.04	0.01
Element (ppm)		
Rb	1.5	0.7
Ba	2.5	1.9
Sr	1.3	0.6
Th	2.2	0.7
U	3.5	1.1
Zr	2.1	1.1
Nb	1.5	0.5
Mo	1.5	0.5
Cr	1.6	0.8
V	1.9	0.9
Sc	0.7	0.3
Ni	0.8	0.4
Co	2.1	0.7
Pb	2.9	1
Zn	0.9	0.4
Cu	1.3	0.5
S *		
Y	1.5	0.5
La	3.5	1.3
Ce	4.5	1.7
Nd	3.5	1.3

* S contamination of pellets by oil fumes in the spectrometer render unreliable S values below concentrations of 200 - 300ppm

Table A.3 Analytical data including volatiles

SAMPLE	SiO2 %	TiO2 %	Al2O3 %	Fe2O3 %	MnO %	MgO %	CaO %	Na2O %	K2O %	P2O5 %	Rb ppm	Ba ppm	Sr ppm	Th ppm	U ppm	Zr ppm	Nb ppm	Mo ppm	Cr ppm	V ppm	Se ppm	Ni ppm	Co ppm	Pb ppm	Zn ppm	Cu ppm	S ppm	Y ppm	C %	DIST m	La ppm	Ce ppm	Nd ppm	SPEC	ENV. HOLE HILL POS.	
Core SS																																				
ALP054	63.558	0.816	20.409	8.701	0.416	1.003	0.296	0.208	4.556	0.036	224	475	44	22	0.001	234	20	0.001	102	75	18	27	42	281	145	29	813	37	0.120	35	40	90	42	SS	BH C	BH123
ALP056	63.138	0.859	20.405	6.837	0.068	2.013	0.181	0.296	4.873	0.061	240	650	64	25	0.001	270	20	5.0	131	237	23	41	16	98	233	60	12691	24	0.770	50	29	66	30	SS	BH C	BH123
ALP057	63.777	0.766	19.670	6.955	0.049	1.757	0.201	0.363	4.910	0.068	231	670	66	19	0.001	235	18	5.8	113	269	20	42	17	92	206	54	14837	21	0.820	55	28	60	28	SS	BH C	BH123
ALP058	63.461	0.738	20.144	7.189	0.036	1.729	0.147	0.252	4.760	0.082	242	569	47	18	0.001	226	16	3.9	107	190	20	39	18	44	158	50	14619	23		65	23	52	24	SS	BH C	BH123
ALP059	64.641	0.772	19.786	6.949	0.034	1.798	0.122	0.246	4.370	0.047	228	567	49	17	0.001	251	15	3.2	113	188	20	39	17	32	150	54	12352	23	0.510	90	26	61	27	SS	BH C	BH123
ALP060	68.472	0.740	17.895	6.129	0.034	1.511	0.110	0.362	3.652	0.025	188	462	49	22	4.6	292	13	0.001	103	109	19	25	16	32	117	29	10694	26	0.780	130	30	68	31	SS	BH C	BH123
ALP087	64.660	0.747	19.936	6.482	0.032	1.920	0.164	0.145	4.656	0.064	235	622	30	18	0.001	219	14	2.9	135	203	19	37	14	51	165	48	11936	23		50				SS	BH C	BH166
ALP087A	63.953	0.782	19.786	7.075	0.040	1.809	0.189	0.189	4.637	0.063	214	548	26	21	0.001	232	17	4.1	106	145	21	31	14	40	140	35	14762	24		50				SS	BH C	BH166
ALP087F	62.129	0.805	19.571	8.414	0.046	1.714	0.150	0.237	4.964	0.043	219	548	24	19	0.001	233	15	3.9	107	130	21	39	20	53	130	48	19270	21		50				SS	BH C	BH166
ALP136	72.659	0.684	16.764	5.364	0.036	1.141	0.098	0.166	3.042	0.045	206	286	16	14	0.001	359	14		96	54	16	24	13	19	78	46	1301	21		350	25	52	22	SS	PH C	BH164
ALP137	71.429	0.727	17.387	5.680	0.095	1.254	0.100	0.153	3.143	0.032	213	306	18	17	4.2	347	16		100	59	17	23	11	125	81	11	702	19	0.010	360	24	57	23	SS	PH C	BH164
ALP138	71.501	0.745	16.496	5.336	0.033	1.283	0.094	0.200	3.309	0.033	207	390	23	13	0.001	338	16	2.7	103	119	18	27	13	5.3	74	38	9708	19		370	25	58	24	SS	PH C	BH164
ALP139	72.433	0.713	16.396	5.030	0.028	1.295	0.154	0.318	2.949	0.022	182	434	42	17	0.001	360	15		96	78	16	21	11	13	68	22	6613	19	0.001	380	26	57	20	SS	PH C	BH164
ALP140	75.137	0.600	14.998	4.825	0.033	1.063	0.112	0.210	2.975	0.047	205	316	24	15	0.001	355	14		87	48	15	18	10	73	56	10	830	20		390	21	51	22	SS	PH C	BH164
ALP141	74.287	0.652	15.259	5.428	0.033	1.038	0.095	0.173	3.011	0.023	213	339	24	13	0.001	362	18		97	52	16	23	13	6.8	66	7.4	550	27		400	24	60	24	SS	PH C	BH164
ALP142	73.270	0.676	16.009	5.459	0.027	1.166	0.117	0.235	3.008	0.033	210	373	30	15	0.001	368	16		98	54	16	22	11	8.2	58	6.2	621	24		410	24	59	25	SS	PH C	BH164
ALP154	66.871	0.706	19.039	5.811	0.032	1.643	0.166	0.316	4.576	0.049	250	560	33	19	3.9	237	15	2.9	104	151	20	24	14	31	150	27	7923	28	0.320	65				SS	BH C	BH156
ALP154A	64.287	0.778	20.480	6.490	0.037	1.942	0.171	0.179	4.695	0.043	253	572	28	21	0.001	250	17	3.5	119	202	23	36	17	23	205	46	8986	29		65				SS	BH C	BH156
ALP155	66.855	0.810	19.616	5.747	0.034	1.661	0.153	0.289	3.943	0.037	226	472	40	17	0.001	298	18	2.1	109	111	19	22	14	113	124	26	8536	28		95	31	67	31	SS	BH C	BH156
ALP156	66.631	0.808	18.782	6.395	0.040	1.810	0.193	0.409	3.937	0.032	240	490	42	20	0.001	288	18	2.1	114	117	20	30	14	17	118	33	9606	24	0.240	125	34	75	32	SS	BH C	BH156
ALP157	65.289	0.664	19.696	6.201	0.024	1.526	0.262	0.510	4.524	0.072	240	582	51	16	4.8	187	14	2.9	98	159	18	38	17	133	117	46	12316	27	0.260	150	37	70	34	SS	BH C	BH156
ALP158	71.647	0.671	16.939	5.575	0.033	1.188	0.159	0.192	3.099	0.046	174	365	32	18	6.2	319	15	0.001	101	96	16	23	12	10	72	19	4512	22	0.040	170	23	54	24	SS	BH C	BH156
ALP160	73.583	0.658	16.194	5.176	0.021	1.010	0.123	0.196	3.007	0.033	181	298	29	16	0.001	350	16		92	53	16	22	11	6.1	36	1.7	134	18	0.060	200	20	52	20	SS	BH C	BH156
ALP161	70.509	0.747	17.349	5.721	0.029	1.308	0.159	0.318	3.090	0.037	179	421	42	12	0.001	329	17		103	103	18	24	15	8.2	62	28	7327	17		230	21	50	21	SS	BH C	BH156
ALP162	71.858	0.698	16.770	5.330	0.030	1.157	0.142	0.342	2.758	0.055	168	400	46	19	4.2	337	16		92	75	16	22	12	62	70	24	8594	25	0.010	260	25	65	29	SS	BH C	BH156
ALP183	65.084	0.773	20.768	5.454	0.036	1.913	0.074	0.210	4.864	0.060	254	588	23	19	5.0	222	16	4.3	122	256	20	47	23	38	410	55	7642	27	0.180	240	26	55	25	SS	BH C	BH163
ALP184	65.098	0.745	20.251	6.115	0.033	1.829	0.081	0.264	4.652	0.054	245	549	23	15	0.001	220	15	3.9	114	211	20	36	16	24	134	52	8768	20		245	28	62	27	SS	BH C	BH163
ALP185	67.999	0.757	18.867	5.604	0.032	1.541	0.163	0.333	3.882	0.033	205	423	38	18	0.001	278	16		104	116	17	24	13	24	106	32	7883	25	0.240	260	32	69	32	SS	BH C	BH163
ALP186	67.962	0.801	18.607	5.712	0.034	1.552	0.196	0.368	3.827	0.041	212	470	51	18	0.001	291	18		111	119	19	24	12	22	104	32	8992	23		280	27	59	27	SS	BH C	BH163
Surface SS																																				
ALP222	72.104	0.767	17.272	5.896	0.047	0.961	0.084	0.101	2.708	0.059	213	317	16	18	0.001	372	17	0.001	108	64	18	37	13	16	96	8.3	189	20	4720	26	58	23	SS	MK S E		
ALP224	70.252	0.755	17.495	6.373	0.046	1.369	0.068	0.155	3.374	0.112	254	503	17	40	0.001	363	17		104	63	18	21	13	50	69	30	123	16	4720	26	59	23	SS	MK S E		
BGZ																																				
ALP053	65.028	0.770	18.467	7.345	0.350	1.810	0.400	0.240	4.541	0.073	229	629	47	21	5.1	239	18	7.3	114	294	18	43	17	240	333	72	9766	26	0.940	30	34	73	32	BGZ	BH C	BH123
ALP120	63.602	0.874	19.931	7.967	0.250	1.618	0.231	0.250	4.830	0.088	243	500	39	25	0.001	232	17	4.3	132	164	19	53	22	503	1018	148	3581	24	1.360	28	40	89	43	BGZ	BH C	BH114
ALP153	62.255	0.856	22.815	6.143	0.096	2.165	0.196	0.185	5.220	0.068	279	760	35	16	0.001	244	16	4.5	141	260	23	48	15	10	375	50	1865	22	0.820	55	29	57	25	BGZ	BH C	BH156
ALP234	65.461	0.735	19.474	6.909	0.151	1.918	0																													

Table A.3 continued

SAMPLE	SiO2 %	TiO2 %	Al2O3 %	Fe2O3 %	MnO %	MgO %	CaO %	Na2O %	K2O %	P2O5 %	Rb ppm	Ba ppm	Sr ppm	Th ppm	U ppm	Zr ppm	Nb ppm	Mo ppm	Cr ppm	V ppm	Se ppm	Ni ppm	Co ppm	Pb ppm	Zn ppm	Cu ppm	S ppm	Y ppm	C %	DIST m	La ppm	Ce ppm	Nd ppm	SPEC	HILL	ENV. HOLE POS.			
WQ																																							
ALP009	95.334	0.069	2.470	1.166	0.015	0.094	0.059	0.049	0.689	0.054	34	94	2.2	0.001	0.001	133	3.8	0.001	7.7	2.7	1.9	2.9	0.001	11	43	35	296	6.0											
ALP040	97.794	0.060	1.064	0.665	0.011	0.045	0.014	0.028	0.303	0.015	18	36	2.0	0.001	0.001	129	2.5	0.001	4.4	3.1	1.4	0.001	1.5	8.2	13	20	73	10	0.001	115									
ALP067	97.485	0.052	1.108	0.778	0.014	0.092	0.012	0.118	0.304	0.037	17	24	0.001	0.001	0.001	100	2.1	0.001	6.1	3.1	0.001	0.001	0.001	6.3	24	39	421	7.3											
ALP124	94.567	0.056	1.820	2.454	0.086	0.416	0.162	0.059	0.369	0.012	40	24	8.4	3.3	0.001	69	1.7	0.001	4.5	6.9	1.0	1.9	5.9	21	106	79	329	11	5100	8.9	20	8.2	WQ	MK	C	BH166			
ALP196	97.805	0.041	0.680	1.204	0.011	0.015	0.001	0.052	0.177	0.015	8.9	35	4.5	4.1	0.001	66	0.001	0.001	6.8	3.3	0.001	0.001	0.001	0.001	6.4	3.5	31	4.2	290	12	28	12	WQ	BH	S	TS11			
ALP204	98.333	0.037	0.339	1.127	0.016	0.009	0.001	0.030	0.091	0.017	4.8	25	2.6	0.001	0.001	56	0.001	0.001	5.9	2.8	0.001	0.001	0.001	0.001	8.1	3.5	44	2.3	650										
ALP215	97.956	0.043	0.577	1.166	0.015	0.027	0.001	0.043	0.172	0.001	9.2	20	1.7	0.001	0.001	84	1.7	0.001	6.3	3.2	2.1	0.001	0.001	0.001	5.6	4.5	4.1	67	2.6	1500	8.2	19	7.1	WQ	KK	S			
ALP227	98.692	0.043	0.732	0.219	0.007	0.001	0.009	0.045	0.229	0.024	18	40	3.9	4.9	0.001	68	2.8	0.001	4.4	2.2	0.8	0.001	0.001	0.001	1.2	0.001	0	3.5	9100	10	22	9.1	WQ	FK	S				
ALP232	97.008	0.060	1.725	0.491	0.013	0.042	0.009	0.056	0.581	0.014	37	53	3.0	4.5	0.001	88	7.0	0.001	5.1	2.7	4.4	0.001	0.001	0.001	6.4	0.001	130	6.5	5050	8.7	15	7.9	WQ	MK	S				
ALP237	98.429	0.035	0.751	0.370	0.012	0.063	0.007	0.032	0.250	0.050	14	18	0.001	0.001	0.001	88	3.6	0.001	4.1	2.0	0.001	1.1	0.001	0.001	5.1	0.001		3.2	3950	10	15	8.2	WQ	MK	S				
DQ																																							
ALP011	96.380	0.034	1.585	1.446	0.070	0.062	0.035	0.039	0.338	0.012	18	33	0.001	3.7	0.001	79	1.5	0.001	7.6	2.4	2.6	2.4	0.001	8.8	26	21	132	15	80										
ALP042	94.738	0.134	2.297	2.096	0.042	0.132	0.019	0.050	0.492	0.001	27	56	0.001	7.9	0.001	264	5.6	0.001	13	6.7	2.2	1.4	4.9	5.8	67	79	532	6.8	55	20	36	16	DQ	BH	C	BH004			
ALP069	96.094	0.071	1.545	1.649	0.031	0.045	0.015	0.043	0.507	0.001	26	48	2.1	3.8	0.001	119	0.001	0.001	6.9	5.4	0.001	0.001	2.3	12	65	28	408	8.1	25	12	10	DQ	BH	C	BH123				
ALP126	97.577	0.026	1.398	0.356	0.008	0.098	0.021	0.049	0.447	0.021	24	36	2.0	0.001	3.1	133	2.4	0.001	4.7	2.8	1.0	0.001	2.3	10	12	565	602	3.0	5100										
ALP195	97.956	0.042	1.072	0.402	0.010	0.108	0.001	0.071	0.330	0.010	16	46	3.1	0.001	0.001	90	0.001	0.001	4.7	2.8	0.8	0.001	0.001	4.6	2.5	7.8	21	3.2	260	7.6	16	6.7	DQ	BH	S	TS11			
ALP233	97.095	0.062	1.704	0.478	0.004	0.032	0.008	0.058	0.559	0.001	30	51	4.0	0.001	0.001	79	3.2	0.001	6.5	1.7	4.4	0.001	1.3	0.001	3.9	1.3	54	3.8	5050	7.1	16	7.9	DQ	MK	S				
ALP238	98.121	0.035	1.090	0.268	0.012	0.059	0.001	0.041	0.372	0.001	19	28	2.3	3.2	0.001	53	3.0	0.001	4.5	2.8	1.2	0.001	0.001	0.001	3.6	0.001	13	3.7	3950	14	28	11	DQ	MK	S				
ALP239	98.621	0.042	0.735	0.223	0.007	0.043	0.001	0.036	0.261	0.031	16	63	4.9	0.001	0.001	122	2.8	0.001	4.1	2.3	0.9	0.001	0.001	0.001	7.1	0.001		8.1	9200	11	23	10	DQ	FK	S				
ALP240	97.383	0.046	0.767	1.637	0.020	0.048	0.011	0.024	0.021	0.042	0.001	27	2.6	0.001	0.001	101	2.8	0.001	4.0	2.3	0.001	0.001	5.4	47	25	66	299	7.6	1500	13	26	13	DQ	KK	S				
MDS																																							
ALP041	71.721	0.709	14.739	8.362	0.162	0.712	0.072	0.118	3.365	0.042	199	358	9.0	19	0.001	424	18	0.001	83	66	12	15	18	43	168	20	266	32	0.010	80	42	91	44	MDS	BH	C	BH123		
ALP068	72.701	0.672	14.248	7.633	0.232	0.628	0.160	0.090	3.552	0.084	218	419	17	12	0.001	352	18	0.001	69	54	10	11	13	55	313	63	821	35	60	35	68	34	MDS	BH	C	BH166			
ALP125	82.790	0.125	4.110	10.140	0.362	1.358	0.587	0.076	3.359	0.094	37	67	25	14	0.001	188	2.4	0.001	13	19	2.5	22	36	32	309	263	991	74	5100	22	47	24	MDS	MK	C	TS11			
ALP226	85.983	0.254	5.765	6.138	0.145	0.204	0.110	0.082	1.227	0.091	73	426	27	13	0.001	292	5.7	0.001	31	50	4.4	6.0	11	53	58	14	136	29	5120	29	50	27	MDS	MK	S				
Q																																							
ALP143	98.758	0.017	0.454	0.475	0.046	0.042	0.016	0.068	0.125	0.001	7.9	5.0	0.001	0.001	13	49	0.001	2.6	2.3	1.3	0.001	1.8	0.001	3.7	5.2	859	6.3		420	7.5	0.001	0.001	Q	PH	C	BH164			
ALP223	93.759	0.070	2.026	2.876	0.044	0.591	0.035	0.055	0.524	0.020	71	54	2.9	0.001	0.001	57	4.1	0.001	16	6.5	1.8	7.4	4.9	8.5	80	20	56	3.3	4720	3.6	13	0.001	Q	MK	S				
DTQ																																							
ALP426	97.734	0.030	1.038	0.680	0.029	0.001	0.026	0.044	0.399	0.019	25	47	21	1.0	0.001	60	3.3	0.001	3.7	3.8	0.8	1.0	1.8	5.9	17	14	483	10											
ALP428	98.244	0.025	0.655	0.816	0.019	0.001	0.016	0.026	0.196	0.002	14	14	1.0	1.0	0.001	50	1.6	0.001	2.9	3.5	5.1	1.0	1.0	2.5	1.0	11	70	2247	4.5	0.001	11	19	8.2	DTQ	NB	C	VG1		
ALP437	96.168	0.076	1.967	0.757	0.007	0.001	0.118	0.338	0.549	0.019	32	64	8.9	6.2	0.001	166	4.4	0.001	7.3	4.2	1.3	1.8	1.7	1.0	8.8	2.3	11	7.4											
ALP448	93.073	0.258	3.607	1.580	0.026	0.024	0.061	0.212	1.123	0.036	55	233	15	10	0.001	214	6.5	0.001	15	16	4.3	7.2	4.9	7.9	13	4.4	385	12	0.001	12	26	13	DTQ	WTL	C	WTL3			
ALP408	98.996	0.029	0.439	0.365	0.009	0.001	0.004	0.007	0.124	0.025	7.5	42	5.8	0.001	4.5	38	1.6	0.001	1.3	2.6	4.8	0.001	0.001	5.5	0.001	10	18	338	5.0										
ALP413	98.720	0.022	0.619	0.392	0.015	0.001	0.001	0.031	0.199	0.001	25	15	0.001	0.001	0.001	31	1.8	0.001	3.9	2.3	0.8	0.001	0.001	0.001	5.8	12	290	1.7		3.2	4.8	0.001	DTQ	NB	S				
ALP414	99.095	0.016	0.386	0.350	0.012	0.001	0.001	0.029	0.109	0.001	15	7.9	5.7	0.001	0.001	42	3.4	0.001	2.7	2.4	1.3	0.001	0.001	0.001	6.8	12	266	5.3		5.3	9.0	3.4	DTQ	NB	S				
MDTS																																							
ALP436	70.647	0.719	13.680	7.660	0.045	0.981	0.423	0.747	5.000	0.098	290	620	72	13	0.001	560	18	2.8	77	76	11	22	13	23	47	3.8	38	29											
ALP449	73.484	0.848	13.483	5.877	0.100	1.637	0.756	0.427	3.312	0.075	203	721	85	18	0.001	301	18	1.8																					

Table A.3 continued

SAMPLE	SiO2 %	TiO2 %	Al2O3 %	Fe2O3 %	MnO %	MgO %	CaO %	Na2O %	K2O %	P2O5 %	Rb ppm	Ba ppm	Sr ppm	Th ppm	U ppm	Zr ppm	Nb ppm	Mo ppm	Cr ppm	V ppm	Se ppm	Ni ppm	Co ppm	Pb ppm	Zn ppm	Cu ppm	S ppm	Y ppm	C %	DIST m	La ppm	Ce ppm	Nd ppm	SPEC	HILL	ENV. HOLE POS.	
Pegmatite																																					
ALP028P	77.533	0.170	12.976	1.618	0.028	0.393	0.300	1.007	5.904	0.071	249	1289	85	0.001	0.001	61	10	0.001	10	15	6.5	3.6	3.1	48	15	1.7	84	16	370	16	29	15	PNS	BH	C	BH123	
ALP039P	92.348	0.049	4.771	1.191	0.037	0.180	0.040	0.039	1.317	0.026	72	97	4.7	3.1	0.001	68	1.9	0.001	12	2.5	0.8	3.1	0.001	17	17	7.5	29	15	240				PNS	BH	C	BH123	
ALP051P	86.031	0.093	8.685	1.617	0.095	0.255	0.062	0.133	2.990	0.039	114	991	20	4.9	0.001	23	3.7	0.001	12	10	2.3	5.1	0.001	275	42	4.2	54	6.9	10				PUPS	BH	C	BH123	
ALP059P	84.579	0.036	9.536	1.428	0.012	0.340	0.231	0.735	2.639	0.063	115	485	56	12	0.001	66	9.1	0.001	2.7	6.0	1.7	4.0	3.1	73	15	8.1	4013	58	90	11	26	11	PSS	BH	C	BH123	
ALP066P	80.703	0.066	11.093	1.326	0.001	0.177	0.248	0.361	5.823	0.202	236	688	55	7.8	0.001	3.2	212	6.2	0.001	15	2.6	1.7	1.5	0.001	246	112	1.2	28	14	160				PNS	BH	C	BH166
ALP087P	79.774	0.025	12.638	0.933	0.044	0.421	0.136	2.071	3.860	0.098	152	649	93	17	0.001	10	17	1.7	0.001	3.7	8.7	0.001	0.001	1.8	200	13	0.001	1236	46	50	30	57	24	PLFS	BH	C	BH166
ALP101P	74.452	0.077	13.762	0.872	0.044	0.001	0.061	0.555	10.095	0.081	364	1855	66	0.001	0.001	26	1.9	0.001	4.7	6.8	1.1	2.1	3.0	552	19	4.2	78	8.1	25	6.4	15	7.0	PNS	BH	C	BH114	
ALP122P	81.707	0.045	10.034	1.158	0.001	0.252	0.315	0.891	5.554	0.042	296	1012	66	4.9	0.001	28	3.4	0.001	12	0.001	1.2	4.0	0.001	46	9.0	1.4	110	7.5	5100				PNS	MK	C	TS11	
ALP128P	80.579	0.285	11.815	2.596	0.017	0.387	0.195	0.108	3.870	0.148	188	330	18	6.6	0.001	237	16	0.001	21	18	6.8	6.5	4.5	57	50	11	27	8.2	5100				PUPS	MK	C	TS11	
ALP135P	71.525	0.051	16.410	1.001	0.001	0.379	0.398	0.749	9.410	0.076	341	1526	125	0.001	0.001	13	1.7	0.001	6.5	2.7	1.2	3.5	0	316	19	0.010	93	3.5	5100				PLFS	BH	C	BH164	
ALP141P	76.576	0.108	14.867	2.061	0.001	0.682	0.267	2.724	2.670	0.045	189	392	142	10	0.001	10	8.5	0.001	10	4.2	3.9	5.2	1.8	123	36	2.3	227	97	400				PLFS	BH	C	BH156	
ALP159P	74.052	0.018	14.953	0.697	0.001	0.115	1.124	2.173	6.819	0.047	225	480	159	6.4	0.001	7.9	17	0.001	0.001	3.9	0.001	2.4	1.8	0.001	116	2.4	0.0	83	185				PLFS	BH	C	BH112	
ALP173P	96.578	0.022	1.417	0.913	0.016	0.122	0.016	0.051	0.840	0.025	32	245	8.0	0.001	0.001	2.9	0.001	0.001	4.1	0.001	0.001	2.7	0.001	29	48	3.6	151	1.4	120				OESP	BH	C	BH112	
ALP424P	78.019	0.073	13.771	2.740	0.055	1.074	0.271	0.658	3.171	0.168	191	759	14	-4.5	-3.5	38	2.8	-1.3	4.4	7.3	2.2	5.4	9.1	303	91	5.1	914	17	9.4	16	10	PSTS	NB	C	VG1		
ALP430P	75.059	0.109	15.395	4.025	0.059	1.243	0.325	0.063	3.513	0.208	204	657	17	8.5	-3.7	53	3.2	-1.4	7.1	11	4.5	6.1	10	370	102	12	414	18	12	21	10	P	WTL	C	WTL3		
ALP438P	85.216	0.084	9.435	0.902	-0.038	0.385	0.409	0.531	3.029	0.048	140	487	61	5.3	-3.3	16	4.9	-1.3	5.3	6.9	2.0	3.6	2.2	14	6.4	3.1	45	84	12	21	10	P	WTL	C	WTL3		
ALP441P	74.118	0.086	15.047	0.612	-0.037	-0.117	3.214	0.745	6.271	0.060	211	518	225	-4.6	57	36	2.2	3.0	-1.4	6.0	3.9	-1.2	2.0	57	8.4	-1.2	17	5.1	4.3	6.2	-2.3	P	WTL	C	WTL3		
Surface NS																																					
ALP205	73.738	0.365	11.349	10.430	0.101	0.200	0.095	0.215	3.344	0.161	159	1099	17	15	0.001	281	10	0.001	70	88	8.4	10	5.5	101	296	13	37	49	250	50	116	56	NS	BH	S		
ALP236	76.330	0.319	9.563	10.098	0.010	0.207	0.120	0.301	2.900	0.151	184	409	13	11	0.001	249	10	0.001	67	72	6.9	11	8.8	0	16	0.001	143	33	4000	38	91	46	NS	MK	S		
ALP242	80.614	0.520	11.074	2.943	0.001	0.308	0.035	0.186	4.271	0.049	250	658	39	16	-3.5	339	16	-1.3	62	21	5.7	8.1	3.7	43	22	1.8	20	33	18	29	15	NS	MK	S			
ALP243	83.968	0.213	7.295	4.935	0.276	0.315	0.173	0.137	2.652	0.035	203	870	22	5.5	-3.7	230	6.7	3.3	264	18	4.5	16	6.0	18	52	7.6	16	24	18	29	15	NS	BH	S			
Surface NS and equivalent rocks at Tank Hill																																					
ALP241	96.649	0.092	2.185	0.189	0.007	0.066	0.032	0.056	0.685	0.038	35	564	14	0.001	0.001	100	3.0	1.2	64	12	1.3	0.001	0.001	57	10	0.001	5.3	3.7	5.7	15	7.6	GRQ	TH	S			
ALP244	72.391	0.687	13.373	6.439	0.074	0.399	0.022	0.190	3.742	0.160	347	4191	20	16	-4.7	226	16	6.3	70	93	15	-2.0	-2.4	7353	7890	112	5926	3.7	26	59	32	NS	TH	S			
Surface NTS																																					
ALP401	74.107	0.632	15.210	5.850	0.001	0.994	0.097	0.116	2.952	0.041	204	509	24	15	-3.8	354	15	2.4	97	64	15	25	12	15	84	40	248	26	0.030	31	66	32	NTS	NB	S		
ALP402	80.685	0.556	12.011	3.927	0.001	0.705	0.073	0.081	1.929	0.032	173	253	9.4	20	4.3	509	17	-1.4	79	42	13	16	8.4	6.3	57	11	90	18	26	52	23	NTS	NB	S			
ALP403	75.954	0.616	15.044	4.911	0.001	1.080	0.070	0.100	2.191	0.034	210	293	20	21	-4.1	483	17	-1.5	95	46	15	20	8.6	-5.8	107	9.0	67	34	0.030	34	74	33	NTS	NB	S		
ALP404	78.036	0.572	12.945	4.891	0.001	0.988	0.095	0.080	2.363	0.029	169	289	16	13	-3.7	396	15	-1.4	84	47	14	27	15	8.8	188	37	84	20	25	49	21	NTS	NB	S			
ALP409	67.491	0.695	19.035	5.428	0.047	1.577	0.208	0.409	5.057	0.053	312	940	53	21	3.9	225	17	5.8	114	187	18	40	12	-5.5	27	51	67	28	0.010	37	75	36	NTS	NB	S		
ALP410	70.322	0.621	18.642	4.458	0.001	1.220	0.108	0.126	4.458	0.044	318	987	24	19	4.1	272	17	2.7	103	91	12	26	5.8	10	69	56	173	25	0.020	27	55	26	NTS	NB	S		
ALP411	77.257	0.537	14.455	4.757	0.001	0.666	0.046	0.093	2.161	0.026	154	467	14	19	3.8	395	14	2.2	83	45	12	20	7.4	5.3	76	30	153	25	28	60	26	NTS	NB	S			
ALP415	71.500	0.681	17.395	5.410	0.001	1.114	0.080	0.127	3.651	0.042	234	843	25	17	-3.8	314	15	1.7	106	80	17	23	9.4	22	63	52	197	19	28	60	27	NTS	NB	S			
ALP416	74.554	0.606	16.173	4.747	0.001	0.730	0.098	0.115	2.940	0.037	169	714	25	15	-3.7	351	16	-1.4	94	55	15	22	10	11	44	7.5	183	17	25	52	23	NTS	NB	S			
Core NTS																																					
ALP433	83.166	0.437	8.873	3.372	0.001	0.532	0.366	0.713	2.499	0.042	180	407	45	15	-3.5	576	12	1.4	100	20	5.7	13	4.6	7.6	25	-1.3	80	27	0.040	33	71	37	NTS	WTL	C	WTL3	
ALP434	88.183	0.415	7.515	1.947	0.001	0.463	0.018	0.141	1.300	0.016	112	161	4.4	12	-3.3	836	13	-1.3	68	16	4.1	8.9	4.5	-4.8	17	-1.2	27	37	36	76	39	NTS	WTL	C	WTL3		
Core NS																																					
ALP028	65.088	0.860	19.093	7.085	0.128	1.494	0.507	0.451	5.187	0.108	33																										

Table A.3 continued

SAMPLE	SiO2 %	TiO2 %	Al2O3 %	Fe2O3 %	MnO %	MgO %	CaO %	Na2O %	K2O %	P2O5 %	Rb ppm	Ba ppm	Sr ppm	Th ppm	U ppm	Zr ppm	Nb ppm	Mo ppm	Cr ppm	V ppm	Sc ppm	Ni ppm	Co ppm	Pb ppm	Zn ppm	Cu ppm	S ppm	Y ppm	C %	DIST m	La ppm	Ce ppm	Nd ppm	SPEC	HILL	ENV. POS.	HOLE POS.	
HS																																						
ALP043	71.386	0.747	16.171	7.665	0.218	0.690	0.090	0.132	2.878	0.024	200	521	6.1	20	0.001	365	20	0.001	89	66	14	16	19	62	259	2.3	115	26	0.001	40	39	88	41	HS	BH	C	BH123	
ALP044	70.336	0.758	15.875	8.092	0.445	0.915	0.155	0.151	3.247	0.025	215	654	10	18	0.001	338	19	0.001	93	70	16	19	16	114	247	0.001	75	40		25	33	74	37	HS	BH	C	BH123	
ALP100	69.178	0.813	15.823	9.895	0.190	0.756	0.062	0.082	3.176	0.026	215	389	7.1	17	0.001	327	19	0.001	102	84	16	19	22	59	191	15	345	24	0.050	40				HS	BH	C	BH114	
ALP101	72.702	0.700	15.268	5.979	0.485	0.998	0.151	0.109	3.543	0.065	196	643	15	19	0.001	312	17	0.001	86	60	13	18	13	63	79	0.001	42	36	0.010	25				HS	BH	C	BH114	
ALP103	73.340	0.495	11.139	11.713	0.542	0.655	0.158	0.062	1.839	0.057	190	1218	7.2	17	0.001	264	13	0.001	53	79	9.3	16	21	269	537	46	478	31	0.010	2.5				HS	BH	C	BH114	
ALP165	65.295	0.887	20.214	7.629	0.567	0.921	0.132	0.109	4.197	0.047	236	517	18	22	0.001	255	21	0.001	112	90	22	32	17	55	658	47	38	38	0.030	220				HS	BH	C	BH112	
ALP166	70.598	0.799	17.222	6.360	0.441	1.006	0.111	0.084	3.333	0.047	200	337	8.5	23	0.001	261	20	0.001	94	70	18	24	100	35	242	17	40	33		200				HS	BH	C	BH112	
ALP168	67.075	0.750	16.771	11.195	0.359	0.682	0.104	0.094	2.913	0.056	191	383	7.5	16	0.001	261	20	0.001	99	101	14	20	29	37	243	35	92	35		240	32	69	36	HS	BH	C	BH112	
ALP170	67.370	0.817	19.422	6.456	0.245	1.478	0.140	0.102	3.906	0.065	243	441	8.8	21	0.001	302	22	0.001	103	79	18	28	16	48	331	135	45	36		185				HS	BH	S E		
ALP163	68.845	0.693	18.079	7.484	0.658	0.656	0.139	0.072	3.303	0.072	182	407	16	20	0.001	209	19	0.001	85	68	17	22	16	28	166	69	80	43	0.040	300				HS	BH	S E		
ALP164	66.606	0.819	19.785	7.848	0.583	1.093	0.091	0.094	3.034	0.047	194	345	12	25	0.001	234	19	2.315	104	89	23	29	15	18	181	2.8	102	37		300				HS	BH	S E		
ALP214	66.797	0.862	19.651	5.518	0.104	1.401	0.096	0.147	5.378	0.045	291	901	35	17	0.001	219	21	0.001	100	92	19	28	13	133	109	13	121	31		1450	33	68	36	HS	KK	S E		
IS																																						
ALP076	64.244	0.841	20.941	6.493	0.308	0.940	0.086	0.139	5.742	0.057	314	2095	34	15	0.001	233	19		102	84	19	17	10	1034	282	66	714	30		5.0	39	88	44	IS	BH	C	BH166	
ALP145	62.335	0.892	20.980	9.521	0.700	0.940	0.091	0.093	4.387	0.061	258	841	12	15	0.001	190	23	0.001	108	92	20	18	10	109	231	0.001	116	43		2.5	44	101	50	IS	BH	C	BH156	
ALP147	67.444	0.826	18.315	8.343	0.262	1.018	0.047	0.074	3.636	0.035	246	470	10	19	0.001	273	21		101	77	16	29	16	22	593	12	734	32		15	42	82	43	IS	BH	C	BH156	
ALP177	67.966	0.773	17.979	6.927	0.488	0.749	0.087	0.102	4.861	0.069	248	627	22	14	0.001	244	17	0.001	96	96	18	24	12	33	388	0.001	187	43		35	37	71	38	IS	BH	C	BH112	
OES																																						
ALP115	62.351	1.049	20.811	8.705	0.312	1.358	0.093	0.173	4.475	0.025	371	2499	10	19	0.001	366	41	0.001	130	97	21	10	6.9	295	655	192	3991	16	0.020	2.5	29	69	35	S	BH	C	BH114	
ALP127	78.542	0.618	11.779	5.131	0.126	0.601	0.115	0.176	2.847	0.066	173	318	15	16	0.001	321	17	0.001	67	49	10	10	12	48	110	12	116	22		5100	28	73	37	OES	MK	C	TS11	
ALP131	71.343	0.888	16.125	7.139	0.042	1.158	0.039	0.085	3.148	0.034	240	235	15	22	0.001	325	25	0.001	113	85	10	22	26	19	197	0.001	58	11		5100	41	99	46	OES	MK	C	TS11	
ALP171	67.786	0.807	18.856	6.328	0.229	1.257	0.136	0.092	4.430	0.079	256	547	13	18	0.001	249	21		93	73	16	27	14	47	397	17	208	30		160	33	75	36	OES	BH	C	BH112	
ALP172	63.724	0.935	20.391	8.794	0.258	1.464	0.134	0.077	4.173	0.051	265	508	7.9	18	0.001	274	26	0.001	111	86	18	36	18	52	501	15	348	30		145	30	74	36	OES	BH	C	BH112	
ALP173	64.985	0.871	19.242	9.826	0.374	1.144	0.125	0.059	3.343	0.031	243	415	7.6	25	0.001	273	27	0.001	99	83	22	34	19	31	554	92	1094	36		120	39	83	38	OES	BH	C	BH112	
ALP175	66.112	0.839	18.812	8.700	0.312	0.971	0.124	0.066	4.004	0.060	245	448	8.4	20	0.001	309	20	0.001	105	82	19	25	16	29	584	50	1041	37	0.020	70	29	72	36	OES	BH	C	BH112	
ALP176	62.684	0.890	20.870	9.031	0.497	0.957	0.147	0.065	4.815	0.044	275	462	11	23	0.001	224	20	2.2	107	92	21	27	15	42	593	3.6	381	42		45				OES	BH	C		
ALP014	65.859	0.874	18.455	7.484	0.145	2.054	0.193	0.240	4.638	0.058	272	430	26	17	0.001	298	22		107	85	21	33	18	23	111	22	85	41		5160	34	73	35	OES	MK	S E		
ALP034	62.501	0.908	21.290	7.113	0.134	2.093	0.263	0.286	5.334	0.078	302	679	35	20	0.001	223	21		115	91	22	31	19	62	126	5.5	55	31		4780	35	73	34	OES	MK	S E		
ALP035	63.640	1.533	20.426	6.604	0.147	1.643	0.195	0.363	5.395	0.055	297	709	45	25	0.001	276	21	0.001	104	82	24	30	15	46	112	28	72	49		4780	44	102	53	OES	MK	S E		
ALP037	37.265	1.720	29.623	22.965	0.904	2.339	0.690	0.162	4.307	0.027	315	358	11	21	0.001	309	27	0.001	162	128	36	50	36	31	232	12	55	97		4760	44	99	47	OES	MK	S E		
ALP189	66.499	0.818	18.225	6.593	0.172	1.964	0.190	0.358	5.094	0.087	278	814	31	19	0.001	286	19	0.001	99	69	19	27	18	36	445	4.5	41	34		170	36	78	38	OES	BH	S W		
ALP190	61.230	1.024	23.179	7.156	0.127	1.821	0.122	0.135	5.153	0.053	297	518	22	26	0.001	277	23	0.001	131	97	26	36	19	54	578	5.9	36	34		160				OES	BH	S W		
ALP191	67.185	0.754	17.788	9.715	0.327	1.286	0.147	0.072	2.687	0.039	202	252	15	18	0.001	226	20	0.001	89	74	23	31	16	27	979	55	52	39		150				OES	BH	S W		
ALP192	71.190	0.634	15.305	9.337	0.030	0.486	0.043	0.169	2.742	0.064	195	332	22	16	0.001	243	17	0.001	8.5	79	64	14	20	17	132	1414	265	112	16		140	26	47	20	OES	BH	S W	
ALP194	75.477	0.547	11.937	9.288	0.026	0.441	0.070	0.125	2.013	0.076	137	301																										

Table A.4 Additional analyses: INAA and fire assay analytical data

Additional analyses																
INAA Data																
	LA	CE	ND	SM	EU	TB	YB	LU	HF	TA	TH	U	AS	SB	CS	W
	ppm	ppm	ppm	ppm	ppm	ppm	ppm	ppm	ppm	ppm	ppm	ppm	ppm	ppm	ppm	ppm
Core NS																
ALP028	63.9	135.9	64.8	10.76	1.82	1.33	3.73	0.58	8.70	1.10	22.40	2.7	15.7		16.60	
ALP030	63.1	148.2	67.0	12.29	2.21	1.59	4.88	0.81	10.10	0.90	19.30	3.7			9.00	1.6
ALP122	52.5	118.6	50.0	9.72	1.91	1.10	3.54	0.58	13.30	0.90	14.80	2.2		0.00	9.60	
Core SS																
ALP057	47.2	103.3	40.8	7.55	1.23	0.84	2.38	0.38	7.00	1.30	21.20	5.0	2.0	0.10	11.70	1.1
ALP059	45.1	98.8	37.0	7.29	1.22	0.84	2.46	0.39	7.38	0.95	19.95	4.1		-0.10	14.13	1.6
ALP158	39.5	89.7	31.0	6.31	0.91	0.77	3.11	0.48	9.48	1.05	18.07	3.0		-0.10	9.96	1.3
ALP184	46.6	102.4	47.3	7.53	1.22	0.92	2.89	0.43	6.70	0.90	19.60	4.7	3.3		19.20	
OES Surface																
ALP190	69.0	147.1	55.0	11.25	1.31	1.25	4.13	0.62	7.90	1.30	25.60	3.5	0.6		21.90	
ALP194	29.4	63.0	27.0	5.31	0.90	0.71	2.44	0.36	5.90	0.90	10.70	2.3	0.5		9.50	
ALP198	23.1	54.3	19.0	4.48	0.91	0.67	2.30	0.35	6.00	0.90	9.20	1.6	0.3		11.50	
ALP208	59.5	125.8	48.8	9.69	1.70	1.11	3.48	0.54	5.60	1.20	21.30	2.9	1.5		21.80	
ALP219	46.8	112.1	48.6	11.13	1.28	1.60	5.64	0.85	7.30	1.10	18.50	4.6	0.7		13.00	0.8
ALP225	28.1	64.4	26.8	5.93	0.91	0.88	4.93	0.84	7.00	0.90	10.80	2.0	0.3		13.90	0.6
NQ																
ALP067	9.4	21.8	9.3	1.60	0.30	0.24	0.75	0.13	3.00	0.20	2.50	0.8	0.4		0.80	0.5
QM																
ALP072	15.2	33.4	14.5	4.33	0.90	0.72	1.79	0.22	6.10	0.60	6.30	2.5	0.6	0.20	2.50	1.0
Surface MnQ																
ALP213	7.0	20.9	14.3	0.16	0.33	0.11	0.23	0.00	0.40	0.10	1.40	27.8	279	8.80	0.30	0.3
HS Core																
ALP043	56.9	123.5	47.0	9.93	1.59	1.06	3.29	0.51	10.43	1.36	21.41	2.9		-0.10	13.97	2.0
ALP101	47.6	99.5	41.0	7.78	1.41	1.06	4.52	0.70	9.30	1.00	17.70	2.4			14.20	
Massive sulfide																
ALP081	20.0	35.3	15.0	3.52	0.90	0.30	1.40	0.24	4.20	0.50	5.40	0.5		247	4.20	
ALP110	24.4	37.3		3.71	1.79	0.30	0.90	0.11	3.50	0.90	4.80	8.3	17	36.80	35.50	
UFS																
ALP052	57.9	123.1	42.0	9.50	1.54	1.17	5.25	0.77	7.65	1.41	21.97	3.0		-0.10	13.97	1.5
IS																
ALP147	62.6	131.5	51.0	10.59	1.60	1.29	3.95	0.59	8.39	1.30	23.72	3.3		0.05	19.40	3.0
BGZ																
ALP153	47.1	103.7	43.0	7.73	1.03	0.92	2.90	0.46	7.21	0.86	21.52	4.4		0.12	19.90	1.0
Fire Assay Data																
	Au	Ag	Spec													
	g/t	g/t														
ALP028	0.01	0.5	NS													
ALP061	0.01	0.1	NS													
ALP057	-0.01	0.6	SS													
ALP184	0.01	0.3	SS													
ALP234	-0.01	0.8	BGZ													
ALP235	0.01	0.6	BGZ													
ALP190	0.02	0.1	OES													
ALP194	0.03	0.7	OES													
ALP208	-0.01	0.2	OES													
ALP209	0.01	0.1	OES													
ALP212	0.03	0.7	OES													
ALP219	-0.01	1.9	OES													
ALP121c	-0.01	9.8	CS													
ALP121g	-0.01	1.1	MnQ													
ALP213	0.01	28.0	MnQ													

Table A.5 Analytical data recalculated volatile-free

SAMPLE	SiO2	TiO2	Al2O3	Fe2O3	MnO	MgO	CaO	Na2O	K2O	P2O5	H2O-	LOI	TOTAL	Rb	Ba	Sr	Th	U	Zr	Nb	Mo	Cr	V	Se	Ni	Co	Pb	Zn	Cu	S	Y	C	Dist	La	Ce	Nd	SPEC	ENV. HOLE		
	%	%	%	%	%	%	%	%	%	%	%	%	%	ppm	ppm	ppm	ppm	ppm	ppm	ppm	ppm	ppm	ppm	ppm	ppm	ppm	ppm	ppm	ppm	ppm	ppm	ppm	ppm	ppm	ppm	ppm	ppm	ppm	HILL	POS.
Core SS																																								
ALP054	61.630	0.791	19.790	6.437	0.403	0.973	0.287	0.202	4.418	0.035	0.399	2.689	100.100	217	461	43	21	0.001	227	19	0.001	99	73	17	26	41	272	141	28	788	36	0.120	35	39	87	41	SS	BH	C	BH123
ALP056	60.400	0.822	19.520	6.541	0.065	1.926	0.173	0.283	4.662	0.058	0.428	4.853	99.740	230	622	61	24	0.001	258	19	4.8	125	227	22	39	15	94	223	57	12141	23	0.770	50	28	63	29	SS	BH	C	BH123
ALP057	61.280	0.736	18.900	6.683	0.047	1.688	0.193	0.349	4.718	0.065	0.407	4.923	99.990	222	644	63	18	0.001	226	17	5.6	109	258	19	40	16	88	198	52	14256	20	0.820	55	27	58	27	SS	BH	C	BH123
ALP058	61.180	0.711	19.420	6.931	0.035	1.667	0.142	0.243	4.589	0.079	0.365	4.872	100.200	233	549	45	17	0.001	218	15	3.8	103	183	19	38	17	42	152	48	14094	22	0.000	65	22	50	23	SS	BH	C	BH123
ALP059	61.910	0.739	18.950	6.655	0.033	1.722	0.117	0.236	4.185	0.045	0.345	5.067	100.000	218	543	47	16	0.001	240	14	3.1	108	180	19	37	16	31	144	52	11830	22	0.510	90	25	58	26	SS	BH	C	BH123
ALP060	66.730	0.721	17.440	5.973	0.033	1.473	0.107	0.353	3.559	0.024	0.290	3.089	99.790	183	450	48	21	0.001	100	13	0.001	100	106	19	24	16	31	114	28	10422	25	0.280	130	29	66	30	SS	BH	C	BH123
ALP087	62.526	0.722	19.278	6.268	0.031	1.857	0.159	0.140	4.502	0.062	0.035	4.389	99.970	227	601	29	17	0.001	212	14	2.8	131	196	18	36	14	49	160	46	11542	22	0.000	50	0	0	0	SS	BH	C	BH166
ALP087A	61.510	0.752	19.030	6.805	0.038	1.740	0.182	0.182	4.460	0.061	0.382	5.190	100.300	206	527	29	17	0.001	223	16	3.9	102	139	20	30	13	38	135	34	14198	23	0.000	50	0	0	0	SS	BH	C	BH166
ALP087F	59.650	0.773	18.790	6.078	0.044	1.646	0.144	0.228	4.766	0.041	0.277	5.421	99.860	210	526	23	18	0.001	224	14	3.7	103	125	20	37	19	51	125	46	18501	20	0.000	50	0	0	0	SS	BH	C	BH166
ALP136	70.170	0.661	16.190	5.180	0.035	1.102	0.095	0.160	2.938	0.043	0.275	3.530	100.400	199	276	15	14	0.001	347	15	0.000	93	52	15	23	13	18	75	44	1256	20	0.000	350	24	51	21	SS	PH	C	BH164
ALP137	68.730	0.700	16.730	5.465	0.091	1.207	0.096	0.147	3.024	0.031	0.221	3.866	100.300	205	294	17	16	4.0	334	15	0.000	96	57	16	22	11	120	78	11	675	18	0.010	360	23	55	22	SS	PH	C	BH164
ALP138	69.350	0.723	16.000	5.175	0.032	1.244	0.091	0.194	3.209	0.032	0.247	3.514	99.810	201	378	22	13	0.001	248	16	2.6	100	115	17	25	13	5.1	72	37	9416	18	0.000	370	24	56	23	SS	PH	C	BH164
ALP139	69.490	0.684	15.730	4.826	0.027	1.242	0.148	0.305	2.829	0.021	0.416	4.138	99.850	175	416	40	16	0.001	345	14	0.000	92	75	15	20	11	12	65	21	6344	19	0.001	380	25	54	19	SS	PH	C	BH164
ALP140	72.190	0.576	14.410	4.636	0.032	1.021	0.108	0.202	2.858	0.045	1.038	3.274	100.400	197	304	23	14	0.001	341	13	0.000	84	46	14	17	10	70	54	10	797	18	0.000	390	20	49	21	SS	PH	C	BH164
ALP141	71.760	0.630	14.740	5.243	0.032	1.003	0.092	0.167	2.909	0.022	0.255	3.284	100.100	206	327	23	13	0.001	350	17	0.000	94	50	15	22	13	6.6	64	7.1	531	26	0.000	400	23	58	24	SS	PH	C	BH164
ALP142	70.710	0.652	15.450	5.268	0.026	1.125	0.113	0.227	2.903	0.032	-0.002	3.663	100.200	203	360	29	14	0.001	355	15	0.000	95	52	15	21	11	7.9	56	6.0	599	23	0.000	410	23	57	24	SS	PH	C	BH164
ALP154	64.240	0.678	18.290	5.582	0.031	1.578	0.159	0.304	4.396	0.047	0.513	4.141	99.970	240	538	32	18	3.700	228	14	2.8	100	145	19	23	13	30	144	26	7611	23	0.320	65	0	0	0	SS	BH	C	BH156
ALP154A	61.210	0.741	19.500	6.179	0.035	1.849	0.163	0.170	4.470	0.041	0.609	5.011	99.970	241	545	27	20	0.001	238	16	3.3	113	192	22	34	16	22	195	44	8556	28	0.000	65	0	0	0	SS	BH	C	BH156
ALP155	64.210	0.778	18.840	5.520	0.033	1.595	0.147	0.278	3.787	0.036	0.335	4.127	99.690	217	453	38	16	0.001	286	17	2.0	105	107	18	21	13	109	119	25	8198	27	0.000	95	30	64	30	SS	BH	C	BH156
ALP156	64.460	0.782	18.170	6.187	0.039	1.751	0.187	0.396	3.809	0.031	0.377	3.749	99.940	232	474	41	19	0.001	279	17	2.0	110	113	19	29	14	16	114	32	9293	23	0.240	125	33	73	31	SS	BH	C	BH156
ALP157	62.750	0.638	18.930	5.960	0.023	1.467	0.252	0.490	4.348	0.069	0.494	4.452	99.880	231	559	49	15	4.6	180	13	2.8	94	153	17	37	16	128	112	44	11837	26	0.260	150	36	67	32	SS	BH	C	BH156
ALP158	68.900	0.645	16.290	5.361	0.032	1.142	0.153	0.185	2.980	0.044	0.214	3.949	99.910	167	351	31	17	6.0	307	14	0.001	97	92	15	22	12	10	69	18	4339	21	0.040	170	23	52	23	SS	BH	C	BH156
ALP160	70.840	0.633	15.590	4.983	0.020	0.972	0.118	0.189	2.895	0.032	0.186	3.414	99.870	174	287	28	15	0.001	337	15	0.000	89	51	15	21	11	5.9	35	1.6	129	17	0.060	200	20	50	19	SS	BH	C	BH156
ALP161	67.870	0.719	16.700	5.507	0.028	1.259	0.153	0.306	2.974	0.036	0.337	4.080	99.970	172	405	40	12	0.001	317	16	0.000	99	99	17	23	14	7.9	60	27	7053	16	0.000	230	20	48	20	SS	BH	C	BH156
ALP162	69.200	0.672	16.150	5.133	0.029	1.114	0.137	0.329	2.656	0.053	0.327	4.114	99.910	162	385	44	18	4.0	325	15	0.000	89	72	15	21	12	60	67	23	8276	24	0.010	260	24	63	27	SS	BH	C	BH156
ALP183	62.050	0.737	19.800	5.200	0.034	1.824	0.071	0.200	4.637	0.057	0.353	5.120	100.100	242	561	22	18	4.8	212	15	4.1	116	244	19	45	22	36	391	52	7286	26	0.280	240	25	53	24	SS	BH	C	BH163
ALP184	62.330	0.713	19.390	5.855	0.032	1.751	0.078	0.253	4.454	0.052	0.300	4.919	100.100	235	526	22	14	0.001	211	14	3.7	109	202	19	34	15	23	128	50	8395	19	0.000	245	27	60	26	SS	BH	C	BH163
ALP185	65.630	0.731	18.210	5.409	0.031	1.487	0.157	0.321	3.747	0.032	0.274	4.237	100.300	198	408	37	17	0.001	288	15	0.000	100	112	16	23	13	23	102	31	7608	24	0.240	260	31	67	31	SS	BH	C	BH163
ALP186	65.380	0.771	17.900	5.495	0.033	1.493	0.189	0.354	3.682	0.039	0.492	4.219	100.000	204	452	49	17	0.001	280	17	0.000	107	114	18	23	12	21	100	31	8650	22	0.000	280	26	57	26	SS	BH	C	BH163
SURFACE SS																																								
ALP222	68.340	0.727	16.370	5.588	0.045	0.911	0.080	0.096	2.567	0.056	0.326	4.595	99.720	202	300	15	17	0.001	353	16																				

Table A.5 continued

SAMPLE	SiO2 %	TiO2 %	Al2O3 %	Fe2O3 %	MnO %	MgO %	CaO %	Na2O %	K2O %	P2O5 %	H2O-%	LOI %	TOTAL %	Rb ppm	Ba ppm	Sr ppm	Th ppm	U ppm	Zr ppm	Nb ppm	Mo ppm	Cr ppm	V ppm	Sc ppm	Ni ppm	Co ppm	Pb ppm	Zn ppm	Cu ppm	S ppm	Y ppm	C %	Dist m	La ppm	Ce ppm	Nd ppm	SPEC	ENV. HOLE HILL POS.	
Peg																																							
ALP028P	76.600	0.168	12.820	1.599	0.028	0.388	0.296	0.995	5.833	0.070	0.142	1.267	100.200	246	1273	84	0.001	0.001	60	9.4	0.001	10	15	6.4	3.6	3.1	47	15	1.7	83	16	0.100	370	15	29	15	PNS	BH C	BH123
ALP039P	91.688	0.049	4.737	1.182	0.037	0.179	0.040	0.039	1.308	0.026	0.101	0.552	99.940	71	96	4.7	3.1	0.001	68	1.9	0.001	12	2.5	0.8	3.1	0.001	17	17	7.4	29	15	0.100	240	0	0	0	PNS	BH C	BH123
ALP051P	85.430	0.092	8.624	1.606	0.094	0.253	0.062	0.132	2.969	0.039	0.074	0.371	99.750	113	984	20	4.9	0.001	23	3.7	0.001	12	10	2.3	5.1	0.001	273	42	4.2	54	6.9	0.100	10	0	0	0	PUPS	BH C	BH123
ALP059P	83.440	0.036	9.408	1.409	0.012	0.335	0.228	0.725	2.603	0.062	0.127	1.608	99.990	113	478	55	12	65	9.0	0.001	0.000	2.7	5.9	1.7	3.9	3.1	72	15	8.0	3959	57	0.100	90	11	26	11	PSS	BH C	BH123
ALP066P	79.614	0.065	10.943	1.308	0.001	0.175	0.245	0.356	5.744	0.199	0.125	0.938	99.710	233	679	54	7.7	3.2	209	6.1	0.001	15	2.6	1.7	1.5	0.001	243	110	1.2	28	14	0.100	160	0	0	0	PNS	BH C	BH166
ALP087P	78.284	0.025	12.402	0.916	0.043	0.413	0.133	2.032	3.788	0.096	0.239	1.446	99.817	149	637	91	17	10	17	1.7	0.001	3.6	8.5	0.001	0.001	1.8	196	13	0.001	1213	45	0.100	50	29	56	24	PLFS	BH C	BH166
ALP101P	73.900	0.076	13.660	0.866	0.044	0.001	0.061	0.551	10.020	0.080	0.093	0.590	100.100	361	1841	66	0.001	0.001	26	1.9	0.000	4.7	6.7	1.1	2.1	3.0	548	19	4.2	77	8.0	0.100	25	6.3	15	7.0	PHS	BH C	BH114
ALP122P	80.945	0.045	9.940	1.147	0.001	0.250	0.312	0.883	5.502	0.042	0.177	0.687	99.952	293	1003	65	4.9	0.001	28	3.4	0.001	12	0.001	1.2	4.0	0.001	46	8.9	1.4	109	7.4	0.100	5100	0	0	0	PNS	MK C	TS11
ALP128P	79.165	0.280	11.608	2.550	0.017	0.380	0.192	0.106	3.802	0.145	0.076	1.642	99.960	185	324	18	6.5	0.001	233	16	0.001	21	18	6.7	6.4	4.4	56	49	11	27	8.1	0.100	5100	0	0	0	OESP+GOMK	MK C	TS11
ALP135P	70.263	0.050	16.120	0.983	0.001	0.372	0.391	0.736	9.244	0.075	0.124	1.326	99.696	335	1499	123	0.001	0.001	13	1.7	0.001	6.4	2.7	1.2	3.4	0.001	310	19	0.010	91	3.4	0.100	5100	0	0	0	PUPS	MK C	TS11
ALP141P	75.150	0.106	14.590	2.023	0.001	0.669	0.262	2.673	2.620	0.044	0.180	1.754	100.102	185	385	139	10	4.9	30	8.3	0.001	10	4.1	3.8	5.1	1.8	121	35	2.3	223	95	0.100	400	0	0	0	PLFS	BH C	BH164
ALP159P	73.776	0.018	14.897	0.694	0.001	0.115	1.120	2.165	6.794	0.047	0.035	0.400	100.079	224	478	158	6.4	7.9	17	0.001	0.001	3.9	0.001	2.4	1.8	0.001	116	2.4	0.010	0	83	0.100	185	0	0	0	PLFS	BH C	BH156
ALP173P	96.538	0.022	1.416	0.913	0.016	0.122	0.016	0.051	0.840	0.025	0.043	0.054	100.060	32	245	8.0	0.001	0.001	2.9	0.001	0.001	4.1	0.001	0.001	2.7	0.001	29	48	3.6	151	1.4	0.100	120	0	0	0	OESP	BH C	BH112
ALP424P	75.717	0.071	13.365	2.659	0.053	1.042	0.263	0.639	3.077	0.163	0.487	2.775	100.075	185	737	14	-4.4	-3.4	37	2.8	-1.3	4.3	7.1	2.2	5.3	8.9	294	88	4.9	887	17	9.1	15	10	PSTS	NB C	VG1		
ALP430P	72.707	0.106	14.913	3.899	0.057	1.204	0.315	0.061	3.403	0.201	0.573	3.266	100.359	198	636	17	8.3	-3.5	52	3.1	-1.3	6.9	10	4.3	5.9	9.3	358	99	12	401	17	20	34	20	PSTS	NB C	VG1		
ALP438P	83.513	0.082	9.246	0.884	-0.037	0.377	0.401	0.520	2.968	0.047	0.203	0.992	99.154	138	478	60	5.2	-3.3	16	4.8	-1.2	5.2	6.8	2.0	3.6	2.2	14	6.3	3.1	44	82	12	21	10	P	WTL C	WTL3		
ALP441P	73.948	0.086	15.013	0.611	-0.037	-0.117	3.207	0.743	6.257	0.060	0.130	0.715	100.714	210	517	224	-4.6	57	36	2.2	3.0	-1.4	5.9	3.9	-1.2	2.0	57	8.4	-1.2	17	5.1	4.3	6.2	-2.3	P	WTL C	WTL3		
Surface NS																																							
ALP205	72.250	0.358	11.120	10.220	0.099	0.196	0.093	0.211	3.277	0.158	0.202	1.825	100.000	156	1077	17	15	0.001	275	10	0.001	69	86	8.2	10	5.4	99	290	13	36	48	0.100	250	49	114	55	NS	BH S	
ALP236	75.051	0.314	9.403	9.929	0.010	0.204	0.118	0.296	2.851	0.148	0.157	1.456	99.927	181	402	13	11	0.001	245	10	0.001	66	71	6.8	11	8.7	0.001	16	0.001	141	32	0.100	4000	37	89	45	NS	MK S	
ALP242	79.161	0.511	10.874	2.890	0.001	0.302	0.034	0.183	4.194	0.048	0.199	1.816	99.956	246	646	38	16	-3.5	333	16	-1.3	61	20	5.6	8.0	3.7	42	22	1.7	20	32	38	77	41	NS	MK S			
ALP243	82.829	0.210	7.196	4.868	0.272	0.311	0.171	0.135	2.616	0.035	0.253	1.401	99.869	200	859	22	5.4	-3.7	227	6.6	3.3	260	18	4.5	15	5.9	18	51	7.5	16	23	17	28	15	NS	BH S			
Surface NS and equivalent rocks at Tank Hill																																							
ALP241	96.067	0.091	2.172	0.188	0.007	0.066	0.032	0.056	0.681	0.038	0.060	0.390	99.773	35	561	14	0.001	0.001	99	3.0	1.2	64	12	1.3	0.001	0.001	57	10	0.001	0	5.3	0.100	0	5.7	15	7.6	GRQ	TH S	
ALP244	69.992	0.664	12.930	6.226	0.072	0.386	0.021	0.184	3.618	0.155	0.177	3.785	97.658	336	4052	19	15	-4.5	219	16	6.1	67	90	14	-1.9	-2.3	7109	7628	108	5730	3.6	0	25	57	31	NS	TH S		
Surface NTS																																							
ALP401	70.717	0.603	14.514	5.582	0.001	0.949	0.093	0.111	2.817	0.039	0.581	4.253	99.764	195	486	23	15	-3.7	338	14	2.3	92	61	15	24	12	14	80	39	237	25	0.100	30	63	30	NTS	NB S		
ALP402	78.263	0.539	11.650	3.809	0.001	0.684	0.071	0.079	1.871	0.031	0.505	3.168	100.332	168	245	9.1	19	4.2	494	17	-1.3	77	41	13	16	8.1	6.1	55	11	87	18	0	0	0	0	NTS	NB S		
ALP403	65.464	0.531	12.966	4.233	0.001	0.931	0.060	0.086	1.888	0.029	0.470	13.611	99.895	181	252	17	18	-3.5	416	15	-1.3	82	40	13	18	7.4	-5.0	92	7.7	58	30	0.100	29	64	28	NTS	NB S		
ALP404	74.740	0.548	12.398	4.684	0.001	0.946	0.091	0.077	2.263	0.028	0.505	3.790	99.655	162	276	15	12	-3.6	379	14	-1.3	81	45	13	25	14	8.4	180	35	80	19	24	47	20	NTS	NB S			
ALP409	64.567	0.665	18.210	5.193	0.045	1.509	0.199	0.391	4.838	0.051	0.527	4.106	99.842	298	899	51	20	3.8	215	16	5.6	109	179	18	39	11	-5.3	26	48	64	27	0.100	36	71	34	NTS	NB S		
ALP410	66.933	0.591	17.744	4.243	0.001	1.161	0.103	0.120	4.243	0.042	0.903	4.143	99.851	303	940	23	18	3.9	259	16	2.6	98	87	11	25	5.5	10	66	53	165	23	0.100	26	53	24	NTS	NB S		
ALP411	73.598	0.512	13.770	4.532	0.001	0.634	0.044	0.089	2.059	0.025	0.807	4.320	99.988	147	445	13	18	3.6	376	13	2.1	79	43	12	19	7.1	5.0	72	29	146	24	26	57	25	NTS	NB S			
ALP415	67.748	0.645	16.482	5.126	0.001	1.056	0.076	0.120	3.459	0.040	0.911	4.732	99.942	221	799	23	16	-3.6	297	15	1.6	100	76	16	22	8.9	21	60	49	187	18	26	57	25	NTS	NB S			
ALP416	70.661	0.574	15.328	4.499	0.001	0.692																																	

Table A.5 continued

SAMPLE	SiO2 %	TiO2 %	Al2O3 %	Fe2O3 %	MnO %	MgO %	CaO %	Na2O %	K2O %	P2O5 %	H2O- %	LOI %	TOTAL %	Rb ppm	Ba ppm	Sr ppm	Th ppm	U ppm	Zr ppm	Nb ppm	Mo ppm	Cr ppm	V ppm	Sc ppm	Ni ppm	Co ppm	Pb ppm	Zn ppm	Cu ppm	S ppm	Y ppm	C %	Dist m	La ppm	Ce ppm	Nd ppm	SPEC HILL	ENV. POS.	HOLE POS.	
OS+GQ																																								
ALP045	70.180	0.525	13.520	10.200	0.499	0.802	0.112	0.137	3.116	0.019	0.251	0.603	99.920	195	842	8.7	19	0.001	309	14	0.001	72	70	14	14	18	140	243	199	485	31	0.001	15	32	77	37	HS+GQ	BH	C	BH123
ALP046	75.800	0.538	11.990	7.519	0.754	0.707	0.101	0.098	2.076	0.018	0.220	0.328	100.200	137	412	6.5	13	0.001	266	12	0.001	68	55	10	16	18	65	224	2.8	81	30	0.000	10	25	59	29	HS+GQ	BH	C	BH123
ALP047	57.770	0.549	10.130	27.700	0.855	0.626	0.286	0.083	2.178	0.122	0.116	-0.511	99.910	132	981	11	23	0.001	360	9.4	0.001	70	182	13	17	26	195	913	140	983	48	0.020	0.1	39	112	52	UOES+GQBH	C	BH123	
ALP048	71.740	0.538	13.270	9.556	0.545	0.746	0.148	0.087	2.646	0.057	0.138	0.439	99.920	170	2081	14	18	0.001	291	15	1.7	66	62	11	12	20	406	669	287	3304	42	0.001	5	37	79	41	IS+GQ	BH	C	BH123
ALP049	66.730	0.568	11.690	15.330	1.120	0.664	0.614	0.074	2.481	0.162	0.126	0.418	99.950	251	1067	6.9	24	0.001	278	14	0.001	74	123	13	19	23	780	2002	210	6703	38	0.040	0.1	37	93	43	LOES+GQBH	C	BH123	
ALP102	66.980	0.513	11.230	15.030	0.623	0.958	0.190	0.064	2.767	0.087	0.183	0.679	99.290	260	911	8.0	16	0.001	287	14	0.001	66	96	12	17	22	108	337	6.7	162	31	0.000	10	0	0	0	HS+GQ	BH	C	BH114
ALP128	74.750	0.657	13.840	5.215	0.836	0.815	0.036	0.143	2.756	0.014	0.117	1.862	100.200	196	212	12	19	0.001	276	17	0.001	76	54	7.7	13	19	30	117	0.001	53	24	0.000	5100	33	73	36	OES+GQ	MK	C	TS11
ALP129	68.230	0.724	15.620	8.793	0.281	1.139	0.166	0.133	3.506	0.034	0.231	1.089	99.910	236	337	12	18	0.001	297	18	22	98	72	15	22	21	38	107	0.001	78	39	0.000	5100	35	80	40	OES+GQ	MK	C	TS11
ALP174	58.240	0.884	20.300	10.080	0.297	1.139	0.106	0.053	4.245	0.039	0.484	3.815	99.690	259	475	8.9	21	0.001	259	22	0.001	102	85	19	33	21	41	707	110	2346	31	0.020	95	30	70	35	OES+GQ	BH	C	BH112
ALP036	63.430	1.452	17.630	7.686	0.896	1.180	0.229	0.224	5.110	0.059	0.534	2.855	100.500	264	754	50	20	0.001	274	19	0.001	102	88	18	22	17	38	107	14	85	30	0.020	4760	28	72	35	OES+GQ	MK	S E	
OEGQ																																								
ALP130	71.920	0.418	11.850	10.420	0.739	0.790	0.550	0.148	3.054	0.119	0.139	0.224	100.400	165	404	22	16	0.001	275	12	64	53	40	21	9.4	17	75	116	2.3	154	103	0.000	5100	27	60	31	OEGQ	MK	C	TS11
ALP132	67.710	0.666	14.140	11.450	0.392	1.200	0.349	0.082	2.838	0.054	0.106	0.756	99.750	205	339	11	17	0.001	270	18	0.001	78	90	16	22	27	38	167	0.001	62	46	0.000	5100	32	74	35	OEGQ	MK	C	TS11
ALP172G	77.161	0.586	6.934	10.651	1.446	1.339	0.247	0.038	0.625	0.023	0.002	0.728	99.780	50	72	0.001	15	0.001	654	15	1.6	56	28	31	37	19	17	403	219	6149	102	0.000	145	26	57	31	OEGQ	BH	C	BH112
ALP202Q	74.030	0.229	2.961	21.110	0.305	0.057	0.082	0.059	0.174	0.191	0.238	0.779	100.000	8.0	363	37	13	0.001	220	0.001	2.7	26	158	6.0	7.2	14	681	814	262	123	42	0.000	60	23	49	25	OEGQ	BH	S	
Ore																																								
ALP072	39.330	0.488	2.421	57.080	0.191	0.189	0.276	0.050	0.373	0.242	0.048	-1.381	99.380	25	53	7.3	28	0.001	208	4.5	5.5	82	46	3.0	0.001	58	301	1795	2007	2149	18	0.000	0.1	11	21	11	UMQ	BH	C	BH166
ALP075	34.858	0.149	2.003	61.083	0.015	0.460	0.509	0.035	0.262	0.399	-0.035	-1.036	98.700	23	66	4.7	46	8.6	45	0.001	7.9	19	29	2.8	28	126	897	3160	2980	11623	18	0.000	0.1	7.3	35	15	UMQ	BH	C	BH166
ALP077	86.700	0.178	2.994	8.248	0.320	0.384	0.097	0.029	0.292	0.059	0.633	0.212	100.100	27	484	3.1	10	0.001	152	3.9	2.1	22	14	1.9	3.3	20	1770	2330	654	6253	11	0.000	5	31	36	12	LQ	BH	C	BH166
ALP113	41.432	0.289	5.577	40.289	8.886	1.089	0.548	0.051	0.093	0.348	-0.073	-0.301	97.430	10	1273	37	18	0.001	118	5.0	9.0	29	37	4.3	43	47	8000	10100	1390	40192	30	0.001	0.1	13	33	22	LMA+GQ	BH	C	BH114
ALP114	87.667	0.211	2.870	5.912	0.135	0.455	0.081	0.045	0.840	0.024	-0.018	1.285	99.510	56	477	4.6	0.001	0.001	456	7.2	7.3	104	28	1.7	22	30	364	1825	168	21390	0.001	0.000	1	0.001	7.1	2.2	LQ+GQ	BH	C	BH114
ALP149	87.120	0.259	3.991	5.525	0.606	0.432	0.156	0.123	1.142	0.025	0.084	0.696	100.100	55	6463	27	5.8	0.001	198	5.3	0.001	30	27	3.4	3.9	6.2	103	811	42	7209	16	0.020	30	16	32	15	LQ	BH	C	BH156
ALP228	28.430	0.508	4.516	62.660	0.184	0.001	0.220	0.149	0.676	0.345	0.122	1.103	98.960	46	160	266	34	12	627	5.6	5.2	76	387	15	20	24	0.001	143	194	254	85	0.000	9100	75	237	117	MQ	FK	S	

Table A.6 Analyses of three aliquots of one sample for C, H and N using gas chromatography

Sample No.	Weight (mg)	C %	N %	H %
ALP057	2.011	0.79	0.18	0.42
ALP057	5.747	0.83	0.05	0.41
ALP057	10.755	0.82	0.02	0.41

Table A.7 Three duplicate INAA REE analyses (ppm) of sample ALP190

ALP190								
	First analysis		Second analysis		Third analysis		Mean	S.D.
	1 sigma counting error		1 sigma counting error		1 sigma counting error			
La	68.2 +- 0.7	71.7 +- 0.7	67 +- 0.7				69	2.44
Ce	145.9 +- 2.4	153.3 +- 2.5	142.2 +- 2.3				147.1	5.5
Nd	54 +- 3	59 +- 4	52 +- 3				55	3.6
Sm	11.14 +- 0.28	11.68 +- 0.3	10.93 +- 0.27				11.25	0.39
Eu	1.3 +- 0.02	1.34 +- 0.03	1.3 +- 0.02				1.31	0.023
Tb	1.21 +- 0.1	1.3 +- 0.1	1.25 +- 0.1				1.25	0.045
Yb	4.09 +- 0.12	4.03 +- 0.13	4.26 +- 0.13				4.13	0.12
Lu	0.62 +- 0.02	0.59 +- 0.02	0.66 +- 0.02				0.62	0.035

Table C.1 List of mineralogical abbreviations used

AM = AMPHIBOLE	MP = MICROPERTHITE
AP = APATITE	MS = MUSCOVITE
BI = BIOTITE	MT = MAGNETITE
CB = CARBONATE	OL = OLIVINE
CH = CHLORITE	OP = OPAQUE MINERALS
CL = CLAY	PL = PLAGIOCLASE
CP = CHALCOPYRITE	PO = PYRRHOTITE
CZ = CLINOZOISITE	PX = PYROXENE
DI = DIOPSIDE	PY = PYRITE
EP = EPIDOTE	QZ = QUARTZ
GA = GALENA	RT = RUTILE
GH = GAHNITE	SL = SILLIMANITE
GP = GRAPHITE	SN = SPHENE
GR = GARNET	SP = SPHALERITE
HM = HEMATITE	SR = SERICITE
HR = HERCYNITE	TM = TOURMALINE
KF = K-FELDSPAR	ZR = ZIRCON

Table C.2 Estimated Namies Schist modal percentages

SLIDE NO.	QZ	BI/CH	MS	SR	SL	MP	PL	OP	ZR	TM	GR	SN	GH	AP	SP
ALP 28	40	15	10		15-20	10	2	3	TR		TR	TR			
ALP 29	45-50	15	10	5	15-20	3		5	TR		5				
ALP 30	55	5-10	25		15			8	TR			TR			
ALP 39	60-65	3	8-10		15	5		8	TR						
ALP 61	50	20-25	5-10		20			5	TR		2				
ALP 63	40	1-2	30-35	5	10			2-3	TR		2				
ALP 64	55-60	15	5		15-20			8	TR						
ALP 65	50	5	20-25		10			3-5	TR		TR				
ALP 122	40-50	10-15	20	1-3	5-10	5		10	TR		2				
ALP 123	40-50	5-10	5	10-15	5-10	3-5		TR	TR						
ALP 205	50	20-25	3	10	10			1-2	TR	TR					
ALP 236	55-60	1	15-20		10			5	TR						
ALP242	60	3	25			8		2	TR						
ALP243	55	5	5		3	20		3	TR		3				
ALP244X	40		40					10	TR				1	TR	4
ALP244Y	20		20	3		35		15	0		TR		5	TR	TR

Table C.3 Estimated Shaft Schist modal percentages

SLIDE NO.	USS or LSS	QZ	BI	MS	SR	SL	MP	OP	ZR	AP	TM	GR
ALP 56	USS	25-30	20	15	10-15	10		5-10	TR		TR	
ALP 57	USS	40	15-20	3	20-25			5	5-10	TR		
ALP 58	USS	30	15	10	25	3			8	TR	TR	1
ALP 59	USS	35-40	20	5-10	10-15	15			5-8	TR		
ALP 87	USS	35-40	25	8	5	20			10	TR		
ALP 140	LSS	35	25	15-20	15	5-10			2			
ALP 142	LSS	45-50	8-10	3-5	10-15	5-10	TR		2	TR		
ALP 154	USS	25	35	10-15	15				8	TR	TR	
ALP 162	LSS	45	15	15	15							
ALP 183	USS	30	20	5	10	25			5	TR		
ALP 186	LSS	50	20-25	5	5	5	TR		5		TR	
ALP 222	USS	40	20	15	15-20					TR		

Table C.4 Estimated Biotite Graphite Zone modal percentages

SLIDE NO.	QZ	BI	MS	SR + CL	SL	KF	GR	GP	ZR	AP	CP	PO	PY	CL
ALP 53	15-20	15-20	10-15	15-20	10-15	30-35		TR	TR	TR	TR		2	TR
ALP 53 QTE	70					20	5-8		-				0.5	
ALP 120	35	15	15-20	10	25		5					5-8		
ALP 153	40	15	5-10	15	3-5				TR					2
ALP 234	30	10-15		45-50					TR			8-10		
ALP 235	30	15-20		40	10				TR					

Table C.5 Estimated Calc Silicate Rock plus Manganese Quartzite modal percentages

ROCK TYPE	SLIDE NO.	PX (D1)	AM	GR	QZ	CH	AP	SR	ZR	OP	TM	EP	BI	GH	CL
CALC SILICATE ROCK	ALP 55a	90	3	2					Tr	Tr					
	ALP 55b	90	5	1	3				0.5	2					
	ALP 121C a			80	8	7	3			2					
	ALP 121C b			80	8	5	1			2					
	ALP 188			10	20	5	45	1	2			8	10		
MANGANESE QUARTZITE	ALP 121G			10	80					1			5	2	
	ALP 187			15	85					Tr					
	ALP 213			5	90								Tr		5
	ALP 216		1	10	85						Tr				5

Table C.6 Estimated Hangingwall Schist modal percentages

ROCK TYPE	S/C	SLIDE N°	AM	AP	BI	CH	GH	GR	KF	MS	OP	QZ	RT	SL	SN	SR	TM	ZR	TOTAL
HS	C	ALP101			20			3	15			35		25				TR	98
HS	C	ALP100			20			10	3	5		45		15				TR	98
HS	C	ALP102			10	15		15	3	15	1	40		TR				TR	99
HS	C	ALP170		TR	25			8	5	5		50		5				TR	98
HS	C	ALP165			10			5	25	15		40						TR	95
HS	C	ALP044			25					10	2	35		25				TR	97
HS	S	ALP214			10				10	20		30		10		20		TR	100
HS PETRO	C	ALP102			30			30	0		10	10		15			2	TR	97
HS+GQ	C	ALP045			8			10	10	5		60		5				TR	98
S	S	ALP230			10			2	2	15	3	60		5				TR	97
S	S	ALP229		TR	15			8	3	2	8	50		12				TR	98

S = Surface C = Core

Table C.7 Estimated Ore Equivalent Schist modal percentages

ROCK TYPE	S/C	SLIDE N°	AM	AP	BI	CH	GH	GR	KF	MS	OP	QZ	RT	SL	SN	SR	TM	ZR	TOTAL
IS	C	ALP048			25			15	10	5		30		15				TR	100
OES	C	ALP172			20			5		25		40		5				TR	95
OES	C	ALP176			10			10	25	5		40		5				TR	95
OES	S	ALP014			30			8	5	1	1	35		10		10		TR	100
OES	S	ALP208			20			35	5	10	5	25						TR	100
OES	S	ALP037			45			25		10	3	0		15				TR	98
OES	S	ALP219		TR	10			20				60		5				0	95
OES	S	ALP190			15			1	30	5		40		3				TR	94
OES	S	ALP036			20				2	45		15		15				TR	97
OES	S	ALP198			10		TR	5	5	5	5	70						TR	100

S = Surface C = Core

Table C.8 Estimated Ore Equivalent Schist plus Garnet Quartzite modal percentages

ROCK TYPE	S/C	SLIDE N°	AM	AP	BI	CH	GH	GR	KF	MS	OP	QZ	RT	SL	SN	SR	TM	ZR	TOTAL	OPAQUE MINERALS					
																				CP	GA	MT	PO	PY	SP
OES+GQ	C	ALP049A			15			5	50	15	TR	10		2				TR	97						
OES+GQ	C	ALP049B			30			5	0	20	3	20		20				TR	98						
OES+GQ	C	ALP129			30			10	25			25		10				TR	100						
OES+GQ	C	ALP174			25			15		15		10				30		TR	95						
OES+GQ	C	ALP047A			2			15		53	25				TR			0	95	2	50		1		
OES+GQ	C	ALP047B			25			10		20	3	20		20				TR	98						
OES+GQ GR-BI**	C	ALP047C			30			5	50		5	10						0	100			10			
OES+GQ QZ-GH**	C	ALP047C		1		5	20				10	60						TR	96						
OES+GQ GR-KF**	C	ALP047C			20		12	20	20	5		10		10				TR	97						

** = Individual bands
S = Surface C = Core

Table C.9 Estimated Upper Footwall Schist modal percentages

ROCK TYPE	S/C	SLIDE No.	AM	AP	BI	CH	GH	GR	KF	MS	OP	QZ	RT	SL	SN	SR	TM	ZR	TOTAL
S	S	ALP230			10			2	2	15	3	60		5				TR	97
S	S	ALP229		TR	15			8	3	2	8	50		12				TR	98
UFS	C	ALP117B		TR	15			15	0	15	2	35		15				TR	97
UFS	C	ALP135			25	5				45		15		10				TR	100
UFS	C	ALP119			20					20	15	20		5		20		TR	100
UFS	C	ALP051			20			20	0	2	10	33		15				TR	100
UFS	C	ALP086		TR	25					5	3	60		5				TR	98
UFS	C	ALP118			20			5	20	15		20		15				TR	95
UFS	C	ALP117A			20	3		5	25	15		30		TR				TR	98
UFS	C	ALP050			20			15	8	25	1	15		15				TR	99

S = Surface C = Core

Table C.10 Estimated Orebody silicate assemblage modal percentages

ROCK TYPE	S/C	SLIDE No.	AM	AP	BI	CH	GH	GR	KF	MS	OP	QZ	RT	SL	SN	SR	TM	ZR	TOTAL
AMPH MAG	C	ALP113	5	TR		5		65			20							TR	95
MASSIVE SUL	C	ALP081			1			10		5	50	35	TR		TR			0	101
QTZ MAG	C	ALP075									60	40						0	100
QTZ MAG	S	ALP228		0.	1					3	40	50		2	TR			TR	96.5

S = Surface C = Core

Table C.11 Estimated Garnet Quartzite modal percentages

ROCK TYPE	S/C	SLIDE No.	AM	AP	BI	CH	GH	GR	KF	MS	OP	QZ	RT	SL	SN	SR	TM	ZR	TOTAL	OPAQUE MINERALS
																				CP GA MT PO PY SP
LGQ	C	ALP077A			3	1	2			5	90							0	101	TR TR 2 2 TR
LGQ PSC *CLAST*	C	ALP077B		5		TR	TR			TR	90							TR	95	
LGQ PSC MATRIX*	C	ALP077B		15			40	0	10	15	20							TR	100	
LGQ	C	ALP172G		10			15			2	70							TR	97	
GQ	S	ALP202Q					15			10	75	TR						TR	100	10
LGQ	C	ALP149		5			15	10	5	1	60							TR	96	
OEGQ	C	ALP130		10	5		10	3	10		60							TR	98	
UGQ	C	ALP114		3		5			1	3	85							TR	97	1 2

* PSC = Pseudoconglomerate

S = Surface C = Core

Table C.12 Estimated Broken Hill Quartzite modal percentages

	SLIDE NO.	QZ	BI/CH	MS	GR	SL	GH	OP	ZR	TM	SN	KF	Opaque minerals recognised in hand specimens
White Quartzite:	ALP009	97		2					TR				CP MT
	ALP124	93	1		3			2	TR				PY CP
	ALP227	96		3				TR	TR				
	ALP232	85		15					TR				
	ALP237	94	TR	5					TR				
Dark Quartzite:	ALP126	84		15					TR			1	CP
	ALP238	97		2					TR	TR			
	ALP239	93		5	1				TR		TR		
	ALP240	93	3		1		TR	2	TR				
	ALP011	94	3	2					TR				MT
Median Schist	ALP041	40	25	25		10		TR*	TR				
	ALP125	70	8		5	5	1	3*	TR				MT CP
	ALP226	80	2	1	5	3		2	TR			5	

* Mainly chalcopyrite

Table C.13 Estimated Namies-type Schist modal percentages

ROCK TYPE	SITE/S/C	SLIDE NO.	AP	BI	CH	KF	MS	OL	OP	PL	QZ	RT	SL	SN	SR	TM	ZR	TOTAL	OPAQUE MINERAL
																			HM
NTS	A	C	ALP451	TR	25		5	3	3	10	40		10				TR	96	
NTS	A	C	ALP453		20	10	10	5	2		25		15		10		TR	97	
NTS	A	C	ALP455 QITE		15		10		2	10	60						TR	97	
NTS	A	C	ALP455		15		5	10		15	35		15				TR	95	
NTS	N	S	ALP409		25		30	15	0.5		20		5	0.5			TR	96	
NTS	N	S	ALP410		25		10	10	3		35		10		5		TR	98	
NTS	N	S	ALP415		10		30	25	10		20		2				TR	97	10
NTS	N	S	ALP404		30		10		2		45		5		5		TR	97	
NTS	N	S	ALP401		10		5	10	12		35	2	15		5	1	TR	95	
NTS	N	S	ALP402		20		0	5	3		65		2				TR	95	
NTS	W	C	ALP434		3	3	20	3			60	1	5				TR	95	
NTS	W	C	ALP433	TR	10		45	5	5	8	20		2				TR	95	
DK QITE in NTS	N	S	ALP413		2			1	1		97							101	

S = Surface C = Core
A = Achab N = Namiesberg
W = Wortel

Table C.14 Estimated Shaft-type Schist modal percentages

ROCK TYPE	SITE/S/ C	SLIDE NO.	AP	BI	CH	GR	KF	MS	OP	PL	QZ	RT	SL	SN	SR	ZR	TOTAL	OPAQUE MINERALS		
																		PO	PY	
STS+Q	W	C	ALP423	TR	25						75					TR	100			
S	W	C	ALP438		20	2		20	25	TR			5	30			TR	102		
S	W	C	ALP447		20	5		10	5	2			40	15			TR	97		2
STS	W	C	ALP442		20	5		10	5	2			50	10			TR	102	1	1
STS	W	C	ALP431		20	15			10	TR			30	10		10	TR	95		TR
STS	W	C	ALP424		15	10							35	30		5	TR	100		
STS	W	C	ALP430		30		5		10	TR			25	15		10	TR	95		TR
STS	W	C	ALP440		30	3			5	3	2		35	20			TR	98		2
STS	W	C	ALP445		20				5	1			55	15			TR	96		1
STS	W	C	ALP422		30			0	25	TR	0	15		30			TR	100		TR
STS	W	C	ALP443		20	3			5	10	3		40	15			TR	96	1	2
MASS.SIL	W	C	ALP444						40	4			10	1	40	2	TR	97		

S = Surface C = Core
 A = Achab N = Namiesberg
 W = Wortel

Table C.15 Estimated Calc-type Silicate plus Manganese Quartzite modal percentages

ROCK TYPE	SITE/S/ C	SLIDE NO.	AM	AP	BI	GR	OL	OP	PX	QZ	ZR	TOTAL	OPAQUE MINERAL		
													MT		
CTS	W	C	ALP446C Y	10	2	10	25			50	3		100		
CTS	W	C	ALP446C X	15	2	5	20	50	5				97		5
GTQ	W	C	ALP446G		1	20	30				45	TR	96		

S = Surface C = Core
 A = Achab N = Namiesberg
 W = Wortel

Table C.16 Estimated Regional Quartzite modal percentages

ROCK TYPE	SITE/S/ C	SLIDE NO.	AP	BI	CB	CH	CZ/EP	GR	KF	MS	OP	PL	QZ	SL	SN	SR	ZR	TOTAL	OPAQUE MINERAL		
																			PY		
WTQ	N	S	ALP406							TR	TR		99					TR	99		
WTQ	N	S	ALP405		5								90					TR	95		
WTQ	N	C	ALP432		2		TR		TR		5	2	90			TR		TR	99		2
WTQ	N	S	ALP412								3		97					TR	100		
WTQ	W	C	ALP450		TR	8		1		5	2	TR	15	65				TR	96		
WTQ	W	C	ALP435			3		10		20	5	1	60					TR	99		
LTQ	N	C	ALP428		2	TR	1		TR		TR	TR	95	TR				TR	98		TR
LTQ	N	S	ALP414		2						1	TR	95					TR	98		
LTQ	N	S	ALP408		2		TR			0.5	2		95			TR		TR	99.5		
LTQ	N	C	ALP426		TR		1			3	1		95					TR	100		1
LTQ	W	C	ALP448		7		3			25		2	60	2				TR	99		2
LTQ	W	C	ALP437			4	TR			20	10	TR	65					TR	99		
MDTS	N	S	ALP407		5					20	15	3	50	5				TR	98		
MDTS	W	C	ALP436 BI*		20					20	5	3	5	45				TR	98		
MDTS	W	C	ALP436 SIL*							25	5		45	20				TR	95		
MDTS	W	C	ALP449		15		5			20	10	TR	30	10		5	TR	95			

* = Individual bands
 S = Surface C = Core
 A = Achab N = Namiesberg
 W = Wortel

Table F.1 Factor loadings for OS "ore factors"

Element	Ore Schist (core)		Ore Schist (surface)
	Factor 2	Factor 3	Factor 3
SiO ₂	-0.317		
TiO ₂			
Al ₂ O ₃			
Fe ₂ O ₃	0.516		
MnO		0.899	
MgO			-0.572
CaO		0.439	-0.474
K ₂ O			
Rb	0.347		
Ba	0.459	0.58	
Pb	0.509	0.434	0.585
Zn	0.499		0.87
Zr			
Cr			
Y		0.906	-0.49
Nb			
S	0.883		
Cu	0.711		0.615
V	0.577	-0.363	
Se		0.331	
Ni			-0.33

Note: Loadings less than 0.3 have been omitted

Table K.1 Comparison between Namies Schist at Gamsberg and at Broken Hill

Gamsberg Namies Schist *	Broken Hill Namies Schist
1. 70 m thick	1. 103 m thick
2. Quartzite interbands	2. Quartzite interbands
3. Quartz content increases towards quartzite	3. Quartz content increases towards quartzite
4. Well foliated	4. Well foliated
5. Nodular with sillimanite-quartz nodules	5. Nodular to mottled with sillimanite-quartz-muscovite nodules
6. Major minerals are: quartz biotite sillimanite muscovite	6. Major minerals are: quartz muscovite sillimanite (biotite)
7. Accessory minerals are: garnet tourmaline rutile anatase hematite ilmenite	7. Accessory minerals are: garnet tourmaline zircon sphene pyrite pyrrhotite magnetite

* After Rozendaal (1978)

Table K.2 Comparison between Quartzite descriptions at Gamsberg and at Broken Hill

Gamsberg *	Broken Hill
Triad of (a) thicker, whiter quartzite gradational into Namies Schist separated by (b) highly variable schist from (c) thinner, darker quartzite	Triad of (a) thicker, whiter quartzite gradational into Namies Schist separated by (b) highly variable schist from (c) thinner, darker quartzite
<u>White Quartzite Member</u>	<u>Upper Quartzite</u>
1. 200 - 250 m thick	1. 65 m thick
2. Major minerals are: quartz	2. Major minerals are: quartz
3. Minor minerals are: muscovite apatite zircon pyrite rutile needles	3. Minor minerals are: biotite/chlorite muscovite zircon magnetite pyrite chalcopyrite garnet
<u>Pelitic Schist Member</u>	<u>Median Schist</u>
1. 10 - 25 m thick	1. 40 m thick
2. Very variable in composition	2. Very variable in composition
3. Micaceous dark quartzite layers in the schist	3. Muscovite-rich dark quartzite lenses in schist
4. Major minerals are: quartz biotite muscovite sillimanite garnet	4. Major minerals are: quartz biotite/chlorite muscovite garnet sillimanite magnetite
5. Minor minerals are: magnetite hematite : totalling anything up to 10% pyrrhotite :	5. Minor minerals are: zircon gahnite pyrite chalcopyrite
<u>Dark Quartzite Member</u>	<u>Lower Quartzite</u>
1. 40 - 100 m thick	1. 23 m thick
2. Occasional pebble bands	2. No pebble bands noted
3. Bands of 1-2m wide schist	3. Minor interbanded schists
4. Major minerals are: quartz	4. Major minerals are: quartz
5. Minor minerals are: zircon biotite apatite muscovite sillimanite hematite magnetite pyrite	5. Minor minerals are: biotite/chlorite muscovite garnet gahnite zircon tourmaline sphene pyrite chalcopyrite magnetite

* After Rozendaal (1978)

Table K.3 Broken Hill oxygen isotope data (permil) from Reid et al. (1987)

Borehole	Sample	Rock Type	Quartz	Biotite	Garnet	Magnetite
BH166	ALP076	WQ	9.36			
	ALP069	DQ	8.92			
	ALP072	UOB QM	8.87			0.79
	ALP077	LOB GQ	7.86	2.41	4.82	-0.32
	ALP081	LOB MS			2.96	
BH123	ALP029	NS	6.37			
	ALP030	NS	5.71			
	ALP040	WQ	9.17			
	ALP042	DQ	9.69			
	ALP047	UOES+GQ	7.7	2.42	3.72	
	ALP049	LOES+GQ	9.4	4.92	7.23	
	ALP057	SS	14.1			
	ALP059	SS	13.9			
BH114	ALP110	LOB MS	6.6			
BH156	ALP153	BGZ	13.34			
Surface outcrops	ALP190	UFS	12.87			
	ALP198	OES	8.39	5.69	4.83	1.87
	ALP208	OES	6.9	3.7	2.83	
	ALP213	MNQ	11.18			

Table K.4 U, Th and Pb ion microprobe analyses on zircons from White Quartzite at Froneman se Kop. (Analyst: R. A. Armstrong)

Grain area	U ppm	Th ppm	204 ppb	%comm. 206	208/232	206/238	207/235	207/206	207/206 age (Ma)
1-1	959	106	48	0.46	0.0771+-4	0.2009	2.345	0.0847+-11	1308+-26
2-1	929	58	41	0.50	0.0616+-8	0.1659	1.748	0.0764+-15	1106+-41
3-1	152	75	66	2.33	0.0962+-7	0.3420	5.730	0.1215+-44	1979+-64
3-2(rim)	969	119	92	0.80	0.0458+-5	0.2205	3.344	0.1100+-15	1800+-24
4-1	163	129	97	3.95	0.0722+-4	0.2710	3.637	0.0973+-54	1574+-104
5-1	451	97	80	1.18	0.0844+-5	0.2795	4.755	0.1234+-18	2006+-26
6-1	454	607	49	0.87	0.0397+-1	0.2309	3.711	0.1166+-20	1904+-31
7-1	191	149	24	0.72	0.1028+-2	0.3207	5.366	0.1213+-21	1976+-31
8-1	532	247	85	1.22	0.0728+-3	0.2417	3.460	0.1038+-24	1693+-42
9-1	392	634	94	2.63	0.0272+-9	0.1667	2.605	0.1133+-29	1853+-47
9-2(rim)	233	290	68	1.97	0.0767+-2	0.2730	4.141	0.1100+-35	1800+-58
10-1	390	89	77	1.12	0.0676+-6	0.3250	5.682	0.1268+-21	2054+-29
11-1	217	125	122	3.23	0.0745+-4	0.3137	4.481	0.1036+-36	1690+-64
12-1	173	87	85	2.75	0.0847+-4	0.3241	5.509	0.1233+-31	2004+-45
13-1	283	76	59	1.14	0.0888+-5	0.3340	5.702	0.1238+-21	2012+-30
14-1	112	66	79	4.11	0.0808+-5	0.3064	4.716	0.1116+-48	1826+-77
14-1(repeat)	116	69	45	2.31	0.0839+-5	0.3084	4.313	0.1014+-48	1651+-88
15-1	192	93	49	1.97	0.0718+-3	0.2392	3.877	0.1175+-28	1919+-43
16-1	78	83	101	7.51	0.0731+-5	0.2969	3.681	0.0899+-75	1424+-161
17-1	208	122	108	2.80	0.0933+-3	0.3362	5.428	0.1171+-26	1912+-40
18-1	415	284	176	2.44	0.0853+-2	0.1780	5.089	0.1162+-19	1898+-29